UNIVERSITÀ DEGLI STUDI DI PALERMO

Dottorato di Ricerca in Scienze della Terra e del Mare

Dipartimento di Scienze della Terra e del Mare

SSD GEO/02

Active tectonics, sedimentation history and geomorphological features in the northern Sicily continental margin: implications for the marine geohazard assessment.

PhD STUDENT

ELISABETTA ZIZZO

COORDINATOR

PROF. ALESSANDRO AIUPPA

TUTOR

PROF. ATTILIO SULLI

CO TUTOR

PROF. AARON MICALLEF

CYCLE XXXII

YEAR OF QUALIFICATION 2020

Contents

Acknowledgements

At the end of these three years of doctoral studies, I would like to express my sincerest gratitude to all those who, to varying degrees and in different ways, have contributed to achieving this goal.

I would first like to thank my tutor Prof. Attilio Sulli, for offering me, since I was a student until today, continuous teachings that made me grow both from a personal and a professional point of view, dedicating and giving myself, without ever sparing himself, his time and precious knowledge, as well as his enthusiasm for work, which nowadays distinguishes me. Without his support and his encouragement to go beyond my limits and my insecurities, I would never have become what I am today, without fear of measuring myself against difficulties but rather with the desire to do better and better. I thank you because your advice has always been useful, to help me think right and finally make the right decisions. Thanks Sulli, you have been a source of inspiration!

I also thank all those who have offered me their precious support despite their many commitments. I am grateful to Dr. Daniele Spatola, researcher at the University of Malta, who supported me during my stay abroad, but above all for his friendship, support and fundamental scientific help given to me along the way. I thank Prof. Aaron Micallef, professor at the University of Malta, for having hosted me for the period abroad, providing me with resources and people. A special thanks to Prof. Christian Gorini of the Sorbonne University in Paris, for having welcomed me for several weeks, with professionalism and kindness, and for offering me useful comments and his competence.

I also thank my Marine Geology group, which includes Dr. Maurizio Gasparo Morticelli and Dr. Mauro Agate, for their support during the three-year period, both personally and professionally. My deep appreciation goes to Prof. Raimondo Catalano, a retired professor of my Department, for teaching me that knowledge has no time, that even a person like him, with his advanced career, can talk and help a doctoral student like me. Thanks to Prof. Pepe of the Department of Earth and Marine Sciences and to Dr. Lo Iacono of the CSIC of Barcelona, for encouraging me especially at the beginning of my studies dispensing valuable advice.

I strongly thank the Coordinator of the Doctorate, Prof. Alessandro Aiuppa, for his support and his availability at all times and wherever he was, and for the valuable advice he gave me during these three years. I would also like to express my thanks to the entire administrative sector and to the present and past management of the Department, in particular Maria Cannilla and Lucia Randazzo for the professionalism and kindness that they have always shown me, and for having always solved in the simplest way the problems that I met during the three-year period.

I also thank Prof. Paolo Orrù of the University of Cagliari and Dr. Fabiano Gamberi of the CNR of Bologna for the revision of the doctoral thesis.

I would like to thank my colleagues Marta, Maria, Vincenzo, Silvia, Eleonora, and Samantha and David, for sharing joys and sorrows, pauses and paranoia that have accompanied me during these three years, and for encouraging me not to give up during difficult times .

I am also grateful to all the relatives who have always shown me their love and support, believing in me, even not knowing exactly what I was doing. Thank you for having been, especially Anna and uncle Giacomo.

Last, certainly not least, my very special thanks go to my Family, Mamma, Papà, Anna, Giovi and Alessandro, to whom I dedicate my thesis, because their Love and Support have accompanied me in every phase of my life, always believing in me, and above all always supporting my choices even if different from their opinion. Thanks Family, with all my heart!

Abstract

Starting from the assumption that seismic events in the active margins are accompanied by evidence of a depositional, geomorphologic and structural type, which constitutes the geological record of their activity, we analysed different features of the Northern Sicily continental margin (NSCM) to reconstruct the deformational field and related stress field in the Southern Tyrrhenian sea. As an outcome of this project we were going to obtain seismotectonic setting and mapping to provide a powerful tool in managing and assessing the marine geological hazards.

The study area extends from the San Vito Peninsula to the Termini Gulf along the NSCM, including the Ustica island, and is located in a transitional area between the Sicilian-Maghrebian chain (SMC) to the south and the Tyrrhenian back-arc basin (TBAB) to the north. We mapped different features (tectonic, geomorphological, depositional, geophysical) in order to collect in a seismotectonic map driving forces and triggering factors, as well as their products along the NSCM.

In order to reconstruct the Recent evolution of the study area we analyzed the whole Plio-Quaternary time interval (defining the interval of neotectonics), with emphasis to the Late Pleistocene-Holocene (which define the interval of active tectonics). Products of the tectonic activity are pockmarks, mud volcanoes, structural escarpment, and other seismic induced features (submarine landslides, chaotic deposits, megafloods, channels and canyons and related sedimentary processes).

As a second step of this study we investigated geometry, age and kinematics of the tectonic structures, both buried and outcropping (at the seafloor or in the field), and correlate them to the sedimentary evolution of the Plio-Quaternary succession.

With the aim to verify whether and where the recently active structures can give rise to tsunamis through the bottom shift associated with slope failures, as the submarine landslides, we implemented a method to assess quantitatively the characteristics of anomalous waves and related coastal run-ups.

In detail, following the main aims of the research project, we obtained some major achievements:

Timing and kinematic characters of the neotectonic features. Based on the analysis of recent and active faults, seismicity and geodetic data, we reconstructed the present deformational pattern in the NSCM. We analysed the present processes along the Africa Europa boundary, giving new contribution on the characterization of crustal features produced by a change in the polarity of deformation and related seismotectonic setting.

Fault systems pattern. We mapped in great detail outcropping and shallow buried faults and fold axes and related morphological features. We found that these structures are in agreement with the present stress field as derived from the focal mechanisms in the study region. The resulting data were used to compile the marine geomorphological and structural layers of the Sheet 585 “Mondello” (Geological Map of Italy on 1:50,000, CARG Project).

Submarine morphology, stratigraphy and structures of the Ustica volcanic complex. We analyzed the complex features of the Ustica volcanic edifice and contributed to the knowledge of the

geological-geodynamic processes acting in the northern sector of the study region, which occurs on the Africa-Europe plate boundary, just along the thrust front separating the Kabilian-Calabrian tectonic element from the Sicilian-Maghrebian domain.

Late Quaternary Tectonics vs Sedimentation history. We investigate the tectonically active NSCM, with a focus on the Termini basin (central Southern Tyrrhenian Sea). This region originated as a consequence of a complex interaction of compressional events, crustal thinning, and strike-slip faulting, which the prevailing control on the morphology of the present day shelf and coastal areas during the Pleistocene. We focused on those related to gravitational mass movement and fluids escape, and dated the seismic-induced landslides in relation to the Late Quaternary depositional sequence. In this way we tentatively calculated the recurrence times of the main earthquakes.

Seabed sedimentary structures and bottom currents. We studied for the first time the bottom sedimentary structures along a gully system in a selected area of the NSCM (the Capo Zafferano offshore), to understand the interactions between the depositional processes and the complex morphology of the coastal-offshore areas. We identified bedforms, known as cyclic steps, which are linked to the dynamics of the bottom currents along the canyons. The results point out that turbidity currents might have been few meters thick and have had velocities in the range of 0.2–1.5 m/s.

Seismotectonic Map. Starting from the analysis of the processes active in the NSCM we realized the seismotectonic map of this region. The results, managed with a GIS-database, are potential indicators of geohazard for human settlements and infrastructures in the offshore and coastal zones.

Tsunami risk generated by submarine landslides. To provide an assessment of the geological hazards including tsunamigenic potential in coastal areas that could be subject to erosion, flooding and seismic activity, we tested some main submarine landslides as potential tsunamigenic source, in two selected sectors of the NSCM, the Gulf of Palermo and the Patti offshore. We calculated the associated theoretical run-ups, and are going to produce simulation models of the propagation of anomalous waves, coastal run-ups and inundation.

Introduction

The topic of this research is to analyse the role of active tectonics, sedimentation history and geomorphological features in the geological, geomorphological and geodynamic evolution of the Northern Sicily Continental Margin (NSCM), in order to evaluate the driving forces and the main parameters for the marine geo-hazard assessment. The research project has been carried out integrating: a) single- and multi-channel seismic profiles, with different resolution/penetration, available (from ViDePi project) and unpublished (acquired from the Department of Earth and Marine Science of the University of Palermo); b) morpho-bathymetric data (mainly unpublished); c) sedimentological analysis on cores collected along the NSCM; d) heat flow, gravimetric, magnetometric data, e) GPS and seismicity data, f) onshore structural and stratigraphic data; g) morphometric characterization, including statistical tools; h) computational methods for tsunami assessment; i) GIS and geo-databases. The new data have been integrated with those available in the literature to provide constraints on the marine geological features of the study area.

In detail, the main aims of the research project deal with the following topics:

- Timing and kinematic characters of the neotectonic features. The analysis of recent and active faults, constrained by seismicity and geodetic data, will be aimed to reconstruct the present deformational pattern in the southern Tyrrhenian Sea-northern coastal belt of Sicily.
- Fault systems geometry. We mapped in great detail structural elements (outcropping and shallow buried faults and fold axes), tectonic domains, and related morphological features, in the NSCM.
- Submarine morphology of the Ustica volcanic complex. New swath bathymetry of the submarine region of the Ustica Volcano (UV), 58 km north-northwest of the Sicily coast (south-western Tyrrhenian Sea), revealing the complex features of the volcanic edifice, contributed to the knowledge of the geological-geodynamic processes acting in the northern sector of the study region, which occurs on the Africa-Europe plate boundary.
- Late Quaternary Tectonics vs Sedimentation history. Focusing on the Termini basin (central Southern Tyrrhenian Sea) we investigated the tectonically active NSCM, using high-resolution seismic profiles and multibeam bathymetric data. Many morphological features of the present day shelf and coastal areas are the result of tectonics acting during the Quaternary on the margin, among which we focused on those related to gravitational mass movement and fluids escape. We used the sequence stratigraphy analysis of the Late Quaternary depositional sequence to date the seismic-induced landslides, in order to tentatively calculate the recurrence times of the main earthquakes.
- Seabed sedimentary structures and bottom currents. We used multibeam bathymetric data to verify the occurrence of bedforms in a selected region (the Capo Zafferano offshore, east of the Palermo gulf), to understand the interactions between the depositional processes and the complex morphology of the coastal-offshore areas.

- Seismotectonic Map. The active processes in the NSCM have been analysed to realize the seismotectonic map and the related database. The multidisciplinary analysis of geodynamic, tectonic and sedimentary processes was aimed to estimate the interplay between plate margins dynamics, seismic activity, geomorphic processes, tectonics and sedimentation along the continental margin. The results, managed with a GIS-database, are potential indicators of geohazard for human settlements and infrastructures in the offshore and coastal zones.
- Tsunami risk generated by submarine landslides. To provide an assessment of the geological hazards including tsunamigenic potential in coastal areas that could be subject to erosion, flooding and seismic activity, we tested some main submarine landslides as potential tsunamigenic source, in two selected sectors of the NSCM, the Gulf of Palermo and the Patti offshore, to calculate the associated theoretical run-ups. We are still working to produce simulation models of the propagation of anomalous waves, coastal run-ups and inundation.

The study area was chosen because it represents a key sector for the central Mediterranean geodynamic setting, as it has peculiar geological, geophysical and geomorphological characteristics that make it unique, like the presence of tectonic and volcanic structures, as well as erosive and depositional processes, which create a very complex architecture at different scales from that related to seabed morphology to the crustal structures. So far many issues regarding the characteristics and evolution of the NSCM are still debated, as timing and pattern of the different tectonic processes; present and past kinematics (both shallow and deep); the interplay of two plates (African and European plates) in relation to the seismicity, the role of fluids (from volcanic to sedimentary), and, last but not least, the interaction between tectonics, sedimentation and sea level change. As a consequence the analysis and interpretation of this area has an important impact on the understanding and assessment of marine geological geo-hazards.

Our study was facilitated by the huge availability of seismic reflection profiles, at different scale of resolution and penetration, geophysical data linked to the strong seismicity, morpho-bathymetric data from MBES surveys, and a deep geological background in the outcropping region (Northern Sicily coastal belt).

The geophysical features of the NSCM show the Moho depth ranges from about 10 km, in the Marsili bathyal plain, to about 40 km, towards the northern Sicily coast. The Bouguer anomalies change from 180 mGal in the Tyrrhenian region to negative anomalies in central Sicily (-100 mGal), while positive magnetic anomalies characterize the volcanic edifices, both submerged and buried. The heat flow values are high in the Tyrrhenian Sea (200 mW/m-2), decreasing (30-40 mW/m-2) towards the stable sector of the foreland area (Iblean plateau in SE Sicily).

The NSCM originated as a consequence of a complex interaction of compressional events, crustal thinning and strike-slip faulting, related to two main geodynamic complexes: 1) a Fold and Thrust Belt system deriving from the Africa-Europe convergence and 2) an extensional tectonic environment in the Tyrrhenian plain deriving from rifting and stretching episodes (Trincardi and Zitellini 1987; Sulli

2000; Pepe et al., 2005) in the back of the Ionian-Tyrrhenian subduction system. The Tyrrhenian basin opened since the Late Tortonian because of the rollback of the Ionian slab subducting beneath the Calabrian arc (Malinverno and Ryan, 1986). The Sicilian Fold and Thrust Belt formed as a consequence of the Neogene convergence of Africa promontory with the Corsica-Sardinia and the Kabylian-Calabrian elements (pertaining to the European plate).

The Meso-Cenozoic sedimentary successions along the NSCM are the marine prolongation of those outcropping along the Northern Sicily coastal belt. In the continental shelf, they are covered by Quaternary deposits, which are truncated by an erosional surface formed during the last glacio-eustatic oscillation. Local uplift caused non-preservation of portions of the oldest sequences. Prograding sedimentary wedges of coastal deposits formed during the Last Glacial Maximum (LGM, about 18 ka) along the shelf margin (Caruso et al. 2011).

During the last 125 ky in northern Sicily vertical tectonic movement are recorded, whose rates show a decrease from E to W, with the highest uplift rates in the eastern coast (0.8-1.63 mm/y). Further on, while the mainland sectors are uplifted, contemporaneously the offshore areas are subsiding, suggesting the existence of tectonic process causing differential vertical movements.

During the Quaternary, tectonics with different kinematic characters (strike slip, extensional, compressive) has controlled the evolution of this sector; it is still controversial what role each specific tectonic regime played on the evolution of the NSCM.

The tectonic activity of the margin is outlined by a large crustal and deep seismicity, located in two main seismogenic volumes. The deep seismicity is concentrated in the eastern part of the margin, related to the subduction of the Ionian lithosphere below the Calabrian Arc; the shallow seismicity is the result of the brittle deformation mainly of the submerged portion of the Maghrebian Chain. In the western sector of the margin the shallow (<25 km) seismic events of low to moderate magnitude (max Mw 5.9 on September 2002) occur along an E-W trending belt (Sulli, 2000; Giunta et al. 2009) included in the INGV catalogue in the Southern Tyrrhenian seismogenic sources (ITCS222 and ITCS014). The focal mechanisms related to the main seismic shocks are in agreement with a dominant NW-SE compressive offset direction, with a right strike-slip component, and an antithetic NE-SW fault trend. In the eastern sector the shallow seismicity is linked both to extensional fault systems (Pollina, Messina strait) and to right-lateral NW-SE transcurrent systems (Vulcano-Lipari and Tindari-Giardini).

One of the most important innovations of this research is the integrated analysis of different types of seismic reflection data with geophysical, structural, stratigraphic-sedimentological and geomorphological data to analyse with a holistic approach a continental margin, with the aim to produce a sea-land seismotectonic map. It also represents the starting point for thematic maps related to the geological risks, such as the coastal geological map and the seismic risk map along the margin that is an important tool for monitoring and assessing potential geohazards (earthquakes, tsunamis,

coastal to submarine failures, coastal erosion and flooding) in marine and coastal environments. In detail, important progresses beyond the state of the art have been achieved as follows:

1- identification of tectonic elements related to the retro-wedging deformation in the northern part of the NSCM, which constitute the starting point to define correctly: a) the distribution and pattern of seismogenetic sources, b) the accurate interpretation of the parameters of the seismic events, such as focal mechanisms and hypocentral/epicentral location, and c) model the evolution of the NSCM in the frame of the plates convergence;

2- the chronostratigraphic correlations of unconformities and systems tract of the LQDS with recognized seismo-induced elements, such as submarine landslides, which made it possible to estimate the recurrence times of earthquakes that triggered them. This could be a very useful information for the present earthquake assessment;

3- mapping and georeferenced of geological features into a GIS database, which represent a starting point for making maps of the Geo-Hazard and Geo-Risk in the southern Tyrrhenian Sea;

4- parametrization of anomalous waves, evaluation of run-up heights along the Sicilian coasts and modelling of tsunami and coastal inundation.

References

Caruso A, Cosentino C, Pierre C, Sulli A. (2011) Sea-level changes during the last 41,000 years in the outer shelf of the southern Tyrrhenian Sea: Evidence from benthic foraminifera and seismostratigraphic analysis. Quaternary International 232: 122-131 doi:10.1016/j.quaint.2010.07.034

Giunta, G., Luzio, D., Agosta, F., Calò, M., Di Trapani, F., Giorgianni, A., Oliveri, E, Orioli, S., Perniciaro, M., Vitale, M., Chiodi, M., Adelfio, G., 2009. An integrated approach to investigate the seismotectonics of northern Sicily and southern Tyrrhenian. Tectonophysics 476, 13-21.

Malinverno A. & Ryan W. B. F. (1986) - Extension in the tyrrhenian sea and shortening in the apennines as result of arc migration driven by sinking of the lithosphere. Tectonics, 5 (2), 227-245.

Pepe F, Sulli A, Bertotti G, Catalano R (2005) Structural highs formation and their relationship to sedimentary basins in the north Sicily continental margin (southern Tyrrhenian Sea): Implication for the Drepano Thrust Front. Tectonophysics 409: 1–18

Sulli A (2000). Structural framework and crustal characteristics of the Sardinia Channel Alpine transect in the central Mediterranean. Tectonophysics 324: 321–336

Trincardi F & Zitellini N (1987) The Rifting of the Tyrrhenian Basin. Geo-Marine Letters 7: 1-6

CHAPTER 1

Active hinterland-verging thrusting in the northern Sicily continental margin in the frame of the Quaternary evolution of the Sicilian Fold and Thrust Belt collisional system

NOTE This chapter is a scientific paper submitted to "Tectonics" journal. The authors are the followings: Attilio Sulli, Maurizio Gasparo Morticelli, Mauro Agate and Elisabetta Zizzo

Abstract

In this paper we present new geological and geophysical data to illustrate the tectonic activity in the Northern Sicily continental margin in the frame of the Quaternary evolution of the Sicilian collisional system. The Sicilian Fold and Thrust Belt (SFTB) has been characterized by a three-stage evolution during the last 15 My: two main thin-skinned shortening events involving mainly Meso-Cenozoic carbonate units, followed by thick-skinned thrusting involving Plio-Pleistocene deposits in the frontal area as well as the crystalline basement in the inner and deeper sector of the chain.

We investigated the northern Sicily continental margin, by using differently-penetrative seismic reflection data calibrated with detailed field surveys. Overall, the tectonic edifice appears to be affected, both offshore and onshore, by northward-verging compressional structures active during Quaternary time. These structures, correlated with the kinematic setting pointed out by seismicity and GPS measurements, are indicative of an important change in distribution and orientation of deformation in the frame of the Africa-Europe convergence.

Our hypothesis is that the most recent tectonic processes in the Northern Sicily continental margin are representative of a jump of the deformation of the SFTB from the frontal area in the Sicily Channel to the inner sector in the Southern Tyrrhenian Sea, and they could be a precursor of the change in the subduction polarity in the central Mediterranean orogenic system, as a consequence of the ongoing collision of the African promontory with the thinned continental to oceanic sectors (Algerian and Tyrrhenian basins) of the European plate.

The seismic activity associated with the northward-verging thrust could have implication for the assessment of the seismic risk in the Central Mediterranean and understanding of active structures in marine areas that could be responsible for tsunami hazard.

Keywords: Backthrust; Fold and Thrust Belt; Subduction; Seismicity; Active Tectonics

1. Introduction

The structure of a thrust belt may provide information about the kinematics and history of plate convergence and lithosphere subduction (Bally et al., 1985; Dewey et al., 1989, Doglioni, 1991, 1992). When continental margins converge, the resulting process is the continental collision that produces orogens. Many Authors have documented that during the building-up of an orogen, the deformation proceeds from inner to outer sector (forward breaking sequence), affecting deeper and deeper structural levels (Bally et al., 1966, 1985; Dhalstrom, 1970; Boyer & Elliott, 1982; Roure et al., 1990, among the others), even if there are many evidence of thrusts nucleated in the hangingwalls of older thrusts (break-back thrusting; Butler, 1987; McClay, 1992). In the past it was a common conviction that continents do not subduct, accommodating the shortening within lithosphere through large thickening. Modern petrologic, tectonic, and geophysical studies, among which seismic reflection

surveys, have demonstrated that continental lithosphere can subduct (Ducea, 2016), and the two colliding plates can be separated by convective upper mantle (mantle wedge). The delamination process can favor the continental subduction, as well as old and cold continental plates are likely to get subducted under hotter and more ductile upper plates that hosted the magmatic/volcanic arcs during subduction periods which preceded collisional events.

Collisional zones can show either shallow foreland-verging thrust sequences (frontal accretion) or deep-seated, out-of-sequence, structures (underthrusting); moreover, many thrust systems are not unidirectional but contain thrust wedges verging away from the toe of a subduction thrust (backthrusting), antithetic to the forward-directed transport (Butler, 1987), accomodating the strain transferred from the subducting plate.

The fold and thrust belts deriving from an arc-continent collision forms Alpine-type orogens, frequently characterized in their mature stage by a change of tectonic transport with retro-wedging thrust, nappe refolding, and normal faulting. The resulting final structure is typically a double-verging orogenic belt, as in the Pyrenees, Himalaya, and Alps, all showing a symmetrical or near-symmetrical structure with a pro-wedge and a retro-wedge (Poblet & Lisle, 2011; Carminati & Doglioni, 2012; Johnson & Harley, 2012). Often this evolves to a change of subduction polarity, which leads to the formation of the final suture zone.

Analog and numerical models demonstrated that frontal accretion, underthrusting, underplating and retro-wedging can represent different stages of an orogeny building, depending on the lithospheric rheology and inherited geometries of colliding plates, composition of the thrust wedge, erosional and exhumation processes, decoupling processes and levels of decollements (Peacock, 1990; Storti & McClay,1995; Beaumont et al., 1996; Royden, 1996; Gutscher et al., 1998; Couzens-Schultz et al., 2003; Burov & Yamato, 2008; Faccenda et al., 2008; Willingshofer & Sokoutis, 2009; Konstantinovskaya & Malavieille, 2011). Therefore, analysis of geometry and shortening of the tectonic wedges, displacements along thrust planes, and stratal pattern in the associated syn-kinematic sedimentary systems is useful to estimate tectonic evolution of thrust belts, including their timing and magnitude, improving understanding of plate convergence processes.

Along the central Mediterranean orogens, such deformational mode produced earlier “thin-skinned” thrust tectonics (with décollement style, basement not involved), and later thick-skinned thrust tectonics, as in the Southern Apennines and Sicily (basement deeply involved in thrusting; Scrocca et al., 2005; Gasparo Morticelli et al., 2015 among others). In the southern Mediterranean, along the Neogene Africa-Europe plate boundary, the development of retro-wedges, at the back of the accretionary complex, i.e. in the southern Tyrrhenian, was related to a plate boundary reorganization during the latest 0.8–0.5 My (Goes et al., 2004). A northern-ward migration of the plate margin was documented through the recognition of Late Miocene-Quaternary opposite-verging structures in the NW Algeria Neogene margin (Yelles et al., 2009) and double-verging structures have been recognized in the northern Africa plate boundary (Mauffret, 2007; Kherroubi et al., 2009; Hamai et al., 2015). A

reorganization of the Africa-Europe boundary was already hypothesized based on tectonic, seismological, geodetic, tomographic, and seismic reflection data, with the reconstruction of Wilson-type phases of deformation, starting with the northward subduction of Africa and contemporaneous Mediterranean back-arc extension, followed by a progressive slowdown of the main subduction, onset of compression and progressive, from W (e.g., off Algeria; Strzerzynski et al., 2010) to E, southwards subduction, or subduction inception, of back-arc basins (inversion; Billi et al., 2011).

Detailed field surveys and differently-penetrative seismic reflection data, including a deep crustal seismic profile, calibrated with borehole data, played an important role to document the features and to discuss the geodynamic context of the recent tectonic activity in the northern Sicily continental margin-southern Tyrrhenian sector, both offshore and onshore. This is a key sector to investigate tectonic structures that accommodate deformation along the transition belt between collision and subduction systems in the frame of the Africa-Europa convergence (Sulli et al., 2018). As a matter of fact, in this sector convergence is accommodated by both the subduction of the Ionian oceanic lithosphere beneath the European Calabrian Arc (Faccenna et al., 2014; Polonia et al., 2017; Scarfì et al., 2018) and collision along the N-Sicily continental margin, where African thinned continental crust is subducted beneath the European Sardinian and Kabylian-Calabrian belts (Roure et al., 1990; Catalano et al., 2013). The roll-back of the Ionian slab, producing frontal accretion in the Outer Calabrian accretionary wedge, opened a young oceanic crust in the southern Tyrrhenian back-arc basin (Kastens & Mascle, 1988; Doglioni et al., 2012).

Seismicity and geodetic data, and deformational features reconstructed along the southern Tyrrhenian Sea, addressed by several authors in the recent past, has been used to infer a new subduction inception along the Northern Sicily continental margin (Billi et al., 2011).

The main aim of this paper is to assess the Quaternary tectonic structures along the seismically active segment of the Sicilian orogeny by interpreting and dating field and seismic reflection data, and by organizing them into geodetic and seismological data-sets. Doing so we tried to shed light on the present processes along the Africa-Europe plate boundary, giving new contribution on the understanding of crustal features and related seismotectonic setting along the Northern Sicily continental margin.

2. Geological setting

The investigated area is a segment of the Apennine-Tyrrhenian System (Figure 1), developed along the Africa-Europe plate boundary (Figure 1a) as result of both the post-collisional convergence between a migrating “European“ sliver, the AlKaPeCa (for Alboran, Kabylies, Peloritani, Calabria, Boullin, 1986; Bonardi et al., 2001) region, and the African northern promontory, and the coeval roll-back of the subduction hinge of the Ionian lithosphere (Doglioni, Gueguen, Harabaglia, & Mongelli, 1999; Faccenna et al., 2004; Chiarabba et al., 2008). This geodynamic process, which produced a collisional system (Figure 1b), the Sicilian Fold and Thrust Belt (FTB), beside a subduction system (Figure 1c), the Ionian-Tyrrhenian arc-trench complex, is believed to be related to the two-phase

opening of the Ligurian/Provençal basin and the Tyrrhenian Sea respectively (Faccenna et al., 2001) and the continuing slow northward advance of the African lithospheric plate (Gueguen et al., 1998; Doglioni, Gueguen, Harabaglia, & Mongelli, 1999 and Doglioni, Harabaglia, Merlini, Mongelli, et al., 1999; Cavazza et al., 2004; Goes et al., 2004).

As a consequence of the rollback of the Ionian slab, the Tyrrhenian back-arc basin opened producing extension offshore northern Sicily (Agate et al., 1993; Pepe et al., 2003), where NW-SE to E-W-striking high-angle normal faults dissected since Late Miocene the northernmost Sicilian FTB, forming extensional basins also in the coastal areas of northern Sicily (Di Stefano & Lentini, 1995; Lentini et al., 1996). NW-SE compressional/transpressional faulting affected the offshore area during the Early Pliocene (Pepe et al., 2005), followed, during the Late Pliocene, by E-W, NW-SE and NE-SW trending normal faulting (Fabbri et al., 1981; Barone et al., 1982) and crustal thinning (Pepe et al., 2000). A NNW-SSE trending main regional tectonic fault system (Lanzafame & Bousquet, 1997; Billi et al., 2006) with predominantly right-lateral transcurrent kinematics transversally dissected the south-eastern Tyrrhenian.

As documented by surface and subsurface geological and geophysical researches (Roure et al., 1990; Casero & Roure, 1994; Lentini et al., 1994; Albanese & Sulli, 2012; Catalano et al., 2013), the Sicilian continental subduction complex (Figure 1), up to 20 km thick, is characterized by the following regional tectonic elements: a) the Pelagian-Iblean foreland with its African crust; b) a Late Pliocene-Quaternary narrow foredeep, onlapping the frontal sector of the thrust belt in southern Sicily and its offshore; c) a complex, south to southeast-vergent FTB. This consists of: i) a “European” element (Kabilian-Calabrian tectonic units) exposed in north-eastern Sicily; ii) a “Tethyan” element (Sicilide units); iii) an African element composed of carbonate thrust systems (Sicilian-Maghrebian units); iv) a thrust wedge, named Gela Thrust System (GTS), composed of Cenozoic terrigenous and clastic-carbonate deformed rocks.

The African element derive from the deformation of both shallow and deep-water Meso-Cenozoic, passive continental margin-type sequences and foreland basin system successions (foredeep and wedge-top basins). The Sicilian sector of the Meso-Cenozoic African passive continental margin, reconstructed from regional facies analyses (Catalano & D’Argenio, 1978; Patacca et al., 1979; Bernoulli, 2001 among others) was formed by a carbonate-platform depositional environment, recorded by shelf-to-pelagic carbonate successions (Panormide, Trapanese, Saccense and Iblean), laterally linked to slope-to-basin areas (Imerese and Sicanian) filled with deep-water carbonates, bedded cherts and sandy mudstone successions.

During the Late Oligocene–Early Miocene the passive continental margin successions were progressively buried beneath several hundred meters thick terrigenous deposits (Numidian Flysch) accumulated in a wide foredeep basin and afterwards involved in the compressional events originating the Sicilian Fold and Thrust Belt (Pescatore et al., 1987; Pinter et al., 2016; Butler et al., 2019).

The Sicilian FTB was characterized by a multi-stage evolution during the last 15 My. Forward migration of the FTB started as from the early Miocene with the progressive detachment of the Meso-Cenozoic, passive continental margin succession from its basement, triggered by the collision between the Corsica-Sardinia sliver and the northern African margin. During this thin-skinned thrusting phase, two main subsequent southeastward-verging tectonic events (Figure 1d), generated and developed at different structural levels and at different time intervals and accompanied by substantial clock-wise rotations, occurred (Oldow et al., 1990; Roure et al., 1990; Bello et al., 2000; Cifelli et al., 2007; Avellone et al., 2010; Speranza et al., 2018). The early phase involved the Sicilide, Imerese and Sicanian thin, deep-water, shales and carbonates, which overthrust thick, more external, platform carbonates, producing duplex geometry and major tectonic transport since Serravallian time (shallow-seated tectonic Event 1, Figure 1d). During the latest Miocene–early Pleistocene, deep-seated thrusts detached and deformed the platform carbonates, forming axial culminations and ramp structures (deep-seated tectonic Event 2, Figure 1d). Triangle-like and duplex structures affected the carbonate ridges (Albanese & Sulli, 2012; Gasparo Morticelli et al., 2017), at places (Rocca Busambra and Kumeta ridges in Figure 1) alternatively interpreted as E-W-striking, right-lateral wrench structures, connected to a crustal discontinuity inherited from the African margin dissection (Ghisetti & Vezzani, 1984; Giunta et al., 2000; Nigro & Renda, 2001). The wedging at the depth of the carbonate platform substrate produced re-embrication and shortening within the overlying deep-water carbonate thrust pile (Avellone et al., 2010) as well as the deformation of the Upper Tertiary deposits filling syn-tectonic basins (Gugliotta et al., 2014). Giunta et al. (2000), Nigro and Renda (2001) described coeval compressional and extensional structures in the Sicilian-Maghrebides and in the Tyrrhenian back-arc basin, as structures related to an E-W-trending simple shear system. Tortorici et al. (2001) interpreted the deformation in western Sicily as a result of lateral escape processes. Butler et al (2019) indicate that the eastern Sicily-Maghrebian-Thrust-System developed as an emergent-imbricate-fan characterized by a slow and poor syn-kinematic deposition on top of the thrust wedge. This model implies a moderate shortening of the sedimentary tectonic units above the top crystalline-crust basal detachment. Backthrusting in the inner sector of the Sicilian FTB was already documented by mesostructural and seismic reflection data in central-western Sicily (Albanese & Sulli, 2012; Gasparo Morticelli et al., 2017), in the E-W trending and ~20 km long carbonate ridges of Mt. Kumeta and Rocca Busambra, as well as in the Cervi Mt (western sector of Madonie Mountains). In this case it is possible to directly correlate the syn-tectonic stratal pattern of the upper Tortonian succession filling the wedge-top basin to the development of north-verging high-angle faults (Gugliotta & Gasparo Morticelli, 2012; Gugliotta et al., 2013). In the central-northern Sicily (Avellone et al., 2011), a N-ward migration of depocenters during the Lower Pliocene related to the tilting of the southern margins was produced by uplift of the carbonate substrate along southward-dipping compressive-transpressive high-angle-faults (Sulli et al., 2016). Also the Plio-Pleistocene deposits of the northern edge of the Gela Thrust System (in the central-southern Sicily) are deformed by N-vergent structures, correlated at

depth with the thick-skinned tectonic event, which involves the crustal layers in the inner sector of the chain (Gasparo Morticelli et al., 2015).

This strain-propagation mode is inferred also by comparing the horizontal and vertical displacement rates of the thrust belt. During the thin-skinned tectonics, shortening prevails in the frontal thrust belt, with vertical displacement accommodating the deformation during the thick-skinned thrust tectonics (Mazzoli et al., 2000; Ferranti & Oldow, 2005).

A wedge-shaped body of high-density (3.1 g/cm3) sub-crustal material (Cassinis et al., 1969; Ferri et al., 2008; Accaino et al., 2011), was found beneath the northernmost Sicily, and interpreted as part of the southern wedge of the Tyrrhenian mantle (Catalano et al., 2013). The wedge appears to split the subducting Iblean (African) continental slab from the overlying stack of thrust sheets (Figure 1b).

Both seismicity and GPS data, as well as vertical movements rates, indicate active tectonics and convergence mainly in the northern Sicily offshore.

The deep seismicity, concentrated in the eastern part of the margin and northeastern corner of Sicily, is related to the subduction of the Ionian lithosphere below the Calabrian Arc and SE Tyrrhenian sea, while the shallow seismicity (< 15 km) is the result of the brittle deformation of the submerged portion of the Maghrebian Chain. The latter is characterized by low-to-medium magnitude (Pondrelli et al., 2006), with focal mechanisms of the major shocks of a thrust type, with horizontal compressive to transpressive maximum axes (Figure 2b), generally NNW-SSE trending (Pondrelli et al., 2006; Giunta et al., 2004; Vannucci & Gasperini, 2004), but its kinematics is still being debated. Seismic events from the Madonie to Peloritani Mts. (northern Sicilian belt) and beneath central Sicily have been related to compressional mechanisms to the west and extensional/transtensional in the east (Pondrelli et al., 2006). A geologic and tectonic “singularity” regards the extensional regime occurring in the Cefalù-Etna seismic zone that was related to the lateral extension on pre-existing faults by an inferred, mantle-upwelling beneath north-eastern Sicily (Etna volcano) (Billi et al., 2010). Available data do not image the deep structures in this area, as mantle seismic velocities are poorly constrained beneath the Sicilian orogenic wedge (Chiarabba et al., 2008). GPS site velocities in Sicily (Figure 2), up to 10 mm/y, are consistent with right-transpressional deformation and convergence between Sardinia and Sicily along the NW-SE contractional axis recorded by earthquake focal mechanisms (Oldow et al., 2002). Pondrelli, et al. (2006), Serpelloni, et al. (2007), Devoti, et al. (2008), Cuffaro, et al. (2011) and Palano, et al. 2012 described the active processes in Sicily, indicating for northern Sicily velocity ranging from 2.5 mm/y to 7 mm/y, moving toward the east, and for the foreland area a velocity of about 4.5 mm/y (NNW-wards drift movement when compared to Eurasia). Vertical movements during the last 125 ky are decreasing from NE to NW Sicily, with the highest uplift rates in the eastern coast (0.8-1.63 mm/y), where the Holocene rates are higher than those calculated for the Tyrrhenian (MIS 5.5) terraces (Ferranti et al., 2006). Further on, while the mainland sectors are uplifted, contemporaneously the offshore areas are subsiding, suggesting the existence of tectonic processes causing differential vertical movements (Sulli et al., 2013).

3. Data and methodologies

In order to analyze the Sicily-southern Tyrrhenian system we studied a set of geological and geophysical data, both offshore and onshore.

Geological mapping, facies analysis and structural fieldwork were carried out on the outcropping units of the Sicilian FTB, the overlying syn-tectonic successions, and the post-tectonic Plio-Quaternary sequences, in order to identify and date the structural features, to infer the related style of deformation, and to constrain the tectono-depositional events. The deformational patterns related to folding and faulting were reconstructed by several sites of structural measurements located along the main tectonic elements. Mesostructural analysis of fault planes and fold axes was used to reconstruct fault kinematics, fold-trending and stress-field orientations. The structural data have been summarized using statistical methods (stereograph projection obtained with Daisy 3.0 software, Salvini, 2001).

Submerged and buried structures were investigated through the geological interpretation of seismic reflection profiles with different resolution and penetration, calibrated with borehole data and integrated with other geophysical data. In the offshore areas we used sets of seismic profiles acquired by different seismic sources during previous researches in marine areas or extracted from public databases. The high resolution seismic profiles were acquired employing a multi-tip sparker array, with a base frequency of around 600 Hz, fired each 12.5 m. Data were received with a single-channel streamer with an active section of 2.8 m, containing seven high-resolution hydrophones, recorded up to 3.0 s two way time (t.w.t.) at a 10 kHz (0.1 ms) sampling rate. Data processing was performed by applying the following mathematical operators: traces mixing, time variant filters, automatic gain control, time variant gain and spherical divergence correction. The achieved signal penetration exceeded 400 ms (t.w.t.) and the vertical resolution reached 2.5 m at the seafloor. The medium penetration seismic data were acquired by using both high power sparker source (16 kJ) coupled with single-channel streamer or airgun array coupled with multi-channel (six) streamer; penetration depth ranges from 2 to 4 s (t.w.t.), with vertical resolution between 4 and 20 m, respectively. The airgun data were processed applying the following mathematical operators: normal move-out correction, stack, true amplitude recovery, 25-50 Hz and 150.200 Hz band-pass filtering, automatic gain control. A dense grid of high penetration seismic data, obtained from a freely accessible database (VIDEPI Project: http://www.videpi.com/videpi/videpi.asp) were acquired by airgun array coupled with 2.400 m long multi-channel streamer, achieving a penetration up to 6 s (t.w.t.), with vertical resolution of about 60 m. The following mathematical operators have been applied to process raw data: resample to 4 ms, demultiplex edit, true amplitude recovery, spherical divergence compensation, mutes, deconvolution, velocity analysis, NMO correction, time variant filter, trace equalization.

The seismic lines were interpreted using seismic facies analysis, which allowed depositional units, characterized by different seismic attributes, to be distinguished; then, structural interpretation was performed. The interpreted seismic lines were depth converted adopting average velocities derived from lithostratigraphy and sonic log data recovered in the southern and western Sicilian offshore.

Already published regional crustal sections (Bello et al., 2000; Catalano et al., 2002; Finetti et al., 2005; Catalano & Sulli, 2006; Catalano et al., 2013) were used to reconstruct a 2.5 D geological model of the Sicilian FTB and the surrounding marine areas, including the Ionian-Tyrrhenian system. The model was generated with the Software-Move2016 by correlating the surfaces that separate the main geological features, which are the depth of: Moho, Sicilian crystalline basement, Ionian oceanic crust, top of Kabylian-Calabrian tectonic wedge, Sicilian regional monocline, Sicilian FTB sole thrust, Kabylian-Calabrian sole thrust, top of Ionian slab beneath the Calabrian Arc. This model was used to generate automatically crustal geological sections along selected directions.

Most of the region is covered by geological maps and Multibeam data, acquired in the past in the frame of different projects by researchers from the University of Palermo (CARG: http://www.artasicilia.eu/old_site/web/carg/index.html; MaGIC: https://www.cnr.it/en/institutes-databases/database/978/progetto-magic). Morpho-bathymetric data were used to individuate the main morphostructural elements in the offshore areas. Digital Terrain Models (DTM) were produced with a footprint resolution of 2 m. The lacking data were covered by using morpho-bathymetry obtained by the GEBCO database (General Bathymetric Chart of the Oceans, gebco.net).

Finally we integrated the geological model with seismological data (since 1970) from international database (ISIDe http://cnt.rm.ingv.it/iside; ISC http://csi.rm.ingv.it; EMSC https://www.emsc-csem.org/Earthquake; Italian CMT rcmt2.bo.ingv.it/Italydataset1976-2015.dek; RCMT http://rcmt2.bo.ingv.it/data/EuroMedCentrMomTensors.csv) and projected hypocenters along regional cross sections.

We plotted the attitude of conjugate fault planes (Strike, Dip and Rake), from international earthquake databases, using Stereonet software (Cardozo & Allmendinger, 2013; Allmendinger et al., 2013), with the aim to realize “beach balls” of the seismic events. We projected the attitude of nodal and auxiliary fault planes of the focal mechanism along a vertical surface whenever indicated along regional cross sections.

4. Recent deformational Pattern in the Sicilian FTB and Northern Sicily Continental Margin

Geological mapping and structural surveys in Northern Sicily and geoseismic investigations along the Northern Sicily continental margin (Figure 2) highlighted that the inner sector of the Sicilian FTB is affected by a younger deformation than those related to the deformational events 1 and 2. The huge carbonate ridges developing along the northern coastline show at their northern walls sub-vertical southwards-dipping faults (Fig. 2). In order to date these structural elements, we analyzed their relationships with continental and marine Pleistocene deposits and correlated the field data to the seismic reflectors interpreted in the adjacent offshore region.

4.1. The inner sector of the Sicilian Fold and Thrust Belt

An essential contribution to dating the North-verging thrust faults comes from Rosamarina Mt., in the Termini Imerese area (central-northern coastal sector of Sicily; Figure 3).

Here the activation of the north-verging tectonic structures has led to the deformation of cemented and poorly stratified carbonate breccias immersed in a reddish sandy-silty matrix, accumulated in the continental environment as deposits of mountain slope, forming stratified slope deposits.

On the basis of lithology, texture and unconformable stratigraphic relationships with the bedrock, these deposits can be correlated with the Buonfornello/Raffo Rosso synthem deposits. Both these synthems, composed of paralic to continental deposits (Di Maggio et al., 2009), extensively crop out along the north-western Sicily coastal belt (Agate et al., 2017). Based on scattered vertebrate fossil remnants (Bada et al., 1991; Bonfiglio et al., 2003; Masini et al., 2008) and local, numerical dating worked out by thermoluminescence method on littoral and aeolian deposits (Mauz et al., 1997), both these synthems have been dated to the middle-late Pleistocene time interval.

Mesostructural field data, collected in 10 structural sites (Figure 3e) highlight the geological setting of this sector of the SFTB. In particular Rosamarina Mt. consists in a SW-vergent asymmetrical ramp anticline growing on a thrust plane affecting the Imerese tectonic units (St. 5 and 6 in Figure 3e). The anticline shows a general NW-SE trending hinge line that swings to a W-E direction in its western sector (St.3 and 4 in Figure 3e). Toward East, the Rosamarina anticline is cut by a NE-SW tectonic structure belonging to San Leonardo Fault system (Gugliotta et al., 2014), which shows the kinematic characters of a left-lateral strike-slip fault (St. 7-9 in Figure 3e). The southern limb of the anticline is well preserved, while the northern limb is involved in thrusting, tilted and uplifted northward, and strongly eroded (Figure 3a). Here we recognized a S-dipping thrust surface displaying striated planes with 200° dip direction (that is SSW-ward) and 35° dip, and with a general N-ward tectonic transport direction (St. 1-2 in Figure 3e). Along the thrust, both foot-wall and hanging-wall are overlain by a sedimentary wedge made up of the middle-upper Pleistocene continental deposits of the Buonfornello/Raffo Rosso synthem. The wedge is arranged in growth strata deposited with onlap geometry characterized by decreasing-upward dips (St. 10 in Figure 3e); this divergent stratal pattern suggests a syn-tectonic deposition (Figure 3 b, c, d; Burbank & Vergés, 1994).

Another sedimentary wedge lies at the base of the Rosamarina Mt. northern slope, composed of pebbly sands in ochre silty matrix, alternating with yellowish sandy silt, that belongs to the San Leonardo River synthem (Catalano et al., 2011; Figure 3a). Also this deposit is arranged in layers with upwards-decreasing-dips, testifying to a tilting of the straight flank of the Rosamarina anticline.

Summarizing the achieved results from the stratigraphic and structural evidence from the Rosamarina Mt., on the basis of the age of the continental deposits involved in the north-verging tectonic deformations, and the stratal pattern that suggest their syntectonic deposition, it is possible to date as middle-late Pleistocene the North vergent reverse fault system detected in this area of the central-northern Sicily.

4.2. The Northern Sicily continental margin (southern Tyrrhenian)

Seismic reflection profiles crossing the south-western Tyrrhenian margin and the Sardinia Channel (Figure 2) were used to define the active deformational pattern and the relationships with the regional geodynamics along the northern Sicily-southern Tyrrhenian seismogenic belt. Seismic data were correlated to the structural pattern reconstructed from the Northern Sicily chain and allowed to constrain the deep structural setting of the submerged sectors of the Sicilian FTB as well as to date relatively the structural elements.

The interpretation of both the medium to high resolution seismic reflection profiles, combined with high resolution morphobathymetric data, and the deep seismic reflection data, led us to define both the shallow and the deeper structural setting of the study area, revealing recent structural variations in the tectonic setting of the inner sector of the Sicilian FTB.

The offshore investigated area is not provided of deep boreholes, thus seismo-stratigraphic interpretation and correlation methods have been applied to date the detected tectonic features.

In this offshore sector, the north-verging tectonic structures affect a seismic unit made up of reflectors lying above a continuous, high amplitude seismic horizon, separating very different seismic facies above and down the reflector (Figures 4 and 5); the rocky surface generating this reflector is characterized by an enhanced acoustic impedance contrast and it usually acts as a low-band pass filter that cut the high frequencies, so that a very prominent change of vertical resolution can be observed between the seismic horizons above and down this surface. The very peculiar acoustic attributes of this seismic marker can be confidently correlated with the corresponding seismic horizon that has been calibrated by boreholes in the adjacent offshore western Sicily (Egadi Island), as well as in the central Mediterranean region on the whole. Well data revealed as this peculiar reflector can correspond to the top of evaporitic to clastic Messinian deposits or to an enhanced, regional scale unconformity, both (depositional and erosional) features related to the final stage of the Messinian salinity crisis occurred in the Mediterranean basin at the end of the Miocene (Ryan, 1973). This seismic marker (here labelled M-reflector, corresponding to the Messinian salinity crisis units LU-MU-UU following Lofi, et al. 2011) allows us to date as Plio-Quaternary the package of seismic horizons unconformably lying above it.

In the area of Cefalù Basin, sub-bottom cores (Sbaffi et al., 2001) document uppermost Pleistocene-Holocene sediment accumulated at the top of the Plio-Quaternary seismic unit, and, along the northern Sicily continental shelf, the analysis of high resolution single channel seismic profiles allow us to recognize the seismic reflectors belonging to the Late Quaternary Depositional Sequence (LQDS), which is a stratigraphic unit, extensively recognized across the continental shelf and upper slope off north-western Sicily coast (Sulli et al., 2012), deposited since about 128 ky BP during the last glacial-eustatic cycle (Caruso et al., 2011). In these sectors (southern margin of Cefalù Basin) we have detected hinterland verging reverse faults affecting the oldest reflecting horizons belonging to the LQDS (Figure 4a-b). This interpretation is confirmed by the displacement of the unconformity at the

base of the LQDS (tse in Fig. 4 a-b), which here represents the "regional" level: at the shelf edge it is as deep as 130 m, in agreement with the depth reached by the sea level during the last glacial sea fall (about -125 m); landward the faulted blocks are less deep, showing they have been uplifted along the interpreted reverse faults (Fig. 4 a-b).

In the Solunto High, along the northern boundary of the Cefalù basin, the high resolution single-channel seismic profile shows North-vergent reverse faults affecting the Plio-Quaternary sequence up to the horizons immediately below the sea-bottom (Figure 4c), suggesting that the deformation could have occurred also during the latest Pleistocene-Holocene time interval.

Three multichannel seismic reflection profiles crossing the central Sardinia Channel in a NNW-SSE direction (Figure 5a, b and c) shows the M-reflector steeply dipping towards SE, passing under a wedge-shaped body composed of a stack of seismic packages each one showing different thickness, acoustic attributes and geometry. On the whole this complex seismic body displays the characters of a North-verging tectonic wedge affected by reverse faulting and folding. Divergent geometries recognized in the basin fill both in the tip of the interpreted thrusts (insets A and C in Fig. 5) and above the thrust wedge (inset B in Fig 5) evidence the syn-kinematic deposition during the Plio-Pleistocene time interval.

Based on the detected depth, more than 3 s/TWT of the S-dipping M-reflector and considering the top of the overlying thrust wedge at 1 s/TWT, assuming an average P-velocity of 3000 m/s, the tectonic complex in the Cornaglia Terrace is as thick as 3000 m. The high-penetration seismic profiles shows that the north-verging thrusts involve not only near-surface, unrooted sediments but also deeper levels of the tectonic edifice, with until 10 km slip above the basal thrust (Fig. 5 a-c).

To confirm the involvement of thick tectonic wedges in the N-verging thrusting, a seismic profile crossing the Drepano Thrust Front (Figure 5d), which is the structural element along which the Kabylian-Calabrian units (Beccaluva et al., 1986; Compagnoni et al., 1989) overthrust the Sicilian-Maghrebian FTB (Sulli, 2000), shows that a recent S-dipping thrust inverted the original relationships between the tectonic bodies. This is a very important information because it documents that north-verging thrust affect not only the sedimentary wedges but the crystalline units too.

Morpho-bathymetric data show that in most cases the north-verging reverse faults are responsible of the geometry of the main submerged structural highs (e.g. the Solunto high, Figure 4c) defining the irregular shape development of the Southern Tyrrhenian continental slope, interrupting its overall northward-deepening trend.

4.3. Crustal geological-cross section and seismicity

We also used the distribution of epicenters and localization at depth of hypocenters to identify the seismically active tectonic structures (Figure 6). We divided the investigated area into three, about 100 km wide, NNW-SSE/NW-SE trending belts, crossing the Central Mediterranean from the Southern Tyrrhenian, across Sicily and Calabria, to the Sicily Channel-Ionian sea. In the middle of each belt we

carried out a vertical crustal section (geo-seismological section), on which we projected, along the perpendicular direction, the hypocentres of all earthquakes distributed in the pertaining zone (1-3 in Figure 6). Figure 6, beside the distribution of the epicenters of the earthquakes recorded since 1970 (ISIDe, ISC, EMSC, CMT, RCMT databases; Pondrelli, 2002; Pondrelli & Salimbeni, 2006; Sgroi et al., 2012), skimmed by events recorded at depths of 5-10 km, show also the main thrust fronts originating from the Africa-Europe convergence.

The generated geo-seismological sections cross the Sicilian FTB and the Kabylian-Calabrian belt, parallel to the convergence direction. Each section shows the Moho discontinuity for both lower and upper plate (African and "Tyrrhenian" Moho respectively), the top of the crystalline basement of the different crustal domains (Iblean, Ionian, Sicilian and Kabylian-Calabrian), the main sole-thrust separating the crustal bodies, the hypocenters of earthquakes projected along a band of 100 km across the trace and associated focal mechanisms.

The sections 1 and 2, which cross the western sector of the Sicilian FTB, show hypocenters up to a depth of 100 km and a few clusters gathered at the main sole-thrust, recognized from seismic reflection profiles (Drepano thrust-front, Sicilian main thrust). In the NW sector they show an alignment of very deep hypocentres along a S-ward dipping plane (characterized by compressive focal mechanism) which differs strikingly from the regional NW-dipping of the major fronts of Sicilian FTB (1 and 2 in Figure 6), as well as from the NW-dipping Benioff zone, related to the Ionian subduction (section 3), and imaged by the alignment of up to 400 km deep hypocenters.

5. Discussion

Geological and geophysical investigation enable to distinguish successive deformational events and different tectonic styles of the orogenic belts during the different stages of shortening. Generally the deformation propagate towards the foreland (forethrusting phase), involving from shallow to deep-seated layers, with ramp-flat geometries (underthrusting phase) or duplexing (underplating), with or without strike-slip displacements or nappe rotations, depending on different factors, such as crustal thickness, convergence angle and rate, paleo-margin geometry, age, lithology and homogeneity of the sedimentary cover (Bally et al., 1966, 1985; Dhalstrom, 1970; Boyer & Elliott, 1982; Butler, 1987; Channell et al., 1990; Speranza et al., 2003; Roure et al., 1990; Avellone et al., 2010; Poblet & Lisle, 2011; Carminati & Doglioni, 2012; Johnson & Harley, 2012; Speranza et al., 2018).

The late Neogene to Quaternary Sicilian collisional system (Figure 1), extending to the whole southern-central Mediterranean region, as revealed by field surveys and seismic reflection and borehole data, supported by gravimetry, magnetometry, heat flow and seismicity, as well as Global Positioning Satellite Array (GPSA), developed in the frame of a foreland-basin system evolution and experienced transition from thin-skinned to thick-skinned thrust tectonics. The last compressional event in the outer sector of the orogeny lasted until 0.8 Ma along the Gela Thrust Front (Catalano et al., 1993). In this area seismicity is very faint and active tectonics limited only to extensional to transtensional processes linked to the Sicily Channel rift zone or to major strike-slip fault systems, the

Belice-Sciacca and Comiso systems, respectively to the W and E of the more advanced front of the thrust belt (Figure 2).

Considering that the larger seismic activity of the Central Mediterranean is located in the northern Sicily continental margin, we analyzed the tectonic activity in this sector, which represents the inner sector of the orogen (Figures 2 and 6). Structural field surveys and seismic reflection interpretation revealed widespread south-dipping, north-verging thrusts both in the outer (innermost Gela TS) and inner sectors.

In the Gela TS the north-verging structures, which are Early Pleistocene in age, involve the uppermost structural level in the tectonic edifice and, together with the south-verging fault system of the Gela TS, depict on the whole a triangle-zone geometry (Figure 1b).

Differently, north-verging compressional structures affecting the inner sector of the Sicilian FTB, along the northern Sicily coastal belt and its offshore (Figures 3-5), provided two useful elements: 1) the deformation involves deeper structural levels of the Sicilian FTB, considering that in most of the cases they affect both the deep-water and shallow-water Meso-Cenozoic carbonates; 2) the occurrence of a preserved sequence of continental deposits of different ages, which have been attributed to "Unconformity Bounded Stratigraphic Units" (UBSU; Agate et al., 2017), allow to date retro-wedge-thrusting to Middle-Late Pleistocene (Figure 3). This evidence demonstrates that these structures are not associated to the older (Neogene) foreland-verging thrusts wedge.

The interpretation of high resolution seismic reflection profiles in the SW Tyrrhenian continental shelf to slope system (Figure 4) confirms the occurrence of south-dipping reverse faults affecting the Holocene deposits, shaping at place also the sea-bottom morphology. Trend of canyons, rills and pockmark alignments (Pennino et al., 2014), parallel to these structures, suggest their present-day activity. In some place these faults invert Neogene-Pleistocene extensional faults (Catalano & Milia, 1990).

Geodetic and seismological data contribute to define the tectonic activity shown by geological and seismic reflection data. The GPS data document the ongoing convergence of Europe and Africa at a rate of about 4-5 mm/yr (Figure 7; Hollenstein et al., 2003; D'Agostino & Selvaggi, 2004; Serpelloni et al., 2007, Devoti et al., 2011; Palano et al., 2012) with the NNW-wards displacement of both central-western Sicily and southern Tyrrhenian sectors (Serpelloni et al., 2007). Conversely, between the northern Sicilian coast belt and the Sicilian Channel GPS velocity along a NNW-SSE direction indicates no or very little active shortening in the southern, external sector of the chain (Serpelloni et al., 2007; Devoti et al., 2011), where the front of the Gela Thrust System is buried beneath middle-upper Pleistocene deposits (Catalano et al., 1993) and the seismic activity is very weak. Velocity profiles along the NW-SE direction (Figure 7c), worked out by projecting GPS velocity values from the stations located in the Sicily mainland and surrounding areas (Figure 7b), show, in correspondence with the less inclined segments (black line in Figure 7c), weak velocity variations in the area between the Hyblean region and the inner sector of the chain in the northwestern Sicily; the same velocity

profiles show, in correspondence with the more inclined segments (red band in Figure 7 a and c) higher velocity variations in the northern Sicily offshore. A such trend confirms a higher compression in the inner sector of the chain then in the outer one.

In this area, seismological data (Pondrelli et al., 2004) highlight an east-west directed seismic zone (ITCS014 and ITCS222 seismogenic sources, http://diss.rm.ingv.it/diss/) between the northern Sicily coast and the Ustica Island, west of Aeolian Islands, characterized by earthquakes with compressional or transpressional focal mechanisms and hypocentral depths of 20-30 km, up to 5.9 Md (September 2002; Giunta et al., 2004). Moreover deeper hypocenters alignment (around 100 km) and related focal mechanism (compressional) in this area seem to indicate a probable south-ward dipping thrust (Figure 6).

For a more clear description of double-verging FTB-tectonic evolution, it is necessary to refer main thrusts and backthrusts at the position of the lower plate on which the tectonic wedge grows. For this purpose, we called Neogene southward-verging fore- and back-thrusts, the compressional structures developed as a consequence of building of the Sicilian FTB above and towards the Hyblean-Pelagian foreland. Instead, we called Quaternary northward-verging fore- and back-thrusts, the more recent tectonic structures developed as a consequence of the overlapping of the Sicilian FTB above the southern Tyrrhenian crust.

Many Authors agree that this seismic and kinematic setting is linked to a tectonic reorganization of the Central Mediterranean orogeny (Goes et al., 2004; Serpelloni et al., 2005; Billi et al., 2011 among others). The southward-verging fore- and back-thrust evolution of the Sicilian FTB started since the Early Miocene, developed through three subsequent tectonic events (Gasparo Morticelli et al., 2015 and references therein) and it stopped at 0.8 Ma (Catalano et al., 1993; Lickorish et al., 1999). Since 0.8 Ma the Sicilian FTB records a new tectonic stage characterized by jumping of the seismic and tectonic activity towards the inner sector of the belt (southern Tyrrhenian Sea); here tectonics acts mainly as Quaternary northward-verging fore- and back-thrust, corresponding to the youngest tectonic structures illustrated in this paper (Figure 8).

6. Conclusions

The Sicilian Fold and Thrust Belt developed during Neogene-Quaternary times characterized by main African-wards tectonic transport direction (Figure 8). The dense set of geological and geophysical investigations carried out along the Northern Sicily continental margin, including the north-central Sicily, and illustrated in this paper, highlighted extensive hinterland-verging tectonic structures active during the Quaternary. These structures, correlated with the kinematic setting pointed out by seismicity and GPS measurements, are indicative of an important change in distribution and orientation of deformation in the frame of the ongoing convergence of the African and European plates.

The results of this study depict, in the northern Sicily mountain building, a structural framework comparable with that recognized in other orogens resulting from continent-continent or arc-continent

collision and interpreted like representative of a late collisional stage (Poblet & Lisle, 2011; Carminati & Doglioni, 2012; Johnson & Harley, 2012). This late evolutionary stage could be, at a larger scale, a consequence of the already inferred change in the subduction polarity in the central Mediterranean orogeny, following the ongoing collision of the tectonically accreted African promontory with the thinned continental to oceanic sectors (Algerian and Tyrrhenian basins; Figure 8) of the European plate (Mauffret et al., 2004; Billi et al., 2011; Arab et al., 2016; Hamai et al., 2018). Indeed, similar structures were envisaged along the north African offshore (inner sector of Western Mediterranean orogen) where, from late Miocene to Present, the Algerian-Tunisian margin has been uplifted and thickened by transpressional tectonics and oceanic crust is deformed by south dipping blind thrusts; moreover, the distribution of hypocenters suggest that this change involve the plates tectonic processes (Auzende et al., 1974; Tricart et al., 1994; Devérchère et al., 2005; Mauffret, 2007; Yelles et al., 2009; Strzerzynski et al., 2010; Arab et al., 2016).

The recent tectonic changes are as following summarized:

- end of the southward fore- and back-thrusting migration, about 0.8 Ma, of the external belt (Gela Thrust System);
- active tectonics shifted in the innermost belt (Northern Sicily continental margin);
- active northward-verging fore- and back-thrusting and uplift, mostly in the inner sectors of the orogen, and partly in the inner sector of the Gela thrust system during the Quaternary;
- active NW-SE convergence between Sicily and Sardinia;
- maximum horizontal displacement in the inner sector of the SFTB, minimum in the external sector of the chain;
- strong seismic activity along the northern Sicilian continental margin.

The latter could have important implications for the assessment of seismic risk in the Central- Western Mediterranean and for the understanding of active structures in marine areas that could be responsible for tsunami hazard.

Acknowledgements

Funding for research was provided by CARG and MAGIC projects (CONISMA/URL Palermo) and MIUR/University of Palermo (PJ_AUTF_008539) (resp. A. Sulli). The MUltibeam bathymetry data are available at https://www.cnr.it/en/institutes-databases/database/978/progetto-magic and www.gebco.net. The geological maps are available at http://www.artasicilia.eu/old_site/web/carg/index.html. The seismological data were obtained from http://cnt.rm.ingv.it/iside; http://csi.rm.ingv.it; https://www.emsc-csem.org/Earthquake; rcmt2.bo.ingv.it/Italydataset1976-2015.dek;

http://rcmt2.bo.ingv.it/data/EuroMedCentrMomTensors.csv. Multichannel seismic data are available at http://www.videpi.com/videpi/videpi.asp, while 3D crustal modelling are archived in Figshare repository (https://figshare.com/s/c3c44cce6f964ba8d497).

References

Accaino, F., Catalano, R., Di Marzo, L., Giustiniani, M., Tinivella, U., Nicolich, R., et al. (2011). A crustal seismic profile across Sicily. Tectonophysics, 508, 52-61.

Agate, M., Basilone, L., Di Maggio, C., Contino, A., Pierini, S., & Catalano, R. (2017). Quaternary marine and continental unconformity-bounded stratigraphic units of the NW Sicily coastal belt. Journal of Maps, 13 (2), 425-437.

Agate, M., Catalano, R., Infuso, S., Lucido, M., Mirabile, L., & Sulli, A. (1993) - Structural evolution of the northern Sicily continental margin during the Plio-Pleistocene. In: Max M.D. & Colantoni P. (Eds), Geological development of the Sicilian-Tunisian Platform, UNESCO Reports in Marine Science, 58, 25-30.

Albanese, C., & Sulli, A. (2012). Backthrusts and passive roof duplexes in fold-and-thrust belts. The case of Central-Western Sicily based on seismic reflection data. Tectonophysics, 514–517, 180–198.

Allmendinger, R. W., Cardozo, N. C., & Fisher, D. (2013). Structural Geology Algorithms: Vectors & Tensors: Cambridge, England, Cambridge University Press, 289 pp.

Arab, M., Rabineau, M., Bracene, R., Déverchère, J., Belhai, D., Roure, F., et al. (2016). Tectono-sedimentary evolution of the Eastern Algerian margin and basin from seismic data and onshore–offshore correlation. Marine Petroleoum Geology, 77, 1355–1375. https://doi .org /10 .1016 /j .marpetgeo .2016 .08 .021.

Avellone, G., Barchi, M.R., Catalano, R., Gasparo Morticelli, M., & Sulli A. (2010). Interference between shallow and deep-seated structures in the Sicilian fold and thrust belt, Italy. Journal of the Geological Society, London, 167, 109–126.

Avellone, G., Gennaro, C., Gugliotta, C., Barchi, M.R., & Agate, M. (2011). Tectono-stratigraphic evolution of a basin generated by transpression: The case of the Early Pliocene Lascari Basin (northern Sicily). Italian Journal of Geosciences, 130, 93–105.

Auzende, J.M., Olivet, J.L., & Bonnin, J. (1974). Le Detroit sardano-tunisien et la zone de fracture nord-tunisienne. Tectonophysics, 21(4), 357-374. doi.org/10.1016/0040-1951(74)90003-1

Bada, J. L., Belluomini, G., Bonfiglio, L., Branca, M., Burgio, E., & Delitala, L. (1991). Isoleucine epimerization ages of quaternary mammals from Sicily. Il Quaternario, 4(1a), 49–54.

Bally, A.W., Catalano, R., & Oldow, J. (1985). Elementi di tettonica regionale. Pitagora, Bologna.

Bally, A.W., Gordy, P.L., & Stewart, G.A. (1966). Structure, seismic data and orogenic evolution of Southern Canada Rocky Mountains. Bulletin of Canadian Petroleum Geology, 14, 337–381.

Barone, A., Fabbri, A., Rossi, S., & Sartori R. (1982). Geological structure and evolution of the marine areas adjacent to the Calabrian arc. Earth Evol. Sci., 3, 207-221.

Beaumont, C., Ellis, S., Hamilton, J., & Fullsack, P. (1996). Mechanical model for subduction-collision tectonics of Alpine-type compressional orogens. Geology, 24(8), 675-678.

Beccaluva, L., Morlotti, E., & Torelli, L. (1986). Notes on the geology of the Elimi chain area (southwestern margin of the Tyrrhenian sea). Mem. Soc. Geol. It. 27, 213–232.

Bello, M., Franchino, A., & Merlini, S. (2000). Structural model of eastern Sicily. Memorie della Società Geologica Italiana, 55, 61–70.

Bernoulli, D. (2001). Mesozoic-Tertiary Carbonate Platform, Slopes and Basins of the external Apennines and Sicily. In: G.B. Vai, & I.P. Martini (Eds.), Anatomy of an Orogen: the Apennines and Adjacent Mediterranean Basins (pp. 307-326). Springer, Dordrecht.

Billi, A., Barberi, G., Faccenna, C., Neri, G., Pepe, F., & Sulli, A. (2006). Tectonics and seismicity of the Tindari Fault System, southern Italy: Crustal deformations at the transition between ongoing contractional and extensional domains located above the edge of a subducting slab. Tectonics, 25, TC2006; doi:10.1029/2004TC001763.

Billi, A., Faccenna, C., Bellier, O., Minelli, L., Neri, G., Piromallo, C., et al. (2011). Recent tectonic reorganization of the Nubia-Eurasia convergent boundary heading for the closure of the western Mediterranean. Bull. Soc. Géol. France, 182(4), 279-303.

Billi, A., Presti, D., Orecchio, B., Faccenna, C., & Neri, G. (2010). Incipient extension along the active convergent margin of Nubia in Sicily, Italy: Cefalù-Etna seismic zone. Tectonics, 29, TC4026; doi: 10.1029/2009TC002559.

Bonardi, G., Cavazza, W., Perrone, V., & Rossi, S. (2001). Calabria-Peloritani terrane and northern Ionian Sea. In: G.B. Vai, & I.P. Martini (Eds.), Anatomy of an Orogen: the Apennines and Adjacent Mediterranean Basins (pp. 287-306). Springer, Dordrecht.

Bonfiglio, L., Di Maggio, C., Marra, A. C., Masini, F., & Petruso, D. (2003). Bio-chronology of Pleistocene vertebrate faunas of Sicily and correlation of vertebrate bearing deposits with marine deposits. Il Quaternario, 16 (1bis), 107–114.

Boullin, J-P., Durand-Delga, M., & Olivier, P. (1986). Betic-Rifian and Tyrrhenian Arcs: distinctive features, genesis and development stages. In: WEZEL, F.C. (Ed.), The Origin of Arcs, (pp.281-304) Elsevier.

Boyer, S.E., & Elliott, D. (1982). Thrust system. AAPG Bulletin, 66, 1196–1230.

Burbank, D.W., & Vergés, J. (1994). Reconstruction of topography and related depositional systems during active thrusting. Journal of Geophysical Research, 99(B10), 20281-20297.

Burov, E., & Yamato, P. (2008). Continental plate collision, P–T–t–z conditions and unstable vs. stable plate dynamics: insights from thermo-mechanical modelling. Lithos 103, 178–204.

Butler, R.W.H. (1987). Thrust sequences. J. Geol. Soc. Lond., 144, 619-634.

Butler, R. W., Maniscalco, R., & Pinter, P. R. (2019). Syn-kinematic sedimentary systems as constraints on the structural response of thrust belts: re-examining the structural style of the Maghrebian thrust belt of Eastern Sicily. Italian Journal of Geosciences, 138(3), 371-389.

Cardozo, N., & Allmendinger, R. W. (2013). Spherical projections with OSXStereonet. Computers & Geosciences, v. 51, no. 0, p. 193 - 205, doi: 10.1016/j.cageo.2012.07.021

Carminati, E., & Doglioni, C. (2012). Alps vs. Apennines: The paradigm of a tectonically asymmetric Earth. Earth Science Rev., 112, 67- 96. doi:10.1016/ j.earscirev.2012.02.004.

Caruso, A., Cosentino, C., Pierre, C., & Sulli, A. (2011). Sea-level changes during the last 41,000 years in the outer shelf of the southern Tyrrhenian Sea: Evidence from benthic foraminifera and seismostratigraphic analysis. Quaternary International, 232 (1-2), 122-131

Casero, P., & Roure, F. (1994). Neogene deformations at the Sicilian-North African plate boundary. In: Roure, F. (Ed.), Peri-Tethian Platforms (pp. 27-50). Institut Francaise du Petrole Research Conference, Arles, Proceedings. Editions Technip, Paris.

Cassinis, R., Finetti, I., Giese, P., Morelli, C., Steinmetz, L., & Vecchia, O. (1969). Deep seismic refraction research on Sicily. Boll. Geof. Teor. Appl., 11, 140-160.

Catalano, R., & D'Argenio, B. (1978). An essay of palinspastic restoration across Western Sicily. Geol. Rom., 17, 145-159.

Catalano, R., & Milia, A. (1990). Late Pliocene – Lower Pleistocene structural inversion in offshore western Sicily. In: B. Pinet & C. Bois (Eds.), Potential of deep seismic profiling for hydrocarbon exploration (pp. 445-449). Edition Technip, Paris.

Catalano, R. & Sulli, A. (2006). Crustal image of the Ionian basin and accretionary wedge. BGTA, 47(3), 343-374.

Catalano, R., Avellone, G., Basilone, L., Contino, A. & Agate, M. (2011). Carta geologica d'Italia alla scala 1: 50.000 e Note Illustrative del foglio 609-596 "Termini Imerese – Capo Plaia", ISPRA, Servizio Geologico d'Italia, SystemCart, Roma, 1-224.

Catalano, R., Infuso S., & Sulli, A. (1993). The Pelagian foreland and its northward foredeep. Plio-Pleistocene structural evolution. In: M.D. Max & P. Colantoni (Eds.), Geological development of the Sicilian-Tunisian Platform (Vol. 58, pp. 37-42). Unesco Report in Marine Science. Proceedings of international Scientific Meeting held at the University of Urbino, Italy, 4-6 November, 1992.

Catalano, R., Merlini, S., & Sulli, A. (2002). The structure of Western Sicily, Central Mediterranean. Petroleum Geoscience, 8, 7-18.

Catalano, R., Valenti, V., Albanese, C., Accaino, F., Sulli, A., Tinivella, U., et al. (2013). Sicily's fold/thrust belt and slab rollback: The SI.RI.PRO. seismic crustal transect. Journal of the Geological Society, London, 170, 451-464.

Cavazza, W., Roure, F., & Ziegler, P. (2004). The Mediterranean Area and the surrounding regions: active processes, remnants of former Tethyan oceans and related thrust belts. In: W. Cavazza, F. Roure, W. Spakman, G.M. Stampfli, P. Ziegler (Eds.), The Transmed Atlas (pp. 1–29). Springer, Heidelberg, Berlin, Germany.

Cifelli, F., Mattei, M., & Rossetti, F. (2007). Tectonic evolution of arcuate mountain belts on top of a retreating subduction slab: The example of the Calabrian Arc. Journal of Geophysical Research: Solid Earth, 112(B9).

Channell, J. E. T., Oldow, J. S., Catalano, R., & D'Argenio, B. (1990). Paleomagnetically determined rotations in the western Sicilian fold and thrust belt. Tectonics, 9(4), 641-660.

Chiarabba, C., Jovane, L., & Di Stefano, R. (2005). A new view of Italian seismicity using 20 years of instrumental recordings. Tectonophysics, 395, 251-268.

Chiarabba, C., De Gori, P., & Speranza, F. (2008). The southern Tyrrhenian subduction zone: deep geometry, magmatism and Plio-Pleistocene evolution. Earth Planet. Sci. Lett., 268, 408–423, doi:10.1016/2008.01.036.

Compagnoni, R., Morlotti, E., & Torelli, L. (1989). Crystalline and sedimentary rocks from the scarps of the Sicily–Sardinia trough and Cornaglia Terrace (Southwestern Tyrrhenian Sea): paleogeographic and geodynamic implications. Chem. Geol. 77, 375–398.

Couzens-Schultz, B.A., Vendeville, B.C., & Wiltschko, D.V. (2003). Duplex style and triangle zone formation: insights from physical model. Journal of Structural Geology, 25, 1623-1644.

Cuffaro, M., Riguzzi, F., Scrocca, D., & Doglioni, C. (2011). Coexisting tectonic settings: the example of the southern Tyrrhenian Sea. Int. J. Earth Sci. (Geol Rundsch), 100, pp 1915-1924, doi:10.1007/s00531-010-0625.

D'Agostino, N., & Selvaggi, G. (2004). Crustal motion along the Eurasia-Nubia plate boundary in the Calabrian Arc and Sicily and active extension in the Messina Straits from GPS measurements. Journal of Geophysical Research, 109, B11402, doi:10.1029/2004JB002998.

Devoti, R., Riguzzi, F., Cuffaro, M., & Doglioni, C. (2008). New GPS constraints on the kinematics of the Apennines subduction. Earth and Planetary Science Letters, 273, 163–174.

Devoti, R., Esposito, A., Pietrantonio, G., Pisani, A.R., & Riguzzi, F. (2011). Evidence of large scale deformation patterns from GPS data in the Italian subduction boundary. Earth and Planetary Science Letters, 311, 230-241, doi:10.1016/j.epsl.2011.09.034.

Dewey, J. F., Helman, M. L., Turco, E., Hutton, D. H. W., & Knott, S. D. (1989). Kinematics of the western Mediterranean. In: M. P. Coward, D. Dietrich & R. G. Park (eds.), Alpine Tectonics (vol. 45, pp. 265–283). Geol. Soc. (Lond.) Spec. Publ.

Dhalstrom, C.D.A. (1970). Structural geology in the eastern margin of the Canadian Rocky Mountains. Bull. Can. Petrol. Geol., 18(3), 332–406.

Di Maggio, C., Agate, M., Contino, A., Basilone, L., & Catalano, R. (2009). Unconformity-bounded stratigraphic units of quaternary deposits mapped for the CARG project in northern and western Sicily. Alpine and Mediterranean Quaternary, 22, 345–364.

Di Stefano, A.., & Lentini., R. (1995). Ricostruzione stratigrafica e significato paleotettonico dei depositi Plio-Pleistocenici del margine tirrenico tra Villafranca Tirrena e Faro (Sicilia Nord-Orientale). Studi Geol. Camerti, vol. spec. 1995/2, 219-237.

Doglioni, C. (1991). A proposal for the kinematic modelling of W-dipping subductions. Possible applications to the Tyrrhenian Apennines system. Terra Nova, 3, 423–434.

Doglioni, C. (1992). Main differences between thrust belts. Terra Nova, 4, 152-164.

Doglioni, C., Gueguen, E., Harabaglia, P., & Mongelli, F., (1999). On the origin of west-directed subduction zones and applications to the western Mediterranean. In: B. Durand, L. Jolivet, F. Horváth, M. Séranne (eds.), The Mediterranean Basins: Tertiary Extension within the Alpine Orogen (vol. 156, pp. 541–561). Geological Society, London, Special Publications.

Doglioni, C., Harabaglia, P., Merlini, S., Mongelli, F., Peccerillo, A., & Piromallo, C. (1999). Orogens and slab vs. their direction of subduction. Earth-Science Reviews, 45, 167–208.

Doglioni, C., Ligi, M., Scrocca, D., Bigi, S., Bortoluzzi, G., Carminati, E., et al. (2012). The tectonic puzzle of the Messina area (Southern Italy): Insights from new seismic reflection data. Scientific Reports, Nature, 2, 970; DOI:10.1038/srep00970

Ducea, M. N., 2016. Understanding continental subduction: A work in progress. Geology, 44(3), 239–240.

Fabbri, A., Gallignani, P., Zitellini, N. (1981). Geological evolution of the Peri-Tyrrhenian sedimentary ba sins of Mediterranean margins. In: F. C. Wezel (Eds.), Sedimentary basins of Mediterranean margins. Tecnoprint, Bologna, Italy, 101-126.

Faccenda, M., Gerya, T.V., & Chakraborty, S. (2008). Styles of post-subduction collisional orogeny: Influence of convergence velocity, crustal rheology and radiogenic heat production. Lithos, 103(1-2), 257-287, doi: 10.1016/j.lithos.2007.09.009.

Faccenna, C., Becker, T.W., Auer, L., Billi, A., Boschi, L., Brun, J. P., et al. (2014). Mantle dynamics in the Mediterranean. Reviews of Geophysics, 52(3), 283-332.

Faccenna, C., Funiciello, F., Giardini D., & Lucente F. P. (2001). Episodic back-arc extension during restricted mantle convection in the central Mediterranean. Earth Planet. Sci. Lett., 187, 105-116; doi: 10.1016/S0012-821X(01)00280-1.

Faccenna, C., Piromallo, C., Crespo-Blanc, A., Jolivet, L., & Rosetti, F. (2004). Lateral slab deformation and the origin of the western Mediterranean arcs. Tectonics, 23, TC1012, http://dx.doi.org/10.1029/2002TC001488.

Ferranti, L., Antonioli, F., Mauz, B., Amorosi, A., Dai Pra, G., Mastronuzzi, G., et al., 2006. Markers of the last interglacial sea-level high stand along the coast of Italy: Tectonic implications. Quaternary International 145-146, 30-54, doi: 10.1016/j.quaint.2005.07.009.

Ferranti, L., & Oldow, J.S. (2005). Latest Miocene to Quaternary horizontal and vertical displacement rates during simultaneous contraction and extension in the Southern Apennines orogen, Italy. Terra Nova, 17, 209-214.

Ferri, F., Zanolla, C., Porfidia, B., Coren, F., Giori, L., & Cesi, C. (2008) La cartografia gravimetrica digitale d'Italia alla scala 1:25000. GNGTS abs. 437-438, Trieste, 6-9 October, Italy.

Finetti, I.R., Lentini, F., Carbone, S., Del Ben, A., Di Stefano, A., Forlin, E., Guarnieri, P., Pipan, M. & Prizzon, A. (2005). – Geological out line of Sicily and litospheric tectono-dynamics of its Tyrrenian margin from new CROP seismic data. In: I.R. Finetti, (Edr.), CROP PROJECT: Deep

seismic exploration of the Central Mediterranean and Central Italy. – Atlas in Geosciences 1, Elsevier B.V., Amsterdam, 319-376.

Gasparo Morticelli, M., Avellone, G., Sulli, A., Agate, M., Basilone, L., Catalano, R., & Pierini, S. (2017). Mountain building in NW Sicily from the superimposition of subsequent thrusting and folding events during Neogene: structural setting and tectonic evolution of the Kumeta and Pizzuta ridges. Journal of Maps, 13(2), 276-290. http://dx.doi.org/10.1080/17445647.2017.1300546

Gasparo Morticelli, M., Valenti, V., Catalano, R., Sulli, A., Agate, M., Avellone, G., et al. (2015). Deep controls on Foreland Basin System evolution along the Sicilian Fold and Thrust Belt. Bull. Soc. Géol. France, 186(4-5), 273-290.

Ghisetti, F., & Vezzani, L. (1984). Thin-skinned deformations of the western Sicily thrust belt and relationships with crustal shortening: Mesostructural data on the Mt. Kumeta–Alcantara fault zone and related structures. Boll. Soc. Geol. It. 103, 129–157.

Giunta, G., Luzio, D., Tondi, E., De Luca, L., Giorgianni, A., D'Anna, et al. (2004). The Palermo (Sicily) seismic cluster of September 2002, in the seismotectonic framework of the Tyrrhenian Sea-Sicily border area. Annals of Geophysics, 47(6), 1755-1770.

Giunta, G., Nigro, F., Renda, P., & Giorgianni, A. (2000). The Sicilian-Maghrebides Tyrrhenian margin: A neotectonic evolutionary model. Boll. Soc. Geol. It., 119, 553-565.

Goes, S., Giardini, D., Jenny, S., Hollenstein, C., Kahle, H.-G., & Geiger, A. (2004). A recent tectonic reorganization in the south-central Mediterranean. Earth Planet. Sc. Lett., 226, 335-345.

Gueguen, E., Doglioni, C., & Fernandez, M. (1998). On the post 25 Ma geodynamic evolution of the western Mediterranean. Tectonophysics, 298, 259–269.

Gugliotta, C., Agate, M., & Sulli, A. (2013). Sedimentology and sequence stratigraphy of wedge top clastic succession: insights and open questions from the upper Tortonian Terravecchia Formation of the Scillato Basins (central northern Sicily, Italy). Marine and Petroleum Geology, 43, 239-259.

Gugliotta, C., & Gasparo Morticelli, M. (2012). Using high-resolution stratigraphy and structural analysis to constrain polyphase tectonics in wedge-top basins: Inferences from the late Tortonian Scillato Basin (central-northern Sicily). Sedimentary Geology, 273-274, 30-47.

Gugliotta, C., Gasparo Morticelli, M., Avellone, G., Agate, M, Barchi, M.R., Albanese, C., et al. (2014). Middle Miocene – Early Pliocene wedge-top basins of North-Western Sicily (Italy). Constraints for the tectonic evolution of a "non-conventional" thrust belt, affected by transpression. Journal of the Geological Society, London, 171, 211-226.

Gutscher, M. A., Kukowski, N., Malavieille, J. & Lallemand, S. (1998). Episodic imbricate thrusting and underthrusting: Analog experiments and mechanical analysis applied to the Alaskan accretionary wedge. J. Geophys. Res., 103, 10161–10176.

Hamai, L., Petit, C., Abtout, A., Yelles-Chaouche, A., & Déverchère, J. (2015). Flexural behaviour of the north Algerian margin and tectonic implications. Geophys. J. Int., 201, 1426-1436.

Hamai, L., Petit, C., Le Porhiet, L., Yelles-Chaouche, A., Déverchère, J., Beslier, M.O., & Abtout, A. (2018). Towards subduction inception along the inverted North African margin of Algeria? Insights from thermo-mechanical models. Earth and Planetary Science Letters, 501, 13-23.

Hollenstein, Ch., Kahle, H.-G., Geiger, A., Jenny, S., Goes, S., & Giardini, D. (2003). New GPS constraints on the Africa-Eurasia plate boundary zone in southern Italy. Geophysical Research Letters, 30(18), 4 pp., doi:10.1029/2003GL017554.

Johnson, M.R.W., & Harley, S.L. (2012). Orogenesis. The making of Mountains. Cambridge University Press, 388pp. https://doi.org/10.1017/CBO9781139023924.

Kastens, K., Mascle, J., Auroux, C., Bonatti, E., Broglia, C., Channell, J., et al. (1988). ODP Leg 107 in the Tyrrhenian Sea : Insights into passive margin and back-arc evolution. GSA Bulletin, 100(7), 1140-1156.

Kherroubi, A., Déverchère, J., Yelles, K., Mercier de Lépinay, B., Domzig, A., Cattaneo, A., et al. (2009). Recent and active deformation pattern off the easternmost Algerian margin, Western Mediterranean Sea: New evidence for contractional tectonic reactivation. Marine Geology, Special Issue on EUROMARGINS 261, 17–32.

Kostantinovskaya, E., & Malavieille, J. (2011). Thrust wedges with décollement levels and syntectonic erosion: a view from analog models. Tectonophysics, 502(3), 336-350.

Lanzafame, G., & Bousquet, J.C. (1997). The Maltese escarpment and its extension from Mt. Etna to Aeolian Islands (Sicily): importance and evolution of a lithosphere discontinuity. Acta Vulcanologica, 9, 113-120.

Lentini, F., Carbone, S., & Catalano, S. (1994). Main structural domains of the central Mediterranean region and their Neogene tectonic evolution. Boll. Geofis. Teor. Ed. Appl., 36, 141–144.

Lentini, F., Carbone, S., Catalano, S., & Grasso, M. (1996). Elementi per la ricostruzione del quadro strutturale della Sicilia orientale. Mem. Soc. Geol. It., 51, 145-156.

Lickorish, W.H., Grasso, M., Butler, R., Argnani, A., & Maniscalco, R. (1999). Structural styles and regional tectonic setting of the 'Gela Nappe' and frontal part of the Maghrebian thrust belt in Sicily. Tectonics, 18, 655–668.

Lofi, J., Sage, F., Déverchère, J., Loncke, L., Maillard, A., Gaullier, V., et al. (2011). Refining our knowledge of the Messinian salinity crisis records in the offshore domain through multi-site seismic analysis. Bull. Soc. Géol. Fr., 182(2), 163-180.

Masini, F., Petruso, D., Bonfiglio, L., & Mangano, G. (2008). Origination and extinction patterns of mammals in three central western Mediterranean islands from the late miocene to quaternary. Quaternary International, 182, 63–79.

Mauffret, A. (2007). The Northwestern (Maghreb) boundary of the Nubia (Africa) plate. Tectonophysics, 429(1-2), 21–44.

Mauffret, A., Frizon de Lamotte, D., Lallemant, S., Gorini, C., Maillard, A. (2004). E–W opening of the Algerian Basin (Western Mediterranean). Terra Nova, 16 (5), 257–264, doi:10.1111/j.1365-3121.2004 00559.x.

Mauz, B., Buccheri, G., Zöller, L., & Greco, A. (1997). Middle to upper pleistocene morphostructural evolution of the NW-coast of Sicily: Thermoluminescence dating and palaeontological-stratigraphical evaluations of littoral deposits. Palaeogeography, Palaeoclimatology, Palaeoecology, 128, 269–285.

Mazzoli, S., Corrado, S., De Donatis, M., Scrocca, D., Butler, R.W.H., Di Bucci, D., et al. (2000). Time and space variability of «thin-skinned » and «thick-skinned » thrust tectonics in the Apennines (Italy). Rend. Fis. Acc. Lincei, 9, 11, 5-39.

McClay, K.R. (1992). Thrust Tectonics. Springer-Science business media, B.V., pp. 447

Nigro, F., & Renda, P. (2001). From Mesozoic extension to Tertiary collision: deformation patterns in the northern Sicily Chain units. Boll. Soc. Geol It., 121, 87-97.

Oldow, J.S., Channell, J.E.T., Catalano, R., & D'Argenio, B. (1990). Contemporaneous thrusting and large-scale rotations in the western Sicilian fold and thrust belt. Tectonics, 9, 661–681.

Oldow, J.S., Ferranti, L., Lewis, D.S., Campbell, J.K., D'Argenio, B., Catalano, R., et al. (2002). Active fragmentation of Adria, the north African promontory, central Mediterranean orogen. Geology, 30(9), 779-782.

Palano, M., Ferranti, L., Monaco, C., Mattia, M., Aloisi, M., Bruno, V., et al. (2012). GPS velocity and strain fields in Sicily and southern Calabria, Italy: Updated geodetic constraints on tectonic block interaction in the central Mediterranean. JGR, 117, B07401, doi:10.1029/2012JB009254.

Patacca, E., Scandone, P., Giunta, G., & Liguori, V. (1979). Mesozoic paleotectonic evolution of the Ragusa zone (Southeastern Sicily), Geol. Rom., 18, 331-369.

Peacock, S. (1990). Fluid processes in subduction zones. Science 248, 329-337. Doi: 10.1126/science.248.4953.329.

Pennino, V., Sulli, A., Caracausi, A., Grassa, F., & Interbartolo, F. (2014). Fluid escape structures in the north Sicily continental margin. In: O. Lacombe, R. Swennen, & A. Caracausi, (Eds.), Fluid-rock-tectonics interaction in basins and orogens, Marine and Petroleum Geology 55, 202-213.

Pepe, F., Bertotti, G., Cella, F., & Marsella, E. (2000). Rifted margin formation in the South Tyrrhenian Sea: a high-resolution seismic profile across the North Sicily passive continental margin. Tectonics 19, 241–257.

Pepe, F., Sulli, A., Agate, M., Di Maio, D., Kok, A., Lo Iacono, C., & Catalano, R. (2003). Plio-Pleistocene geological evolution of the northern Sicily continental margin (southern Tyrrhenian Sea): new insights from high resolution, multi-electrode sparker profiles. Geo Mar. Lett., 23, 53-63.

Pepe, F., Sulli, A., Bertotti, G., & Catalano, R. (2005). Structural highs formation and their relationship to sedimentary basins in the north Sicily continental margin (southern Tyrrhenian Sea): implication for the Drepano Thrust Front. Tectonophysics, 409, 1–18.

Pescatore, T., Renda, P., & Tramutoli, M. (1987). Facies ed evoluzione sedimentaria del bacino Numidico nelle Madonie Occidentale (Sicilia). Mem. Soc. Geol. Ital., 38, 97-316.

Pinter, P.R., Butler, W.H., Hartley, A.J., Maniscalco, R., Baldassini, N., & Di Stefano, A. (2016). The Numidian of Sicily revisited: a thrust-influenced confined turbidite system. Marine and Petroleum Geology, 78, 291-311. http://dx.doi.org/10.1016/j.marpetgeo.2016.09.014

Poblet, J., & Lisle, R.J. (2011). Kinematic evolution and structural styles of fold and thrust belts. In: J., Poblet, R.J. Lisle (Eds), Kinematic evolution and structural styles of fold and thrust belts (vol. 349, pp. 1-24). Geol. Soc. (Lond.) Spec. Publ.

Polonia, A., Torelli, L., Gasperini, L., Cocchi, L., Muccini, F., Bonatti E., et al. (2017). Lower plate serpentinite diapirism in the Calabrian Arc subduction complex. Nature Communications, 8, 2172, doi: 10.1038/s41467-017-02273-x.

Pondrelli, S. (2002). European-Mediterranean Regional Centroid-Moment Tensors Catalog (RCMT) [Data set]. Istituto Nazionale di Geofisica e Vulcanologia (INGV). https://doi.org/10.13127/rcmt/euromed

Pondrelli, S., Morelli, A., & Ekstrom, G. (2004). European-Mediterranean regional centroid-moment tensor catalog: solutions for years 2001 and 2002. Phys. Earth Planet Inter., 145, 127-147.

Pondrelli, S., & Salimbeni, S. (2006). Italian CMT Dataset [Data set]. Istituto Nazionale di Geofisica e Vulcanologia (INGV). https://doi.org/10.13127/rcmt/italy

Pondrelli, S., Salimbeni, S., Ekström, G., Morelli, A., Gasperini P., & Vannucci, G. (2006). The Italian CMT dataset from 1977 to the present. Phys. Earth Planet Inter., 159, 286-303, doi: 10.1016/j.pepi.2006.07.008.

Roure, F., Howell, D.G., Muller, C., & Moretti, I. (1990). Late Cenozoic subduction complex of Sicily. Journal of Structural Geology, 12, 259–266.

Royden, L. (1996). Coupling and decoupling of crust and mantle in convergent orogens: Implications for strain partitioning in the crust. Journal of Geophysical Research, 101(B8), 17679-17705.

Ryan, W.B.F., Hsu, K.J., Cita, M.B., Dumitrica, P., Lort, J.M., Maync, W., et al., (1973). Initial reports of the Deep Sea Drilling Project. US Government Printing Office, Washington, DC, 13, 1-1447.

Salvini, F. (2001). Daisy 3, version 5.07-1. The structural data integrated analyzer [Free Software]. Dipartimento di Scienze Geologiche, Università degli Studi di 'Roma3′, Rome.

Sbaffi, L., Wezel, F.C., Kallel, N., Paterne, M., Cacho, I., Ziveri, P., & Shackleton, N. (2001). Response of the pelagic environmentto palaeoclimatic changes in the central Mediterranean Sea during the Late Quaternary. Marine Geology, 178,39-62.

Scarfi, L., Barberi, G., Barreca, G., Cannavò, F., Koulakov, I., & Patanè, D. (2018). Slab narrowing in the Central Mediterranean: the Calabro-Ionian subduction zone as imaged by high resolution seismic tomography. Scientific Reports, 8, 5178, doi:10.1038/s41598-018-23543-8.

Scrocca, D., Carminati, E., & Doglioni, C. (2005). Deep structure of the Southern Apennines (Italy): thin-skinned or thick-skinned? Tectonics, 24, TC3005, http://dx.doi.org/10.1029/2004TC001634.

Serpelloni, E., Vannucci, G., Pondrelli, S., Argnani, A., Casula, G., Anzidei, M., et al. (2007). Kinematics of the Western Africa–Eurasia plate boundary from focal mechanisms and GPS data. Geophys. J. Int., 169(3), 1180–1200. http://dx.doi.org/10.1111/j.1365-246X.2007.03367.x.

Sgroi, T., De Nardis, R., & Lavecchia, G. (2012). Crustal structure and seismotectonics of central Sicily (southern Italy): new constraints from instrumental seismicity. Geophys. J. Int., 189, 1237-1252, http://dx.doi.org/10.1111/j.1365-246X.2012.05392

Speranza, F., Maniscalco, R., & Grasso, M. (2003). Pattern of orogenic rotations in central–eastern Sicily: implications for the timing of spreading in the Tyrrhenian Sea. Journal of the Geological Society, London, 160,183–195

Speranza, F., Hernandez-Moreno, C., Avellone, G., Gasparo Morticelli, M., Agate, M., Sulli, A., & Di Stefano, E. (2018). Understanding Paleomagnetic Rotations in Sicily: Thrust Versus Strike-Slip Tectonics. Tectonics, 37(4), 1138-1158.

Storti, F., & McClay, K.R. (1995). Influence of syntectonic sedimentation on thrust wedges in analog models. Geology, 23, 999-1002.

Strzerzynski, P., Déverchère, J., Cattaneo, A., Domzig, A., Yelles, K., Mercier De Lepinay, B., et al. (2010). Tectonic inheritance and Pliocene-Pleistocene inversion of the Algerian margin around Algiers: Insights from multibeam and seismic reflection data. Tectonics, 29, TC2008, doi: 10.1029/2009TC002547.

Sulli, A. (2000). Structural framework and crustal characteristics of the Sardinia Channel Alpine transect in the central Mediterranean. Tectonophisics, 324(4), 321-336.

Sulli, A., Agate, M., Mancuso, M., Pepe, F., Pennino, V., Polizzi, S., et al. (2012). Variability of depositional setting along the north-western Sicily continental shelf (italy) during late Quaternary: effects of sea level changes and tectonic evolution. Alpine and Mediterranean Quaternary, 25(2), 141-155.

Sulli, A., Gasparo Morticelli, M., Agate, M., Basilone, L., & Gorini, C. (2016). Origin and evolution of the Messinian Basins developed on top of the Sicilian fold and thrust belt. In: A. Caruso, A. Camerlenghi, G. Aloisi & J.Lofi (Eds.) COST-ANR MEDSALT SYMPOSIUM., 24-28 October 2016, 29-30, Palermo, Italy.

Sulli, A., Gasparo Morticelli, M., Agate, A., & Zizzo, E. (2018). Hinterland-verging thrusting in the northern Sicily continental margin: a late collisional stage of the Sicilian Fold and Thrust Belt?. Geophysical Research Abstracts, 20, EGU2018-8842, EGU General Assembly, 8–13 April 2018.

Sulli, A., Lo Presti, V., Gasparo Morticelli, M., & Antonioli, F. (2013). Vertical movements in NE Sicily and its offshore. Outcome of tectonic uplift during the last 125 kyr. Quaternary International, vol. 288, 168-182, ISSN: 1040-6182, doi: 10.1016/j.quaint.2012.01.021

Tortorici, L., Monaco, C., Mazzoli, S., & Bianca, M. (2001). Timing and modes of deformation in the western Sicilian thrust system, southern Italy. Journal of Petroleum Geology, 24(2), 191-211.

Tricart, P., Torelli, L., Argnani, A., Rekhiss, F., & Zitellini, N. (1994). Extensional collapse related to compressional uplift in the apline chain off northern Tunisia (Central Mediterranean). Tectonophysics, 238(1-4), 317-329. doi.org/10.1016/0040-1951(94)90062-0.

Vannucci, G., & Gasperini, P. (2004). The new release of the database of Earthquake Mechanisms of the Mediterranean Area (EMMA version 2). Ann. Geophys., 47, 303-327.

Willingshofer, E., & Sokoutis, D. (2009). Decoupling along plate boundaries: Key variable controlling the mode of deformation and the geometry of collisional mountain belts. Geology, 37, 39–42, doi:10.1130/G25321A.1

Yelles, A., Domzig, A., Déverchère, J., Bracène, R., Mercier de Lépinay, B., Strzerzynski, P., et al. (2009). Plio-quaternary reactivation of the Neogene margin off NW Algiers, Algeria: The Khayr al Din Bank. Tectonophysics, 475(1), 98–116.

Figure captions

Figure 1. Structural map of Sicily (modified from Catalano et al., 2013). The inset maps show: a) schematic tectonic map of the central-western Mediterranean region; b) geological transect highlighting the subduction of the African continental lithosphere and the overlying Sicilian fold-and-thrust belt (collisional system; from Gasparo Morticelli et al., 2015); c) geological transect highlighting the subduction of the oceanic Ionian crust and the overlying Calabrian arc (subduction system; from Catalano & Sulli, 2006); d) schematic model (not to scale) showing the two compressional tectonic events of the Sicilian fold and thrust belt (from Gugliotta & Gasparo Morticelli, 2012).

Figure 2. Shaded-relief map of the central Mediterranean region showing: main north-verging thrust fronts recognized in Sicily and surrounding marine areas; earthquake focal mechanisms in the southern Tyrrhenian region (data from Pondrelli et al., 2006); GPS velocity vectors with respect to Eurasia according to different Authors; traces of the seismic reflection profiles illustrated in this paper. The inset map (bottom left) shows a schematic tectonic map of the study area.

Figure 3. a) Panoramic view of the northern slope of the Rosamarina Mt, where a middle-upper Pleistocene tectonic structure was recognized. A north-verging ramp anticline, developing on a south-dipping thrust (red lines), involved Mesozoic limestone (white lines) covered in turn by a middle-upper Pleistocene syntectonic sedimentary wedge of continental deposits with growth strata geometry (yellow lines); b) geometry of the syntectonic wedge covering both hangingwall and footwall of the thrust; c, d) detail of onlap geometry in the syntectonic wedge; e) geological map of the Rosamarina Mt. area displaying the sites of the mesostructural measurements and related stereoplots, and the site from where the panoramic picture shown in (a) has been shot.

Figure 4. Seismic reflection profiles crossing the northern submerged SFTB in the Cefalù basin area. a) and b) Single channel (1kJ Sparker source) seismic profiles across the continental shelf at the southern margin of the Cefalù Basin: north-vergent reverse fault affect the basal portion of the LQDS sediments (late Pleistocene-Holocene in age); in b) two small mud volcano are also imaged, problably related to reverse fault activity. c) Structural details of the Solunto Smt. (norther margin of Cefalù basin) are shown in the single channel (16 kJ) Sparker profile, where the involvement of the Plio-Quaternary deposits in north-vergin compressional tectonics is evidenced (traces of seismic profiles are shown in Figure 2).

Figure 5. Multichannel seismic profiles across the Sardinia Channel (a, b and c) and the north-western Sicily offshore (d) showing extensive south-dipping reverse faults. In the Sardinia Channel, a north-verging tectonic wedge overthrusts the M-reflector forming a Plio-Quaternary accretionary wedge. Eastward, along the southern slope of the Elimi Chain, the Sicilian Maghrebian units overthrust the Kabilian-Calabrian unit formerly southward emplaced during Miocene.

Figure 6. Distribution of epicenters recorded since 1970 (red, brown and blue points discrete to geographic position). The related hypocenter depths have been plotted along three regional cross sections (1, 2 and 3) where focal mechanism and main regional tectonic elements have been drawn. See text for more details.

Figure 7. a) Velocity field of the Sicilian region and southern Tyrrhenian area with respect to Eurasia from permanent and non-permanent GPS networks of selected sites according to different authors (b); (c) velocity profiles (traces in a) where the different compressive zone along the trace are indicate (red band).

Figure 8. Schematic structural maps where has been reported the main Quaternary northward-verging fore-thrust and focal mechanism recognized and discussed in this paper. Down, regional geological cross section showing both main tectonic features and geometry of the central Mediterranean orogeny characterized by double verging tectonic structures.

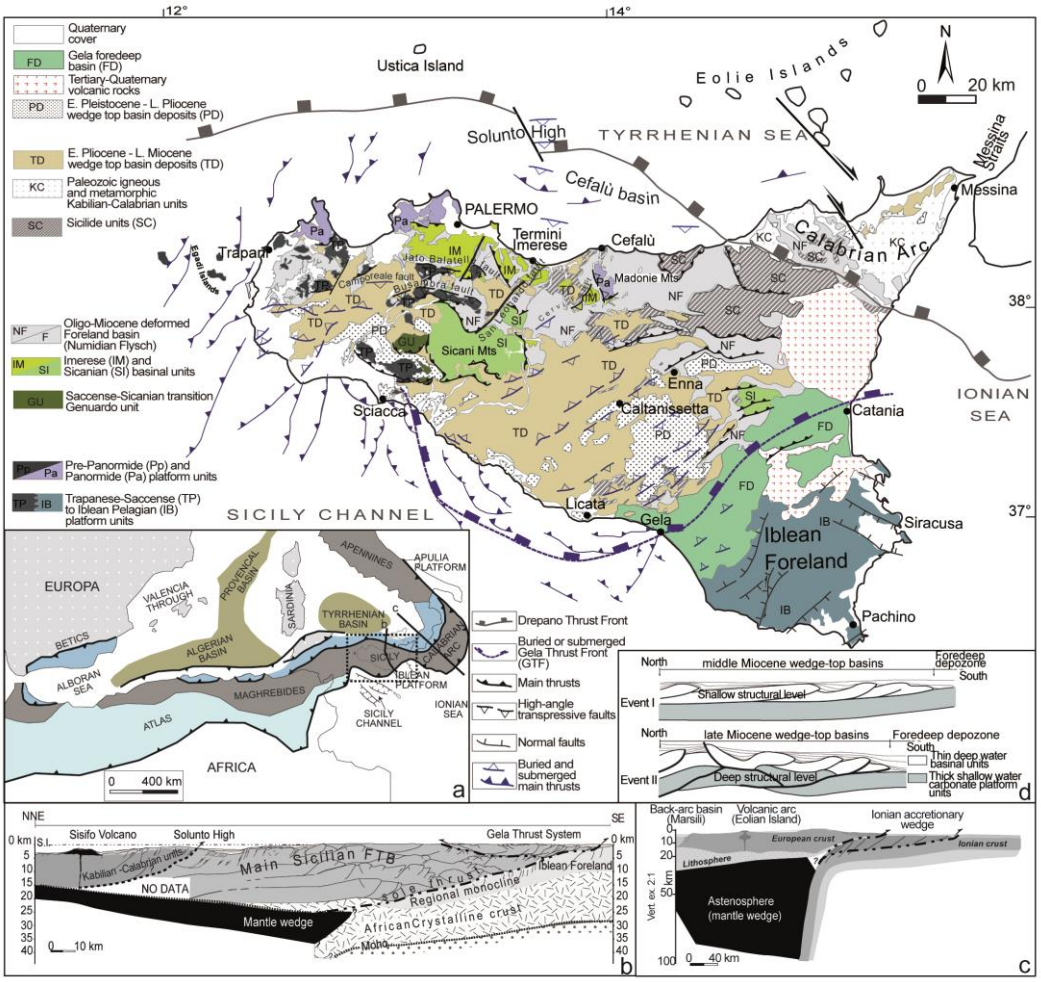

Figure 1. Sulli et al.,2019

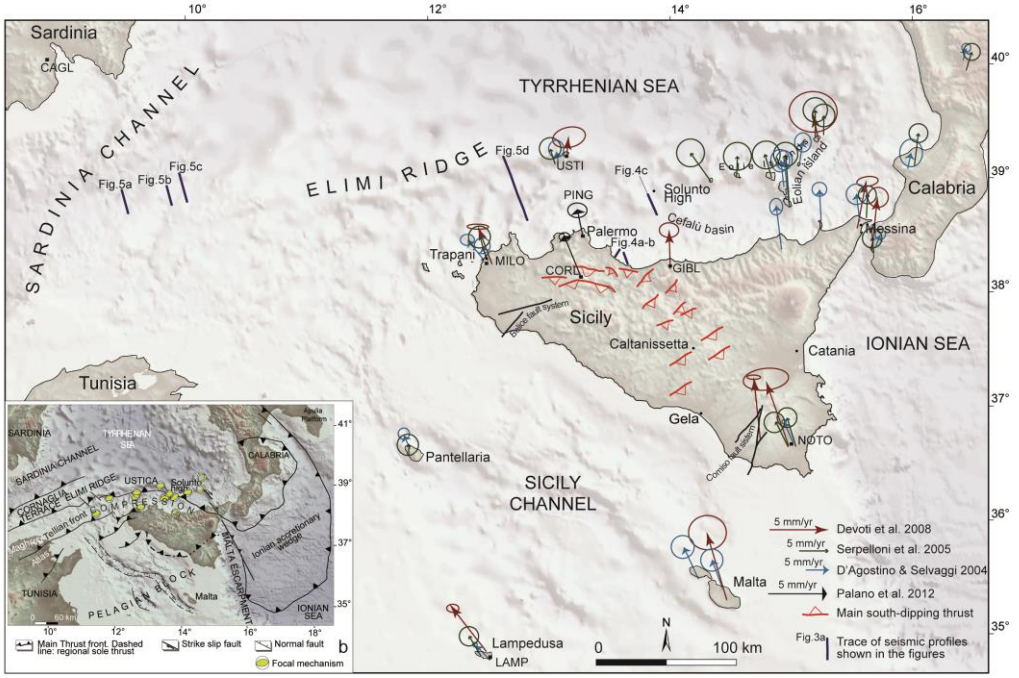

Figure 2. Sulli et al.,2019

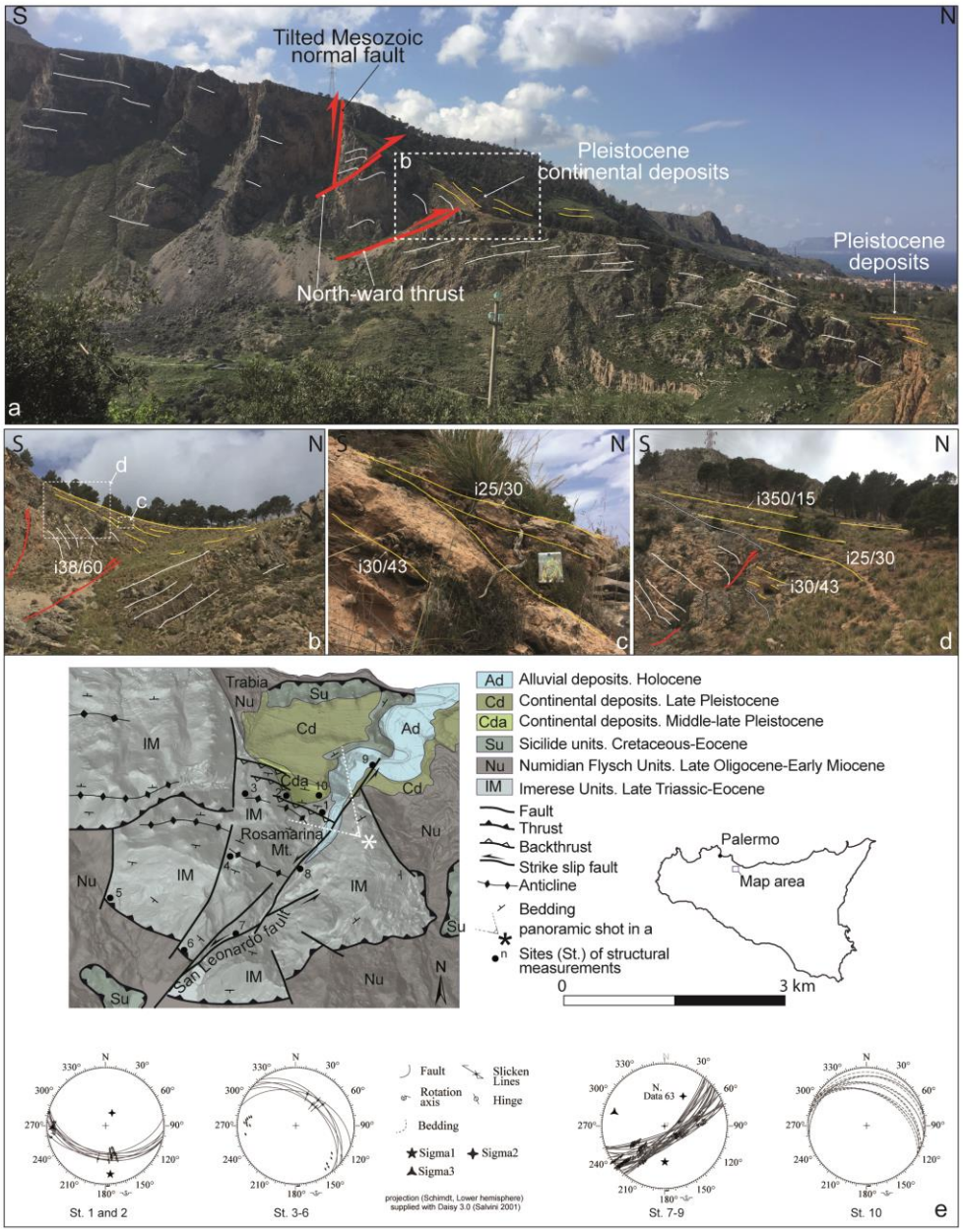

Figure 3. Sulli et al., 2019

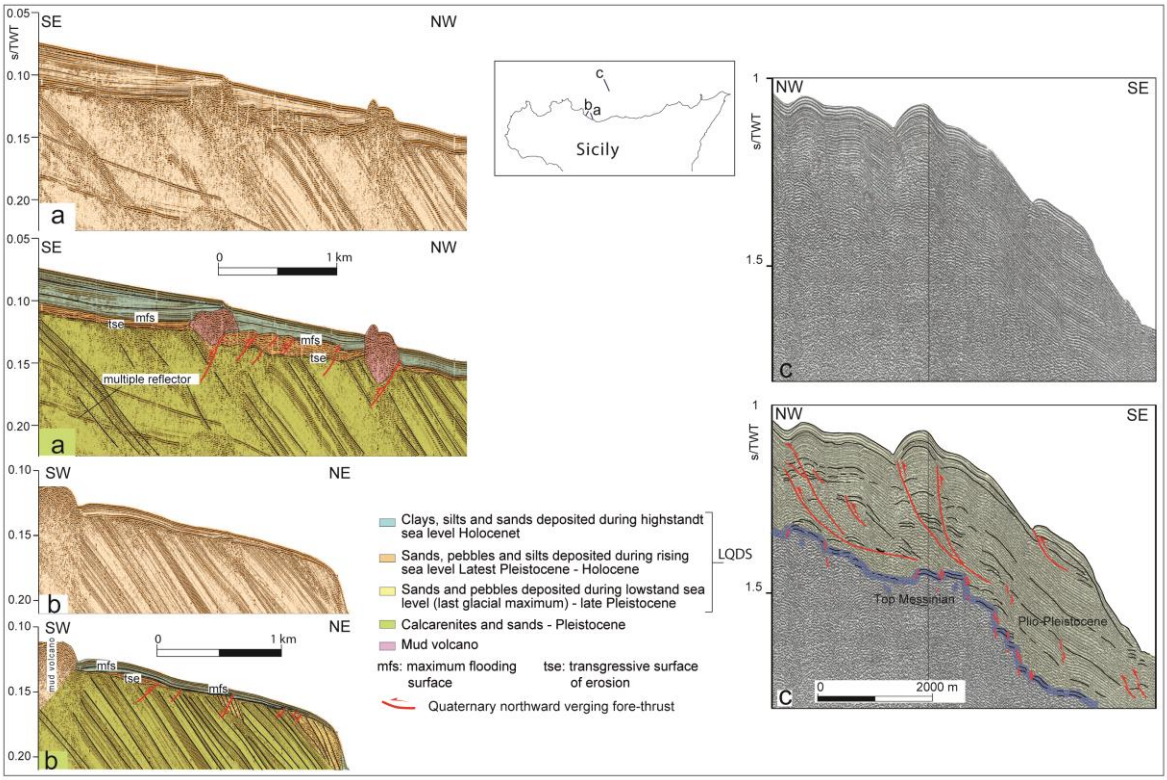

Figure 4. Sulli et al., 2019

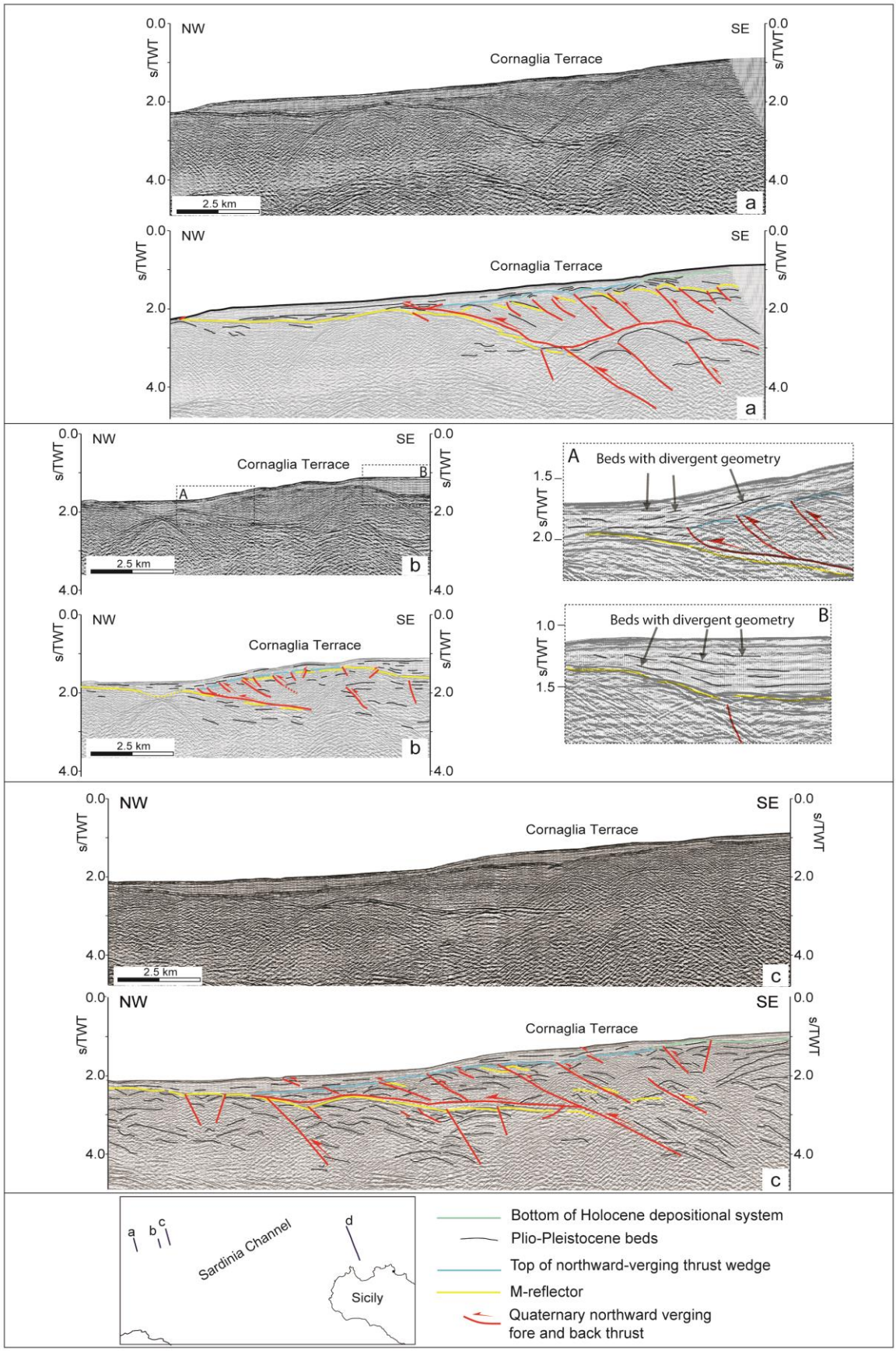

Figure 5a-c. Sulli et al., 2019

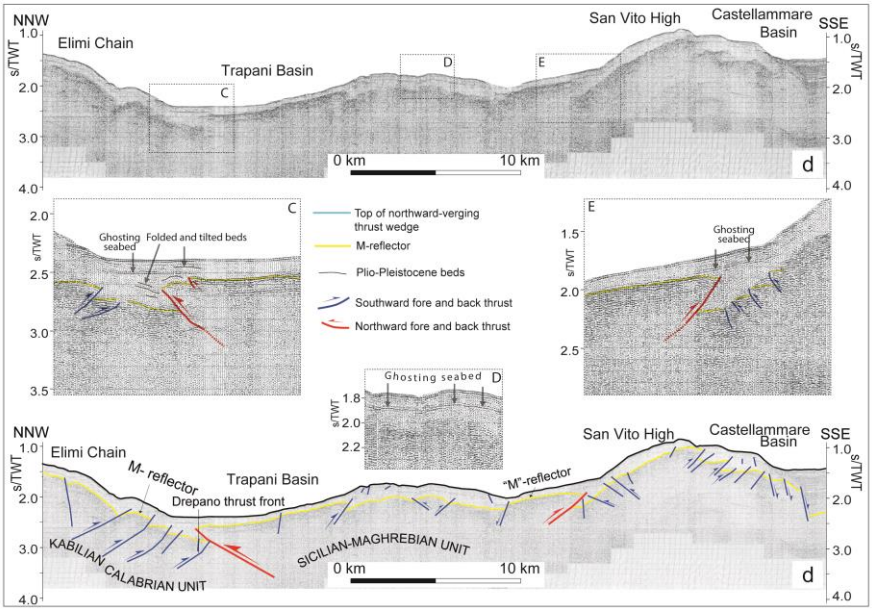

Figure 5d. Sulli et al., 2019

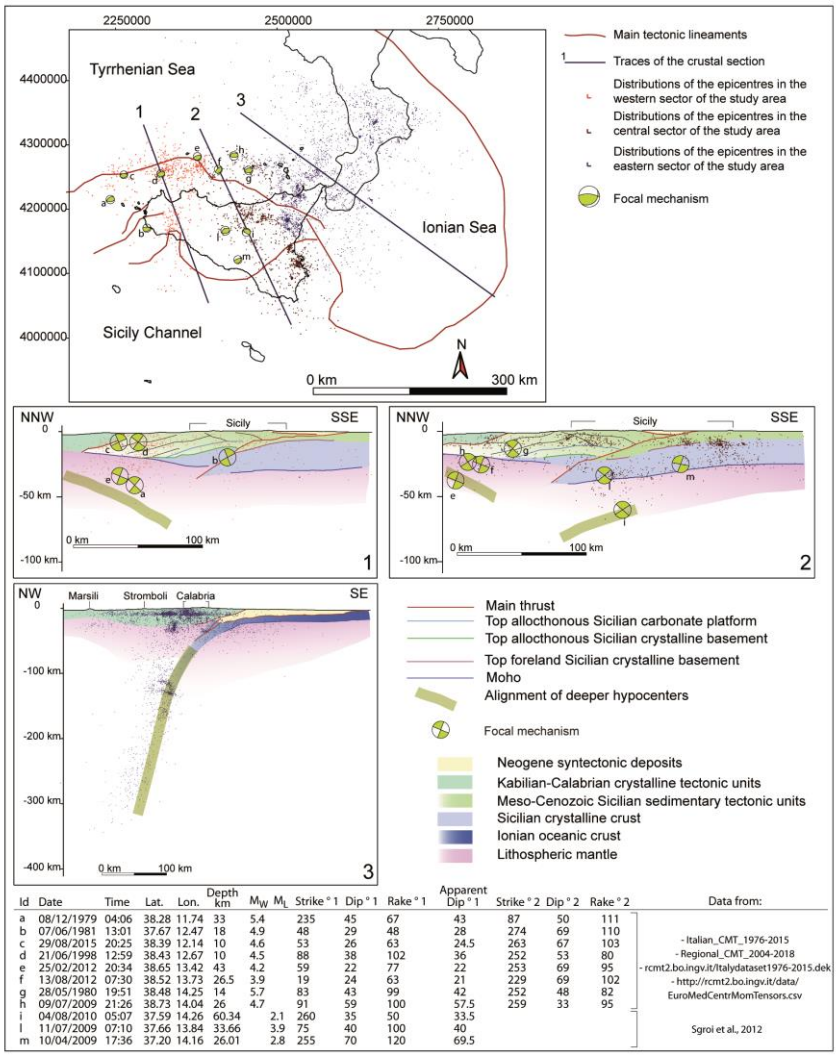

Id	Date	Time	Lat.	Lon.	Depth km	M_W	M_L	Strike ° 1	Dip ° 1	Rake ° 1	Apparent Dip ° 1	Strike ° 2	Dip ° 2	Rake ° 2	Data from:
a	08/12/1979	04:06	38.28	11.74	33	5.4		235	45	67	43	87	50	111	
b	07/06/1981	13:01	37.67	12.47	18	4.9		48	29	48	28	274	69	110	
c	29/08/2015	20:25	38.39	12.14	10	4.6		53	26	63	24.5	263	67	103	- Italian_CMT_1976-2015
d	21/06/1998	12:59	38.43	12.67	10	4.5		88	38	102	36	252	53	80	- Regional_CMT_2004-2018
e	25/02/2012	20:34	38.65	13.42	43	4.2		59	22	77	22	253	69	95	- rcmt2.bo.ingv.it/Italydataset1976-2015.dek
f	13/08/2012	07:30	38.52	13.73	26.5	3.9		19	24	63	21	229	69	102	- http://rcmt2.bo.ingv.it/data/
g	28/05/1980	19:51	38.48	14.25	14	5.7		83	43	99	42	252	48	82	EuroMedCentrMomTensors.csv
h	09/07/2009	21:26	38.73	14.04	26	4.7		91	59	100	57.5	259	33	95	
i	04/08/2010	05:07	37.59	14.26	60.34		2.1	260	35	50	33.5				
l	11/07/2009	07:10	37.66	13.84	33.66		3.9	75	40	100	40				Sgroi et al., 2012
m	10/04/2009	17:36	37.20	14.16	26.01		2.8	255	70	120	69.5				

Figure 6. Sulli et al., 2019

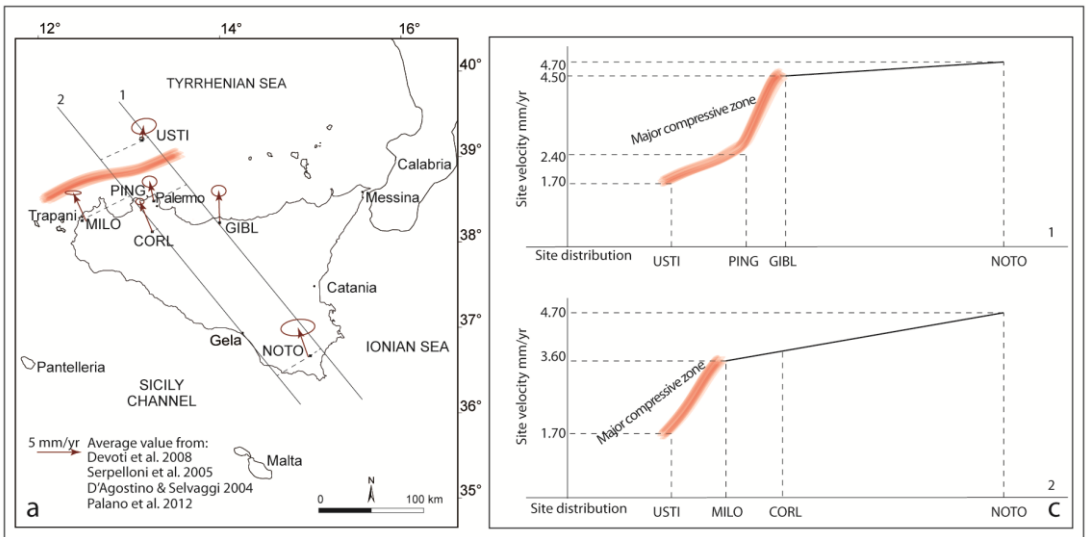

b

	SITE VELOCITY, NORTH AND EAST COMPONENT mm/yr															
	Hollenstein et al. 2003			D'Agostino & Selvaggi 2004			Serpelloni et al. 2005			Devoti et al. 2008			Palano et al. 2012			Averege value
	North mm/yr	East mm/yr	Calcolated value along the movement direction	North mm/yr	East mm/yr	Calcolated value along the movement direction	North mm/yr	East mm/yr	Calcolated value along the movement direction	North mm/yr	East mm/yr	Calcolated value along the movement direction	North mm/yr	East mm/yr	Calcolated value along the movement direction	
USTI	1,5	-0,9	1,6	/	/	/	2,47	-0,91	2,4	1,39	0,14	1,30	1,54	0,10	1,50	1,70
MILO	3,5	-3,9	5,2	3,37	-1,3	3,6	3,52	-0,98	3,6	2,85	-1,09	3,05	2,55	-0,26	2,53	3,60
GIBL	/	/	/	/	/	/	/	/	/	2,98	-0,17	3,0	6,06	-0,41	6,07	4,50
NOTO	3,6	-2,4	4,3	4,49	-1,97	4,9	4,76	-1,71	5,0	4,88	-1,76	5,2	3,94	-1,44	4,19	4,70
PING	/	/	/	/	/	/	/	/	/	/	/	/	2,40	-0,52	2,45	2,40
CORL	/	/	/	/	/	/	/	/	/	/	/	/	3,52	-1,48	3,81	3,80

Figure 7. Sulli et al., 2019

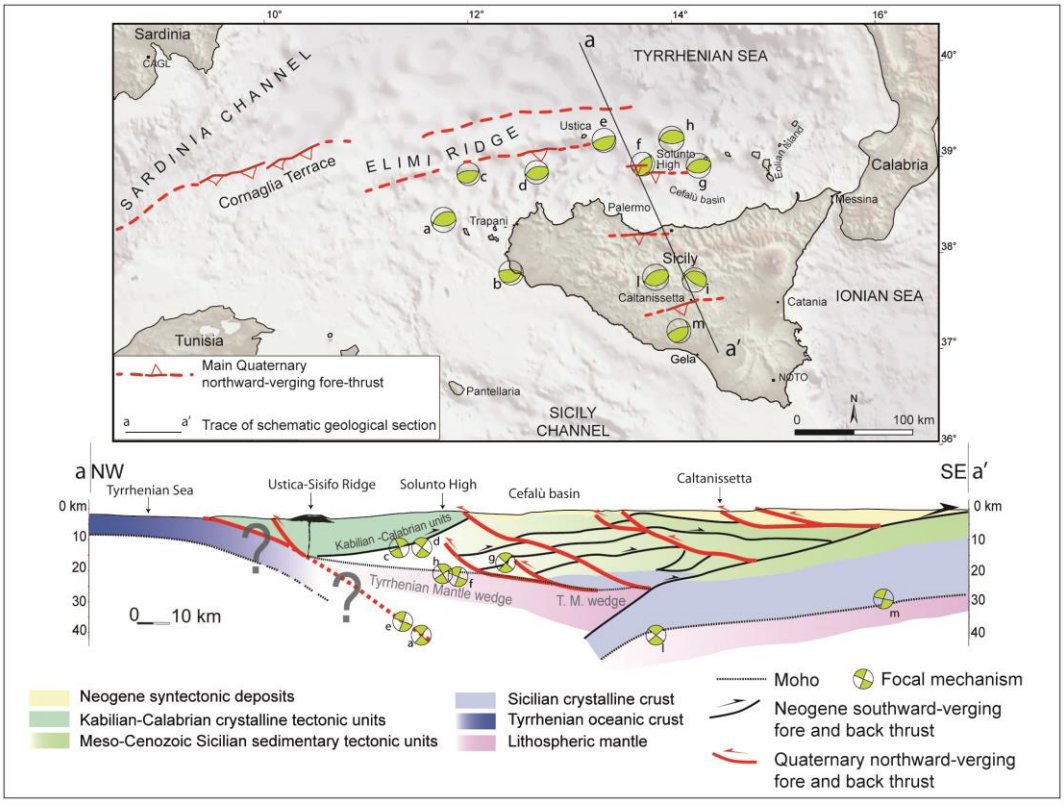

Figure 8. Sulli et al., 2019

CHAPTER 2

Explanatory notes of the 585 “Mondello” map sheet 1:50.000

NOTE This chapter is part of Explanatory notes of the 585 “Mondello” map sheet 1:50.000, to be published by ISPRA in the frame of the Italian official geological mapping project (CARG). The authors are the followings: Raimondo Catalano, Attilio Sulli, Elisabetta Zizzo, Mauro Agate, Maurizio Gasparo Morticelli.

1. Introduction

The Sheet 585 "Mondello" of the Geological Map of Italy on 1: 50,000 scale was carried out in the frame of the CARG Project, based on a scientific agreement between the Department of Earth and Marine Sciences of the University of Palermo and ISPRA. The Sheet covers the marine domain of the eastern sector of the Gulf of Castellammare and large part of the morphotectonic high offshore the Palermo Mountains (Fig. 1). The Mondello sheet includes a small land area in the south-eastern sector (Monte Gallo area) and a wide marine area that is mainly the continuation of the carbonate reliefs outcropping in the eastern sector of the Palermo mountains. It is a large structural high that extends from the Sicilian continental shelf progressively degrading to the Ustica basin.

The marine sector of the "Mondello" sheet extends for 645 km^2, corresponding to the 98% of the total extension of the Sheet and includes two physiographic units, the continental slope in front of the sector between the eastern Gulf of Catellammare and the western Gulf of Palermo and the continental shelf, between the Carini bay and the Bay of Mondello, continuing ENE-wards with La Barra high.

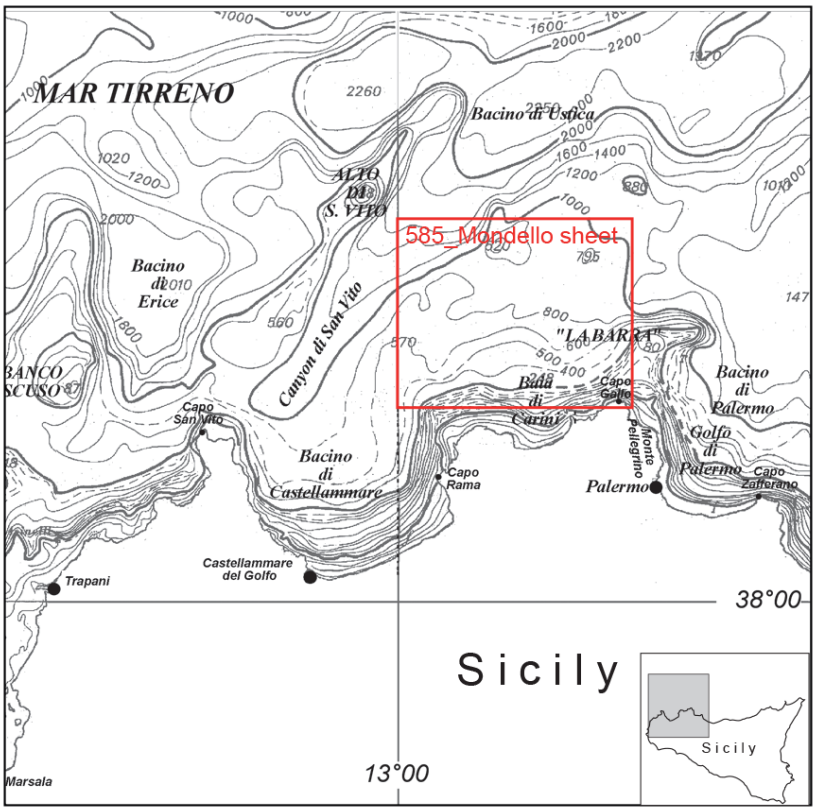

Fig. 1 Bathymetric map of north-western Sicily offshore with the area of the Sheet 585.

The geological and geophysical surveys of the marine area of the Sheet were performed over several years by researchers from the Marine Geology Group of the Department of Earth and Marine Sciences of the University of Palermo. Data acquired in other research projects, in particular the MAGIC project (Marine Geohazards in the Italian Coasts) have also been used.

We used as cartographic basis a bathymetric map obtained from the inversion of digital data provided by the Hydrographic Institute of the Navy (I.I.M) and by morphobathymetric surveys with multibeam echo sounder, unpublished, collected during oceanographic campaigns, and subsequently validated by the I.I.M.

2. Geological Setting

Marine geology studies on this region concern the tectonic structure of the north-western Sicilian continental margin (Selli, 1974; Catalano et al., 1985; Agate et al., 1993; Pepe et al., 2003; Sulli et al., 2012), the geomorphology of the continental shelf (Lucido, 1992; Ferretti et alii, 1996), the stratigraphy of Plio-Quaternary deposits (Agate & Lucido, 1995; Agate et alii, 2004), the sedimentary dynamics, the Late Quaternary sequence stratigraphy (Agate et alii, 2005), and the marine hazards (Sulli et al., 2013, 2018). The Sheet covers an area of the northern Sicily continental margin, that develops in the southern Tyrrhenian Sea, between the north Sicily coastal belt to the Marsili Abyssal Plain, (Fig. 2) in the transitional area between the Sicilian-Maghrebian chain to the south and the Tyrrhenian Basin to the north (Malinverno and Ryan, 1986; Catalano et al., 1996; Pepe et al., 2005; Billi et al., 2006).

The continental margin is composed of: (1) a narrow (<8 km) and steep (up to 2.5°) continental shelf, with the edge between -95 m and -140 m. Around 40 m water depth the internal sector, with higher hydrodynamics and mainly terrigenous and locally biogenic sedimentation, is separated by the external sector of the shelf, mainly characterized by hemipelagic sedimentation; (2) a very steep (7-8°) upper continental slope ranging in depth from 150 to 1500 m; (3) flat intra-slope basin plains at depths of about 1500-2500 m; (4) a wide and gentler lower continental slope, and (5) a bathyal plain from a depth of 3000 m.

The large continental slope appears tectonically unstable and incised by numerous canyons. The wave regime is characterized by NW, NE and E directions (Astraldi et al, 2002). The storm waves reach usually 3-4 m in height, have a period of 6 s and an annual frequency of 3% (Istituto Idrografico della Marina, 1982). The tidal excursion indicate a microtidal regime with a tide height varying between 0.37 and 0.60 m a.s.l. The water salinity has no considerable variation between summer and winter, remaining between 37.6‰ and 38.2‰ (Demirov & Pinardi, 2002).

The Northern Sicily continental margin originated as a consequence of a complex interaction of compressional events, crustal thinning and strike-slip faulting. Following the early-middle Miocene deformation and thrusting of the Kabilian-Calabrian units and the most internal units of the Sicilian-Maghrebian chain (Catalano et al., 1985; Sulli, 2000; Pepe et al., 2005), related to the collision between Corsica-Sardinia and the Sicilian passive continental margin, the opening of the Tyrrhenian Sea led to the subsidence of the northern Sicilian margin since the Late Tortonian (Baghi et al., 1980; Fabbri et al., 1981).

The Elimi chain extends along a west-east ridge from the Drepano Smt to the Anchise-Ustica volcanic complex and the Sicilian coast. It represents the southern edge of a wedge of imbricate crystalline units (Kabilian-Calabrian Units) that overthrusted, since the Burdigalian and during a consequent event just after the Messinian, the Sicilian-Maghrebian units, which represent part of the shortened African crustal segment (Appeninic units) along the Drepano front (European/African boundary in Fig. 2) The Sicilian-Maghrebian units show southern and south-eastern vergence and derive from the deformation of Meso-Cenozoic carbonate and silici-clastic deep sea and shallow-water platform domains, considered as equivalent to the units outcropping along the Sicilian mainland (Catalano et alii, 1985).

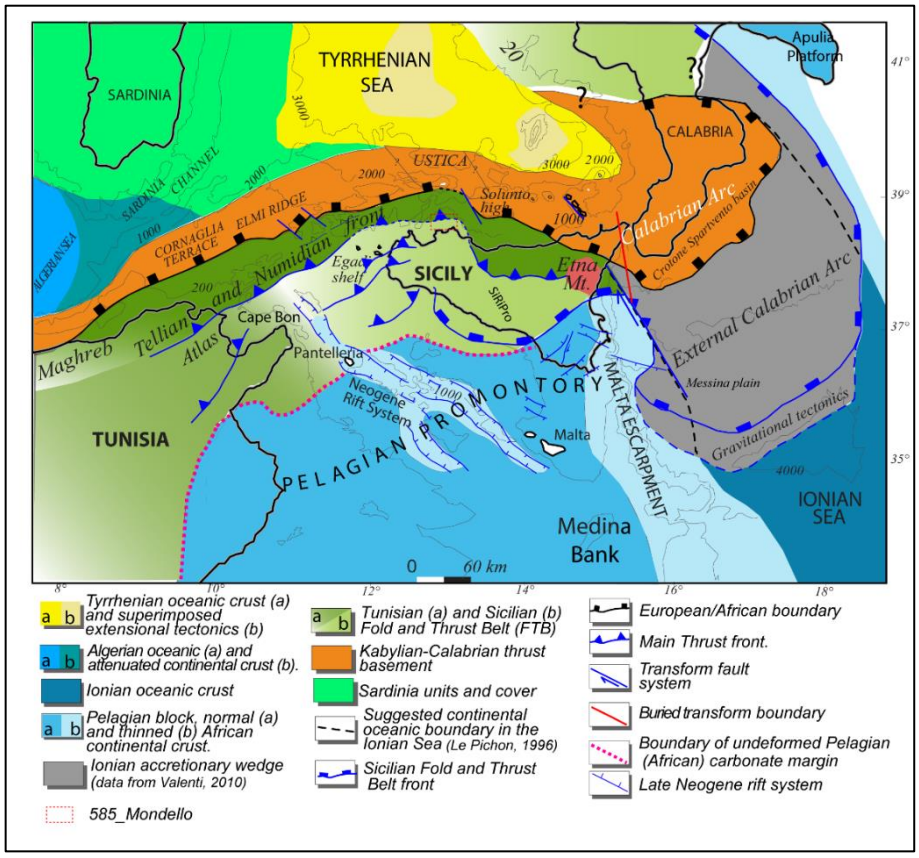

Fig. 2. Tectonic-geodynamic map of the Central Mediterranean region.

Late Miocene-early Pliocene north-dipping high-angle reverse faults, involving mainly deep seated, carbonate platform units, produced structural highs (Avellone et al., 2010), among which those seaward bounding the intraslope basins, termed peri-Tyrrhenian basins by Selli (1970), filled with Late Neogene to Quaternary evaporitic, hemipelagic, siliciclastic and volcaniclastic deposits, up to 1200 m thick (Baghi et al., 1980). Later, normal faults partly dissected the back- and fore-limb of the structural high. Middle-upper Pliocene reflectors clearly diverge towards the normal fault bordering the basin, thereby demonstrating syn-extensional deposition (Pepe et al., 2003).

NW-SE, E-W and NE-SW-trending normal faults exerted during the Pleistocene a control on the morphology of the present day shelf and coastal areas (Fig. 3). The tectonic activity of the northern

Sicily continental margin is outlined by a large upper plate seismicity, producing a seismogenic region characterized by compressional focal mechanisms to the west, while in the eastern sector extensional and strike-slip mechanisms prevail. Shallow (<25 km) seismic events of low to moderate magnitude (max Md 5.6 on September 2002) occur along an E-W trending belt located northward. The focal mechanisms related to the main seismic shocks are in agreement with a dominant NE-SW fault trend coupled with a NW-SE compressive offset direction (Agate et al., 2000; Giunta et al., 2009).

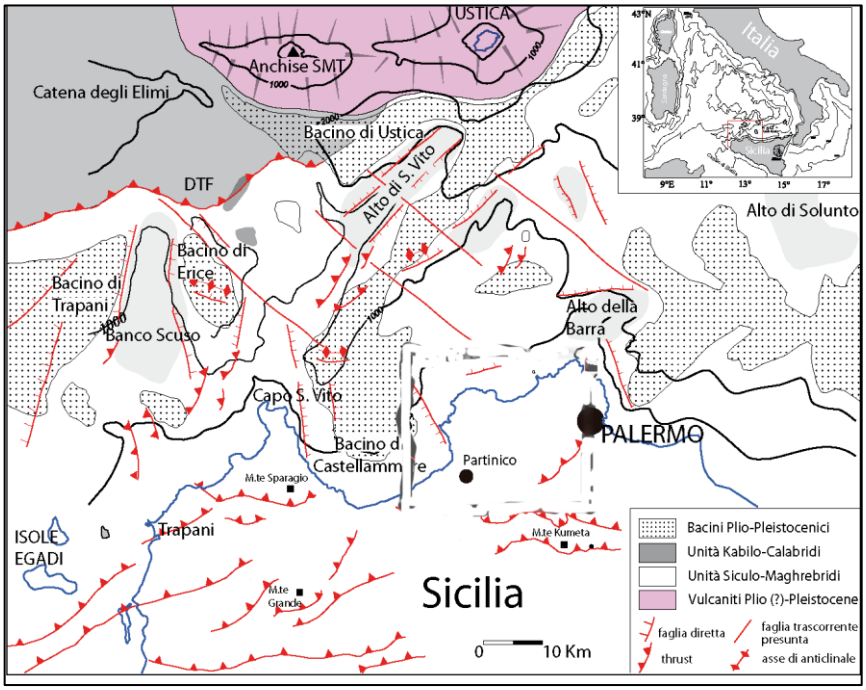

Fig. 3 Structural map along the Northern Sicily continental margin.

As a consequence deep basins (Trapani Basin, Erice Basin, Castellammare del Golfo Basin, and Palermo Basin, Fig. 4) alternate with high carbonatic structures (Banco Scuso, Capo San Vito promontory, Palermo high, Fig. 4), Plio-Pleistocene antiformal structures and Pleistocene volcanic edifices (Anchise and Ustica, Fig. 4).

The Palermo high represents the marine continuation of the carbonate units outcropping in the northern sector of the Palermo Mountains (Catalano and D'Argenio, 1982; Catalano et alii, 1996). The land and marine sectors represented in the Sheet Mondello are composed mainly by Meso-Cenozoic carbonate platform successions (Panormide) and Cenozoic clastic-terrigenous successions (Numidian Flysch), covered unconformably by Plio-Quaternary to Recent detritic-organogenic calcarenites marls and shale (marine to continental deposits).

Along the shelf and the upper slope, the Quaternary deposits consist of seawards dipping clastic and terrigenous deposits coming from the northern Sicily (Agate et al., 2005), whereas in the basinal areas hemipelagic sediments are locally intercalated with volcanoclastic sediments (Baghi et al., 1980). In the continental shelf, the Pleistocene deposits are truncated by an erosional surface formed during the

last glacio-eustatic oscillation. Local uplift caused the systematic non-preservation of portions of the oldest sequences (Pepe et al., 2003). Prograding sedimentary wedges of coastal deposits, formed during the Last Glacial Maximum (LGM, about 18 ka), are present along the shelf margin. The prograding wedges are absent where the heads of the canyons or failure scars have indented the outer shelf (Lo Iacono et al., 2011). The highest uplift rates during the last 125 ky in northern Sicily (Ferranti et al., 2010) were found on the inner margin-terraces in the eastern coast (0.8-1.63 mm/y), whilst the Holocene rates are between 20% and 70% higher than those calculated for the Tyrrhenian terraces.

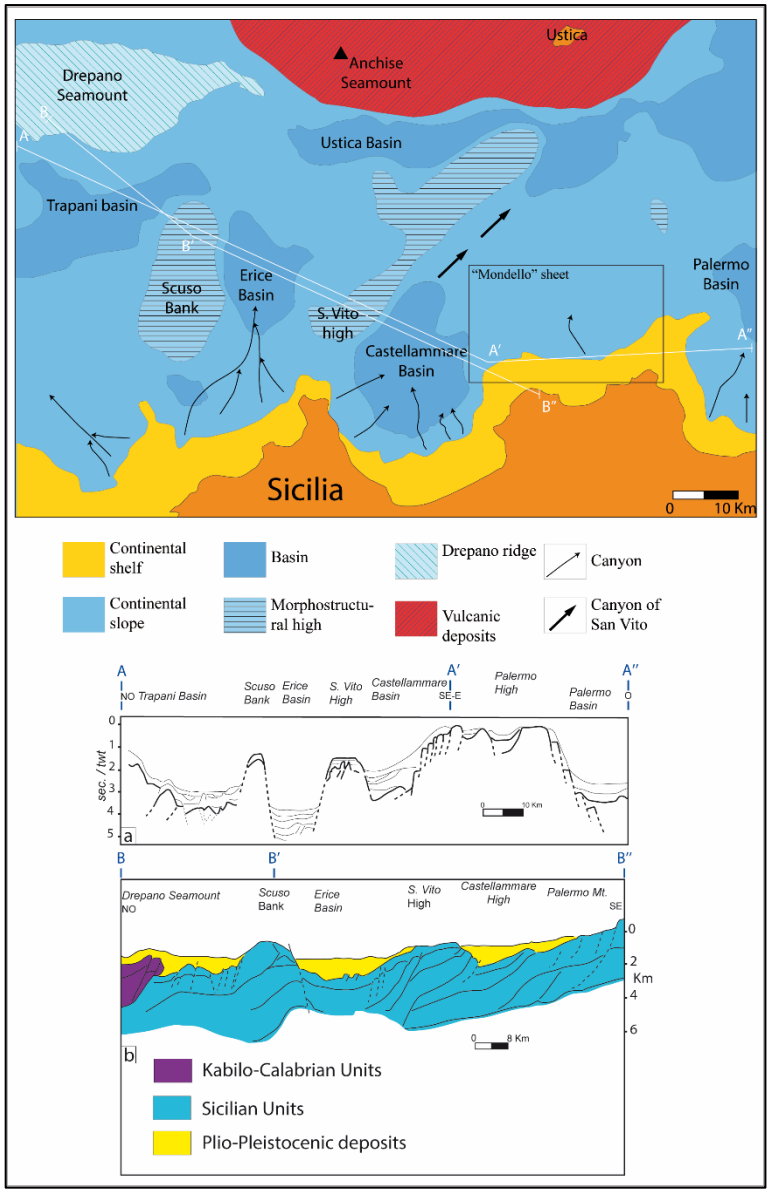

Fig. 4 – Physiography of the Northern Sicily continental margin. (modif. da Agate et alii, 1993). The sections A-A" and B-B" show the morphotectonic setting of this region.

Further on, both coastal geomorphological and marine geology data demonstrate that while the mainland sector is uplifted, contemporaneously the offshore area is subsiding, suggesting the existence

of fault systems parallel to the coastline, separating the inner from outer sector of the continental shelf, causing different vertical movements (subsidence vs. uplift) (Sulli et al., 2012). The vertical tectonic rates show a decrease from E to W. Near Cefalù vertical movement rates are lower than 0.2 mm/y, while between Palermo and the Egadi islands, MIS 5.5 markers show a substantial stability, except for small and local vertical movements (Gulf of Castellammare, Mauz et al., 1997 and Castelluzzo Plain), due to the action of transcurrent faults where uplift rates reach 0.1 mm/y (Antonioli et al., 2006).

3. Materials And Methods

Side Scan Sonar data (SSS, Fig. 5), were acquired with a Klein system, using dual frequencies of 100 and 500 kHz, during the 1994 and 2002 oceanographic campaign carried out on the Urania (CNR) ship, and in the frame of the CARG and GEBEC SUD projects. They cover an area of approximately 8 km^2 extending from coast to about 50 m of depth, and were used to map morphological features, sedimentology fields, sedimentary structures and biocenosis. The acoustic facies were calibrated thanks to the data coming from the numerous seabed sampling carried out using Shypek and Van Veen grabs. High-resolution morphobathymetric data, covering an area of 1900 km^2, were acquired the Multibeam Echo Sounder Reson SeaBat 8160 system, generating 126 beams at a frequency of 50 kHz, for an operational depth range of 30-3000 m. The swath overlap was 20% and the nadir filter was adapted to the different depths. The acquisition of bathymetric data was supported by a Differential Global Positioning System to acquire an accurate vessel position, a motion sensor to determine the attitude of the vessel in terms of pitch, roll and heave; a CTD probe to measure the parameters influencing the sound velocity in seawater. Bathymetric data were stored and processed using the PDS2000 software. Data processing included the graphic removal of erroneous beams, noise filtering, processing of navigation data and correction for sound velocity.

Digital Terrain Models (DTM) were produced with a footprint resolution of 20 m. The Global Mapper and the Golden Software Surfer 9 were used to obtain 3D maps, shaded relief maps, and bathymetric profiles.

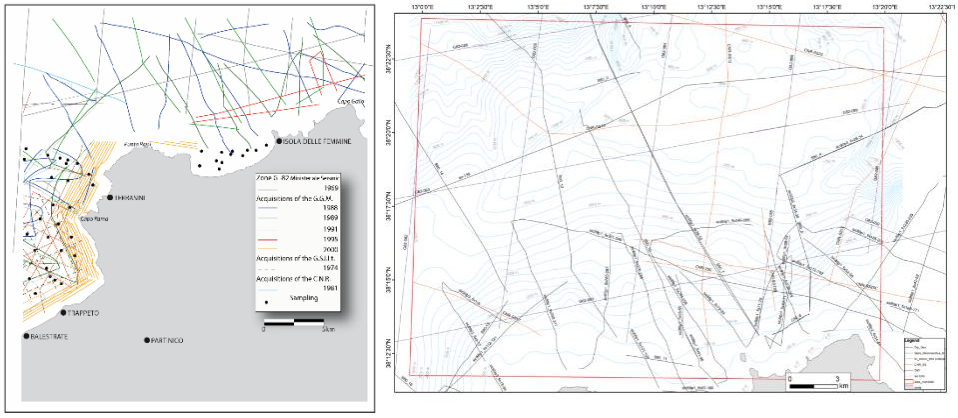

Fig. 5. Geophysical and geological data set (seismic reflection profile, SSS data, sediment samples).

A dense network of single-channel seismic reflection profiles provided high resolution data on the post-Messinian sedimentary succession (Fig. 5). The seismic sources were the Sub Bottom Profiler

Geochirp II - CP931 (Geoacoustics) for the Late Quaternary multilayer and the multi-tip sparker array for the older Plio-Quaternary sequences.

A standard seismic data processing (edit, muting, swell filter, digital filters, AGC, gain) provided good quality seismic data that were interpreted by using seismostratigraphic analysis, which allowed depositional units characterized by seismic facies with different characters (seismic attributes, lateral terminations, internal geometry and external shape) to be distinguished.

The depth of investigation is variable between 100 and 1000 ms while the high resolution power makes it possible to identify bodies of a thickness between one meter and some tens of meters.

Unpublished or available (VIDEPI project) high penetration seismic data were obtained by using both Airgun/Watergun sources coupled with multi-channel streamer. The penetration exceeds 6 s (t.w.t.), with vertical resolution between 10 and 80 m.

4. Marine Geomorphology

The continental shelf extends from 5 to 8 km (Fig. 6). The seabed is characterized by some morphological features with lateral continuity: concave and convex NE-SW and E-W trending break-of-slopes, abrasion marine terraces, submerged cliffs, beach rocks, rocky outcrops. In the intertidal areas, along the rocky coast, furrow grooves, vermetid reefs and abrasion pots have been identified. Ephemeral sedimentary structures such as coastal cusps, submerged dune or megaripple fields, and small mud volcanoes are present. The shelf edge is represented by a predominantly depositional wedge and is erosional only where it is interrupted by the heads of canyons or by the numerous small gullies.

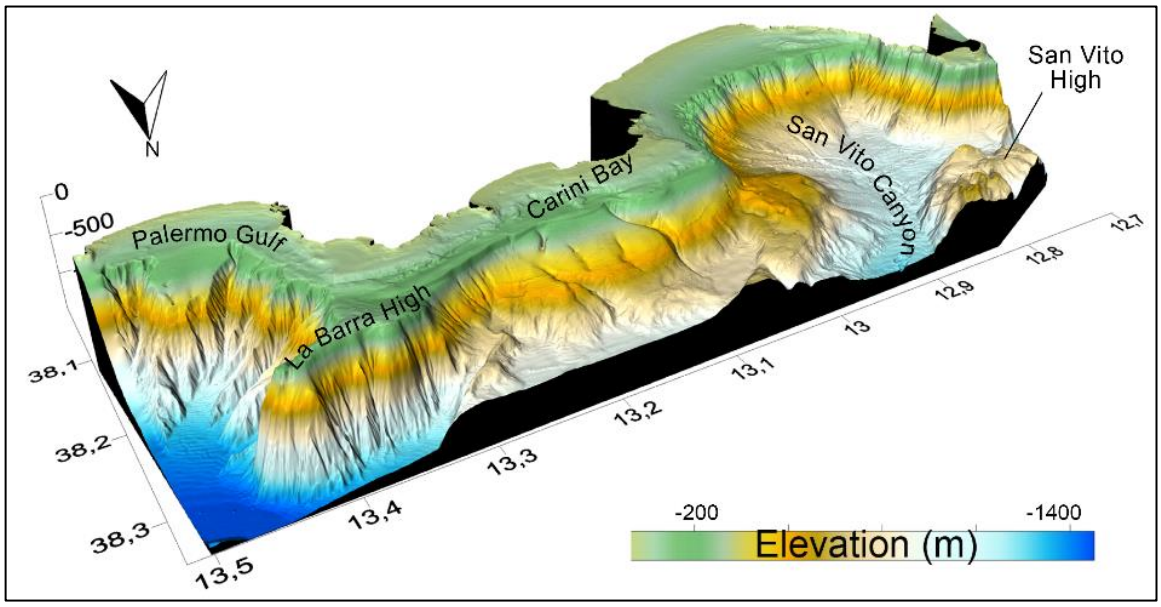

Fig. 6. 3D view of the study area showing its physiographic features.

The morphobathymetric features allows to subdivide the continental shelf into two main morphodynamic zones (see attached Sheet):

- *the inner shelf*, between the coast line and the isobath of -40/-60 m, with variable width and a dip between 0.7° and 3°, influenced by waves and littoral currents, induced by NW, W and SW winds, which produce sedimentary tractive structures; it is bounded seaward by an erosive slope of variable height. Recent marine abrasion terraces, bordered by convex break-of-slope forming semicircular amphitheaters, are present at lower depths;
- *the outer shelf*, which extends to the edge of the platform, located between –120 m and –160 m, more regular by extension and morphology, 1-2° dipping seawards, characterized by buried marine abrasion terrace fault steps, abrasion potholes, and submarine incisions. A series of concave break-of-slopes, at depths ranging from -90 m to -132 m. Ribbon-shaped beach rocks form reliefs parallel to the coastline.

The continental slope is characterized by depositional and erosional morphologies (see attached Sheets), such as turbiditic conduits (canyons, channels, gullies), submarine landslide niches, turbiditic complexes. The channels show single linear NNW-SSE directed conduits, between 50 and 200 m wide, which branch off from the -120 m isobath.
The average steepness of the thalweg reaches 8° in the upper slope, and reduces to 3° near the base of the slope. The incisions have a linear course of about 10 km and show a low sinuosity, conditioned by the tectonic activity. Pockmark aligments are parallel or inside the thalweg of this tectonically controlled NNW-SSE trending incisions.
The E-W directed depression in the northern sector of the Sheet is a significant intraslope basin associated with reliefs of various types that interrupt the continental slope. The basin is filled by Plio-Pleistocene deposits and is characterized by a high subsidence and sedimentation rates.

5. Marine Geological Mapping

The marine geological map of the "Mondello" sheet shows the distribution of depositional systems and facies of marine sediments pertaining to the upper portion of the highstand systems tract (HST) of the Late Quaternary deposition sequence, characterized by a three-dimensional aggradational organization of facies.

5.1 Seabed deposits

The sedimentological analysis of seabed deposits, sampled in the marine area of the “Mondello” sheet with a Shipek grab, allowed to distinguish different grain size facies (Fig. 7). The sediments are classified according to the triangular diagram (Sand–Silt–Clay) proposed by Folk (1954). On the basis of the lithological and stratigraphic characteristics different depositional systems have been distinguished, from the inner shelf to the outer shelf and the continental slope, which develop from the coastline seaward, generally with sharp transition (see attached Sheet): a) shoreface deposits; b) inner shelf deposits; c) outer shelf deposits; d) slope deposits.

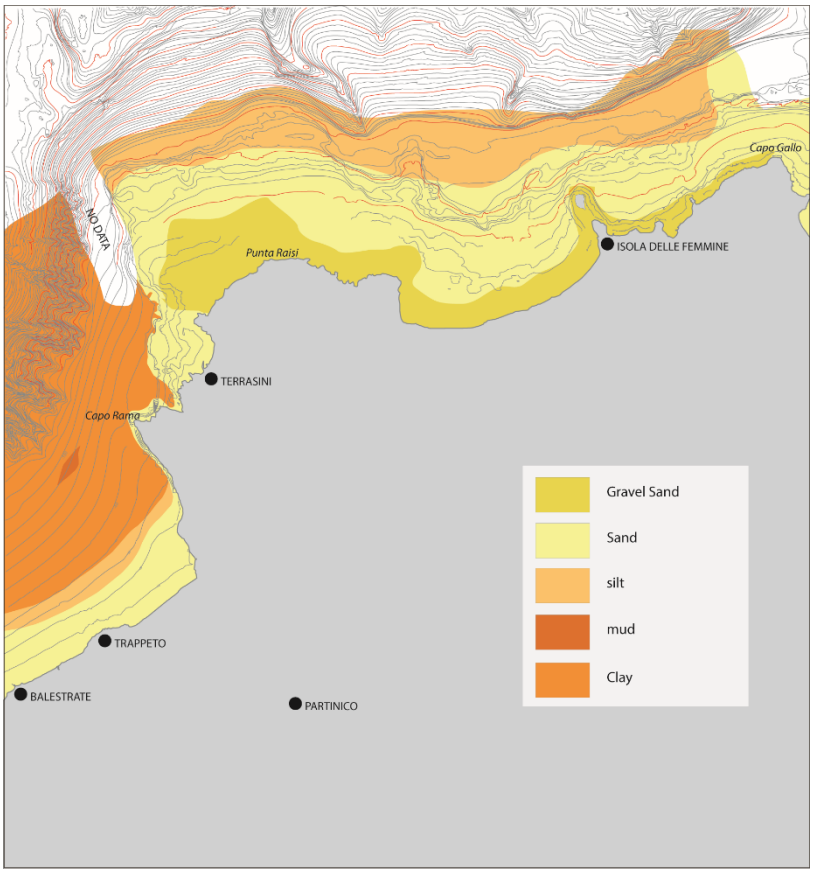

Fig. 7. Sediments distribution

The continental shelf seabed in the Sheet "Mondello" is colonized by extensive Posidonia oceanica (L.) Delile and Cymodocea nodosa (Ucria) Asch. grasslands. The Posidonia oceanica meadows lie on rocky substrate from Capo Rama to Isola delle Femmine. The meadow is in places interrupted in correspondence of depressions and erosive pockets that host megaripple fields. The Cymodocea nodosa populations are located within 30 m of depth in the inner sector of the Bay of Carini.

5.2 The shallow marine substratum

The shallow marine substratum map show the distribution of the Noemi supersynthem deposits and the Late Quaternary Depositional Sequence (Fig. 8).

The most significant seismic units are represented by the Messinian horizon, the Pliocene (PL) to Pleistocene (PQ) sequence, grouped in the Noemi supersynthem, and the Late Quaternary Depositional Sequence (Fig. 8).

Due to the lack of lithostratigraphic data from wells and cores in the southernTyrrhenian sea, the seismic sections were calibrated using data of dredging recovered along submarine slopes beyond the northern boundary of the Foglio (Selli, 1974; Catalano et alii, 1985; D'Argenio, 1999), and gravity cores occurring in areas adjacent to the Sheet, for the shallow quaternary succession.

The cartographic methods used for the marine area of the Sheet comply with the guidelines in the Quaderni del Servizio Geologico Nazionale (Series III n. 1, 1992; Series III n. 12 (II), 2009).

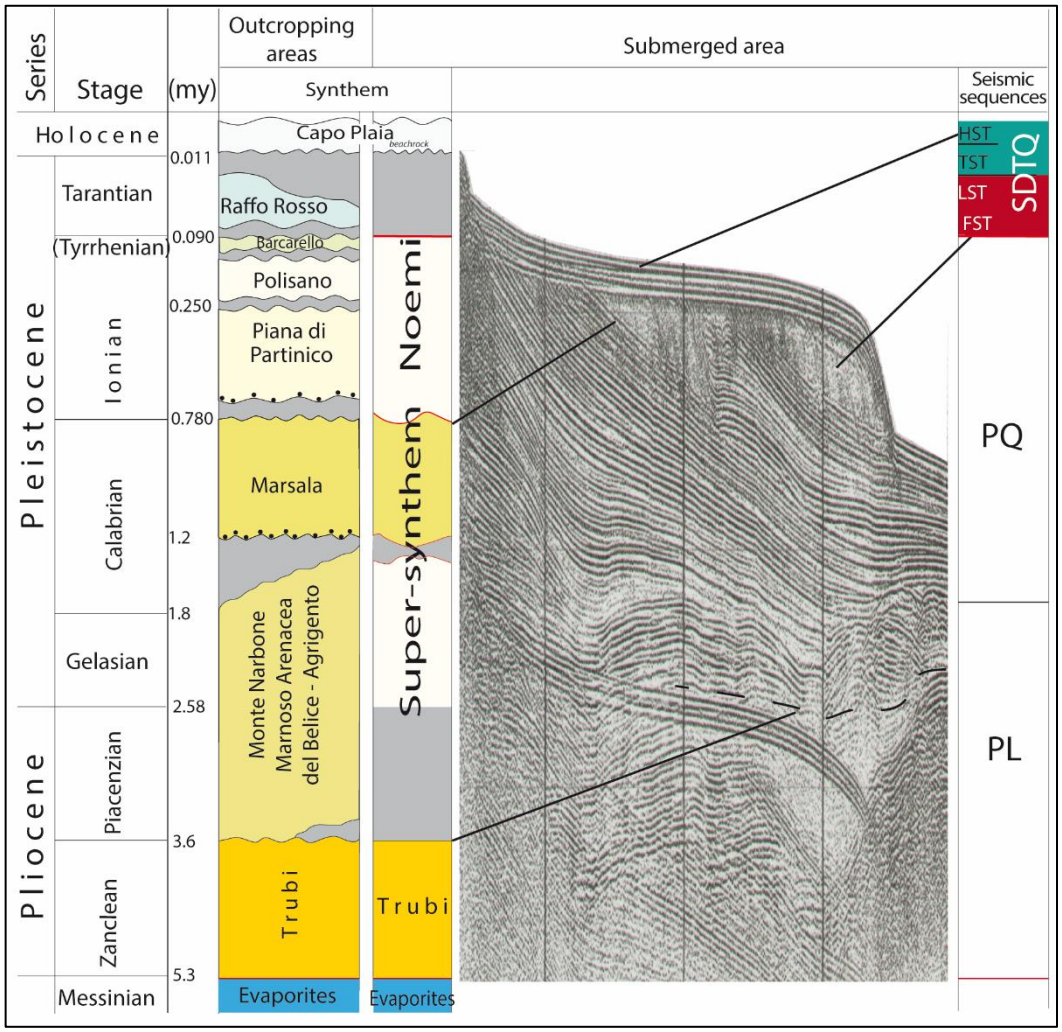

Fig. 8. Seismic section showing the relationships between different seismostratigraphic units. Y, top Messinian; X, Noemi supersynthem lower boundary; lpc, lowstand prograding complex of the LQDS.

The Noemi supersynthem outcrops along the shelf break and the continental slope in the western sector of the Sheet. On the continental shelf between the Bay of Carini and Isola delle Femmine it is characterized by alternating calcarenites and sandy marls (see attached Sheet).

The Late Quaternary Depositional Sequence is mapped from the coastal areas to the base of the upper slope. The lower boundary on the continental shelf is an unconformity associated with erosional truncation passing, along the upper slope, to a paraconformity on which multiple detachment niches are connected. The lower unconformity identifies a type 1 sequence limit (Van Wagoner et alii, 1988) and is characterized by morphological steps in the inner shelf. Within the sequence, four system tracts were distinguished: falling stage systems tract (FST); lowstand ST (LST); Transgressive ST (TST), and highstand ST (HST).

The FST seismic facies is oblique–tangential, more rarely oblique–parallel. The reflectors show low to medium amplitude. The amplitude and continuity of seismic horizons decrease seawards.

The LST shows an oblique prograding geometry, with low to medium amplitude and good lateral continuity reflectors, which towards the sea are arranged in downlap up to pass to greater amplitude and laterally continuous reflectors of the upper slope. The upper boundary of FST and LST coincides in the outer shelf with an erosional transgression surface and along the upper slope with a drowning surface. The TST and HST are bounded at the base by an erosional transgression surface and in the inner shelf by the sequence boundary. Ribbon-like bodies, elongated parallel to the isobaths in the area facing the coast of Sferracavallo at -105 m, -95 m, -85 m, -75 m depths, are indicators of successive stationing of the sea level during its last rise (Lucido, 1992). The upper limit of the TST is a downlap surface, associated with apparent truncation of the reflectors, which corresponds to the of maximum flooding surface (mfs). The HST is identified by a prograding wedge whose lower limit is represented by the maximum flooding surface. The upper limit is represented by the present depositional surface.

6. Marine Tectonic Setting

The interpretation of seismic reflection profiles acquired along the offshore of the Sheet “Mondello” showed the submerged tectonic structures and allowed the reconstruction of the tectonic evolution of the marine areas (Fig. 9).

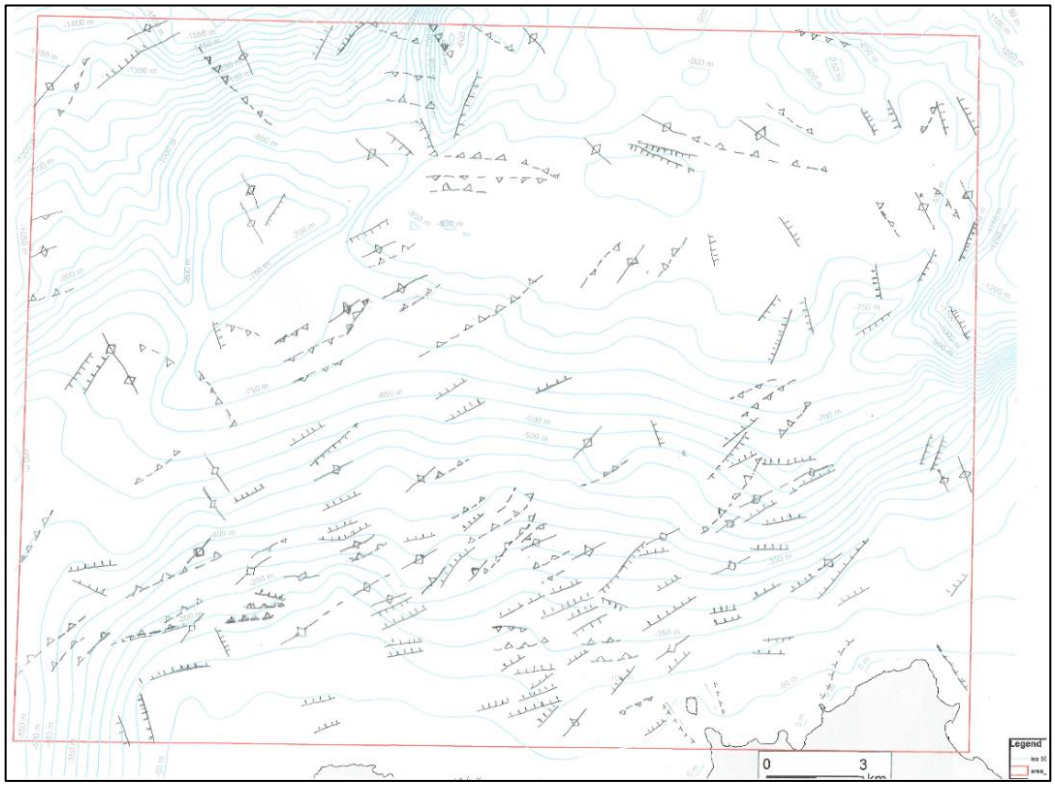

Fig. 9. Tectonic map of the study area

The doubtful chronostratigraphic attribution of the seismic horizons of the Plio-Quaternary succession prevent to determine the age of the unconformities and of the tectonic events but not the relative chronology of them.

In the marine sector the main tectonic edifice is composed mostly Meso-Cenozoic carbonate units, arranged as a pile of tectonic units with apparent vergence towards ESE, involved, since the upper Pliocene, in the extensional and/or transtensional tectonics (Fig. 10).

The most significant faults with main trend NNW-SSE and ENE-WSW, responsible for the current configuration of the shelf-slope system, have their surface morphological expression in the crowns of the retrogressive landslides and in the development of bypass zones (canyons, channels, rills).

The main elements, recognized also in the outcropping sectors, are the following:

i) compressional deformation involving the Meso-Cenozoic carbonates up to the Messinian layer, producing folds and reverse faults with NNE-SSW direction and vergence towards ESE. In the northern sector the tectonic overlap of the Meso-Cenozoic carbonate thrust units is documented;

ii) extensional (to trastensional) deformation that involve the post-Messinian deposits represented by W-dipping listrical growth normal faults with large displacements. These structures generated a system of structural high and depressions.

iii) NNW-SSE to NNE-SSW trending extensional faults involving more recent deposits (mainly up to middle Pleistocene) rarely displacing the seabed; the fault system appears to influence the genesis of submarine canyons and channels.

The deformation of the unconformity at the base of the middle Pleistocene sequences indicates a later compressional phase.

The present-day deformation is in agreement with the focal mechanisms of the earthquakes that indicate a NW-SE directed compressional stress field. The related deformational pattern is represented by two main NNW-SSE and ENE-WSW fault systems with extensional to transtensional kinematics. N-S and E-W trending faults shoe also a strike-slip component. Compressional and transpressional faults with vergence toward North were recently highlighted in this margin (Sulli et al., 2019).

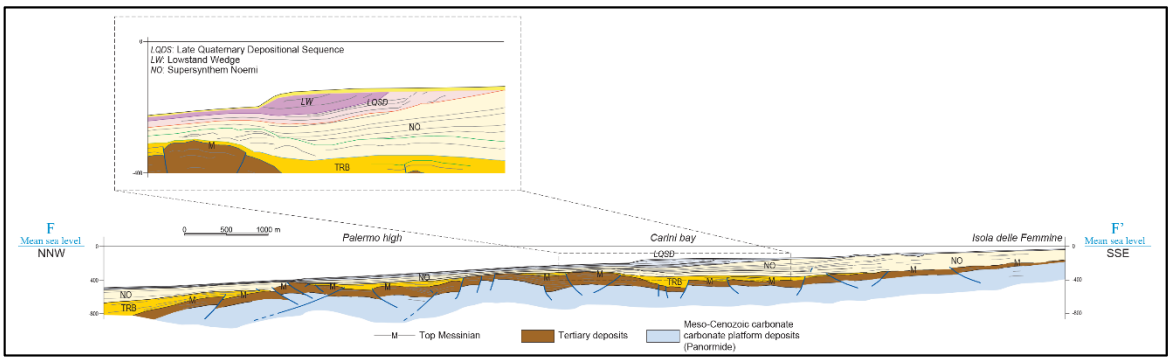

Fig. 10. Geological section from depth-conversion of seismic profile crossing the southern sector of the study area.

Along the outcropping areas, evidence of the Quaternary tectonic activity are given by geomorphological (fault escarpments, tectonic cliffs) and geological (relationships between faults and Quaternary deposits) elements. The progressive increase of the accommodation space in the tectonic depressions on the roof of the normal faults allowed the reworking and the retreating of the scarps of

fault due to the marine erosion and the deposition of the Marsala synthem deposits on marine erosion surfaces.

This deposits seal the faults, which have displacements of hundreds of meters, allowing to date the tectonic event to about 1.5 My (Di Maggio et alii, 2009).

The main directions of these faults are NNW-SSE, ENE-WSW, NE-SW, and NW-SE, In some case they affect the middle-upper Pleistocene marine terraces or the Holocene debrites of the Capo Plaia synthems.

7. Seismicity

The Sheet "Mondello" covers a sector of the north-Sicilian continental margin that develops along the collision limit between African and European plate. For this reason the tectonic processes are still very active, as evidenced by the strong seismicity of the submerged sector (Fig. 11), which was recently revealed by the earthquakes of 1998 and 2002, whose epicenters are located in areas respectively southwest and east of Ustica. These earthquakes are framed within regional seismogenic bands that develop within the shallow interplate zone of the southern Tyrrhenian Sea.The seismogenic sources can be extracted from the DISS (Database of Individual Seismogenic Sources), a georeferenced archive of tectonic structures and seismological data (Fig. 11), created by the National Institute of Geophysics and Volcanology (INGV). The area of the Sheet "Mondello" holds the composite seismogenic sources SC ITCS014 (Southern Tyrrhenian) and SC ITCS222 (Southern Tyrrhenian S). The composite sources are a simplified three-dimensional representation of a crustal fault containing a number of seismogenic sources. They are not associated with a specific set of earthquakes or earthquake distribution.

The seismic hazard inside the Sheet area derives mainly from the active seismogenic structures located in the southern Tyrrhenian (Fig. 11). They are distributed along a compression band that extends in an east-west direction and accommodates most of the convergence between the African and the Euro-Asian plates. Instrumental seismicity shows that in the last 30 years several events with a magnitude greater than 5 originated along this band, including the 2002 Mw 5.9 Palermo earthquake and the 1998 Md max 4.3 earthquake in the area SSO of Ustica (Fig. 11). These are shallow earthquakes with compressive kinematics, with a maximum compression axis oriented in the NNO-SSE direction (Fig. 11). The faults in the marine sector of the Sheet and those along the coastal areas are consistent with the present-day stress field determined by both focal mechanisms and geodetic data. Even some historical earthquakes of moderate magnitude, located inland along the northern Sicilian coast, could belong to these seismic sources (Guidoboni et al., 2003; Jenny et al., 2006).

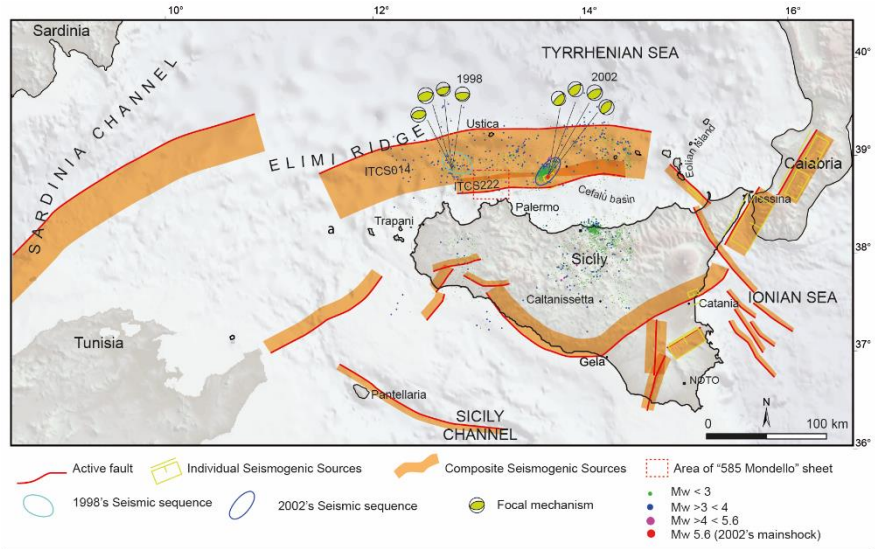

DISS–ID: ITCS014
Name: Southern Tyrrhenian
PARAMETRIC INFORMATION

Parameter		Quality	Evidence
Min depth [km]	2.0	EJ	Inferred from regional tectonic considerations.
Max depth [km]	18.0	EJ	Inferred from regional geological and seismological data.
Strike [deg] min… max	40…100	EJ	Inferred from regional geologic and seismological data.
Dip [deg] min… max	15…40	EJ	Inferred from regional geologic and seismological data.
Rake [deg] min… max	60…120	EJ	Inferred from regional seismological data.
Slip Rate [mm/y] min… max	0.1…1.4	EJ	Inferred from regional geodynamic considerations.
Max Magnitude [Mw]	6.5	EJ	Inferred from the largest known earthquake in the area.

DISS–ID: ITCS222
Name: Southern Tyrrhenian S
PARAMETRIC INFORMATION

Parameter		Quality	Evidence
Min depth [km]	3.0	EJ	Inferred from regional tectonic considerations.
Max depth [km]	16.0	EJ	Inferred from regional tectonic and seismological considerations.
Strike [deg] min… max	200…280	EJ	Inferred from regional tectonic and seismological considerations.
Dip [deg] min… max	40…60	EJ	Inferred from regional tectonic and seismological considerations.
Rake [deg] min… max	80…120	EJ	Inferred from regional geological, seismological and geodynamic considerations.
Slip Rate [mm/y] min… max	0.1…0.5	EJ	Inferred from regional geodynamic considerations.
Max Magnitude [Mw]	6.5	EJ	Inferred from the largest known earthquake in the area.

Fig. 11. Seismicity along the Northern Sicily continental margin. The ITCS014 and ITCS222 Southern Tyrrhenian Seismogenetic source (form DISS-INGV catalogue, Central Mediterranean) and focal mechanisms of the main offshore earthquakes (1998 and 2002) are shown.

The Composite Seismogenic Source ITCS014 (Southern Tyrrhenian Sea) extends in an east-west direction from the Sardinia Channel to the Aeolian Islands, about 50 km off the northern Sicilian coast.

It is a compressional belt that accommodates about 4-5 mm/y of the Africa-Europe convergence (D'Agostino and Selvaggi, 2004; Serpelloni et al., 2005), (Fig. 11) estimated at around 5-8 mm/y overall (Goes et al., 2004; Pondrelli et al., 2004). The compressional stress field is consistent with the motion vectors of the plates derived from the GPS data (Oldow et al., 2002; Pondrelli et al., 2006; Serpelloni et al., 2007; Devoti et al., 2008; Cuffaro et al., 2011), which have estimated slip rates between 0.1 and 10 mm/y.

A structure known as the Kabilian-Calabrian Thrust Front, recently reactivated, is considered the source of the Palermo earthquake of September 6, 2002 in Palermo (Pepe et al., 2005). These compressional deformations, mainly ENE-WSW oriented, are also accompanied by extensional faults

(normally oriented NNW-SSE) and strike-slip, both right-lateral (NW-SE) and left-lateral (NE-SW), in agreement with an Andersonian model of deformation.

The maximum magnitude in this area is that of the earthquake of March 5, 1823, located on the northern coast of Sicily (Mw estimated between 5.9 and 6.2). The maximum potential is estimated between 7.0 and 7.6 (Jenny et al., 2006; Billi et al., 2007).

The ITCS222 Composite Seismogenic Source (Southern Tyrrhenian S) extends along a compressive belt in an east-west direction, just south of SC ITCS014 (Fig. 11), and accommodates about 2-5 mm/y of the Africa-Europe convergence (D 'Agostino and Selvaggi, 2004; Serpelloni et al., 2007). Several historical seismic events have been generated by this structure, developing between the offshore of the San Vito peninsula and the Aeolian islands. It produces shallow compressional events, with a main axis in the NNW-SSE direction (Goes et al., 2004; Pondrelli et al., 2004; Vannucci & Gasperini, 2004). This source could coincide with the north-vergent reverse faults and thrusts, recently reported both onland and in the submerged areas (D'Agostino and Selvaggi, 2004; Goes et al. 2004; Sulli et al., 2019).

The seismic hazard, expressed in terms of peak soil acceleration with a 10% surplus probability in 50 years (return period of 475 years) is estimated in this area between about 0.050 and 0.125 g (Fig. 12).

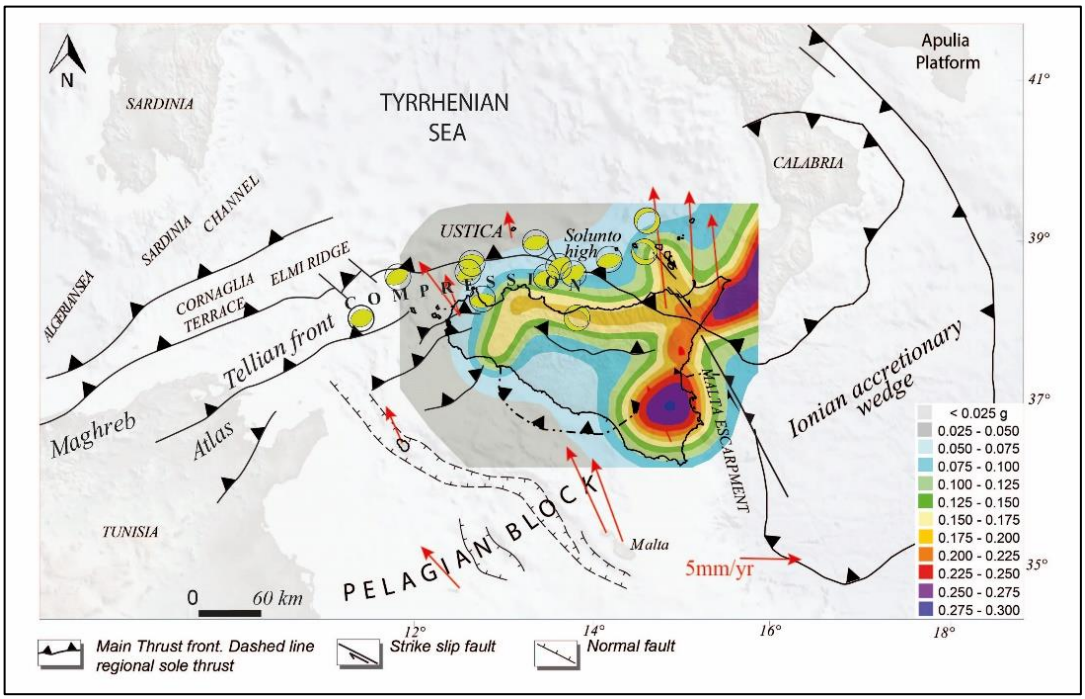

Fig. 12 Seismic hazard map in terms of Peak Ground Acceleration, showing focal mechanisms, GPS values (data from D'Agostino and Selvaggi, 2004; Ferranti et al., 2006, Devoti et al., 2008, Serpelloni et al., 2007).

The historical seismicity, expressed in terms of macroseismic intensity (which evaluates on a macroseismic scale the effects caused by a given event in a certain locality), is obtained from

international databases (such as SHEEC, AHEAD) or from catalogs, like the Italian Macroseismic Historical Archive from 461 BC to 2014, the Parametric Catalog of Italian Earthquakes from 1000 to 2014, the Italian Macroseismic Database from 1000 to 2014, the Catalog of Strong Earthquakes from 461 BC to 1997, which reported numerous historical events located in the area of the sheet.

Destructive events include those of 1726 and 1940. The earthquake of September 1, 1726 (5.48 MW) was the most powerful in the Palermo area (VIII-IX MCS). Out of about 100,000 inhabitants of Palermo in 1726, there were 250 dead and 151 wounded. The earthquake of January 15, 1940 (MW 5.29) had a VII MCS seismic intensity in Palermo; there were one dead and about 50 wounded, some seriously.

Sheet 585 "Mondello"

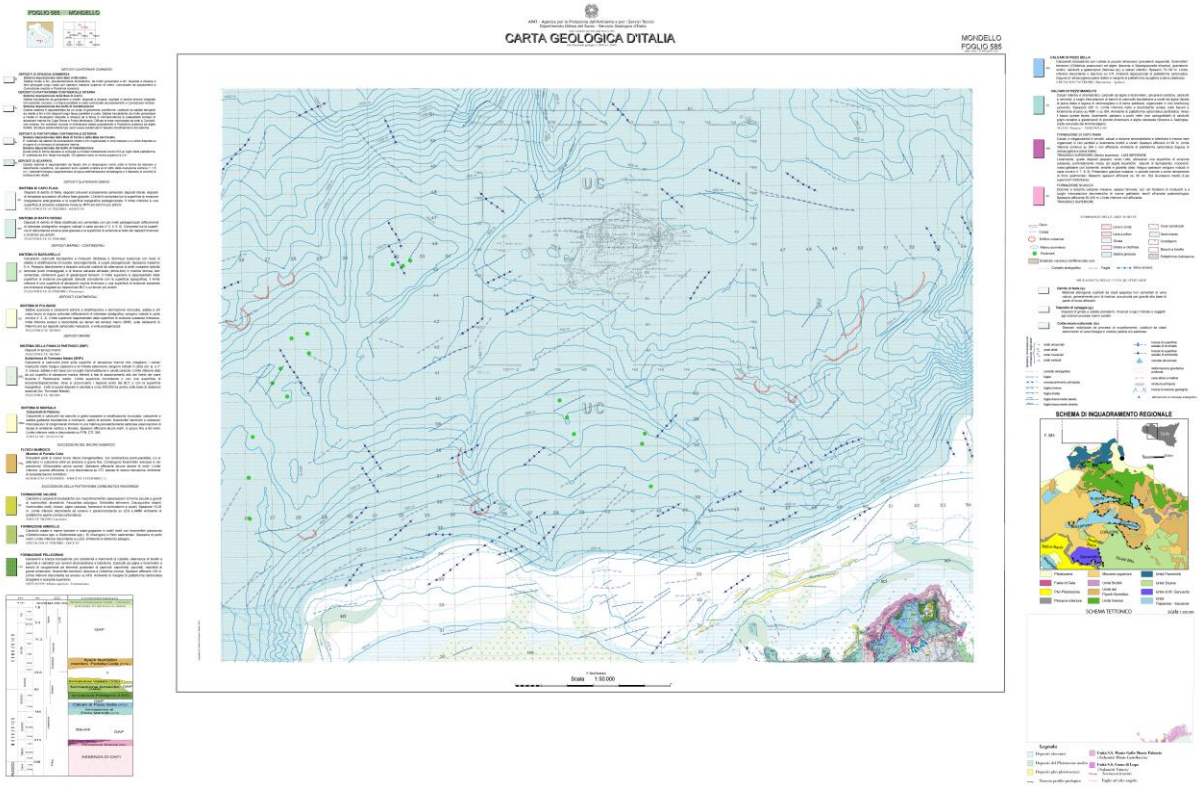

References

Agate M. & Lucido M. (1995) - Caratteri morfologici e sismostratigrafici della piattaforma continentale della Sicilia nord-occidentale. Naturalista Sicil., 19 (1-2): 3 - 25.

Agate M., Beranzoli L., Braun T., Catalano R., Favali P., Frugoni F., Pepe F., Smriglio G. & Sulli A. (2000) - The 1998 offshore NW Sicily earthquakes in the tectonic framework of the southern border of the Tyrrhenian Sea. Mem. Soc. Geol. It., 55: 103-114.

Agate M., Catalano R., Infuso S., Lucido M., Mirabile L. & Sulli A. (1993) - Structural evolution of the northern Sicily continental margin during the plio-Pleistocene. In: Max M. D. & Colantoni P. (Eds.) - Geological development of the sicilian-tunisian platform. Unesco Report in Marine Science, 58: 25-30.

Agate M., Infuso S., Lucido M. & Mancuso M. (2004) – Terrazzi deposizionali sommeri al largo della baia di Carini (Sicilia nord-occidentale). In: Chiocci F. L., D'angelo S., Romagnoli C., Atlante dei terrazzi deposizionali sommersi lungo le coste italiane. Mem. Descrittive della Carta Geologica D'Italia, 58: 115-124.

Agate M., Mancuso M. & Lo Cicero G. (2005) - Late Quaternary sedimentary evolution of the Gulf of Castellammare (NW Sicily offshore). Boll. Soc. Geol. It., 124: 21-40.

Antonioli F, Kershaw S, Renda P, Rust D, Belluomini G, Cerasoli M, Radtke U, Silenzi S (2006) Elevation of the last interglacial highstand in Sicily (Italy): A benchmark of coastal tectonics. Quaternary International 145-146: 3–18

Astraldi, M., Gasparini, G.P., Vetrano, A., Vignudelli, S., 2002. Hydrographic characteristics and interannual variability of watermasses in the Mediterranean: a sensitivity test for long-term changes in the Mediterranean Sea. Deep Sea Res. I 49, 661–680.

Baghi et al. (Bacini Sedimentari Group), 1980. Dati geologici preliminari sul bacino di Cefalù (Mar Tirreno). Ateneo Parmense. Acta Nat. 16, 3–18.

Billi, A., Barberi, G., Faccenna, C., Neri, G., Pepe, F., & Sulli, A. (2006). Tectonics and seismicity of the Tindari Fault System, southern Italy: Crustal deformations at the transition between ongoing contractional and extensional domains located above the edge of a subducting slab. Tectonics, 25, TC2006; doi:10.1029/2004TC001763.

Billi, A., D. Presti, C. Faccenna, G. Neri and B. Orecchio 2007 Seismotectonics of the Nubia plate compressive margin in the south Tyrrhenian region, Italy: Clues for subduction inception. J. Geophys. Res., 112, B08302, 10.1029/2006JB004837.

Catalano R. & D'Argenio B. (1982) - Schema geologico della Sicilia occidentale. In: R. Catalano & B. D'Argenio (Ed.): Guida alla geologia della Siiclia occidentale. Guide geologiche regionali, Mem. Soc. Geol. It., suppl. A, 24, 9-41, Palermo.

Catalano R., D'Argenio B., Montanari L., Morlotti E. & Torelli L. (1985) - Marine geology of the NW Sicily offshore (Sardinia channel) and its relationships with mainland structures. Boll. Soc. Geol. It., 104: 207-215.

Catalano R., Di Stefano P., Sulli A. & Vitale P. F. (1996) - Paleogeography and structure of the Central Mediterranean: Sicily and its offshore area. Tectonophysics, 260, 291-323.

Cuffaro, M., Riguzzi, F., Scrocca, D., Doglioni, C. (2011) - Coexisting tectonic settings: the example

of the southern Tyrrhenian Sea. Int. J. Earth Sci. (Geol Rundsch), DOI 10.1007/s00531-010-0625-z.

D'Argenio B. (1999) - Analisi stratigrafica delle successioni mesozoiche e terziarie dell'offshore della Sicilia nord-occidentale. Naturalista Sicil., S. IV, XXIII (1-2): 43-61.

D'Agostino, N., and G. Selvaggi 2004 Crustal motion along the Eurasia-Nubia plate boundary in the Calabrian Arc and Sicily and active extension in the Messina Straits from GPS measurements. J. Geophys. Res., 109, B11402, 10.1029/2004JB002998.

Demirov, E., Pinardi, N., 2002. Simulation of the Mediterranean Sea circulation from 1979 to 1993: PartI. The interannual variability. J. Mar. Syst. 33–34, 23–50.

Devoti, R., Riguzzi, F., Cuffaro, M., & Doglioni, C. (2008). New GPS constraints on the kinematics of the Apennines subduction. Earth and Planetary Science Letters, 273, 163–174.

Di Maggio C., Agate M., Contino A., Basilone L. & Catalano R. (2009). Unità a limiti inconformi dei depositi quaternari utilizzate per la cartografia nei fogli CARG della Sicilia nord occidentale. Il Quaternario (Italian Journal of Quaternary Sciences), 22 (2): 345-364.

DISS Working Group (2018). Database of Individual Seismogenic Sources (DISS), Version 3.2.1: A compilation of potential sources for earthquakes larger than M 5.5 in Italy and surrounding areas. http://diss.rm.ingv.it/diss/, Istituto Nazionale di Geofisica e Vulcanologia; doi:10.6092/INGV.IT-DISS3.2.1

Fabbri A., Gallignani P. & Zitellini N. (1981) - Geologic evolution of the peri-Tyrrhenian sedimentary basins of Mediterranean margins. In: Wezel, F. C. (Ed.), Sedimentary Basins of Mediterranean Margins, Bologna (Tecnoprint): 101-126.

Ferranti, L., Antonioli, F., Mauz, B., Amorosi, A., Dai Pra, G., Mastronuzzi, G., et al., 2006. Markers of the last interglacial sea-level high stand along the coast of Italy: Tectonic implications. Quaternary International 145-146, 30-54, doi: 10.1016/j.quaint.2005.07.009.

Ferranti L, Antonioli F, Anzidei M, Monaco C, Stocchi P (2010) The timescale and spatial extent of vertical tectonic motions in Italy: insights from relative sealevel changes

studies. Journal of the Virtual Explorer, Electronic Edition. ISSN:1441-8142 ISSN: 1441-8142, 36, paper 23

Ferretti O., Immordino F., Niccolai I., Bertoldo M., Buccheri G. & Setti M. (1996) – Cartografia sedimentologica del Golfo di Castellammare (Sicilia nord-occidentale): informazioni, criteri e finalità. In: A Colella (Ed). Riunione del Gruppo Sedimentologia del CNR., Catania, 147-148.

Folk R. L. (1954) - The distinction between grain size and mineral composition in sedimentary rocks nomenclature. Jour. Geol., 62: 344-359.

Giunta G., Luzio D., Agosta F., Calò M., Di Trapani F., Giorgianni A., Oliveri E., Orioli S., Perniciaro M., Vitale M., Chiodi M., Adelfio G. (2009) - An integrated approach to investigate the seismotectonics of northern Sicily and southern Tyrrhenian, Tectonophysics, 476: 12-21.

Goes, S., Giardini, D., Jenny, S., Hollenstein, C., Kahle, H.G., Geiger, A. (2004) - A recent tectonic reorganization in the south-central Mediterranean. Earth and Planetary Sc. Lett., 266: 335-345.

Guidoboni, E., D. Mariotti, M. S. Giammarinaro and A. Rovelli 2003 Identification of Amplified Damage Zones in Palermo, Sicily (Italy), during the Earthquakes of the Last Three Centuries. B. Seismol. Soc. Am., 93, 4, 1649-1669.

Jenny, S., S. Goes, D. Giardini and H.-G. Kahle 2006 Seismic potential of Southern Italy. Tectonophysics, 415, 1-4, 81-101, 10.1016/j.tecto.2005.12.003.

Lo Iacono et al., 2011

Lucido M. (1992) - Geomorfologia della piattaforma continentale tra Torre del Pozzillo e Torre Mondello (Sicilia nord-occidentale). Naturalista Sicil., IV: 91-107.

Malinverno A. & Ryan W. B. F. (1986) - Extension in the tyrrhenian sea and shortening in the apennines as result of arc migration driven by sinking of the lithosphere. Tectonics, 5 (2), 227-245.

Mauz B., Buccheri G., Zoller L. & Greco A. (1997) - Middle to upper Pleistocene morphostructural evolution of NW Sicily coast: thermoluminescience dating and paleontological-stratigrafical evaluations of littoral deposits. Palaeo, 128: 269 - 285.

Oldow, J.S., Ferranti, L., Lewis, D.S., Campbell, J.K., D'Argenio, B., Catalano, R., et al. (2002). Active fragmentation of Adria, the north African promontory, central Mediterranean orogen. Geology, 30(9), 779-782.

Pepe, F., Sulli, A., Agate, M., Di Maio, D., Kok, A., Lo Iacono, C., & Catalano, R. (2003). Plio-Pleistocene geological evolution of the northern Sicily continental margin (southern Tyrrhenian Sea): new insights from high resolution, multi-electrode sparker profiles. Geo Mar. Lett., 23, 53-63.

Pepe, F., A. Sulli, G. Bertotti and R. Catalano 2005 Structural hights formation and their relationship to sedimentary basins in the north Sicily continental margin (southern Tyrrhenian Sea): Implication for the Drepano Thrust Front. Tectonophysics, 409, 1-18.

Pondrelli, S., Morelli, A., & Ekstrom, G. (2004). European-Mediterranean regional centroid-moment tensor catalog: solutions for years 2001 and 2002. Phys. Earth Planet Inter., 145, 127-147.

Pondrelli S., Salimbeni S., Ekström G., Morelli P., Gasperini A. & Vannucci G., (2006) - The Italian CMT dataset from 1977 to the present. Phys. Earth Planet. Int., 159/3-4: 286-303.

Selli, R., 1970. Cenni morfologici generali sul Mar Tirreno. G.Geol. 37, 5–24.

Selli R. (1974) - Appunti sulla geologia del Mar Tirreno. In: Paleogeografia del terziario sardo nell'ambito del Mediterraneo occidentale. Rend. Sem. Fac. Sc., Univ. Cagliari, suppl.: 327-349.

Serpelloni, E., G. Vannucci, S. Pondrelli, A. Argnani, G. Casula, M. Anzidei, P. Baldi and P. Gasperini 2007 Kinematics of the Western Africa-Eurasia plate boundary from focal mechanisms and GPS data. Geophys. J. Int., 169, 1180-1200.

Serpelloni, E., M. Anzidei, P. Baldi, G. Casula and A. Galvani 2005 Crustal velocity and strain-rate fields in Italy and surrounding regions: new results from the analysis of permanent and non-permanent GPS networks. Geophys. J. Int., 161, 861-880, 10.1111/j.1365-246X.2005.02618.x

Sulli A (2000) Structural framework and crustal characteristics of the Sardinia Channel Alpine transect in the central Mediterranean. Tectonophysics 324: 321–336

Sulli A, Lo Presti V, Gasparo Morticelli M, Antonioli F (2013) Vertical movements in NE Sicily and its offshore: Outcome of tectonic uplift during the last 125 ky. Quaternary International, 288: 168-182. doi:10.1016/j.quaint.2012.01.021

Sulli, A., Gasparo Morticelli, M., Agate, A., & Zizzo, E. (2018). Hinterland-verging thrusting in the northern Sicily continental margin: a late collisional stage of the Sicilian Fold and Thrust Belt?. Geophysical Research Abstracts, 20, EGU2018-8842, EGU General Assembly, 8–13 April 2018.

Sulli A., Morticelli M.G., Agate M., Zizzo E. (2019) Hinterland-Verging Thrusting in the Northern Sicily Continental Margin: Evidences for a Late Collisional Stage of the Sicilian Fold and Thrust Belt?. In: Rossetti F. et al. (eds) The Structural Geology Contribution to the Africa-Eurasia Geology: Basement and Reservoir Structure, Ore Mineralisation and Tectonic Modelling. Advances in Science, Technology & Innovation (IEREK Interdisciplinary Series for Sustainable Development). Springer, Cham, 251-253.

Sulli, A., Agate, M., Mancuso, M., Pepe, F., Pennino, V., Polizzi, S., et al. (2012). Variability of depositional setting along the north-western Sicily continental shelf (italy) during late Quaternary: effects of sea level changes and tectonic evolution. Alpine and Mediterranean Quaternary, 25(2), 141-155.

Van Wagoner J. C., Posamentier H. W., Mitchum R. M., Vail P. R., Sarg J. F. & Loutit T. S. (1988) - An Overview of the Fundamentals of Sequence Stratigraphy and key definitions. In: Wilgus C.K., Hasting B., Ross C., Posamentier H.W., Van Wagoner J., Kendall C. G. St. C. (Eds.), Sea level change: an integrated approach. SEPM Spec. P., 1988, 42: 39-45.

Vannucci, G., & Gasperini, P. (2004). The new release of the database of Earthquake Mechanisms of the Mediterranean Area (EMMA version 2). Ann. Geophys., 47, 303-327.

CHAPTER 3

Growth and geomorphic evolution of the Ustica volcanic complex at the Africa-Europe plate margin inferred from high resolution marine geophysical data

NOTE This chapter is a scientific paper submitted to "Marine Geology". The authors are the followings: Attilio Sulli, Elisabetta Zizzo, Daniele Spatola, Maurizio Gasparo Morticelli, Mauro Agate, Claudio Lo Iacono, Francesco Gargano, Fabrizio Pepe, Gaspare Ciaccio.

Abstract
We present a morpho-structural study based on the new swath-bathymetry, sub bottom profiles, single-channel seismic reflection records acquired during the last two decades on the submarine region of the Ustica Volcano (UV) in the South-western Tyrrhenian sea.

This study has unveiled the occurrence of different geomorphic elements forming the complex morphology of the volcanic edifice and has increased the knowledge of the geological-geodynamic processes acting in this crucial sector of the Central Mediterranean. The physiography of the volcanic edifice shows a narrow shelf and extremely uneven submarine flanks, as a consequence of a long coexistence of volcanic, tectonic, and slope failure processes. We identify four different morphological zones with specific prevailing characters denoting different processes and genetic mechanisms. The northern region is characterized by the massive occurrence of well-preserved volcanic cones in a depth range of 200-1500 m, probably linked to a recent volcanic activity of the area, despite the Ustica edifice is considered an inactive Quaternary volcanic system. Elongate gullies and linear furrows, carving locally the shelf break and developing up to the depth of 1700 m producing slope failures, mainly affect the eastern region. Furrows and gullies may represent the main conduits for flushing sediments from the shallow sectors to the deep plain, through various types of flows. Slope failures processes, carving almost totally the shelf edge and originating mainly from collapses of volcanic cones, shape the southern region. Finally, the western flank is mainly shaped by volcanic features and fault escarpments that have controlled the biggest slope failures of the study area. The seismostratigraphic analysis indicates that UV is composed by a multilayer of lava flows and pyroclastic products, whose geometry can be interpreted as the product of an upward growing and northward shifting of the volcanic centers.

The main results of this study could be a starting point for an assessment of the geo-hazard potential in the offshore of Ustica and for a better knowledge of the geodynamic activity between the Northern Sicily Continental Margin and the Tyrrhenian Basin.

Keywords: Ustica, submarine volcanoes, seamounts, geo-hazard, slope instability, active tectonics.

1. Introduction

Submarine volcanoes are common features in several marine environments and represent an important proportion of the world's seafloor (Harris et al., 2014).Volcanic islands often represent only the emerging part of much larger and more complex volcanic edifices resulting from different processes that contribute to determining their geological and geomorphological features (Quartau et al., 2014; Casalbore, 2018). The overall morphology is the result of volcanic, erosional, depositional, tectonic, isostatic, eustatic, and mass wasting processes (Ramalho et al., 2013). Recently several authors have approximated the shape of individual volcanic edifices to truncated cones (e.g., Smith, 1988; Scheirer and Macdonald, 1995; Spatola et al., 2018), regular elliptical cones (e.g., Rappaport et al., 1997), or

more or less regular cones (Romero Ruiz et al., 2000), in order to simplify the measurement of their shape parameters and their volumes.

Recent studies based on multibeam seafloor mapping have added knowledge on the distributions, structures and evolution of sub-marine volcanic edifices, in particular intraplate volcanic complexes, such as Azores and Canary Islands in the Atlantic Ocean and Hawaii in the Pacific Ocean (Clague et al., 2000; Mitchell et al., 2008; Rivera et al., 2013). Several recent studies, in the Mediterranean Sea have documented the submarine dynamics along the flanks of volcanic edifices developed in different geodynamic settings, as in the Aeolian Islands (Chiocci et al., 2008; Casalbore, 2018), Aegean Archipelago (Nomikou et al., 2013 and references therein), Graham Bank (Spatola et al. 2018), Ischia, Pantelleria (Conte et al., 2014), Linosa (Romagnoli et al., 2020). These studies have revealed considerable variability in flank morphology of the submarine volcanoes, indicating that they are modified by tectonic lineaments, volcanic activity and a range of slope failure processes. The latter range from debris avalanches generated during catastrophic collapses (Ramalho et al., 2013), to slumps of more coherent material on submarine slopes (Smith et al., 1999), slide scars generated by small-scale sliding (Chadwick et al., 2008; Chiocci et al., 2008), flow of volcanogenic sediment away from submarine and subaerial zones as turbidity currents (Walker et al., 2008), or a combination of them. However, the different role of these processes in relation to magma composition, structure, evolution and characteristics of the emerging sectors and associated factors, such as rates of subaerial and coastal erosion, is still poorly known.

Two separated volcanic complexes develop along the Southern Tyrrhenian Sea, (Fig. 1), the Aeolian Islands eastwards and the Ustica-Anchise system to the west. Both complexes include emerged islands as well as submerged seamounts. Some of the eruptive centres of the Aeolian Islands (e.g. Stromboli Island) are still active. On the other hand the Ustica-Anchise system was affected by short-lived eruptive episodes separated in time with different geodynamic significance, but is considered inactive for the last 130 ky (Romano and Sturiale, 1971; de Vita et al., 1998). Anchise seamount was produced during the Pliocene subduction-related calcalkaline magmatism, while the Pleistocene volcanics of Ustica reveal Na-alkaline affinity (Schiano et al. 2004; Fig.1).

The Ustica Island, located 58 km north-northwest of the Sicily coast, represents the emergent part of a wide submarine edifice that rise from the seafloor at about 2200 m (UV in Fig. 1). It lies on the Africa-Europe plate boundary, just along the thrust front separating the Kabylian-Calabrian tectonic units from the Sicilian-Maghrebian domain. Despite being on a plate margin, its magmatic products are considered as being related to anorogenic/intraplate setting (Trua et al 2003). Since it lies in the geological intersection of prominent tectonic and volcanic processes active in the Southern Tyrrhenian Sea, the Ustica edifice represents one of the most significant geo-hazard elements for the neighbouring population in the Southern Tyrrhenian Sea.

Considering the importance of the region in the context of the central Mediterranean geodynamics, this paper describes for the first time the seafloor morphological features of the Ustica volcanic

edifice, developing on a 2020 km2 wide area, extending between 8 m and 3330 m below sea level. We based our analysis on the interpretation of high-resolution multibeam swath bathymetry and single-channel seismic profiles, collected in the framework of the CARG (Italian official geological cartography) and MAGIC (Marine Geohazards in the Italian Coasts) projects. Contrary to the quite well-documented tectonic and volcanological characters of the subaerial edifice, the marine geology of the seafloor around the island was up to now almost unknown.

The main aim of this paper is to highlight the morpho-structural characteristics of the submerged volcanic edifice to give a contribution to the knowledge of the geological and geodynamic processes occurring in this part of the central Mediterranean Sea.

With the aim to describe the main geological processes that control the morphology of the area, we identified and mapped the main morphological-structural lineaments, with reference to erosional and instability processes (e.g. slope failures, furrows, and channels), volcanic features and tectonic structures. The mapping of the seafloor features and related geological processes will contribute to evaluate the potential of marine geohazard in a very active sector liable to multi-risks events (Chiocci et al., 2011).

2. Geological setting

The Ustica-Anchise system is located at the eastern edge of the Elimi Chain (Fig. 1), between the Tyrrhenian Abyssal Plain, floored by young (< 5 Ma) and thin oceanic/transitional crust, and the Northern Sicily continental margin, characterized by a crustal thickness ranging from 25 to 40 km beneath the Apenninian-Maghrebian chain (Catalano et al., 2013). In the E-W direction the Elimi Chain lies above a variably thick continental crust, ranging from 25 km beneath the western Aeolian Islands to 30 km beneath the study area (Sulli, 2000). It results from the alignment of mainly metamorphic (Drepano) and volcanic (e.g. Aceste, Anchise, Ustica, Sisifo, Enarete, Eolo) seamounts and islands (Fig. 1). This area undergoes crustal shortening processes at about 1.5-2.5 mm/yr, as measured by geodetic data (Devoti et al., 2011), and is affected by moderate (Mw 6) crustal (15–20 km deep) compressional earthquakes with P-axes trending NW-SE (Chiarabba et al., 2005; Billi et al., 2007; Giunta et al., 2009) linked to the geodynamic setting in which the volcanic system of Ustica is inserted. One of the most important seismic sequences (about 50 shocks) as reported by Martinelli (1910) occurred in 1906. The parametric catalog of Italian earthquakes (Rovida et al., 2016) allows to estimate for this seismic sequences an energy released by the main shock corresponding to Mw=4.63 ± 0.46.

The volcanic island of Ustica is located approximately 58 km NW off the coast of Sicily (Fig. 1). It rises to 245 m a.s.l., but represents the emergent part of a larger and higher submarine volcanic complex. The island, elongated in a NE–SW direction, 4 km long and 2.5 km wide, is made up of lava flows and pyroclastic products, with alkali-basaltic to trachytic composition, lying above a basal formation formed by oldest pillow lavas, pillow breccias and hyaloclastic breccias (Cinque et al. 1988; Etiope et al. 1999).

The subaerial activity, which took place from 0.735 to 0.132 Ma (Barberi and Innocenti 1980; de Vita et al. 1995), was concentrated along fractures producing small eruptive centres with preferential E–W and NE–SW alignments (Alletti et al., 2005). Two shield-volcanoes, Costa del Fallo Mt. and Guardia dei Turchi Mt. (ca. 500 ka in age), are the main morphologic features of the island and bound a large collapsed caldera to the north; the well-preserved Falconiera volcano (130 ka) forms the eastern part of Ustica, while the Spalmatore Volcano and the Punta Cavazzi Volcano, partially destroyed, are located on the west side of the island.

A submarine saddle at depth between 700 and 1150 m connects the Ustica edifice with the Anchise volcanic seamount to the west, while a depression as deep as 2800 m separates it from the Sisifo, Enarete and Eolo volcanic seamounts to the east (Fig. 1). The Anchise seamount (Fig. 1) shows the orogenic volcanism typical of the whole southern Tyrrhenian area, which derives from a mantle enriched in incompatible elements for subduction (Peccerillo, 2003). The Ustica edifice, younger and much less affected by mantle enrichment, is considered an intraplate anorogenic volcano (Calanchi et al., 1984), and related to a wide crustal transtensional fault system (de Vita et al., 1995). The geochemical characteristics and petrography are similar to those of the eastern Sicily volcanism (Etna, Iblean Plateau; Fig. 1), leading Schiano et al. (2004) to hypothesize a large mantle plume beneath Sicily. A NE-SW relevant, gas-bearing structure is interpreted as a component of the mantle degassing in southern Italy (Etiope et al., 1999).

The structural framework of Ustica is dominated by N–S and NE–SW trending fault systems and N–S and E–W trending dikes (Bousquet and Lanzafame, 1992), well exposed in the western side of the island, which are coherent with the main regional tectonic lineaments; they are characterized generally by alternating extensional and compressional tectonic regimes with left-lateral component (Bousquet and Lanzafame, 1992) that activated during the Late Pleistocene the Arso fault systems in the south-western part of the island. This kinematic signature agrees with the recent geodynamic history of the Southern Tyrrhenian Sea (Billi et al., 2007).

Tectonic activity and erosional processes modified and/or obliterated the former volcanic structures. The morphological variety of the different sectors, both onland and offshore, are related to the recent morphotectonic evolution of Ustica (Romano e Sturiale, 1971, Cinque et., 1988; Furlani et al., 2017), as well as to the different exposure to marine-weather processes. The island is currently widely terraced at different topographic levels, because of the marine erosion related to sea level oscillations and the uplift of this area during the Pleistocene, while submarine abrasion platforms at 50, 75-85 and 90-110 m are evidence of low standing of the sea level (Romano and Sturiale, 1971; Cinque et., 1988; Furlani et al., 2017).

3. Materials and methods

3.1 Dataset

This study is based on data acquired from the Southern Tyrrhenian Sea between 1991 and 2009 (Fig. 2A), including:

Multibeam data, acquired during three oceanographic surveys carried out in 2001, 2004 (in the frame of the CARG project) as well as 2009 (MaGIC project). The 2001's survey was carried out on board of the R/V "Tethis" using a Reason SeaBat 8111 MultiBeam Echosounder (MBES), with a frequency of 100 kHz and operational depth range between 35 and 800 m. In 2004 and 2009, the research expeditions were carried out on board of the R/V "Universitatis" using a Reason SeaBat 8160 MBES, with a frequency of 50 kHz, and operational depth range of 30–3000 m. In all the scientific cruises, the acquisition was supported by a Differential Global Positioning System (DGPS) to obtain an accurate vessel position, a motion sensor to determine the attitude of the vessel in terms of pitch, roll and heave, and different CTD probes to measure electric conductivity and temperature, influencing the sound velocity in seawater. Bathymetric data were processed using the PDS-2000 software at the University of Palermo. Post-processing steps included the processing of navigation data, graphic removal of erroneous beams, noise filtering, and correction for sound velocity. The Digital Terrain Models (Fig. 2b) were produced using different cell sizes, from 2 to 20 m, according to the water depth and merged in a final DTM at 20 m. Maps were generated with open source GIS Software.

High-resolution seismic profiles, acquired during the 1991 cruise (Sicilia 1991) on board of the R/V Minerva-Uno, using a 1 kJ Sparker source and a single-channel streamer (Fig. 2A). During the 2004 survey a multi-tip Sparker array was used, with a base frequency of 600 Hz, fired every 12.5 m and recorded with a single-channel streamer with an active section of 2.8 m, containing seven high-resolution hydrophones, with a recording length of 3.0 s two way time (TWT) at 10 kHz sampling rate. Data processing of 2004 seismic data was performed using the Geo-Suite software running the following mathematical operators: trace mixing, time variant filters, automatic gain control, time variant gain and spherical divergence correction. Signal penetration was found to exceed 400 ms (t.w.t.t.) and the vertical resolution is up to 2.5 m at the seafloor.

Sub bottom profiles, which are about 600 km of high-resolution single-channel seismic reflection lines, acquired using a hull-mounted 4 to 16-transducers GeoAcoustics CHIRP II profiler (Fig. 2a). The instrument has an operating frequency ranging between 1.5 to 11.5 kHz, operational depth between 600 and 2000 m, and a pulse length of 32 ms. The sub bottom data were recorded and processed using the GeoTrace software by carrying out automatic gain control, time variant gain, swell filtering and muting.

3.2 Methods

The profiles were visualised and interpreted using Kingdom and GeoSuite Work software packages. We adopted an average velocity of 1512 m/s for the water and 1700 m/s for the Plio-Quaternary

sedimentary units. This velocity for the Plio-Quaternary sedimentary was derived from lithostratigraphy and sonic log data collected from a freely accessible database in the southern and western Sicilian offshore (VIDEPI Project: http://www.videpi.com/videpi/videpi.asp).

The Digital Terrain Models, obtained from Multibeam data, were the base for morphological mapping and for quantitative morpho-structural analysis.

The morphological mapping was carried out with the Global Mapper software, which allows different main groups of submarine morphological elements to be identified and mapped: channelized features, mounds, escarpments, terraces, scars.

Since the development/application of multibeam techniques in seafloor surveys, an increasing number of papers has demonstrated utility of quantitative morphometric techniques in improving the geological interpretation of submarine features in different settings (Llanes et al., 2009). Considering the geological context of the Ustica volcanic edifice, we focused the quantitative analysis on the mounds, identified as generic, more or less rounded, features rising from the seabottom, whose nature will be debated in the Discussion section.

We selected the 14 biggest mounds, and for all them we measured the minimum (d), maximum (D) and mean axis, minimum axis/2 (R), basal surface (Sb), perimeter base (Pb), height (H), summit (Sd) and basal (Bd) depth, diameter of summit (ds), minimum, maximum and mean slope. We also estimated the volume (V), basal ratio (bsr, d/D), mean height vs. radius (H/R), and flatness (f= (ds / 2)/d). This method has been proposed in Scheirer and Macdonald (1995) and Rappaport et al. (1997) and successively modified by Romero Ruiz et al. (2000) and Spatola et al. (2018). We used the "Cut and Fill" tool to estimate the volume of the mounds. The bases of the features were identified by sharp breaks of slope in the cross-sectional profile using the high-resolution multibeam data.

4. Results

4.1 Seismostratigraphy

The Sub bottom profiles (Fig. 3A) as well as the high-resolution seismic profiles (Fig. 3B) allowed us to identify five main acoustic facies:

(i) Facies A (the deepest) is an acoustically semi-transparent to transparent seismic facies. It occurs all over the study area. It is always bounded at the top by a high-amplitude and discontinuous reflector (Fig. 3A).

(ii) Facies B comprises subparallel, high-amplitude reflectors with good lateral continuity, which alternate with low-amplitude reflectors (Figs. 3A, 3B). It infills basins or drapes low-gradient seafloor areas.

(iii) Facies C is an acoustically impenetrable body with a strong upper reflection and is associated with buried positive relief features (Fig. 3A).

(iv) Facies D occurs mainly on top of facies B. It consists of chaotic seismic reflector packages where continuous reflectors cannot be identified. It corresponds to bodies with an irregular shape and variable thickness, not more than some tens of milliseconds, forming a hummocky surface (Fig. 3A). It is present discontinuously along the slopes and at their toe.

(v) Facies E consists of three main sub-facies, which are organized as follows: Facies E1 has high-amplitude reflectors with poor to good lateral continuity with evidence of irregular gentle folding (Fig. 3B). Facies E2 consists of high-amplitude discontinuous reflectors strongly folded forming clear hyperboles geometry (Fig. 3B). Facies E3 has an internal configuration predominantly showing strong-reflectivity, discontinuously dipping or wavy reflectors. A very high-amplitude reflector that coincides with the top of the sub-facies E1 marks its base (Fig. 3B).

4.2 Morphology

Our study highlighted for the first time the still unknown morpho-structural features of the Ustica continental shelf and slope system, developing in a total area of 2020 km^2, with a depth ranging between 8 m and 3330 m. We divided the study area into four zones, based on morphological/seismostratigraphic features: Zone A, Zone B, Zone C, and Zone D (Fig. 2B), and we present our main observations accordingly in following chapters.

In the northern part (Zone A in Fig. 2B), the continental shelf has a maximum width of 1500 m and average gradient of about 2.5°, narrowing considerably to about 800 m eastward, where it becomes steeper, up to 6° (Fig. 4B). In the western region (Zone B in Fig. 2B), the shelf reaches the maximum width, 1800 m, in the whole offshore of Ustica, with gradient decreasing progressively from 4° to 1° (Fig. 4B). The shelf break is deep up to 120 m, except in the southern part (Zones B, C in Fig. 2B) where the continental shelf is almost absent and the steep and rugged seafloor, which is widely affected by channels, quickly reaches high depths. In the south-western part (Zone B in Fig. 2B), the shelf appear to be largely eroded.

The continental slope has variable gradients in the different sectors, meanly 15° down to a depth of 2000 m, gradually decreasing at deeper depths (Figs. 4A, B), but at places they exceed 40°. The minimum gradient is measured in the western region, about 10° less sloping than the rest of the island (Fig. 4B). On the whole the general morphology appears very rugged and affected by different morphological elements that are characteristic of definite sectors of the offshore of Ustica.

We have identified and distinguished different main groups of submarine morphological elements: channalized features, mounds, escarpments, terraces, scars (Fig. 4A).

4.2.1 Channelized features

More than 130 channelized features (channels and gullies) extend along the submarine flank of Ustica and surrounding continental slope, acting as transport paths for sediment supply (mainly terrigenous to bioclastic material) from the island (Figs. 4A, 5, 6). Some of them are conditioned by the rough seabed morphologies and show a tortuous pattern, while others follow lineaments or main gradient assuming straight, often parallel, directions. Most of them have slopes along the thalweg that decrease from about 14° to about 10° (Fig. 4B). The main channels and gullies were found at and below the insular shelf edge, where the gradients are higher and erosion could act more deeply. The gradient decreases considerably at depths higher than 1000 m, and consequently the erosion along the thalweg is reduced.

4.2.2 Mounds

More than 100 conical-shaped mounds have been recognized on the Ustica submarine flanks down to a water depth of about 2115 m (Figs. 4A, 5A), most of which are located in the northern region (Fig. 2B). The mounds have circular, elliptic or irregular base, while the 3D shapes range from very irregular to perfectly conical. They are either aligned ENE-WSW or NNW-SSE or occur as isolated features (Figs. 4A, 5A).

One of the biggest mounds is the Banco Apollo (BA in Fig. 4A, A in Figs. 5A, 6A), which has been mapped close to the shelf edge in the western zone. It consists of two large cone-shaped mounds (A1 and A2 in Table 1 and Fig. 6). It is altogether ~2000 m long and ~1300 m wide and has a conical-shape, and it is associated to a NE-SW directed depression bounded downward by a positive-relief circular structure, developed at a depth from ~50 to ~450 m, on a surface of 1.8 km2. The gradient is 23° to 29° in the upper part, decreases at 12° just up-slope of the positive-relief structure, where it reaches again 27°, decreasing downward of the relief. Its top is at the depth of the shelf break (about 120 m). We correlate the flat morphology with the Last Glacial Maximum (Caruso et al. 2011) and we infer that the Banco Apollo was emerged during the post-LGM.

All the measured and estimated morphological parameters of the biggest mounds (A-N in Fig. 5A) are tabulated in Table 1. Some values, such as the volumes, were calculated approximating the forms to a regular shape (Rappaport et al., 1997; Romero Ruiz et al., 2000).

We also mapped about 90 ridges, which are variably distributed across the study area, and they mainly are aligned about NE-SW, and NW-SE (Fig. 4A).

4.2.3 Escarpments

The continental slope appears on the whole intensively affected by more than 150 very steep escarpments (Figs. 4A, 5A, 6A-B, 7). They are almost straight lineaments, bounding raised and lowered sectors. Three main set of escarpments and lineaments were recognized, NE-SW to E-W, N-S, and NW-SE (Fig. 4A). Some of these trends are the same that were recognized in the Ustica Island (Cinque et al., 1988; De Vita et al., 1998; Etiope et al., 1999).

The longest escarpment (E1 in Fig. 4A, 6A-B, 7) has been recognized in the south-western region (Zone B in Fig. 2B). It is about 11 km long, up to ~280 m high, and has a NE-SW trend. A smaller N-S trending escarpment (~180 m in high) displaces E1. The seismic reflection profile shown in Fig. 7, acquired across the southern region of the study area, shows two escarpments playing an important role in the shaping of the seafloor. These escarpments involve both the seafloor and the sedimentary multilayer of the sub-seafloor (Fig. 7). The seismic line displays also offset seismic reflectors in the sub-seafloor that seem to be linked to the escarpments (Fig. 7). The second longest escarpment (E2 in Fig. 4A) that is 9 km long has been recognized in the Zone C (Fig. 2B) in the south-easternmost region. It is oriented about NE-SW and is affected by five NW-SE channelized features (Fig. 4A). The third escarpment in length is located in the Zone B (Fig. 2B) in the western region. It is 6 km long and has a N-S trend (E3 in Fig. 4A).

4.2.4 Terraces

We mapped a total length of about 18 km of submarine outer margin of terraces (OMT) which are associated with three main sub-horizontal portions of the seabed (Figs. 4A, 5A, 6A-B). The surfaces of these terraces are smooth, up to 1.2 km in width, and slope at 2° (Fig. 4A-B). They are characterized by a clear concave break of slope along the Zones B (west) and D (east), and share similar orientation to the fault-related escarpments above-mentioned (Fig. 2A). These terraces are elongated about N-S, and their seafloor morphology is smooth and gently-inclined, in places appearing as step-like (Figs. 4A, 5A, 6A). In the western part of the study area, the terraces are narrower to the south and broaden to the north (Figs. 4A, 6A).

4.2.5 Scars

More than 150 scars have been identified and mapped across the offshore of Ustica (Fig. 4A, 6A, 7). They often are associated to seafloor positive-relief structures with different shape, size and depth forming a hummocky surface (Figs. 3A, 4A, 6A-B). The headwalls of the scars are generally linear to arcuate, and steep (10–25°) (Fig. 4A-B). Most of the mapped scars are connected to either another scar or an escarpment at their distal limit.

The smaller scars indent at places the shelf edge (Fig. 4A). They have headwalls 100 m high and an average width of 0.5 km. The edge of the largest escarpment (E1 in Figs. 4A, 6A-B, 7) is deeply incised by a large U-shaped scar composed by theatre-shaped heads (S1 in Figs. 4A, 6A, 7). S1 has headwalls ~250 m high and a width of almost ~2 km, steep up to 20°. It is often associated with large seafloor positive-relief features forming a clear hummocky surface (HM in Figs. 4A, 6A-B). This scar is located at a water depth of more than 650 m (S1 in Figs. 4A, 6A, 7), and covers an area of tens of km2, a perimeter of more than 10 km, and develops in steep slopes. HM1 (Figs. 4A, 6A-B) was recognized at a depth of 750 m, covers an area of 3.5 km2 and develops in a 15° steep slope downward of an uneven indented shelf break. It is formed by wavy high amplitude reflectors as shown by the single-channel sparker profile (Fig. 7).

5. Discussion

5.1 Volcanic processes

We interpret the identified mounds and ridges as volcanic morphologies. Volcanic activities have been already described only on land in the Ustica Island. It consists of mainly subaerial volcanic products, generated from 0.735 to 0.132 Ma (Barberi and Innocenti 1980; de Vita et al. 1995), lying above submarine volcanics (Cinque et al. 1988; Etiope et al. 1999). Similarly, we hypothesize that the cluster of the recognized submarine mounds could be related to volcanic activity affecting the Anchise-Ustica System. Our interpretation is supported by:

1. mound shape and morphometry: a) the basal ratio values of the mapped mounds (bsr in Table 1), which are <1 as the typical submarine volcanic seamounts, according to Rappaport et al. (1997) and Romero Ruiz et al. (2000); b) the flatness values of the mounds (f in Table 1), between 0.03 and

0.12 for the submarine morphology with a cone shape, 0.2 and 0.31 for the flattened truncated cone shape. These values are in accordance with Rappaport et al. (1997), which show that the flatness of submarine volcanic edifices varies from 0.01 (a pointy cone) to 0.57 (a flattened truncated cone).

2. seismic facies: the sub bottom of Figs. 3A shows an acoustic facies (Facies C) that has very strong analogies with the facies described along the NW Sicily Channel, which has been interpreted as volcanic rocks (Civile et al., 2010; Spatola et al., 2018). The high-resolution seismic profile of Fig. 3B shows a complex seismic facies (Facies E1-3). The seismic features of the sub-facies E1, which is composed of alternating parallel and folded reflectors, could be generated by a multilayer of lava flows and pyroclastic products. This seismic body, which represent the largest volume of the Ustic complex, shows an asymmetric shape in section view, considering that it becomes thicker towards the north, suggesting an upward and northward growth of the volcanic edifice (Fig. 3B). The sub-facies E2, characterized by hyperboles geometry, can be ascribable to the oldest pillow lavas, pillow breccias and hyaloclastic breccias, in accordance to Cinque et al. (1988) and Etiope et al. (1999), as well as for the similarity of this facies with those generated by submarine basalts (Catalano et al., 2000; Aiello et al., 2012). The sub-facies E3 can be interpreted as produced by lava flows, considering the wavy internal geometry in the seismic section, and its tabular external shape, as shown by the morphobathymetric data.

3. positive Bouguer anomalies: a detailed gravimetric map of the southern region of the central Mediterranean Sea (Barreca, 2014) shows on the study area gravimetric anomalies similar to those occurring in areas where volcanic activity has been documented (e.g. Graham Bank in the NW Sicily Channel).

4. magnetic anomalies: the magnetic anomalies map of Italy shows around the study area high values that could be interpreted as signature of surface volcanism (AGIP s.p.a. 1994). The magnetic anomalies have high similarity with the values of Marsili Abyssal Plain, Aeolian Islands, and Graham Bank (Calanchi et al., 1984).

Two main morphological kind of submarine volcanoes were distinguished in the study area. We suggest this morphological feature depends on two different typology of submarine eruptions: (i) emission (leakage) of magma from a single source point; (ii) fissional eruptions from a linear source, which produce characteristic shapes such as ridges.

The largest mounds (e.g. Banco Apollo) pertain to the first type. The occurrence of a crest on the flat morphology at the top of the Banco Apollo could be due to the preservation of harder rocks during the phases of submarine and/or subaerial erosion (Fig. 7). While, the minor mounds and the ridges form adjacent aligned seamounts and have been classified as the results of fissional eruptions. They are mainly organized with ENE-WSW and NNW-SSE trends. These trends are also the main trends of faults and volcanic dykes on land and are confirmed by the magnetic anomalies map (Calanchi et al., 1984). These structures are located in the zone A, where probably a greater magmatic rise is produced by fissuration along zones of crustal weakness associated with tectonics.

The main occurrence of preserved submarine volcanoes in the northern region (Fig. 2B, 4A, 5A), the convex-upward shape of the topographic profile along the northern slope, and the upward and northward growth of the volcanic edifice (Fig. 3B) could point out the northward migration of the volcanic activity in the last 130 ky, which is the age of the more recent volcanic activity in the Ustica island.

5.2 Tectonic processes

We interpret the sets of escarpments and straight lineaments as morphological seafloor expressions of faults (Fig. 8). Most of these faults are restricted to the offshore area, although a few of them constitute extensions of outcropping faults.

The most important escarpment (E1 in Figs. 4A, 6A-B, 7,) seems to represent the offshore extension of the N60°E Arso Fault that is the longest outcropping fault. It appears offset by a smaller N-S fault, and onland it is also affected by conjugated synthetic faults (Cinque et al., 1988; De Vita et al., 1998 Etiope et al., 1999). These evidences are signature of alternative extensional and compressional deformations phases (Billi et al, 2007). The Arso Fault together with the N-S fault develops in the southern slope where they are trigger for extensive slope instabilities (Figs. 4A, 6A-B, 7, 9). This deformational system, which forms a widespread set of NE-SW and E-W oriented faults, fractures, and dykes, affecting mainly the western part of Ustica Island and relative offshore region, can be correlated to the transtensional to transpressional system already described in this area (Agate et al., 2000; Sulli, 2000). Extensional to transtensional kinematics of the N-S and NW-SE fault systems is inferred from correlation with onland tectonics and seismic reflection data from adjacent sectors (Agate et al., 2000).

5.3 Erosional processes

The numerous channelized features, evidenced for the first time by the high-resolution morpho-bathymetric data along the slope, show high similarity with the features described by Lo Iacono et al. (2011) along the offshore of Palermo. They are interpreted as submarine erosional channels, generic incisions and gullies. They are mainly erosional grooves, which act as preferential transport routes for the sediment supply from both land and shallow water areas. They show different morphological characteristics (depth, width, length, longitudinal and transverse section, and sinuosity) according to their distribution and genetic mechanisms.

The gullies along the southern and eastern region are usually linked to circular scars suggesting retrogressive movements (Klaus and Taylor 1991; Mulder et al. 2006). Retrogressive movements along the slope facilitate the upslope propagation of the channelized features towards the shelf margin (Lo Iacono et al. 2011, Mitchell 2005).

The channelized features are almost straight structures, with ENE-WSW, N-S and NNW-SSE trends. They develop from the shelf edge (-120 m) to the lower slope (-1570 m), mainly in the southern and eastern regions. Whilst, the channelized features along the northern slope follow the path imposed by

the volcanic structures. Finally, in the western slope they follow the fault direction, enhancing their morphologies due to the erosional processes. In this area, they have minor slopes (about 1° - 4°), owing to the tectonic uplift, which affected the western slope (Furlani et al., 2017).

The terraces that are bordered by minor escarpments are interpreted as shore platforms formed by subaerial weathering as well as by wave erosion during the last marine transgression when the sea level raised relative to the land and the shoreline moves toward higher ground, resulting in flooding.

5.4 Slope Failures

The morphobathymetric and seismic reflection data show that the slope failures along the margin have played a key role in shaping of the seafloor of the offshore of Ustica in both the northern and southern regions, where the shelf get narrower in relation to retrogressive gravitational processes.

We interpret the scars identified as evidence for slope instability, and we suggest as main style of deformation affecting the area:

(i) translational sliding, as suggested by the linear to arcuate steep headwalls (Fig. 9) and relative smooth and planar scars (Micallef et al. 2019; Locat and Lee, 2002);

(ii) debris avalanche (sensu Hampton et al., 1996) sourced by the volcanic seamount through the gullies, because most of the failed material has been evacuated from the scars. The typical morphologies associated with a debris avalanche are an amphitheater depression, which corresponds to the source area, and a hummocks topography in correspondence of the deposit with irregularly scattered hills on the surface (Hampton et al., 1996), which correspond to large blocks immersed into fine-grained sediments.

The seismostratigraphic analysis of the seismic lines shown in Figs. 6, 8 allow us to identify a debris avalanche along the south-eastern slope in correspondence of volcanic morphologies. The seismic lines shows that acoustic facies D (Figs. 3A, 7) is generated by an isolated body with variable thicknesses, and a rugged external shape (hummocky surface). It has been interpreted as a chaotic deposit linked to slope failures according to Masson et al. (2008), Sulli et al. (2013, 2018).

The most likely preconditioning factor for slope failure is over-steepening and loss of support because of the volcanic and tectonic activities affecting the area. While we suggest fault systems and associated seismicity as main trigger. The region between the Arso Fault (E1) and the N-S fault escarpment (E3) is subject to tectonic stress, which generate slope instability, causing several collapses and large breaks of slope.

6. Conclusions

For the first time, the combination of multibeam, sub bottom and Sparker seismic data reveals the geomorphic and structural features along the offshore of Ustica with high-resolution. The main conclusions of this paper are:

1) The northern region is mainly characterized by volcanic features such as cone shape and flattened truncated cone shape volcanoes whose genesis can be easily attributed to magmatic rising associated to the N-S and NW-SE extensional to transtensional fault systems. The presence of submarine volcanoes only in the northern region and the asymmetric growth of the whole volcanic complex points out a northward migration of the volcanic activity in the last 130 ky, which could be related to the plate margin kinematics.

2) The western region is mainly characterized by fault escarpments such as the ~11 km-long ENE-WSW trending Arso Fault. This region is also affected by the bigger slope failures documented in this paper and by numerous N-S channelized features.

3) The southern region is characterized by a narrow continental shelf, widely affected by erosional processes, and very steep continental slope, mainly its upper part. The area mainly hosts the smaller volcanic features, volcanic ridges and slope failures.

4) The eastern region is dominated by channelized features, which develop along the steep and irregular slope from the shelf break down to a depth of 1500 m as well as by NE-SW fault escarpments and NE-SW ridges.

All these zones individuate areas with prevailing marine hazards, which are related to the occurrence of submerged volcanic structures, fault systems and fractures, at local and regional scale, slope failures, and erosional channel. This complex morpho-strucutral setting is enhanced by the strong widespread seismicity of this area, which is located just along the Africa-Eurasia plate margin.

Acknowledgements

We acknowledge the CARG (Geological Maps of Italy) funded by the Italian Geological Survey and the Italian National Research Projects MaGIC (Marine Geological Hazard along the Italian Coast) funded by the Italian Civil Protection Department. We thank also the captains and the crews of the R/V ‘‘Thetis’’ and R/V ‘‘Universitatis’’ for their assistance during the surveys.

References

Agate, M., Beranzoli, L., Braun, T., Catalano, R., Favali, P., Frugoni, F., Pepe, F., Smriglio, G., Sulli A., 2000. The 1998 offshore NW Sicily earthquakes in the tectonic frame work of the southern border of the Tyrrhenian Sea. Mem. Soc. Geol. It. 55, 103-114.

AGIP s.p.a. 1994. Carta Aeromagnetica d'Italia Scala 1:1000000. Istituto Poligrafico e Zecca dello Stato. Servizio Geologico, Roma.

Aiello, G., Marsella, E., Passaro, S., 2012. Stratigraphic and structural setting of the Ischia volcanic complex (Naples Bay, Southern Italy) revealed by submarine seismic reflection data. Rendiconti Lincei 23(4), 387-408.

Alletti, M., Pompilio, M., Rotolo, S.G., 2005. Mafic and ultra-mafic enclaves from Ustica Island lava: inferences on deep magmatic processes. Lithos 84, 151–167.

Barberi, F., Innocenti, F., 1980. Volcanisme Neogene et Quaternarie. Guide a l'excursion. Società Italiana di Mineralogia e Petrologia 122A, 99–104.

Barreca, G., 2014. Gravimetric gradient, Sicily and southern Calabria, Italy (Central Mediterranean). Journal of Maps 10(4), 563-568.

Billi, A., Barberi, G., Faccenna, C., Neri, G., Pepe, F., Sulli, A., 2006. Tectonics and seismicity of the Tindari Fault System, southern Italy: crustal deformations at the transition between ongoing contractional and extensional domains located above the edge of a subducting slab. Tectonics 25(2), TC2006. https://doi.org/10.1029/2004TC001763.

Billi, A., Presti, D., Faccenna, C., Neri, G., Orecchio, B., 2007. Seismotectonics of the Nubia plate compressive margin in the south-Tyrrhenian region, Italy: clues for subduction inception. J. Geophys. Res. 112, B08302, doi:10.1029/2006JB004837.

Bousquet, J.C., and Lanzafame, E.G., 1992. Evidence of north-south compression at Ustica (southern Tyrrhenian Sea) – CNR IIV Open File Rep 2 (93), 1-6.

Bousquet, J.C., and Lanzafame, G., 1995. Transition from Tyrrhenian basin extension to collisional tectonics: evidence of N-S compression during the recent Quaternary at Ustica (southern Tyrrhenian Sea, Italy). CR Acad. Sci. Paris 321 (IIa), 781–787.

Calanchi, N., Colantoni, P., Gabbianelli, G., Rossi, P. L., Serri, G., 1984. Physiography of Anchise Seamount and of the submarine part of Ustica Island (South Tyrrhenian): petrochemistry of dredged volcanic rocks and geochemical characteristics of their mantle sources. Miner. Petrogr. Acta 28, 215-241.

Caruso, A., Cosentino, C., Pierre, C., Sulli, A., 2011. Sea-level changes during the last 41,000 years in the outer shelf of the southern Tyrrhenian Sea: evidence from benthic foraminifera and seismostratigraphic analysis. Quaternary International 232(1-2), 122-131.

Catalano, R., Franchino, A., Merlini, S., Sulli, A., 2000. Central western Sicily structural setting interpreted from seismic reflection profiles. Memorie della Società Geologica Italiana 55, 5-16.

Catalano, R., Valenti, V., Albanese, C., Accaino, F., Sulli, A., Tinivella, U., Gasparo Morticelli, M., Zanolla, C., Giustiniani M., 2013. Sicily's fold/thrust belt and slab rollback: The SI.RI.PRO. seismic crustal transect. – J. Geol. Soc., London 170, 451-464.

Casalbore, D., 2018. Volcanic islands and seamounts. In Micallef, A., Krastel, S., Savini, A. 2018 (Eds.) Submarine Geomorphology (pp. 333-347). Springer, Cham.

Chadwick, Jr, W. W., Cashman, K. V., Embley, R. W., Matsumoto, H., Dziak, R. P., De Ronde, C. E. J., Lau, T. K., Deardorff, N. D., Merle, S. G., 2008. Direct video and hydrophone observations of submarine explosive eruptions at NW Rota-1 volcano, Mariana arc. Journal of Geophysical Research: Solid Earth 113(B8).

Chiarabba, C., Jovane, L., Di Stefano, R., 2005. A new view of Italian seismicity using 20 years of instrumental recordings. Tectonophysics 395, 251–268.

Chiocci, F.L., Romagnoli, C., Bosman, A. 2008. Morphologic resilience and depositional processes due to the rapid evolution of the submerged Sciara del Fuoco (Stromboli Island) after the December 2002 submarine slide and tsunami. Geomorphology 100:356–365. https:// doi.org/10.1016/j.geomorph.2008.01.008

Cinque, A., Civetta, L., Orsi, G., Peccerillo, A., 1988. Geology and geochemistry of the island of Ustica (Southern Tyrrhenian Sea). Rend. Soc. It. Mineral. Petrol. 43, 987-1002

Civile, D., Lodolo, E., Accettella, D., Geletti, R., Ben-Avraham, Z., Deponte, M., Facchin, L., Ramella, R., Romeo, R., 2010. The Pantelleria graben (Sicily Channel, Central Mediterranean): an example of intraplate 'passive'rift. Tectonophysics 490(3-4), 173-183.

Conte, A. M., Martorelli, E., Calarco, M., Sposato, A., Perinelli, C., Coltelli, M., Chiocci, F. L., 2014. The 1891 submarine eruption offshore Pantelleria Island (Sicily Channel, Italy): Identification of the vent and characterization of products and eruptive style. Geochemistry, Geophysics, Geosystems 15(6), 2555-2574.

Devoti, R., Esposito, A., Pietrantonio, G., Pisani, A. R., Riguzzi, F., 2011. Evidence of large scale deformation patterns from GPS data in the Italian subduction boundary. Earth and Planetary Science Letters 311(3-4), 230-241.

de Vita, S., Guzzetta, G., Orsi, G., 1995. Deformational features of the Ustica volcanic island in the Southern Tyrrhenian Sea (Italy). Terra Nova 7(6), 623-629.

de Vita, S., Laurenzi, M.A., Orsi, G., Voltaggio, M., 1998. Application of 40Ar/39Ar and 230Th dating methods to the chronostratigraphy of Quaternary basaltic volcanic areas: the Ustica island case history. Quaternary International 47/48, 117-127.

Etiope, G., Beneduce, P., Calcara, M., Favali, P., Frugoni, F., Schiattarella, M., Smriglio, G., 1999. Structural pattern and CO2 - CH4 degassing of Ustica Island, Southern Tyrrhenian Basin. Journ. Volcanol. Geotherm. Res. 88, 291 – 304.

Furlani, S., Antonioli, F., Cavallaro, D., Chirco, P., Caldareri, F., Martin, F. F., ... and Biolchi, S., 2017. Tidal notches, coastal landforms and relative sea-level changes during the Late Quaternary at Ustica Island (Tyrrhenian Sea, Italy). Geomorphology 299, 94-106.

Giunta, G., Luzio, D., Agosta, F., Calò, M., Di Trapani, F., Giorgianni, A., Oliveri, E, Orioli, S., Perniciaro, M., Vitale, M., Chiodi, M., Adelfio, G., 2009. An integrated approach to investigate the seismotectonics of northern Sicily and southern Tyrrhenian. Tectonophysics 476, 13-21.

Harris, P. T., Macmillan-Lawler, M., Rupp, J., Baker, E. K., 2014. Geomorphology of the oceans. Marine Geology 352, 4-24.

Hampton, M. A., Lee, H. J., Locat, J., 1996. Submarine landslides. Reviews of geophysics 34(1), 33-59.

Innangi, S., Di Martino, G., Romagnoli, C., Tonielli, R., 2019. Seabed classification around Lampione islet, Pelagie Islands Marine Protected area, Sicily Channel, Mediterranean Sea. Journal of Maps 15(2), 153-164.

Klaus, A., and Taylor, B., 1991. Submarine canyon development in the Izu-Bonin forearc: A SeaMARC II and seismic survey of Aoga Shima Canyon. Marine Geophysical Researches 13(2), 131-152.

Llanes, P., Herrera, R., Gómez, M., Muñoz, A., Acosta, J., Uchupi, E., Smith, D., 2009. Geological evolution of the volcanic island La Gomera, Canary Islands, from analysis of its geomorphology. Marine Geology 264(3-4), 123-139.

Locat, J., and Lee, H. J., 2002. Submarine landslides: advances and challenges. Canadian Geotechnical Journal 39(1), 193-212.

Lo Iacono, C., Sulli, A., Agate, M., Presti, V. L., Pepe, F., Catalano, R., 2011. Submarine canyon morphologies in the Gulf of Palermo (Southern Tyrrhenian Sea) and possible implications for geo-hazard. Marine Geophysical Research 32(1-2), 127.

Martinelli, G., 1910. La sismicità all'isola di Ustica e il periodo marzo-aprile 1906. Annali dell'Uff. Centr. Meteorologico e Geodinamico italiano, vol. XXX, I, Roma, 1910. Tipografia Nazionale G. Bertero & c, Roma (16 pp).

Masson, D. G., Le Bas, T. P., Grevemeyer, I., Weinrebe, W., 2008. Flank collapse and large-scale landsliding in the Cape Verde Islands, off West Africa. Geochemistry, Geophysics, Geosystems 9(7), 1-16, doi:10.1029/2008GC001983

Micallef, A., Camerlenghi, A., Georgiopoulou, A., Garcia-Castellanos, D., Gutscher, M. A., Lo Iacono, C., Huvenne, V. A. I., Mountjoy, J. J., Paull, C. K., Le Bas, T., Spatola, D., Facchin, L., Accettella, D., 2019. Geomorphic evolution of the Malta Escarpment and implications for the Messinian evaporative drawdown in the eastern Mediterranean Sea. Geomorphology 327, 264-283.

Mitchell, N. C., 2005. Interpreting long-profiles of canyons in the USA Atlantic continental slope. Marine Geology 214(1-3), 75-99.

Mulder, T., Lecroart, P., Hanquiez, V., Marches, E., Gonthier, E., Guedes, J. C., Thiébo, E., Jaaidi, B., Kenyon, N., Voisset, M., Perez, C., Sayago, M., Fuchey, Y., Bujan, S., 2006. The western part of the Gulf of Cadiz: contour currents and turbidity currents interactions. Geo-Marine Letters 26(1), 31-41.

Nomikou, P., Papanikolaou, D., Alexandri, M., Sakellariou, D., and Rousakis, G., 2013. Submarine volcanoes along the Aegean volcanic arc. Tectonophysics 597, 123-146.

Peccerillo, A., 2003. Plio-quaternary magmatism in Italy. Episodes 26(3), 222-226.

Quartau, R., Hipólito, A., Romagnoli, C., Casalbore, D., Madeira, J., Tempera, F., Roque, C., Chiocci, F. L., 2014. The morphology of insular shelves as a key for understanding the geological evolution of volcanic islands: Insights from Terceira Island (Azores). Geochemistry, Geophysics, Geosystems 15(5), 1801-1826.

Ramalho, R. S., Quartau, R., Trenhaile, A. S., Mitchell, N. C., Woodroffe, C. D., Ávila, S. P., 2013. Coastal evolution on volcanic oceanic islands: A complex interplay between volcanism, erosion, sedimentation, sea-level change and biogenic production. Earth-Science Reviews 127, 140-170.

Rappaport, Y., Naar, D. F., Barton, C. C., Liu, Z. J., Hey, R. N., 1997. Morphology and distribution of seamounts surrounding Easter Island. Journal of Geophysical Research: Solid Earth 102(B11), 24713-24728.

Romano, R., Sturiale, C. 1971. L'isola di Ustica: Studio Geo-vulcanologico e Magmatologico. Rivista Minerararia Siciliana 22, 3–61.

Romero Ruiz, C., García-Cacho, L., Araña, V., Luque, A. Y., Felpeto, A. 2000. Submarine volcanism surrounding Tenerife, Canary Islands: implications for tectonic controls, and oceanic shield forming processes. Journal of volcanology and geothermal research 103(1-4), 105-119.

Rovida, A., Locati, M., Camassi, R., Lolli, B., Gasperini, M., 2016. CPTI15, the 2015 Version of the Parametric Catalogue of Italian Earthquakes. Istituto Nazionale di Geofisica e Vulcanologia (CPTI15-DBMI15).

Savelli, C., 1988. Late Oligocene to Recent episodes of magmatism in and around the Tyrrhenian Sea: implications for the processes of opening in a young inter-arc basin of intra-orogenic (Mediterranean) type. Tectonophysics 146(1-4), 163-181.

Scheirer, D. S., Macdonald, K. C., 1995. Near-axis seamounts on the flanks of the East Pacific Rise, 8° N to 17° N. Journal of Geophysical Research: Solid Earth 100(B2), 2239-2259.

Schiano, P., Clocchiatti, R., Ottolini, L., Sbrana, A., 2004. The relationship between potassic, calc-alkaline and Na-alkaline magmatism in South Italy volcanoes: a melt inclusion approach. Earth and Planetary Science Letters 220(1-2), 121-137.

Smith, D. K., 1988. Shape analysis of Pacific seamounts, Earth Planet. Sci. Lett. 90, 457-466,

Spatola, D., Micallef, A., Sulli, A., Basilone, L., Ferreri, R., Basilone, G., Bonanno, A., Pulizzi, M., Mangano, S. (2018). The Graham Bank (Sicily Channel, central Mediterranean Sea): Seafloor signatures of volcanic and tectonic controls. Geomorphology 318, 375-389.

Sulli, A., 2000. Structural framework and crustal characters of the Sardinia Channel alpidic transect in the central Mediterranean. Tectonophysics 324, 321–336.

Sulli, A, Lo Presti, V, Gasparo Morticelli, M, Antonioli, F., 2013. Vertical movements in NE Sicily and its offshore: outcome of tectonic uplift during the last 125 ky. Quaternary International 288:168–182. https://doi.org/10.1016/j.quaint.2012.01.021

Sulli, A., Zizzo, E., Albano, L., 2018. Comparing methods for computation of run-up heights of landslide-generated tsunami in the Northern Sicily continental margin. Geo-Marine Letters 38(5), 439-455.

Tepp, G., Chadwick Jr, W. W., Haney, M. M., Lyons, J. J., Dziak, R. P., Merle, S. G., Butterfield., D.A., Young III, C. W. (2019). Hydroacoustic, Seismic, and Bathymetric Observations of the 2014 Submarine Eruption at Ahyi Seamount, Mariana Arc. Geochemistry, Geophysics, Geosystems 20(7), 3608-3627.

Trua, T., Serri, G., Marani, M. P., 2003. Lateral flow of African mantle below the nearby Tyrrhenian plate: geochemical evidence. Terra Nova 15(6), 433-440.

Urgeles, R., Canals, M., Baraza, J., Alonso, B., Masson, D., 1997. The most recent megalandslides of the Canary Islands: El Golfo debris avalanche and Canary debris flow, west El Hierro Island. Journal of Geophysical Research: Solid Earth 102(B9), 20305-20323.

Wright, L. D., Friedrichs, C. T., 2006. Gravity-driven sediment transport on continental shelves: a status report. Continental Shelf Research 26(17-18), 2092-2107.

Figure captions

Fig. 1. Bathymetric map of the southern Tyrrhenian Sea showing the main morphological-structural features. Background bathymetry is from EMODnet bathymetry (http://www.emodnet-bathymetry.eu). AS: Anchise Seamount, UV: Ustica Volcano, AI: Aeolian Islands, EI: Egadi Islands.

Fig. 2. A) Study area showing seismic reflection profiles and multibeam data (highlighted the seismic lines displayed in this paper). B) Different zones of the offshore of Ustica based on the morpho-structural setting of the seafloor.

Fig. 3. A) Sub bottom profile acquired on the south-eastern region of the study area showing the identified acoustic facies as well as the seafloor morphology, with hummocky surface and channelized features. B) High resolution seismic line (Sparker source) acquired on the eastern region showing channelized features, offset seismic reflectors. Location of the seismic profiles is shown in Fig. 2A.

Fig. 4. A) Map of principal morphologic elements and features identified across the study area, draped on a shaded relief map of the seafloor. B) Slope map of the study area.

Fig. 5. A) 3D shaded relief bathymetric map showing the main morpho-structures across the northern offshore of Ustica. OMT: Outer Margin Terrace. Vertical exaggeration 1:1.5. B-C) Topographic profiles across the study area. Direction of profiles is illustrated in A. See Table 1 for detail.

Fig. 6. B) 3D shaded relief bathymetric map showing the main morpho-structures of the southern offshore of Ustica. OMT: Outer Margin Terrace. Vertical exaggeration 1:1.5. B-C) Topographic profiles across the study area. Direction of profiles is illustrated in A.

Fig. 7. High resolution seismic line (Sparker source) acquired on the south-western region of the study area showing the escarpments (E1), channelized features, offset seismic reflectors. Location of the seismic profiles is shown in Fig. 2A.

Fig. 8. High resolution seismic line (Sparker source) acquired in the southern region of the study area showing the complexity of the seafloor morphology with escarpments and channelized features. The seismic lines also shows offset seismic reflectors. Location of the profiles is shown in Fig. 2A.

Fig. 9. Sketch map of the translational sliding mapped along the western region of the study area. Location of the slope failure is shown in Fig. 6A.

Table 1. Measured/estimated size parameters of the mapped mounds located in Zone A in the northern region (Figs. 2B, 4A, 5A). The values of the mounds were estimated by using the multibeam data. Location of the mounds is shown in Fig 5A.

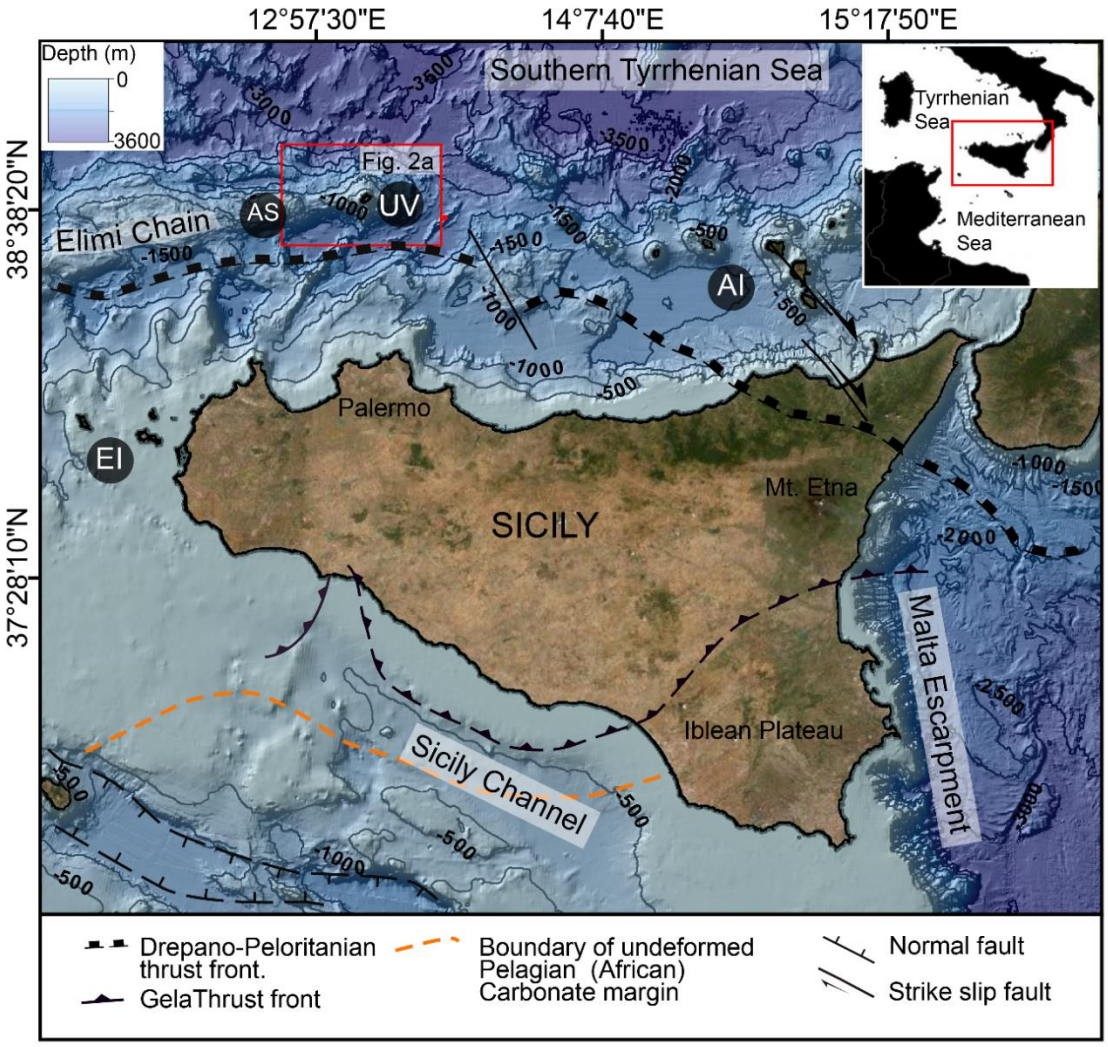

Fig. 1 Sulli et al.,2019

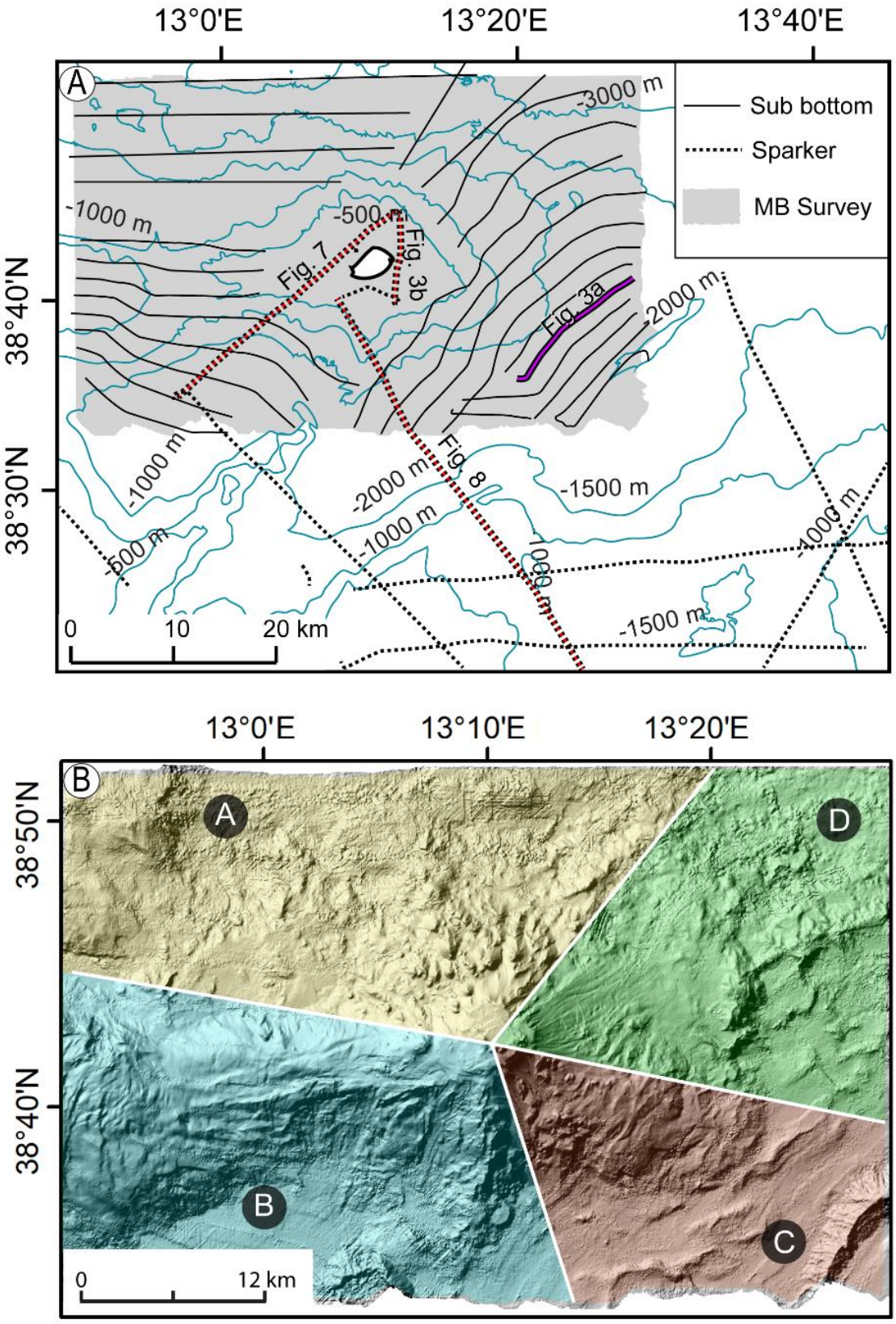

Fig. 2. Sulli et al.,2019

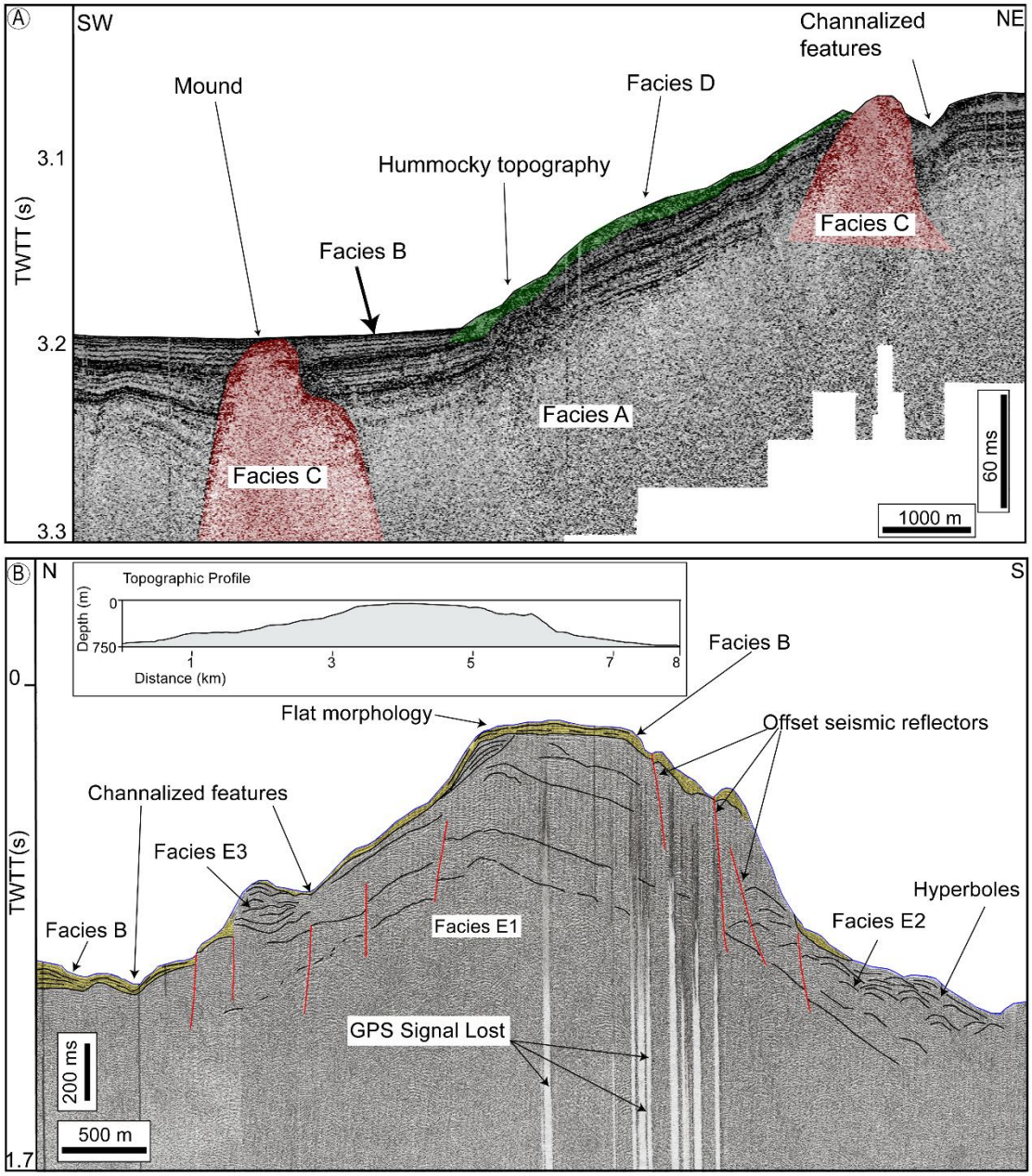

Fig. 3. Sulli et al.,2019

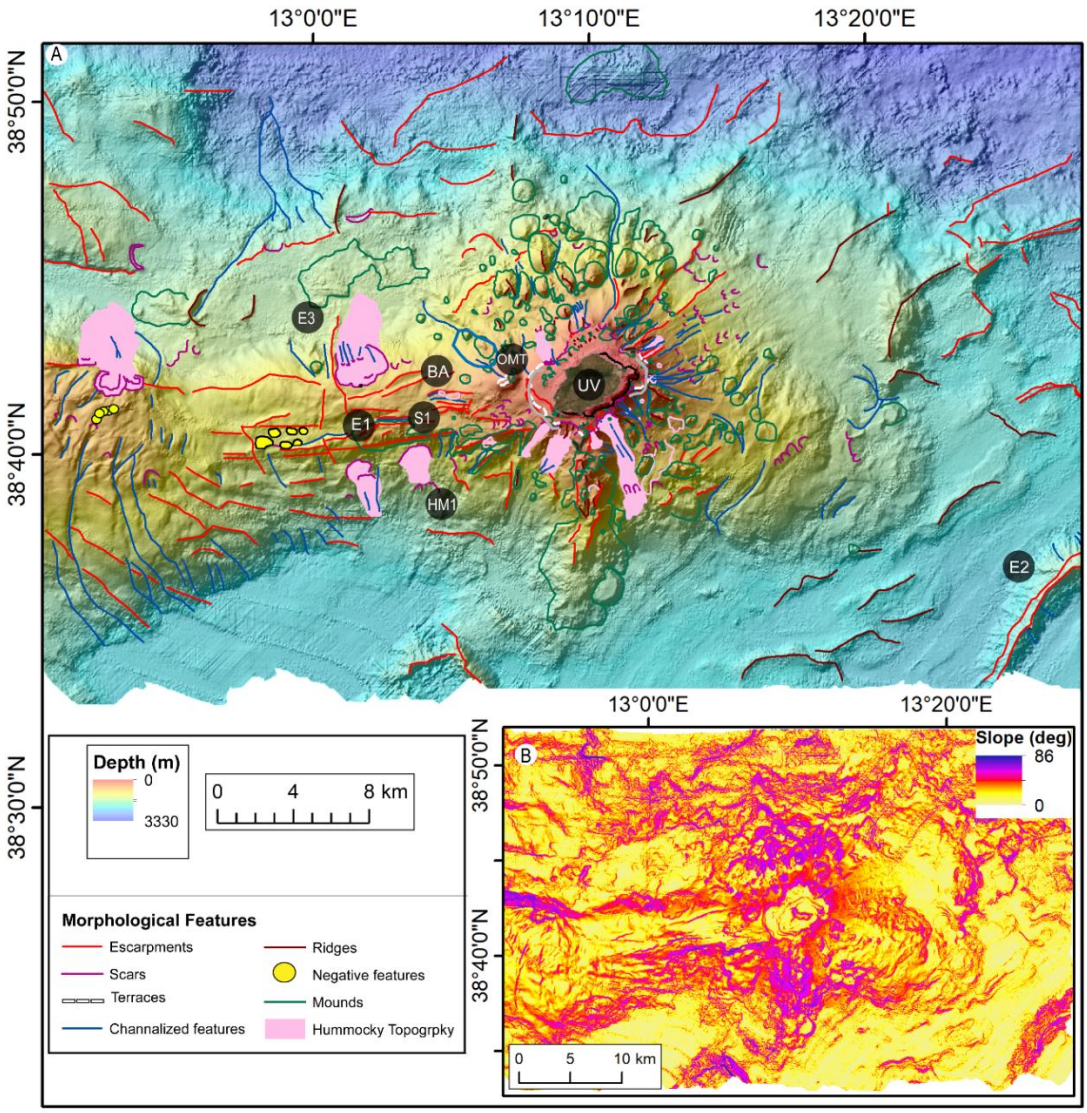

Fig. 4. Sulli et al.,2019

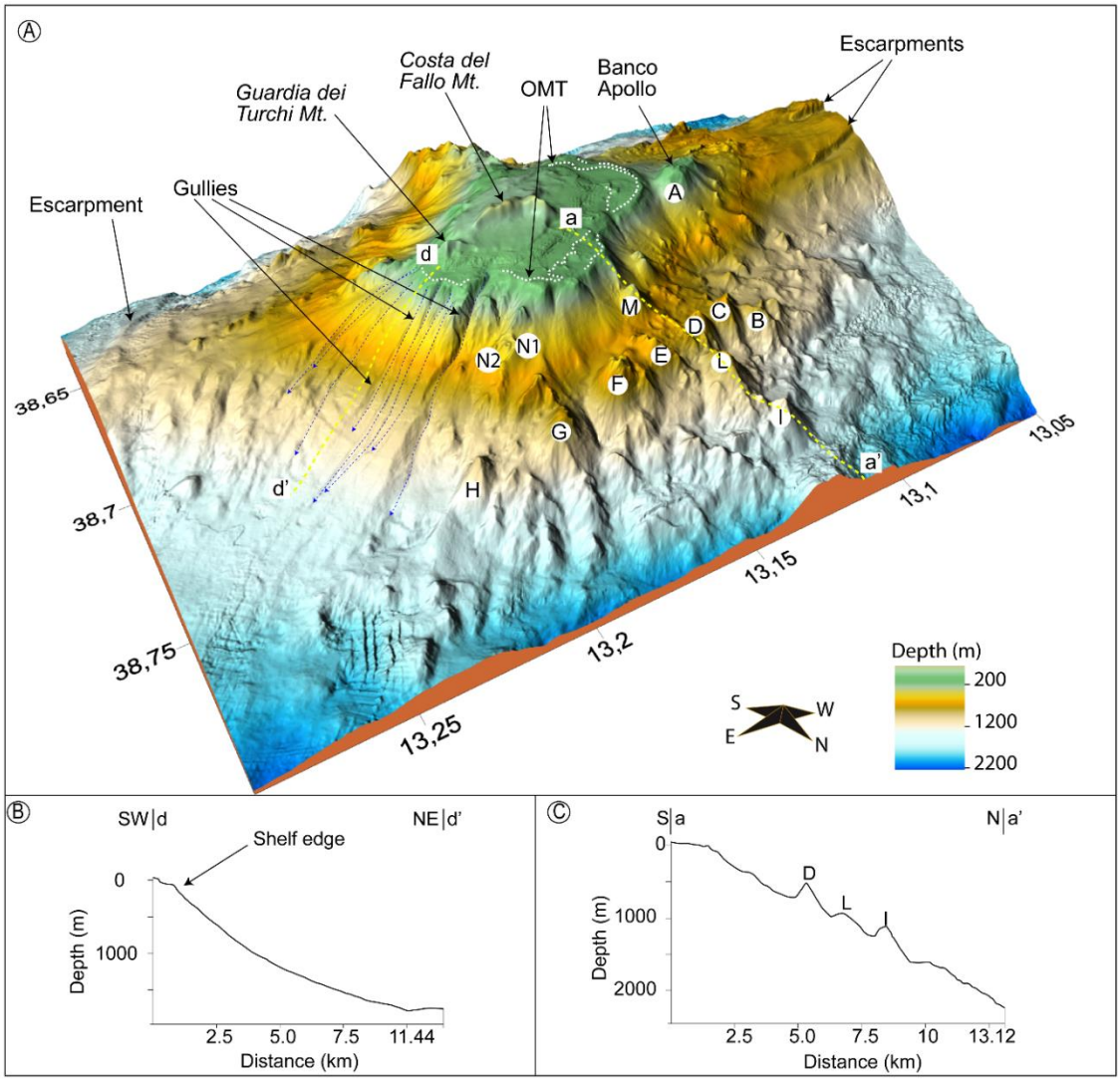

Fig. 5. Sulli et al.,2019

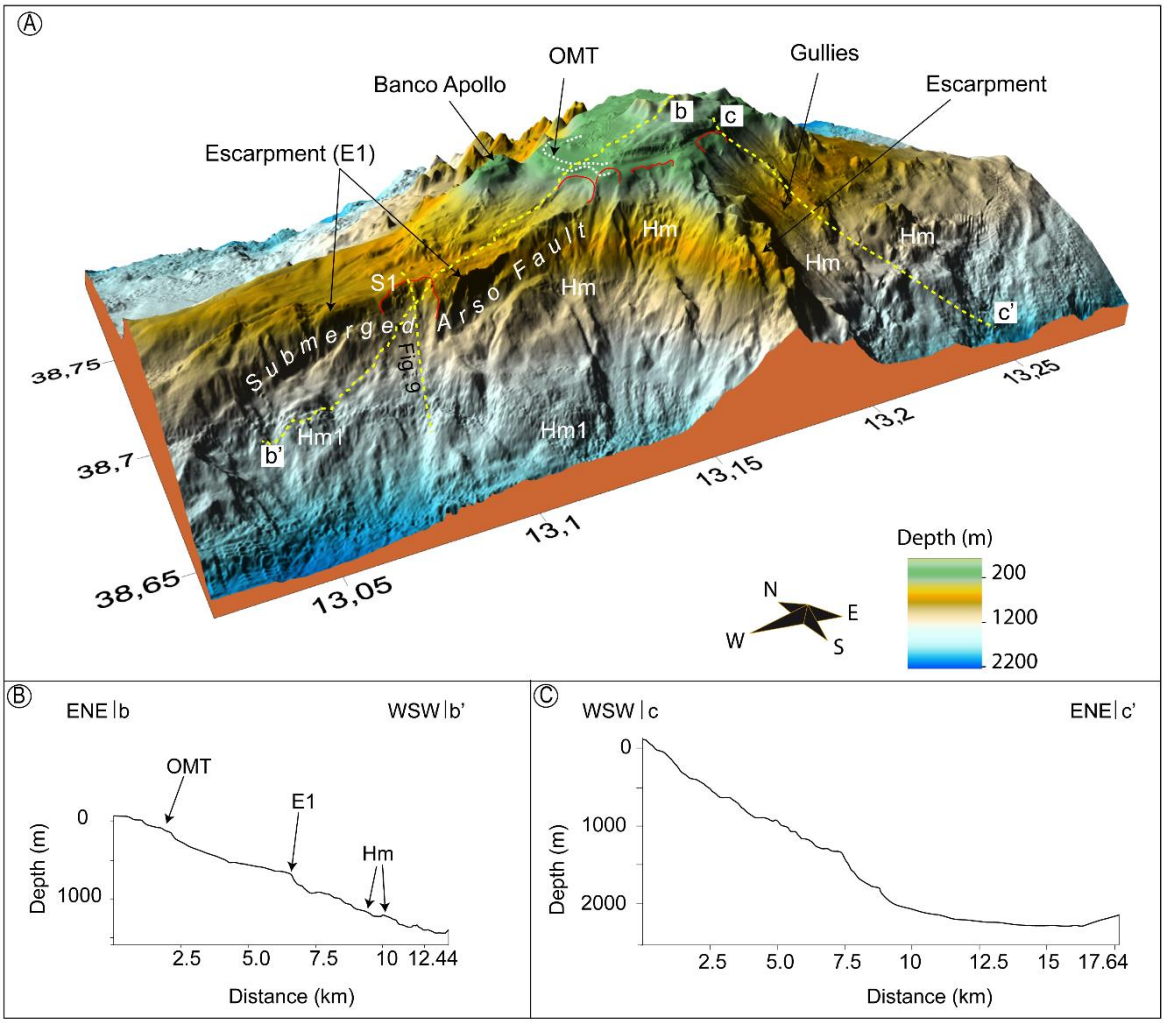

Fig. 6. Sulli et al.,2019

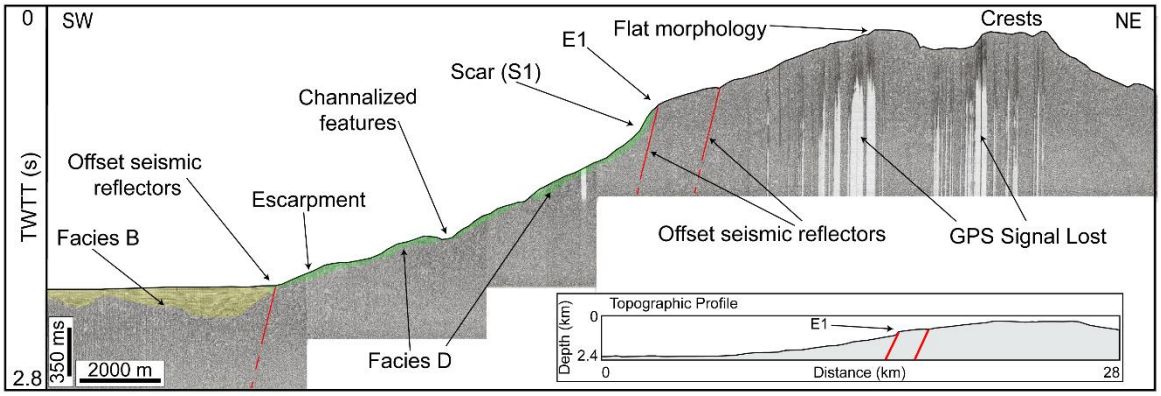

Fig. 7. Sulli et al.,2019

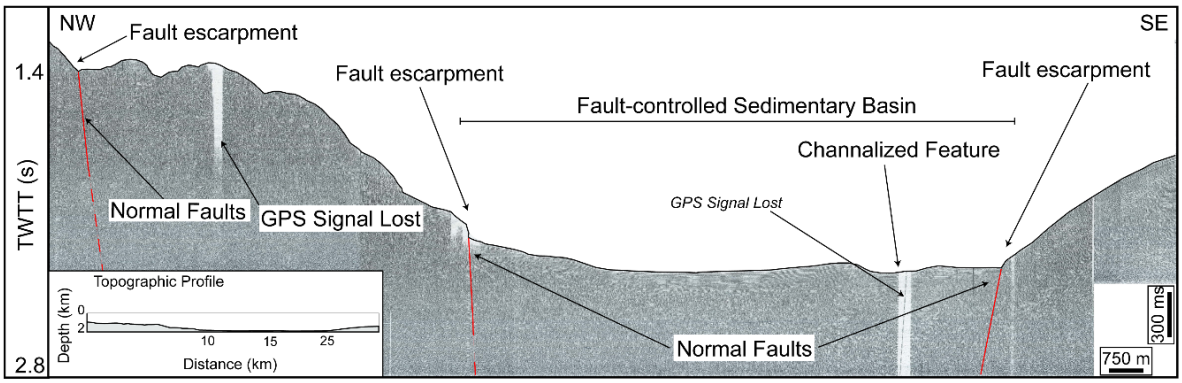

Fig. 8. Sulli et al.,2019

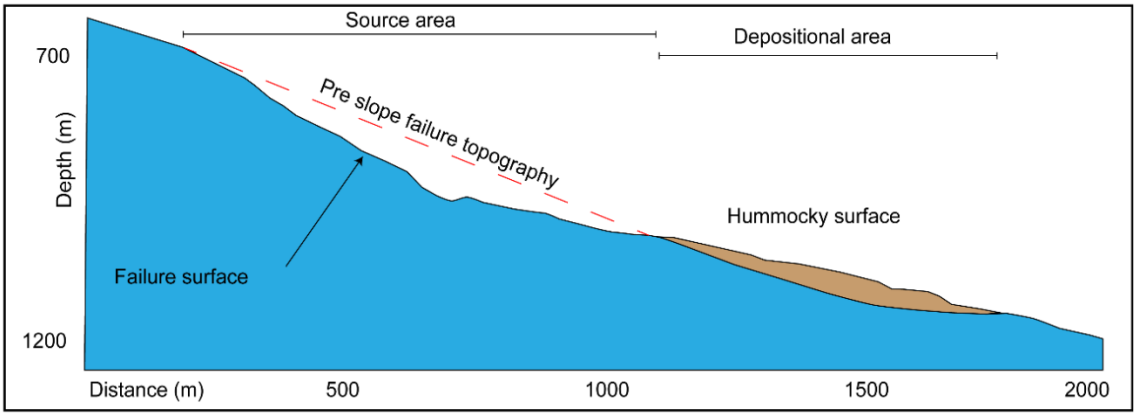

Fig. 9. Sulli et al.,2019

ID	D (m)	d (m)	Mean Axis (m)	R (m)	Sb (km^2)	Pb (km)	V (Km^3)	H (m)	Sd (m)	Bd (m)	bsr	H/R	ds	f	Max slope (deg)	Min slope (deg)	Mean slope (deg)	Shape
A1	1100	1050	1075	525	1.00	3.3	0.10	330	50	450	0.95	0.63	650	0.31	29.00	23.00	26.50	Truncated-Cone
A2	1350	1000	1175	500	1.00	4	0.09	346	100	400	0.74	0.69	391	0.20	29.00	23.00	26.50	Truncated-Cone
B	1500	1380	1440	690	1.60	5.6	0.21	420	780	1200	0.92	0.61	240	0.09	34.00	18.00	26.00	Cone
C	1940	950	1445	475	1.20	5.75	0.12	510	580	1100	0.49	1.07	50	0.03	32.00	24.00	28.00	Cone
D	1380	756	1068	378	0.90	3.5	0.07	480	610	1020	0.55	1.27	70	0.05	36.00	26.00	30.00	Cone
E	2000	850	1425	425	1.10	5	0.09	450	530	980	0.43	1.06	135	0.08	34.00	20.00	27.00	Cone
F	1972	1780	1876	890	3.00	7	0.59	710	450	1160	0.90	0.80	340	0.10	38.00	28.00	33.00	Cone
G	2640	1450	2045	725	2.95	7.2	0.49	890	710	1600	0.55	1.23	260	0.09	36.00	20.00	28.00	Cone
H	1320	950	1135	475	1.10	3.9	0.13	550	910	1460	0.72	1.16	58	0.03	36.00	22.00	29.00	Cone
I	1870	1360	1615	680	1.44	4.9	0.24	490	1130	1620	0.73	0.72	320	0.12	32.00	20.00	26.00	Cone
L	2130	1980	2055	990	2.70	6.95	0.54	530	710	1240	0.93	0.54	120	0.03	32.00	21.00	27.00	Cone
M	1100	1000	1050	500	0.60	2.9	0.18	670	290	600	0.91	1.34	60	0.03	32.00	28.00	30.00	Cone
N1	795	580	687.5	290	0.34	2.2	0.02	203	362	565	0.73	0.70	320	0.28	48.00	7.60	20.28	Truncated-Cone
N2	180	160	170	80	0.02	0.5	0.00	167	398	565	0.89	2.09	129	0.40	34.00	7.00	13.00	Truncated-Cone

Table 1. Sulli et al.,2019

CHAPTER 4

Late Quaternary Tectonics vs Sedimentation history of the offshore Termini in a seismically active segment of the Northern Sicily Continental margin (Southern Tyrrhenian Sea)

NOTE This chapter is a scientific paper in prep. to be submitted to Marine and Petroleum Geology. The authors are the followings: Elisabetta Zizzo, Attilio Sulli, Daniele Spatola, Christian Gorinì, Maurizio Gasparo Morticelli.

Abstract

We investigate the tectonically active Northern Sicily Continental margin, with a focus on the neotectonic processes affecting the Offshore of Termini (Southern Tyrrhenian Sea) by using high-resolution seismic profiles and multibeam data. The Meso-Cenozoic sedimentary successions along the NSCM are the marine prolongation of those outcropping along the Northern Sicily coastal belt. This region originated as a consequence of a complex interaction of compressional events, crustal thinning, and strike-slip faulting. E–W, NW–SE, and NE–SW trending, both extensional and compressional, faults with a local strike-slip component, exerted control on the morphology of the present day shelf and coastal areas during the Pleistocene. Most of morphological structures that shaped the margin during the Quaternary were conditioned by tectonic as well as depositional events, among which we focused on those related to gravitational mass movement and fluids escape. Among these we recognized repeated deformational features affecting the less-lithified deposits lying above the northern Sicily continental shelf. These soft-sediment deformational structures are interbedded with hemipelagic deposits of the transgressive and highstand systems tracts of the Late Quaternary depositional sequence, whose bottom is dated by chronostratigraphy available a few kms far from the identified structures. For each interval of this sequence we elaborated an age-model considering a constant sedimentation rate for the last 11.5 My. In this way we dated the mass movement event, which we considered as seismic induced structures, and indirectly the earthquakes that originated them. As a consequence we were able to calculate the earthquakes recurrence times corresponding to intervals between 680 and 2200 years.

Keywords: Active tectonics, Submarine canyon, Sicilian continental margin, Soft sediment, Southern Tyrrhenian Sea.

1. Introduction

Most of the Earth seismicity occurs along or near active-tectonics coastline and many large earthquakes in these areas are recorded by modern depositional or erosional features (Orange, 1999). In active continental margins uplift and subsidence, erosion and deposition depends largely upon tectonics and the interplay between deformational processes, sea-level fluctuations, geomorphic processes and sediment supply shape the seafloor morphology and the stratal architecture (Green et al., 2002). In most of these regions large-magnitude earthquakes tend to influence occurrence, geometry and distribution of geomorphic features, (Laursen and Normack, 2002; Le Dantec et al., 2010; Pedley et al., 2010; Micallef et al., 2014), as well as sediment thickness, structures and fabric (Griffith et al., 2012).

In the last years multidisciplinary (geological-geomorphological, morphostructural, geophysical) and multi-scales investigation were used to unravel the erosional-depositional processes associated to the

recent tectonic activity and seismicity in different regions both onland (Papanikolaou et al., 2015) and in marine areas (Alonso et al., 1992; von Huene et al., 2004; Lafosse et al., 2018), with the aim to reconstruct the dynamic processes forcing morphological-depositional evolution along the continental margins.

The central sector of the Northern Sicily Continental margin (NSCM) has geological, geophysical and geomorphological characteristics that make it unique, like the presence of tectonic structures, as well as erosive and depositional features, fluid escaping and bottom currents, which affected the region since Neogene and very active up today. The occurrence of a complex morphology enhanced by extensive tectonic processes, induced seafloor instability and drove soft-sediment deformational structures (SSDS; Owen and Moretti, 2011; Waldron and Gagnon, 2011; Basilone et al., 2016). The resulting deformed rocks, known as seismites (Pratt, 1994; Lu et al., 2017)), represents sedimentary indicators of paleoseismicity (Ricci Lucchi, 1995) and their dating has been useful to characterize the chronology of ancient earthquakes (Kagan et al., 2005; Rudersdorf et al., 2015).

In this study we analyse high resolution geophysical and sedimentological data from the offshore of Termini, in the central-western sector of the NSCM, to: (i) reconstruct the geomorphic evolution of the continental shelf-slope system; (ii) understand the role of the Late Quaternary tectonics on the depositional architecture of the buried succession. Starting from the morphostructural evolution of the study region, the main novelty of this research is to propose a methodology to calculate the earthquake recurrence time in this sector of the NSCM from dating seismic induced SSDS. The results of this research will provide qualitative and quantitative information useful to assess the marine geo-hazard, and particularly seismic hazard, along the Northern Sicily coastal region. This study was facilitated by the huge availability of seismic reflection profiles, at different scale of resolution and penetration, sedimentological data, morpho-bathymetry from MBES surveys, and a deep geological background in the outcropping region (Northern Sicily coastal belt).

2. Regional setting

2.1 Geological setting

The Northern Sicily Continental Margin (NSCM) is located in a transitional area between the Sicilian-Maghrebian chain and the south and the Tyrrhenian back-arc basin to the north (Fig. 1). The NSCM is the result of the postcollisional convergence between the Africa plate and a very complex “European” lithosphere (Bonardi et al., 2001), represented by the AlKaPeKa element (Boullin, 1986), and the opening of the Tyrrhenian back-arc basin.

The African element derive from the deformation of both shallow and deep-water Meso-Cenozoic, passive continental margin-type sequences and foreland basin system successions (foredeep and wedge-top basins). The Sicilian sector of the Meso-Cenozoic African passive continental margin was formed by a carbonate-platform depositional environment, recorded by shelf-to-pelagic carbonate successions, laterally linked to slope-to-basin areas filled with deep-water carbonates, bedded cherts

and sandy mudstone successions (Catalano and D'Argenio, 1982). During the Late Oligocene–Early Miocene the passive continental margin successions were buried beneath a thick terrigenous sequence (Numidian Flysch) accumulated in a wide foredeep basin (Pescatore et al., 1987; Pinter et al., 2016) and afterwards involved in the compressional events originating the Sicilian Fold and Thrust Belt (FTB), characterized by a multi-stage evolution during the last 15 My.

Forethrusting of the FTB started in the early Miocene with the progressive detachment of the Meso-Cenozoic succession from its basement, triggered by the collision between the Corsica-Sardinia block and the northern African margin. During this thin-skinned phase, two main subsequent southeastward-verging tectonic events generated and developed at different structural levels and at different time intervals (Oldow et al., 1990; Roure et al., 1990; Bello et al., 2000; Avellone et al., 2010). The early phase involved the thin, deep-water, shales and carbonates, which overthrust thick, more external, platform carbonates, producing duplex geometry and major tectonic transport since Serravallian time. During the latest Miocene–early Pleistocene, deep-seated thrusts detached and deformed the platform carbonates, forming axial culminations and ramp structures. A more recent thick-skinned tectonic event involved the crustal layers in the inner sector of the chain (Gasparo Morticelli et al., 2015), accompanied by crustal delamination (Caracausi and Sulli, 2019).

The deformed FTB is covered unconformably by Upper Miocene to Quaternary clastic, evaporitic and carbonate successions (marine to continental deposits). Along the shelf and the upper slope, the Quaternary deposits consist of seawards dipping clastic and terrigenous deposits coming from the northern Sicily interbedded with hemipelagic sediments in the distal areas (Baghi et al., 1980). The middle Pleistocene deposits are truncated by an erosional surface formed during the last glacio-eustatic oscillation. Prograding sedimentary wedges of coastal deposits, formed during the Last Glacial Maximum (LGM, about 20 ka), are present along the shelf margin.

Due to the intense deformational processes, the physiography of the NSCM is presently composed by a narrow and steep continental shelf, a steep to gentle downward continental slope, interrupted by a flat intra-slope basin plain, and a bathyal plain at a depth of 3000 m (Sulli et al., 2012).

During Late Pliocene-Pleistocene, a late collisional stage of the Sicilian Fold and Thrust Belt seems to have decreased in favour of back-verging thrusts and vertical growth, mostly in the inner sector of the orogen where a large number of N-verging thrusts controlled the tectonic evolution of the uppermost Miocene-Pleistocene deposits. In the offshore sector (southern Tyrrhenian border). Some of these tectonic features seem to be responsible for the geometry of the main submerged structural highs that characterized the physiography of the present day northern Sicily margin. The latest of them were locally reactivated by a compressional stress field with a dominant NW-SE orientation. During the Pleistocene, NNW-SSE, E-W, ENE-WSW trending faults have controlled the present day morphology of the continental shelf and the coastal areas (Sulli et al., 2013). The tectonic activity, during the last 125 ky has triggered an important uplift/subsidence patterns, decreasing from E to W; locally the on

land areas are raised while offshore areas are subsiding, suggesting the occurrence of vertical differential movements (Sulli et al., 2013).

The high tectonic activity affecting the NSMC has strongly influenced the sedimentary and geomorphic processes of the region producing several slope failures, controlled by the gravitational instability all over the continental shelf and the continental slope, furrowing and fluid escaping.

2.2 Seismicity and geophysical characters of the Northern Sicily Continental Margin

The NSMC is characterized by a crustal and deeper seismicity distinct in two main seismogenetic volumes (Pondrelli et al., 2006; Billi et al., 2010). The deeper seismicity, concentrated on the eastern and north-eastern sector of Sicily, is related to the Ionian subduction. In this sector the shallow events are instead prevailingly linked both to extensional fault systems (Pollina, Messina strait) and to right lateral NW-SE transcurrent systems (Vulcano- Lipari and Tindari-Giardini). The crustal seismicity is concentrated in the western sector, resulting from the brittle deformation of the Maghrebian chain. In this area, shallow earthquakes (up to 25 km) of low to moderate magnitude (max Mw 5.9 on September 2002) occurring along an E-W trending belt and their focal mechanisms are in agreement with a dominant NW-SE compressive offset direction, with a right strike-slip component, and an antithetic NE-SW fault trend.

Along the NSMC, the Moho depth ranges from about 10 km, in the Marsili bathyal plain, to about 40 km, towards the northern Sicily coast. The Bouguer anomalies change from 180 mGal in the Tyrrhenian region to negative anomalies in central Sicily (-100 mGal), while positive magnetic anomalies characterize the volcanic edifices, both submerged and buried. The heat flow shows very high values across the southern Tyrrhenian Sea (200 mW/m-2) while decrease (30-40 mW/m-2) towards the stable sector of the foreland area (Iblean plateau in SE Sicily).

GPS measurements document the active deformation with differential movements of individual blocks northward directed, in agreement with the shallow seismicity, as well as with the convergence between Sicily and Sardinia, with values of about 2-6 mm/y (Devoti et al., 2011). This last collisional stage in the northern Sicily chain seems to be a precursor of a change in the subduction polarity by activation of northward back-verging compressional faults as a consequence of the ongoing collision of the African promontory with the thinned continental to oceanic sectors (Algerian and Tyrrhenian basins) of the European plate (Sulli et al., 2019).

3. Materials and Methods

3.1 Marine geological dataset

This study is based on data acquired from the southern Tyrrhenian Sea between 1991 and 2009 (Fig. 2), including:

a) Multibeam data, acquired during three oceanographic surveys carried out in 2001, 2004 (in the frame of the CARG project) as well as 2009 (MaGIC project). The 2001's survey

was carried out on board of the R/V "Tethis" using a Reason SeaBat 8111 Multi Beam Echosounder (MBES), with a frequency of 100 kHz and operational depth range between 35 and 800 m. In 2004 and 2009, the research expeditions were carried out on board of the R/V “Universitatis” using a Reason SeaBat 8160 MBES, with a frequency of 50 kHz, and operational depth range of 30–3000 m. In all the scientific cruises, the acquisition was supported by a “Differential Global Positioning System” (DGPS) to obtain an accurate vessel position, a motion sensor to determine the attitude of the vessel in terms of pitch, roll and heave, and different CTD probes to measure electric conductivity and temperature, influencing the sound velocity in seawater. Bathymetric data were processed using the PDS-2000 software at the University of Palermo. Post-processing steps included the processing of navigation data, graphic removal of erroneous beams, noise filtering, and correction for sound velocity. The Digital Terrain Models (Fig. 2b) were produced using different cell size, from 2 to 20 m, according to the water depth. Maps were generated with open source GIS Software.

We finally integrated the multibeam data with the EMODnet bathymetry (http://www.emodnet-bathymetry.eu) (220 m grid resolution).

b) About 500 km of high-resolution seismic profiles acquired during the 1991 cruise (Sicilia 1991) on board of the R/V Minerva-Uno, using a 1 kJ sparker source and a single-channel streamer. During the 2004 survey a multi-tip sparker array was used, with a base frequency of 600 Hz, fired every 12.5 m and recorded with a single-channel streamer with an active section of 2.8 m, containing seven high-resolution hydrophones, for 3.0 s two way time (TWT) at 10 kHz sampling rate. Data processing was performed using the Geo-Suite software running the following mathematical operators: traces mixing, time variant filters, automatic gain control, time variant gain and spherical divergence correction. Signal penetration was found to exceed 400 ms (t.w.t.t.) and the vertical resolution is up to 2.5 m at the seafloor.

c) About 1000 km of Sub bottom profiles were acquired using a hull-mounted 4 to 16-transducers GeoAcoustics CHIRP II profiler (Fig. 2a). The instrument has an operating frequency ranging between 1.5 to 11.5 kHz, operational depth between 600 and 2000 m, and a pulse length of 32 ms. The sub bottom profiles were recorded and processed using the GeoTrace software by carrying out automatic gain control, time variant gain, swell filtering and muting.

d) Vibrocores: Eighteen cores were recovered using a 6 m-long vibrocoring system during the 2016-2018 oceanographic survey across the offshore of Termini (Tab. 1).

3.2 Methodology

The seismic interpretation of the high-resolution seismic lines has been based on the classic seismic facies analysis methods (*sensu* Selley, 1979) and allow us to identify and characterise different depositional units (e.g. seismic-induced mass movement deposits) showing different seismic attributes along the study area. The mapped depositional units have been classified on the base of the seismic interpretation according to the general principles sequence stratigraphy (Catuneanu et al., 2011), adequate to address analyses of Quaternary high frequency glacio-eustatic signals of fourth (100-200 ka) and fifth orders (40-20 ka) according to Tesson et al. (1990); Posamentier et al. (1992); Posamentier and Morris, (2000). The depositional units have been also accordingly calibrated with the sedimentological/stratigraphic information from the sedimentological analysis in order to infer their extent and timing. The VIB10 core, located in this sector of the southern Thyrrehian Sea (Caruso et al. 2011), was used to correlate the seismic reflection data.

We used the mapped mass-movement deposits, interpreted as Soft Sediment Deformation Structures (SSDS), which are often triggered by local earthquakes, recently highlighted also by Basilone et al. (2016) along the NSCM, to estimate the earthquakes recurrence interval in the study area. We correlated the bottom surface of this depositional unit with the surface dated at 11.5 ka by Caruso et al. (2011) through a high-resolution bio-chronostratigraphic analysis. A constant sedimentation rate has been considered for the entire Holocene sedimentary succession: it was obtained from the ratio between the total thickness of the Holocene unit and the related time interval (11.500 years), since poorly lithified pelagic deposits, whose sedimentation rate can be considered as constant, in this small time interval, usually form the SSDSS. This method allow us to constrain an age-model of the identified SSDSS estimating their timing of deposition and indirectly the timing of each presumed earthquake triggering the Soft Sediment Deformation Structures.

The isopach maps of the seismic sub-unit E1-8 have been generated by interpolating (linear interpolation technique) the depth estimations of the top and bottom surfaces, extrapolated by the seismostratigraphic analysis, by Kingdom suite software considering a seismic P-velocity of 1600 m. The boundaries of the isopach maps have been restricted to the areas where seismic units were identified.

For the first time in the study area, we correlated the tectonic/stratigraphic framework (mapped depositional sequences and structural features) with the present physiography of the margin, interpreted on the basis of its morphometric parameters (e.g. slope gradient, bathymetry), in order to understand the role played by the tectonics in the shaping of the continental margin.

The collected vibrocore samples were visually logged, photographed, and analysed in terms of sediment colour on board. Three samples of sand from each cores were analysed quantitatively for grain size distribution with a complete set of sieves (FRITSCH, analysette 3 PRO) according to the American Society Standard Material ASTM D 422/63 (1998) at the Earth and Marine Science Department of University of Palermo. The same sediment samples were also analysed using X-ray

diffraction (XRD) and X-ray Fluorescence Spectrometers (XRF) in order to determine the qualitative and semi-quantitative mineralogical composition of the sub-seafloor. Mineral identification was performed on dried and ground sub-samples using a Rigaku XRD diffractometer. Elemental composition determination was finally carried out on dried sub-samples using a Rigaku ZSX Primus (WDS).

4. Results

4.1 General physiography of the continental margin system in the Termini Gulf area

The general physiography of the NSCM is presently composed by: (1) a narrow (<8 km) and steep (up to 2.5°) continental shelf, with the edge between -95 m and -140 m; (2) a very steep (7-8°) upper continental slope ranging in depth from 150 to 1000 m; (3) a flat intra-slope basin plain at a depth of 1500 m; (4) a lower continental slope that is wider and gentler than the upper slope, and (5) a bathyal plain from a depth of 3000 m (Sulli et al., 2012). In the continental shelf, the Pleistocene deposits are truncated by an erosional surface formed during the last glacio-eustatic oscillation with the last depositional sequence at its top (Lo Iacono et al. 2011; Sulli et al. 2012). While, the prograding wedges are absent where the heads of the canyons or failure scars have indented the outer shelf (Lo Iacono et al. 2011).

The Gulf of Termini is located between Capo Zafferano and Capo Plaia in the central part of the NSCM (Figure 3). It covers an area of ~2000 km^2 and a depth ranging between 50 and up to a maximum of 1545 m.

We distinguished three physiographic domains based on the geomorphological characters along the Gulf of Termini (Figure 3):

(i) The continental shelf, ranging from between 0 and 150 m depth below sea level, is characterized by a gentle slope gradient decreasing westward from 0.5° (offshore of Capo Zafferano) to 2.7° (offshore of Capo Plaia). The continental shelf is between 2 and 11 km wide. It is wider in the centre of the gulf (11 km), while it narrows both to the west towards Capo Zafferano, where it is less than 2 km, and to the east towards Cefalù, where it is ~5 km wide (Fig. 3) In the study area, the continental shelf can be easily divided into an inner shelf between water depths of 0 and 88 (Is in Fig. 4), and in an outer shelf between 88 and 147 mbsl (Os in Fig. 4). The seafloor of the inner shelf shows a regular morphology except where steep escarpments locally affect it in the central sector of the area. The outer shelf is up to 4 km wide and has a seafloor morphology more articulated than the inner shelf. The shelf-edge, ranging from 130 to 150 m, has been identified as a break of slope between the flat outer shelf and a steep area that bounds upwards the continental slope (slope ledge) (Fig. 3).

(ii) The seafloor of the continental slope is located between water depths of 150 and 1400 m and has a high slope gradient. Its slope gradient is ~4° in the western region and decreases towards the east (Fig.3). The longitudinal bathymetric profiles shown in Fig. 3 display the complex morphology of

the continental slope with a concave upwards profile along the eastern part and convex profile across the western part (Fig. 3).

(iii) The intra-slope basins are bounded by structural highs (Pepe et al., 2005). The region is subdivided into two sub-basins by a clear ~66 km long NNW-ESE break of slope that has been identified at a depth 400 m. The Cefalù Basin is located in the lower continental slope, extending up to 1400 m below sea level. It is a very large basin that develops from the Palermo Gulf offshore to the Eolian Islands but only an area of ~577 km2 is covered by our Multibeam data (Fig. 3). The smaller Termini Basin is located between the continental shelf and the upper continental slope (between 60 and 400 m in water depth) and is elongate about WNW-ESE. It is a narrow basin, 40 km long, up to 5 km wide and covers an area of ~122 km2 that narrows towards both the east and the west.

4.2 Characteristics and distributions of the seafloor geomorphic features

4.2.1 Scars

The high-resolution bathymetric dataset allow us to identify forty-three scars across the offshore of Termini. The headwalls of the scars are generally linear to arcuate, with a steepness of 8°–14°. They mainly are located on the continental slope and only few of them along the shelf edge. The latter are usually connected to the headwalls of the canyons. Along the western part of the continental slope, the scars have been mapped at the depths between 770 and 1200. The scars have headwalls up to 300 m high with amphitheatre shapes, 10-25° steep, and an average width of 2 km. In the eastern region is located the largest scar occurring along the continental slope (S1 in Fig. 3). It is 3.5 km wide, with headwalls up to 180 m in height.

4.2.2 Positive features

The inner shelf as well as the outer shelf are characterised by smooth morphology bounded by steep breaks of slopes. The seafloor is also characterised by fifty positive features, which are either aligned in W-E or/ NNW-SSE direction or occur as isolated features (Fig. 3). They occur in depths ranging between 90 and 100 m and are located 1.5 km from the coast of Sicily and they have elliptical shapes. These positive morphologies are up to 7000 m long, up to 800 m wide.

4.2.3 Negative features

Twenty-seven circular depressions occur in the continental slope and are located 6 km from the coast of Sicily (Fig. 3). These depressions occur in depths ranging between 240 and 800 m. These structures have abrupt edges, and they are circular and elliptical in plan-view and have a U to V shaped cross-sectional shape. They are 150-350 m in diameter, about 15 m deep and the slope gradients of their walls are up to 23°. These negative features either are aligned in NNW-SSE or/and N-S directions or occur as isolated features.

4.2.4 Escarpments

The continental slope appears on the whole intensively affected by more than forty very steep escarpments (Fig. 3). They are almost straight lineaments, bounding raised and lowered sectors. They are up to 12 km long and 180 m high with slope gradients higher than 65°. Three main set of escarpments and lineaments were recognized, NE-SW to E-W, N-S, and NW-SE to WNW-ESE (Fig. 3). These trends are the same that were recognized along the NSCM (Agate et al., 2000; Sulli et al., 2012) and also they are linkable with the distribution of earthquake epicentres recorded between 1981 and 2019 in the region (data from ISIDE: Italian seismological instrumental and parametric database, http://iside.rm.ingv.it).

4.2.5 Break of slopes and Submerged Terraces

The seafloor morphology of the continental shelf shows a flat general morphology that is interrupted by important discontinuous breaks of slope (oriented about E-W) as well as by the continuous shelf break (Fig. 3). The longest discontinuous break of slope is concave in profile and is located at a mean depth of 86 m. It is associated with an E-W elongate positive feature that is ~12 km long and ~350 m wide (Figs. 3). This feature is the physical limit between the Inner and the Outer shelf.

In this paper, we define a submerged terrace as a flat morphology with a slope gradient less than 2°. We mapped three flat morphologies (ST1-3 in Figs. 3, 4) delimited by three discontinuous breaks of slope and characterised by a very low slope gradient that have been considered as submerged terraces by using the high-resolution bathymetric data.

ST1 has been identified in front of the promontory of Capo Zafferano along the continental shelf (Fig. X). We have been not able to measure its extent because ST1 extends out the area covered by the multibeam survey. ST1 is a narrow (<l km wide) with a slope gradient of ~1°. It is characterised by a very discontinuous distal edge that cannot be traced from west to east. ST2 ranging between 61 and 101 m depth is characterized by a slope gradients ranging from 0.5 ° to 1.8 °. It has an edge ~8.5 km long and covers an area of 5 km^2. ST3 is the largest submerged terrace. It is characterized by a slope gradients ranging from 0.6° to 2°. It is bounded by an edge that is ~10 km long and it covers an area of 8 km^2. The bathymetric profiles in Fig. 4 show an asymmetric shape in section view of the ST1-3 as well as how they become smaller and deeper towards the west.

4.2.6 Submarine Canyons

Both the edge of the shelf and the continental slope are strongly incised by more than 300 “elongate steep-sided valleys” definite in this paper as gullies and submarine canyons (Fig. 3). They are aligned in NNW-SSE, N-S and NNE-SSW directions in front of Capo Zafferano (western section of the study area) and they are aligned in NNW-SSE, NO-SE e ENE-WSW directions in front of Capo Plaia (eastern section of the study area) (Fig. 3).

In the western part, the canyons are located 2.4 km from the coast of Sicily and they have a length up to 3 km. They occur in depths ranging between 200 and 750 m as well as between 1000 and 1400 m. While in the eastern part, they are longer and they occur in depths ranging between 160 and 380 m as well as between 1000 and 1200 m.

4.2.6.1 Morphometric analysis of the Capo Plaia Canyon

The longest canyon along the entire continental slope dominates the eastern part of the study area (Capo Plaia Canyon in Fig. 3). It is ~33 km long, up to 1.5 km wide, up to 700 m deep and covers an area of ~28 km^2. Its depth ranges from 100 m at the head to 1345 m at the mouth. The incision has a V-shaped cross-section sharp interfluve and pointed head in its upper part (up to 500 m of water depth) and a U-shaped cross-section sharp in its distal part. We estimate for this feature a sinuosity index of 1.22, a mean slope of 3° and a maximum slope of 22.6°. The orientation of the canyon changes along its thalweg profile. We identified five different transects, each of which following a straight trend and separated from the others by abrupt changes of direction (Fig. 5). In view of this feature, each transect cannot be considered as a sinuous canyon *sensu* Wynn et al. (2007).

4.3 Sub-seafloor Architecture

4.3.1 Seismic reflection profiles

The acquired sub bottom profiles as well as the high-resolution seismic profiles (Sparker) allow us to identify five main seismic units (Fig. 7) on the basis of seismic facies, internal geometry, external configuration, and seismic features of prominent reflectors.

(i) Unit A: It is stratigraphically the deepest and it comprises two sub-units: (A1) seismically transparent unit a very high amplitude reflector at its top. It corresponds to the acoustic basement, and (A2) an unit made of high-amplitude basinward dipping reflectors with good lateral continuity, at times transparent to chaotic internal configuration. Both A1 and A2 are affected by vertical to sub-vertical offset reflectors (Fig. 6).

(ii) Unit B: It overlies unit A and consists of a package of very high-amplitude basinward dipping reflectors with good lateral continuity that does not display vertical and lateral changes in seismic character (Fig. X). Unit 2b has a wedge-shaped geometry (Fig. 6).

(iii) Unit C: It is characterized by parallel high-amplitude basinward dipping reflectors with good lateral continuity, at times undulating or gently folded with sometime very clear concave-upward reflectors (Fig. 6). Its lower boundary generally occurs in angular unconformity with the top of the sub-unit A2 (Fig. 6).

(iv) Unit D: It is made by an acoustically semi-transparent to chaotic facies. It is bounded at the top by a high-amplitude and continuous reflector. It mainly occurs along the inner continental shelf and corresponds to the positive features previously described that we identified by using the high-resolution bathymetric data (Fig. 6).

(v) Unit E: Unit E, stratigraphically located above unit A, is a complex unit displaying vertical and lateral changes in seismic character (Fig. 6).

The high-resolution seismic lines show the occurrence of large hydro-acoustic anomalies in the water column consisting of hyperbolic water-column reflections, which are up to 65 ms high (about 50). They mainly occur in the central part of the study area at the top of mounds formed of seismic unit D and/or of escarpments, and they always are associated to offset seismic reflectors (Fig. 8ì7).

The Unit E is composed of eight sub-units with chaotic to transparent or seismic signatures. The internal configuration of the sub-units hardly contains any discernible pattern. They vary vertically from the seafloor to the top of the unit A, show mostly a wavy to parallel internal geometry, with discontinuous/chaotic to transparent reflectors to a drape featuring intermediate amplitude and discontinuous reflectors (Fig. 7ì6).

Sub-unit E1-8 cover an average area of ~215 km2 (~25 km × 8 km) (Fig. 6). All the estimated physical parameters of the sub-units E1-8 are tabulated in Tab. 2 and shown in Fig.6 .

The detailed chrono-biostratigraphic analysis of the VIB 10 core (Caruso et al., 2011), located in the study area, calibrated the unconformity at the top of the seismic Unit A2 as old as 20.5 ka. The same core identified a horizon dated as old as 11.5 ka, corresponding to the Late Pleistocene-Holocene boundary into the Unit C.

4.4 Sedimentological and mineralogical architecture

Sub-seafloor sediments collected from the seafloor along the offshore of Termini predominantly consist of poorly to moderately well sorted fine to coarse sands covered by a variable thickness, less than 2 m, of pelitic sediments. The samples that were analysed with XRD and XRF are mainly composed of carbonates associated with detrital minerals (clays and quartz) and minor other mineralogical phases (e.g. feldspars, micas). Calcite represents the dominant carbonate phases and is associated with minor quantities of dolomite (Fig. 9).

5. Discussion

5.1 Geomorphological interpretation

The high-resolution bathymetric data evidence how the seafloor of the offshore of Termini is characterised by different submarine geomorphic features linked to different geological processes (Fig. 10). In the following chapters, we discuss the main bathymetric and seismic observation related to the mapped seafloor features suggesting relative potential geological processes.

We interpret the amphitheatre scars on the headwalls of the canyon and/or on escarpment for the high similarity with the features described by Sulli et al. (2018) along the nearby offshore of Palermo as landslide scars resulting from mass movement processes.

In respect of the morphology of the mapped canyons as well as their connection to the subaerial fluvial drainage (Fig. 3), we propose that the submarine canyons mapped on the continental margin are the

result of a coexistence of complex erosional mechanisms such as: (1) downslope surface flows probably during a LGM base level fall (Gerber et al., 2009; Pratson et al., 2007; Micallef 2016) and (ii) continues mass movement processes as supported by the several landslide scars mapped along the headwalls of the canyons (Lo Iacono et al. 2011, 2014). Our interpretation is also supported by the axial incision along the thalweg of the Capo Plaia Canyon demonstrates that active or recent downslope sedimentary fluxes occur along the slope (Baztan et al. 2005) as in the submarine canyons described by Lo Iacono et al. (2011) along the nearby offshore of Palermo. During the LGM, the palaeoshoreline and shore were located more near the shelf margin. We suggest this high-energy hydrodynamics scenario allowed the fluvial sediment supply increased and valleys channelled the sediments to the outer shelf (Lo Iacono et al., 2011; Hernàndez-Molina et al. 2002) because unexposed areas would have been eroded by coarse-grained gravity flows sourced by the fluvial systems. This our inference is supported by the results of the sedimentological analysis showing a quantitative abundance of coarse-grained sands in the sub-seafloor.

At support of our second hypothesis on the genesis of the canyon are also the observation carried out from the occurrence of over imposed chaotic bodies forming the unit E (Fig. 6) mapped by the seismo-stratigraphic analysis and interpreted in the following chapters.

5.2 Stratigraphic interpretation of the mapped systems tracts

Following the sequence stratigraphy interpretation, the seismic facies and their geometric relationships, and based on the calibrating age from the VIB 10 core, we interpreted the identified seismic units as follows:

- Unit A corresponds to the pre 20.5 ka substrate, which in this area is represented mostly by middle Pleistocene clastics and hemipelagites, whose interbedded setting make this unit well stratified (sub-unit A2). The transparent unit A1, on the contrary, correspond to emergent portions of older rocks, which vary from Meso-Cenozoic carbonate successions to Tertiary terrigenous sequences (Catalano et al., 2011);
- Unit B corresponds to the Lowstand Systems tract of the Late Quaternary Depositional Sequence. It was drilled by most of the collected cores (Tab. 1), which recovered poorly to moderately well sorted fine to coarse sands, formed in a littoral environment;
- Unit C corresponds to the Transgressive and Highstand Systems tracts of the Late Quaternary Depositional Sequence. It is composed mainly by interbedded clastic and, prevailing, hemipelagites. The 11.5 ka horizon (Caruso et al., 2011) allows to divide the upper Pleistocene from the Holocene sequence;
- Unit D corresponds to emerging (D1) or buried (D2) mounds, the former corresponding to positive structures in the morphobathymetry. Considering their transparent to chaotic facies and that they are often accompanied to hydroacustical anomalies and are bounded by faults, we interpreted them as fluid flow structures (e.g. mud volcanoes). Also the occurrence of

negative structures that can be interpreted as pockmark points out the abundance of fluids into the buried sequences;

- Unit E, mainly distributed in the subseafloor of the continental shelf, was interpreted as derived from mass movement that formed in a very gentle slope. For this reason we considered them as SSDS induced by earthquakes. We identified almost 7 different bodies interbedded with the hemipelagites attributed to the upper part of the Unit C. Based on the calibration by the VIB 10 core (Caruso et al., 2011), we considered the SSDS as formed during the last 11.5 ky, that is during the Holocene.

5.3 Implication for the neotectonics

5.3.1 Type and age of offshore faults

We interpret the sets of linear and no-linear escarpments as morphological seafloor features related to faults affecting the sedimentary multilayer of the offshore of Termini. The majority of the mapped escarpments have a good correlation with the offset seismic reflectors identified by the seismostratigraphic analysis.

The faults are mainly organized in main orders of fault systems with the same trends already known on land: NE-SW to E-W, N-S, and NW-SE to WNW-ESE fault systems according to Agate et al., (2000), Catalano et al., (2011), Sulli et al., (2012) (Fig. 11). The focal mechanisms of earthquakes recorded between 1981 and 2019 (data from ISIDE: Italian seismological instrumental and parametric database, http://iside.rm.ingv.it) in the vicinity of the faults indicate focal mechanisms in agreement with extensional to transtensional deformation in the NW-SE to WNW-ESE direction (Agate et al., 2000; Sulli et al., 2012), as well as compressional kinematics in the NE-SW to E-W direction (Sulli et al., 2019), as also shown by the displacement of the seismic units (Fig 8). The kinematics of these fault systems can easily be correlated with onland tectonics and seismic reflection data from adjacent sectors (Agate et al., 2000). The mapped offshore faults are likely structures that have recently been active (last 20 ky) because they displace the seismic unit overlaying the angular unconformity dated at ~21.5 ka by Caruso et al. (2011).

5.3.2 Role of the Faults in the evolution of the Capo Plaia canyon

Capo Playa Canyon is the longest submarine canyon in the study area. Its orientation changes at the least five times forming different straight transects along the talweg of the canyon (Figs. 6, 11) that are parallel to the main orientation of the mapped offshore normal faults (Fig. 12) as well as with the as well as with faults documented from different geological data by Agate et al. (2000) and Sulli et al. (2012) along the western region of the NSCM . In view of this geomorphic characters of the Capo Plaia canyon, we suggest that the documented offshore faults have played a key role in shaping of the canyon and that the abrupt changes in canyon orientation are probably fault-controlled.

5.3.3 Nature and activity of the fluid flow structures

The positive features mapped along the inner continental shelf show acoustic facies similar to the acoustic anomalies described in Spatola et al. (2018a) and Ceramicola et al. (2018) in this respect: we interpret these features as mounds resulting from fluid seepage processes.

We interpret the circular negative features, mapped by using the high-resolution bathymetric data on the basis of their morphological parameters (e.g. size, shape) that are comparable to those of similar features in the central Mediterranean Sea (Micallef et al., 2011; Lo Iacono et al., 2014; Pennino et al. 2014; Spatola et al, 2018a, b), as pockmarks associated to seepage of fluids from the seabed (Hovland et al., 2002; Judd and Hovland, 1992, 2007; King and MacLean, 1970). The concave-upward reflectors characterising the unit C have been interpreted as evidence of buried pockmarks (Pennino et al. 2014; Spatola et al, 2018a, Ceramicola et al., 2018). Our interpretation is strongly supported by the occurrence of hydro-acoustic water anomalies (Fig. 7), which are interpreted as fluid/gas associated with active seepage from the seafloor (e.g. Ceramicola et al., 2018; Sauter et al., 2006). The faults displacing the seafloor and the sedimentary multilayer that are associated to the pockmarks can the a preferable pathway for the migration of fluid/gas to seafloor.

The pockmarks have mainly been mapped in proximity of the landslide scars or parallel to the canyons. We suggest, in respect of this spatial distribution, that the fluid flow processes play an important role in the shaping of the landslide scars as well as of the submarine canyons hosted by the continental margin.

5.4 Seismic-induced landslides recurrence time

The eight sedimentary bodies forming the Unit E and characterized by a transparent to chaotic seismic facies show high similarity in terms of seismic features, extent and stratigraphic position with the features described in Basilone et al., (2016) and have been interpreted as Soft Sediment Deformation Structures (SSDS). We suggest, in view of the characters of the physiography of the present continental margin and the spatially distribution of mapped geomorphic features, as most preconditioning factor for mass movement the over-steepening, loss of support as a result of canyon erosion and the fluid escape from the seafloor. The seismicity of the area, which is likely linked to the mapped fault systems, on the other hand, could be the main trigger and in view of this, we interpret the mass movement deposits as seismic-induced landslides. The seismic-induced landslides, as suggested by the chronostratigraphic information provided by the accurate sequence stratigraphy analysis of the Late Quaternary depositional sequence, suggests they have been deposited in the last 11.5 ky with a recurrence time between 680 and 2200 years (Fig. 12).

6. Conclusions

In the central western sector of the NSCM unpublished high-resolution seismic reflection profiles and swath bathymetry highlighted the role of active tectonics in shaping the seafloor morphology and controlling the architecture of Holocene sedimentary sequences. For the first time in the study area

calibration of seismic horizons with bio-chronostratigraphy available in the area and sedimentological characterization of the Upper Quaternary deposits were used to provide a chronology of the seismic events responsible for gravitational processes. The main conclusions of this paper are:

1) the study area is affected by active tectonics coherent with the regional kinematics pointed out by focal mechanisms and GPS-measured plate motion. In the study area the deformational pattern is revealed mainly by NNW-SSE and E-W trending faults, with extensional/transtensional and compressional kinematics, respectively;
2) the seafloor morphology is mostly regulated by neo-tectonic processes as suggested by the alignment of pockmarks and mounds, the direction of gullies and minor submarine canyons. The variable course of the Capo Plaia canyon, which is the largest one in the study area, and one of the principal canyons in the NSCM, is outlined by the trends of the fault systems;
3) the spatial distribution, geometry, and seismic character of mass-wasting deposits suggest that the fluid seepage, oceanographic processes and the slope over steepening could be important preconditioning factors, while the tectonic activity showing fault displacements during earthquakes represent the main triggering factor;
4) the gravitational instability of recent deposits lying above the slightly sloping continental shelf was induced by earthquakes shaking unconsolidated sediments, favoured by high fluid content. Almost 7 seismic-induced landslides were identified into the Holocene sequence;
5) the age-model of the Holocene deposits, supported by bio-chronostratigraphic calibration, provided timing of the seismic-induced events. From this we calculated earthquake recurrence times of 680-2200 years.

These results provide qualitative and quantitative information useful to assess the marine geo-hazard, and particularly seismic hazard, along the Northern Sicily coastal region.

Acknowledgements
We acknowledge the CARG (Geological Maps of Italy) funded by the Italian Geological Survey and the Italian National Research Projects MaGIC (Marine Geological Hazard along the Italian Coast) funded by the Italian Civil Protection Department. We thank also the captains and the crews of the R/V ‘‘Thetis’’ and R/V ‘‘Universitatis’’ for their assistance during the surveys.

References

Agate, M., Beranzoli, L., Braun, T., Catalano, R., Favali, P., Frugoni, F., Pepe, F., Smriglio, G., Sulli, A., 2000. The 1998 offshore NW Siciliy eathquakes in the tectonic frame work of the southern border of the Tyrrhenian Sea. Mem. Soc. Geol. It. 55, 103-114

Alonso, B., Maldonado, A., 1992. Plio-Quaternary margin growth patterns in a complex tectonic setting: Northeastern Alboran Sea. Geo-Marine Letters, 12(2-3), 137-143.

Avellone, G., Barchi, M.R., Catalano, R., Gasparo Morticelli, M., Sulli, A., 2010. Interference between shallow and deep-seated structures in the Sicilian fold and thrust belt, Italy. Journal of the Geological Society, London, 167, 109–126.

Baghi, G, Barbieri, F., Morlotti, E., Raffi, I., Torelli, L., Bartole, R., Polidori, E., Savelli, D., Wezel, F.C., Gallo, F., Mezzadri, G., Pingani, L., Vernia, L., Zerbi, M., Busatti, G., Bortoluzzi, G., Fabbri, A., Ferretti, P., Nanni, T., Ori, C., Zitellini, N., Nicolich R., 1980. Dati geologici preliminari sul bacino di Cefalù (Mar Tirreno). Ateneo Parmense Acta Nat., 16, 3-18

Basilone, L., Sulli, A., Morticelli, M.G., 2016. The relationships between soft-sediment deformation structures and synsedimentary extensional tectonics in Upper Triassic deep-water carbonate succession (Southern Tethyan rifted continental margin—Central Sicily). Sedimentary geology, 344, 310-322.

Baztan, J., Berné, S., Olivet, J. L., Rabineau, M., Aslanian, D., Gaudin, M., ... Canals, M., 2005. Axial incision: The key to understand submarine canyon evolution (in the western Gulf of Lion). Marine and Petroleum Geology, 22(6-7), 805-826.

Bello, M., Franchino, A., Merlini, S., 2000. Structural model of eastern Sicily. Memorie della Società Geologica Italiana, 55, 61–70.

Bonardi, G., Cavazza, W., Perrone, V., Rossi, S., 2001. Calabria-Peloritani terrane and northern Ionian sea. In Anatomy of an orogen: The Apennines and adjacent Mediterranean basins Springer, Dordrecht, pp. 287-306.

Bouillin, J. P., 1986. Le" bassin maghrebin"; une ancienne limite entre l'Europe et l'Afrique a l'ouest des Alpes. Bulletin de la Société géologique de France, 2(4), 547-558.

Caracausi, A., Sulli, A., 2019. Outgassing of mantle volatiles in compressional tectonic regime away from volcanism: the role of continental delamination. Geochemistry, Geophysics, Geosystems, 20(4), 2007-2020.

Caruso, A., Cosentino, C., Pierre, C., Sulli, A., 2011. Sea-level changes during the last 41,000 years in the outer shelf of the southern Tyrrhenian Sea: evidence from benthic foraminifera and seismostratigraphic analysis. Quaternary International, 232(1-2), 122-131.

Catalano, R. D'Argenio, B., 1982. Schema Geologico della Sicilia. In: Catalano, R. & D'Argenio, B. (eds) Guida alla geologia della Sicilia occidentale. Geological Society of Italy, Memoir, XXIV (Suppl. A), 9–41.

Catalano, R., Avellone, G., Basilone, L., Contino, A., Agate, M., 2011. Carta geologica d'Italia alla scala 1: 50.000 e note illustrative dei fogli 609-596 "Termini Imerese – Capo Plaia". –ISPRA, Servizio Geologico d'Italia, Roma.

Catuneanu, O., Galloway, W.E., Kendall, C.G.S.C., Miall, A.D., Posamentier, H.W., Strasser, A., Tucker, M.E., 2011. Sequence stratigraphy: methodology and nomenclature. Newsl. Stratigr. 44, 173–245.

Ceramicola, S., Dupré, S., Somoza, L., Woodside, J., 2018. Cold seep systems. In Submarine geomorphology. Springer, Cham, pp. 367-387.

Devoti, R., Esposito, A., Pietrantonio, G., Pisani, A.R., Riguzzi, F., 2011. Evidence of large scale deformation patterns from GPS data in the Italian subduction boundary. Earth and Planetary Science Letters, 311, 230-241, doi:10.1016/j.epsl.2011.09.034.

Gasparo Morticelli, M., Valenti, V., Catalano, R., Sulli, A., Agate, M., Avellone, G., Albanese, C., Basilone, L., Gugliotta, C., 2015. Deep controls on Foreland Basin System evolution along the Sicilian Fold and Thrust Belt. Bull. Soc. Géol. France, 186(4-5), 273-290.

Gerber, T. P., Amblas, D., Wolinsky, M. A., Pratson, L. F., Canals, M., 2009. A model for the long-profile shape of submarine canyons. Journal of Geophysical Research: Earth Surface, 114(F3).

Greene, H.G., Maher, N.M., Paull, C.K., 2002. Physiography of the Monterey Bay National Marine Sanctuary and implications about continental margin development Marine Geology, 181 (1–3), 55-82

Griffith, W.A., Mitchell, T.M., Renner, J., DiToro, G., 2012. Coseismic damage and softening of fault rocks at seismogenic depths. Earth and Planetary Science Letters 353–354, 219–230.

Hernández-Molina, F. J., Somoza, L., Vázquez, J. T., Lobo, F., Fernández-Puga, M., Llave, E., Dıaz-del Rıo, V., 2002. Quaternary stratigraphic stacking patterns on the continental shelves of the southern Iberian Peninsula: their relationship with global climate and palaeoceanographic changes. Quaternary International, 92(1), 5-23.

Hovland, M., Gardner, J.V., Judd, A.G., 2002. The significance of pockmarks to understanding fluid flow processes and geohazards. Geofluids 2, 127–136.

Judd, A.G., Hovland, M., 2007. Seabed Fluid Flow: The Impact on Geology, Biology and the Marine Environment. Cambridge University Press, Cambridge.

Judd, A.G., Hovland, M., 1992. The evidence of shallow gas in marine sediments.

Continental Shelf Research, 12, 1081-1096

Kagan, E.J., Agnon, A., Bar-Matthews, M., Ayalon, A., 2005. Dating large infrequent earthquakes by damaged cave deposits. Geology, 33, 4, 261–264.

King, L.H., MacLean, B., 1970. Pockmarks on the Scotian Shelf. Geol. Soc. Am. Bull. 81, 3142–3148.

Laursen, J., Normark, W.R., 2002. Late Quaternary evolution of the San Antonio Submarine Canyon in the central Chile forearc (~33°S): Marine Geology , 188, 365–390.

Lafosse, M., Gorini, C., Le Roy, P., Alonso, B., D'Acremont, E., Ercilla, G., Rabineau, M., Vázquez, J.T., Rabaute, A., Ammar, A., 2018. Late Pleistocene-Holocene history of a tectonically active segment of the continental margin (Nekor basin, Western Mediterranean, Morocco). Marine and Petroleum Geology, 97, 370–389

Le Dantec, N., Hogarth, L.J., Driscoll, N.W., Babcock, J.M., Barnhardt, W.A., Schwab, W.C., 2010. Tectonic controls on nearshore sediment accumulation and submarine canyon morphology offshore La Jolla, southern California. Marine Geology, 268, 115–128.

Lo Iacono, C., Sulli, A., Agate, M., Presti, V. L., Pepe, F., Catalano, R., 2011. Submarine canyon morphologies in the Gulf of Palermo (Southern Tyrrhenian Sea) and possible implications for geo-hazard. Marine Geophysical Research, 32(1-2), 127.

Iacono, C. L., Sulli, A., Agate, M., 2014. Submarine canyons of north-western Sicily (Southern Tyrrhenian Sea): Variability in morphology, sedimentary processes and evolution on a tectonically active margin. Deep Sea Research Part II: Topical Studies in Oceanography, 104, 93-105.

Micallef, A., Berndt, C., Debono, G., 2011. Fluid flow systems of the Malta Plateau, central Mediterranean Sea. Marine Geology, 284(1-4), 74-85.

Micallef, A., Mountjoy, J. J., Barnes, P. M., Canals, M., & Lastras, G., 2014. Geomorphic response of submarine canyons to tectonic activity: Insights from the Cook Strait canyon system, New Zealand. Geosphere, 10(5), 905-929.

Micallef, A., Georgiopoulou, A., Mountjoy, J., Huvenne, V. A., Iacono, C. L., Le Bas, T., ... & Otero, D. C., 2016. Outer shelf seafloor geomorphology along a carbonate escarpment: The eastern Malta Plateau, Mediterranean Sea. Continental Shelf Research, 131, 12-27.

Oldow, J.S., Channell, J.E.T., Catalano, R., D'Argenio, B., 1990. Contemporaneous thrusting and large-scale rotations in the western Sicilian fold and thrust belt. Tectonics, 9, 661–681.

Orange, D.L., 1999. Tectonics, sedimentation, and erosion in Northern California; submarine geomorphology and sediment preservation potential as a result of three competing processesMarine Geology, 154 (1–4), 369-382

Owen, G., Moretti, M., 2011. Identifying triggers for liquefaction-induced soft-sediment deformation in sands. Sedimentary Geology 235, 141–147.

Papanikolaou, I.D., van Balen, R., Silva, P.G., Reicherter, K., 2015. Geomorphology of Active Faulting and seismic hazard assessment: New tools and future challenges. Geomorphology, 237, 1-13

Pedley, K.L., Barnes, P.M., Pettinga, J.R., Lewis, K.B., 2010. Seafloor structural geomorphic evolution of the accretionary frontal wedge in response to seamount subduction, Poverty Indentation, New Zealand, Marine Geology, 270, 1–4, 119-138,

Pennino, V., Sulli, A., Caracausi, A., Grassa, F., Interbartolo, F., 2014. Fluid escape structures in the north Sicily continental margin. Marine and petroleum geology, 55, 202-213.

Pescatore, T., Renda, P., Tramutoli, M., 1987. Facies ed evoluzione sedimentaria del Bacino Numidico nelle Madonie occidentali (Sicilia). Memorie della Societa Geologica Italiana, 38, 297-316.

Pinter, P. R., Butler, R. W., Hartley, A. J., Maniscalco, R., Baldassini, N., Di Stefano, A., 2016. The Numidian of Sicily revisited: a thrust-influenced confined turbidite system. Marine and Petroleum Geology, 78, 291-311.

Pratson, L. F., Nittrouer, C. A., Wiberg, P. L., 2007. Seascape evolution on clastic continental shelves and slopes. In C. A. Nittrouer (Ed.),Continen-tal Margin Sedimentation. Oxford: Blackwell Publishing, pp. 340–380.

Pratt, B.R., 1994. Seismites in the Mesoproterozoic Altyn Formation (Belt Supergroup), Montana: a test for tectonic control of peritidal carbonate cyclicity. Geology 22, 1091–1094.

Ricci Lucchi, F., 1995. Sedimentological indicators of paleoseismicity. In: Serva, L., Slemmons, D.B. (Eds.), Perspectives in Paleoseismology. Association of Engineering Geologists Spec. Publ 6, pp. 7–17.

Roure, F., Howell, D.G., Muller, C., Moretti, I., 1990. Late Cenozoic subduction complex of Sicily. Journal of Structural Geology, 12, 259–266.

Lu, Y., Waldmann, N., Ian Alsop, G., Marco, S., 2017. Interpreting soft sediment deformation and mass transport deposits as seismites in the Dead Sea depocenter. Journal of Geophysical Research: Solid Earth, 122, 8305–8325.

Pepe, F., Sulli, A., Bertotti, G., Catalano, R., 2005. Structural highs formation and their relationship to sedimentary basins in the north Sicily continental margin (southern Tyrrhenian Sea): Implication for the Drepano Thrust Front. Tectonophysics, 409(1-4), 1-18.

Posamentier, H. W., Allen, G. P., James, D. P., Tesson, M., 1992. Forced regressions in a sequence stratigraphic framework: concepts, examples, and exploration significance (1). AAPG bulletin, 76(11), 1687-1709.

Posamentier, H. W., Morris, W.R., 2000. Aspects of the stratal architecture of forced regressive deposits. Geological Society, London, Special Publications, 172(1), 19-46.

Rudersdorf, A., Hartmann, K., Yu, K., Stauch, G., Reicherter, K., 2015. Seismites as indicators for Holocene seismicity in the northeastern Ejina Basin, Inner Mongolia. In: Landgraf, A., Kuebler, S., Hintersberger, E. & Stein, S. (eds) Seismicity, Fault Rupture and Earthquake Hazards in Slowly Deforming Regions. Geological Society, London, Special Publications, 432, pp. 1-19.

Sauter, E.J., Muyakshin, S.I., Charlou, J.L., Schlüter, M., Boetiusd, A., Jeroscha, K., Damma, E., Foucherc, J.P., Klagesa, M., 2006. Methane discharge from a deep-sea submarine mud

volcano into the upper water column by gas hydratecoated methane bubbles. Earth Planet Sci Lett 243: 354–365

Selley, R. C., 1979. Concepts and methods of subsurface facies analysis. United States: N. p., 1979. Web

Spatola, D., Micallef, A., Sulli, A., Basilone, L., Ferreri, R., Basilone, G., Bonanno, A., Pulizzi, M., Mangano, S., 2018a. The Graham Bank (Sicily Channel, central Mediterranean Sea): Seafloor signatures of volcanic and tectonic controls. Geomorphology 318, 375-389.

Spatola, D., Micallef, A., Sulli, A., Basilone, L., Basilone, G., 2018b. Evidence of active fluid seepage (AFS) in the southern region of the central Mediterranean Sea. Measurement, 128, 247-253.

Sulli, A., Agate, M., Mancuso, M., Pepe, F., Pennino, V., Polizzi, S., Lo Presti, V., Gargano, F., Interbartolo, F., 2012. Variability of depositional setting along the North-western Sicily continental shelf (Italy) during Late Quaternary: Effects of sea level changes and tectonic evolution. Alp. Mediterr. Quat, 25, 141-156.

Sulli, A., Lo Presti, V., Gasparo Morticelli, M., Antonioli, F., 2013. Vertical movements in NE Sicily and its offshore: outcome of tectonic uplift during the last 125 ky. Quaternary International 288:168–182. https://doi.org/10.1016/j.quaint.2012.01.021

Sulli, A., Zizzo, E., Albano, L., 2018. Comparing methods for computation of run-up heights of landslide-generated tsunami in the Northern Sicily continental margin. Geo-Marine Letters, 38(5), 439-455.

Sulli, A., Gasparo Morticelli, M., Agate, A., Zizzo, E., 2019. Hinterland-verging thrusting in the northern Sicily continental margin: a late collisional stage of the Sicilian Fold and Thrust Belt?. Geophysical Research Abstracts, 20, EGU2018-8842, EGU General Assembly, 8–13 April 2018

Tesson, M., Gensous, B., Allen, G. P., & Ravenne, C., 1990. Late Quaternary deltaic lowstand wedges on the Rhône continental shelf, France. Marine Geology, 91(4), 325-332.

von Huene, R., Ranero, C. R., Vannucchi, P., 2004. Generic model of subduction erosion. Geology, 32(10), 913-916.

Waldron, J.W.F., Gagnon, J.-F., 2011. Recognizing soft-sediment structures in deformed rocks of orogens. Journal of Structural Geology 33, 271–279.

Wynn, R. B., Cronin, B. T., Peakall, J., 2007. Sinuous deep-water channels: Genesis, geometry and architecture. Marine and Petroleum Geology, 24(6-9), 341-387.

Figure captions

Fig. 1. Location map of the southern Tyrrhenian Sea showing the main morphological-structural features. Background bathymetry is from EMODnet bathymetry (http://www.emodnet-bathymetry.eu). CZ: Capo Zafferano Promontory, CP Capo Plaia Promontory:, OT:, UI: Ustica Island, AI: Aeolian Islands, EI: Egadi Islands. Red box is the study area.

Fig. 2. (A) Study area showing seismic reflection profiles (sparker and CHIRP sources), multibeam data (highlighted the seismic lines displayed in this paper) and vibrocores location. CZ: Capo Zafferano Promontory, CP Capo Plaia Promontory. (B) Physiographic features of the study area. Black dashed rectangles: positions of Figs, 3-6.

Fig. 3. (A-B) Map of the main morphologic elements and features identified across the study area. Longitudinal profiles across the study area. SB: Shelf break; Is: Inner shelf margin.

Fig. 4. Shaded relief map (above) and longitudinal profiles (below) across the western sector of the study area. IS: inner shelf; OS: outer shelf; ST1: submerged terrace 1; ST2: submerged terrace 2; ST3: submerged terrace 3; SB: shelf break; SL: slope ledge.

Fig. 5. Shaded relief map showing the detailed morphology of the Capo Plaia Canyon. Lines with different colors indicate the 5 rectified directions identified along the Canyon stream.

Fig. 6. Seismic units identified both on sub bottom (A1) and sparker (A2 to E) profiles.

Fig. 7. Sparker seismic reflection profile across the central sector of the study area (see location in Fig. 2), showing mounds and associated hydro-acoustical anomalies (above) and offset reflectors in correspondence of mounds (below).

Fig. 8. Isopach maps of the sub-units identified in the Unit E. For depth-conversion of travel times from seismic profiles, we used 1.6 km/s sound velocity, as derived from correlation with well velocity logs in adjacent areas.

Fig. 9. Shepard's diagram with the mean grain size of the cores collected in the Gulf of Termini.

Fig. 10. A) 3D view of the study area with the main morphological features; B) Longitudinal profile along the talweg of the Capo Plaia Canyon. Straight lines with different colors point out the transects with different direction; C) Slope map of the study area from morphobathymetric data.

Fig. 11. A) Detail of the sparker seismic profile (location in fig.2). B) Geoseismic interpretation of the seismic profile in A. C) Seismostratigraphy, physical parameters and Age Model of the interpreted SSDS.

Table 1. Location of the vibrocores collected in the Termini Gulf (UTM and Geographic coordinates).

Table 2. Physical parameters and tentative lithological interpretation of the sub-facies identified in the Unit E.

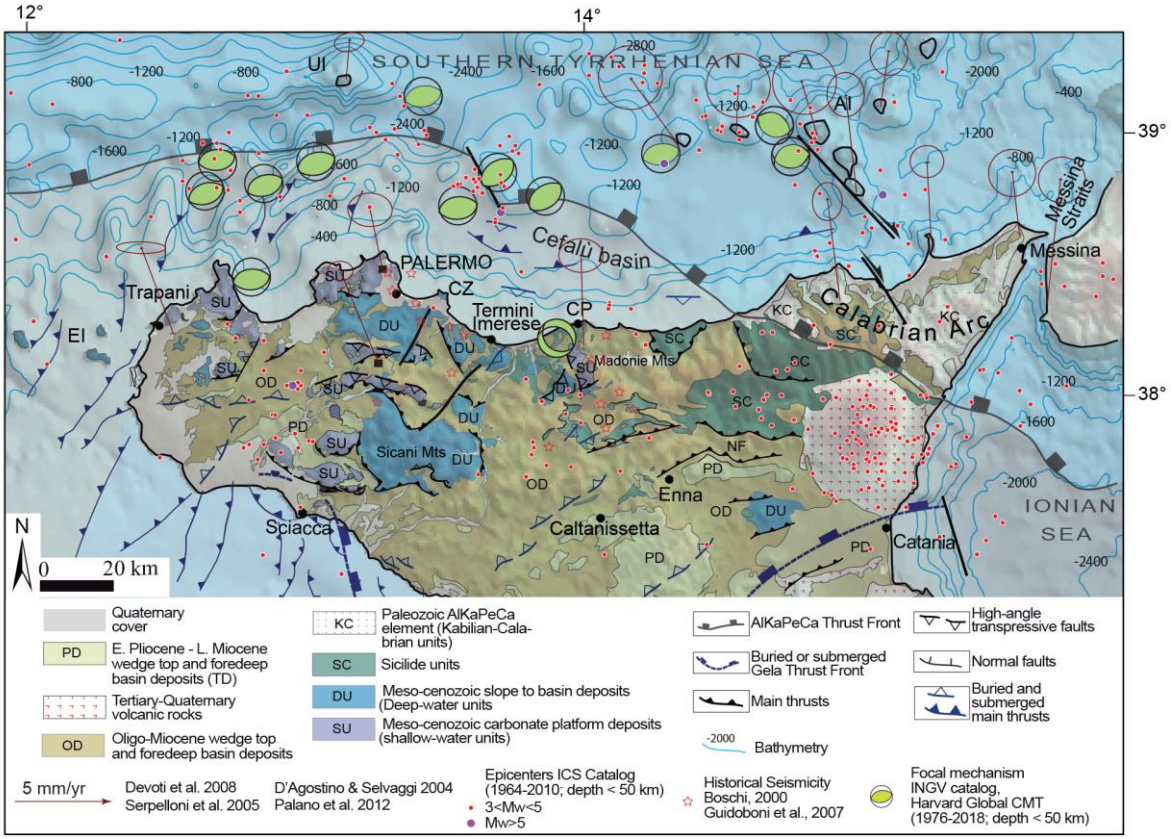

Fig. 1. Zizzo et al., 2019

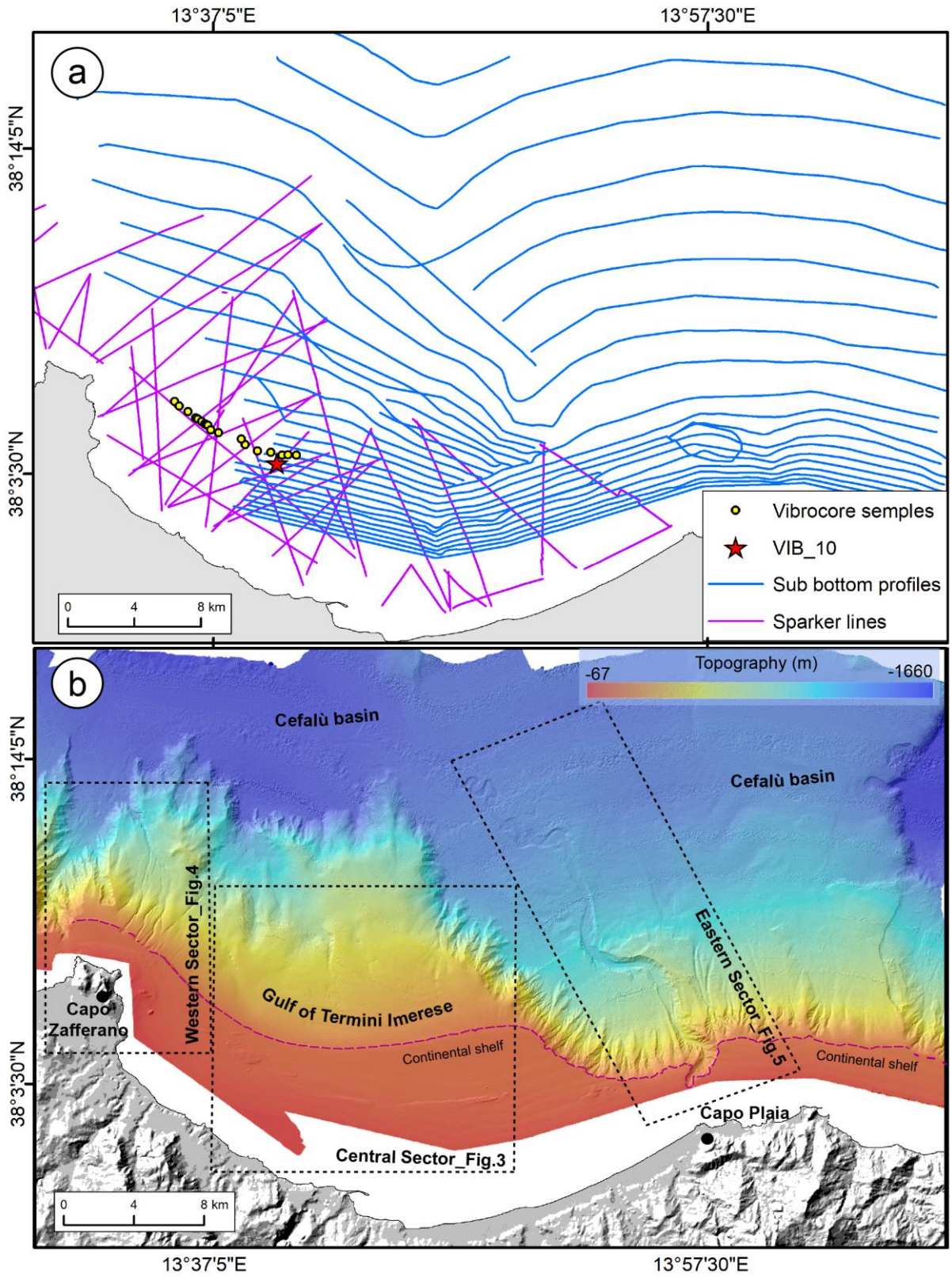

Fig. 2. Zizzo et al., 2019

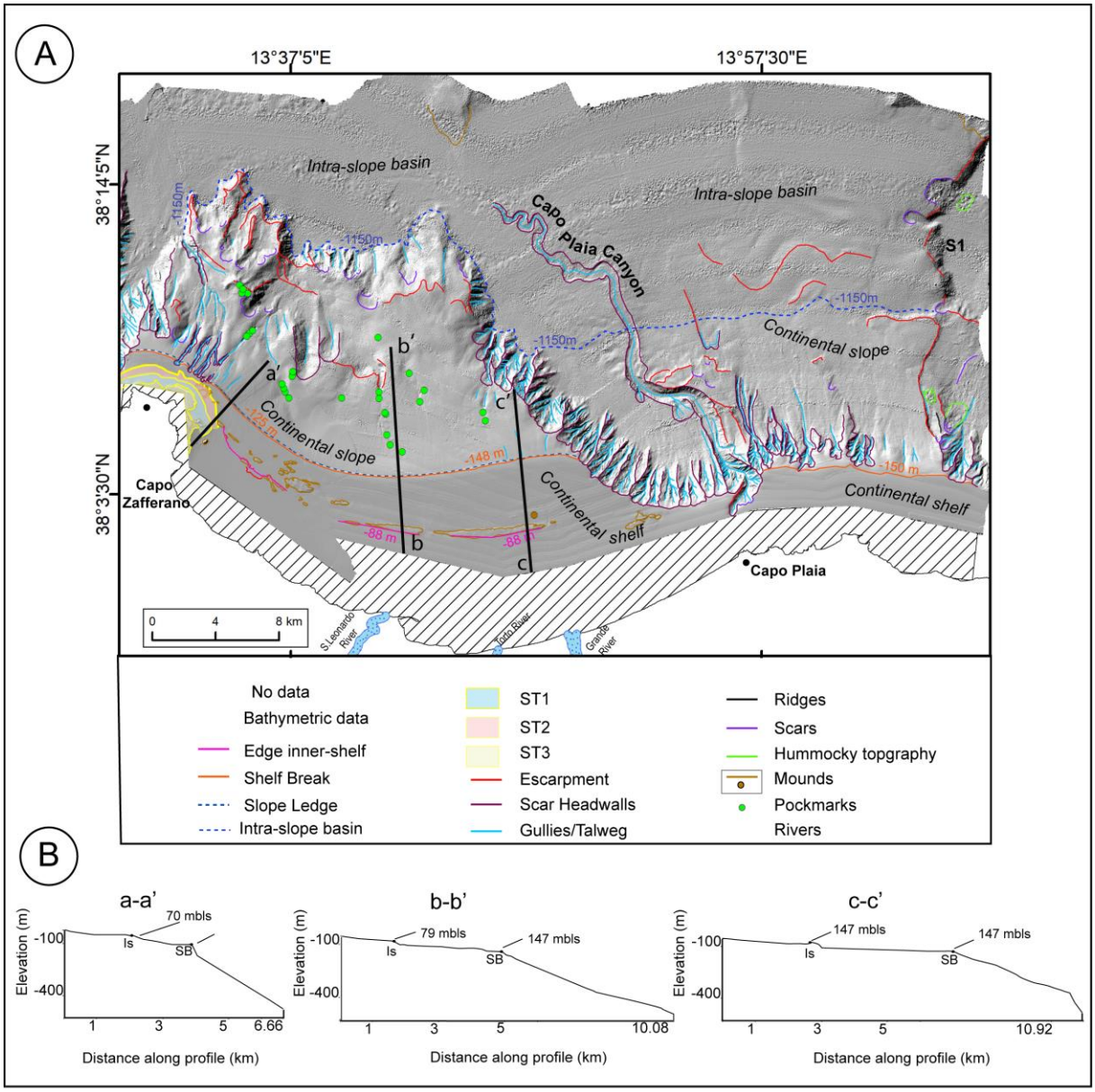

Fig. 3. Zizzo et al., 2019

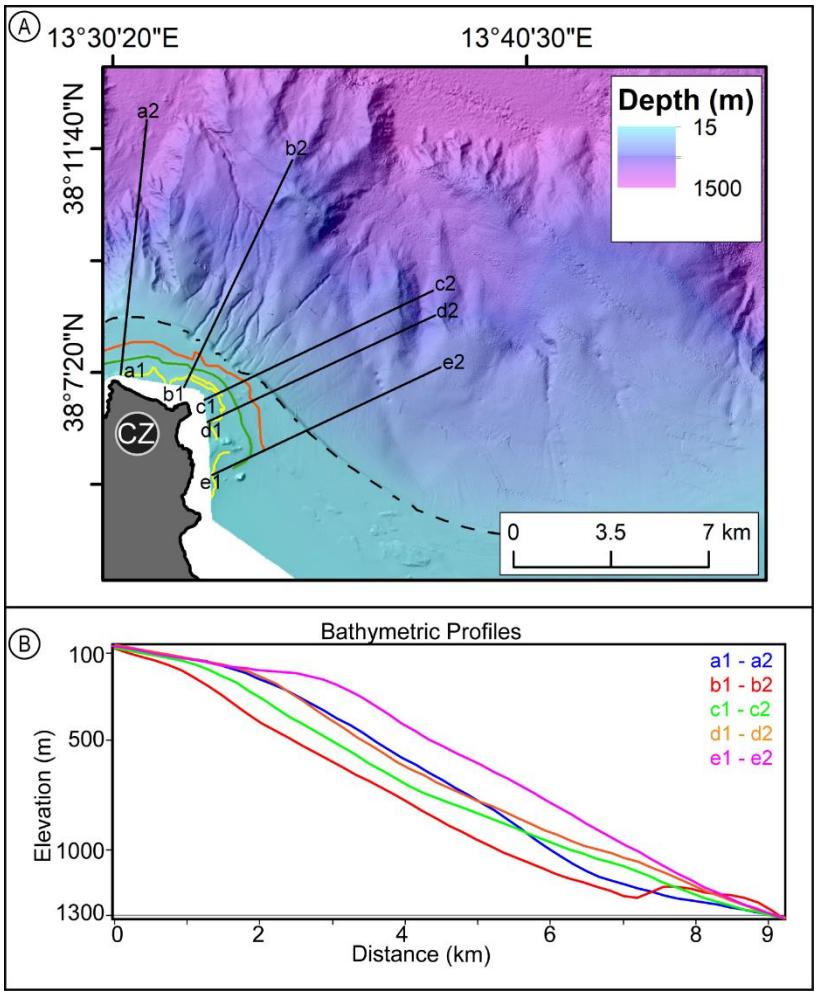

Fig. 4. Zizzo et al., 2019

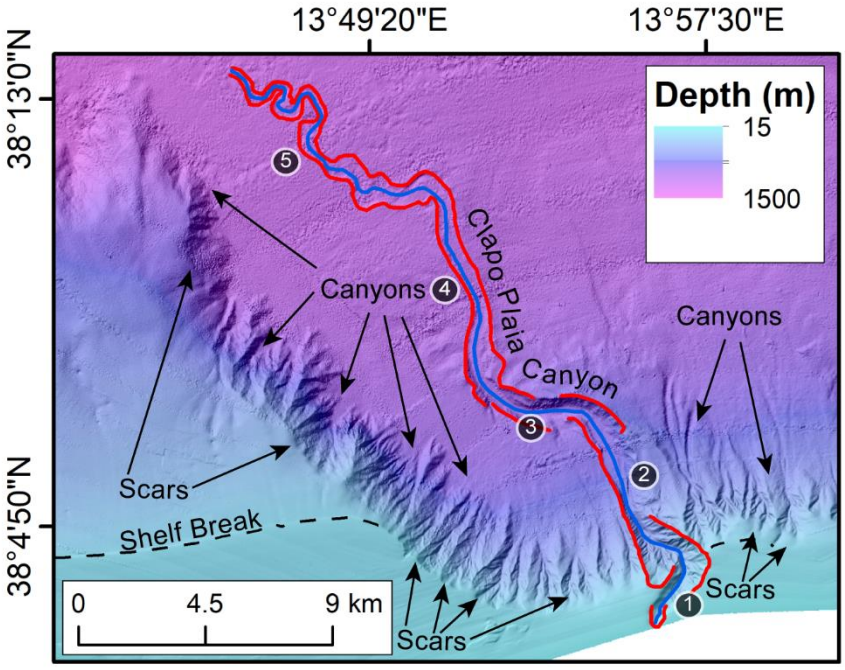

Fig. 5. Zizzo et al., 2019

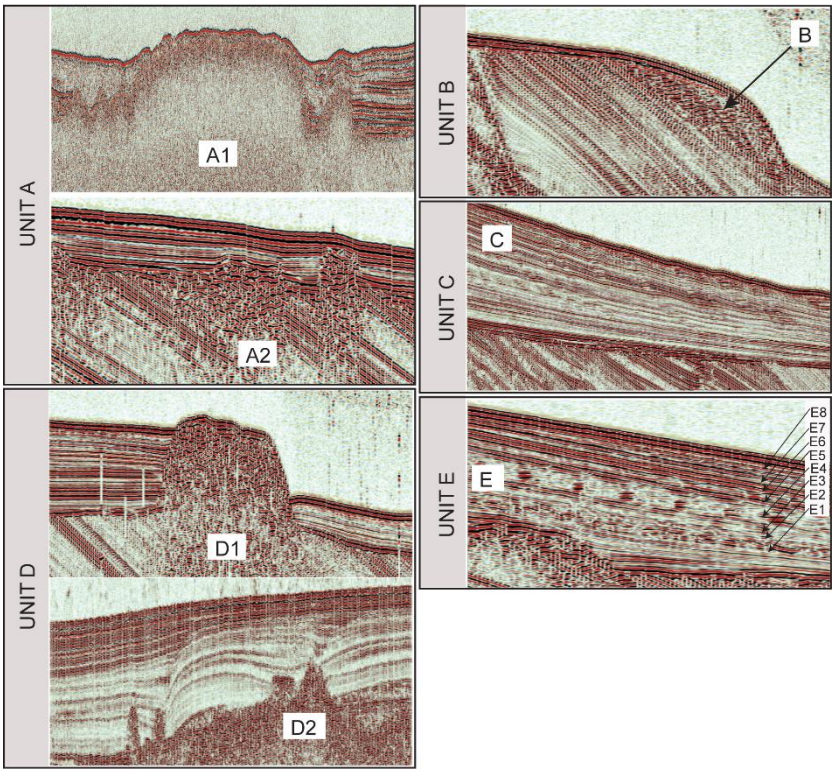

Fig. 6. Zizzo et al., 2019

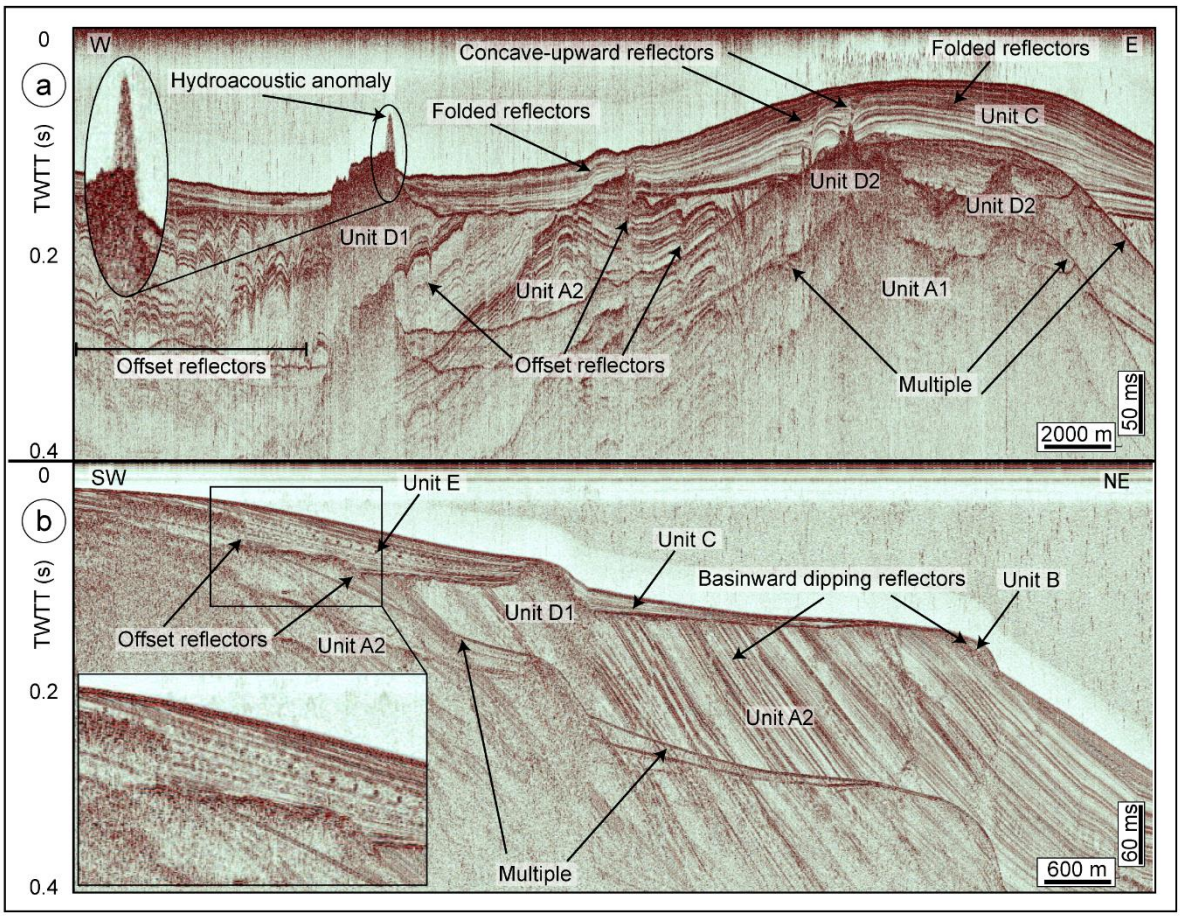

Fig. 7. Zizzo et al., 2019

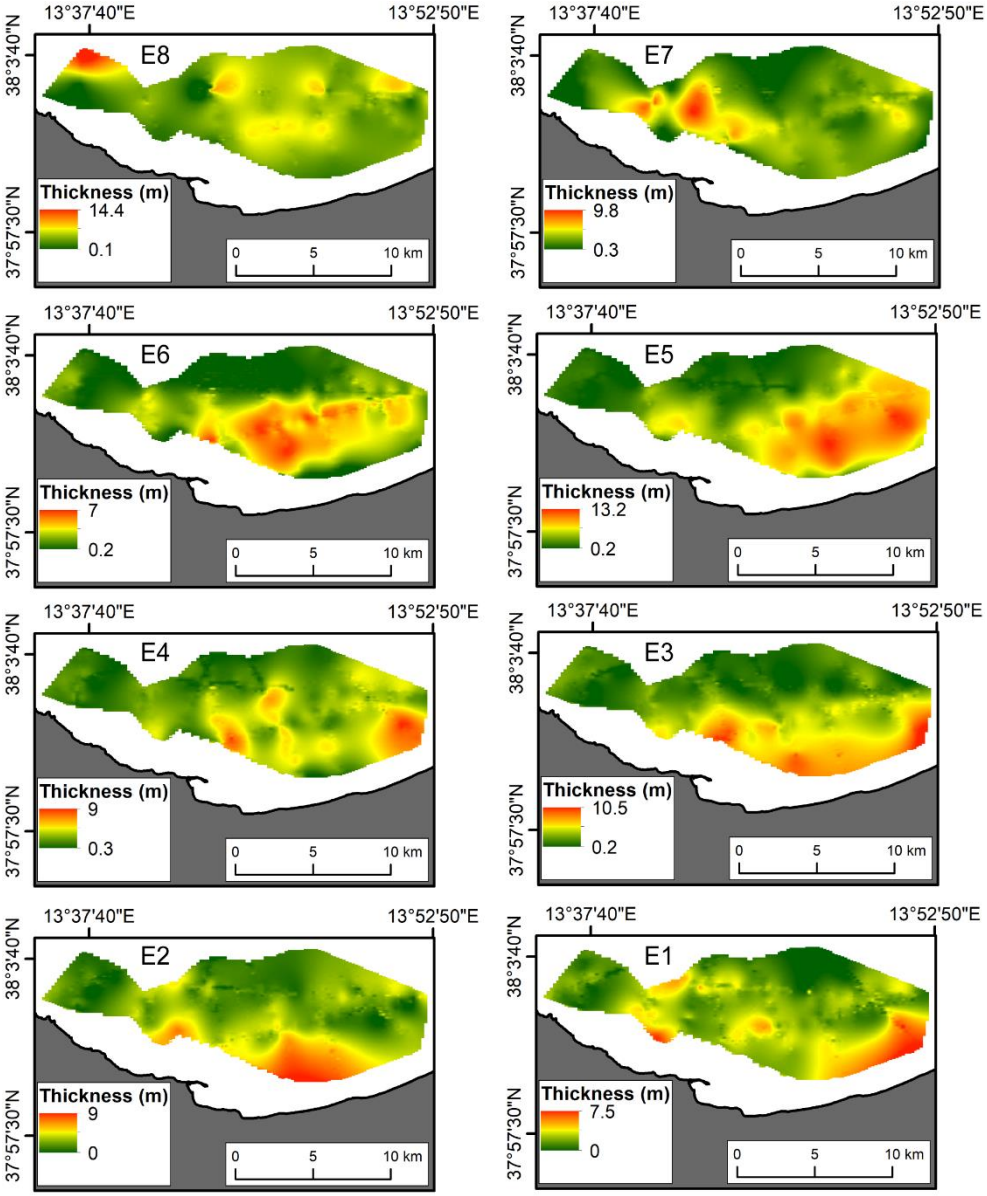

Fig. 8. Zizzo et al., 2019

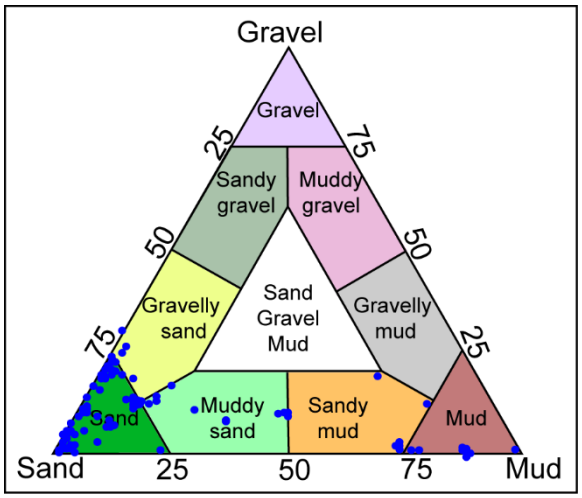

Fig. 9. Zizzo et al., 2019

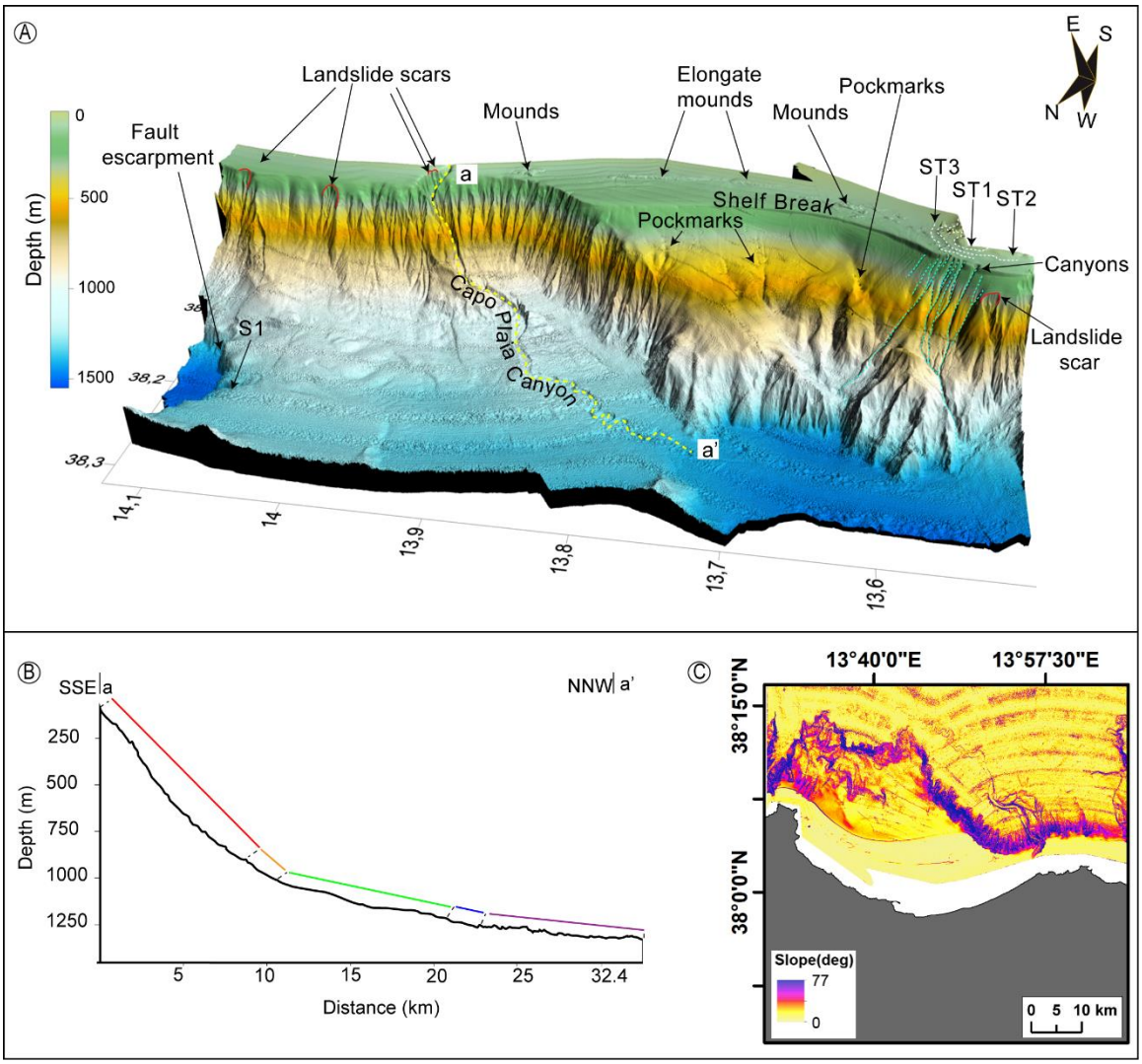

Fig. 10. Zizzo et al., 2019

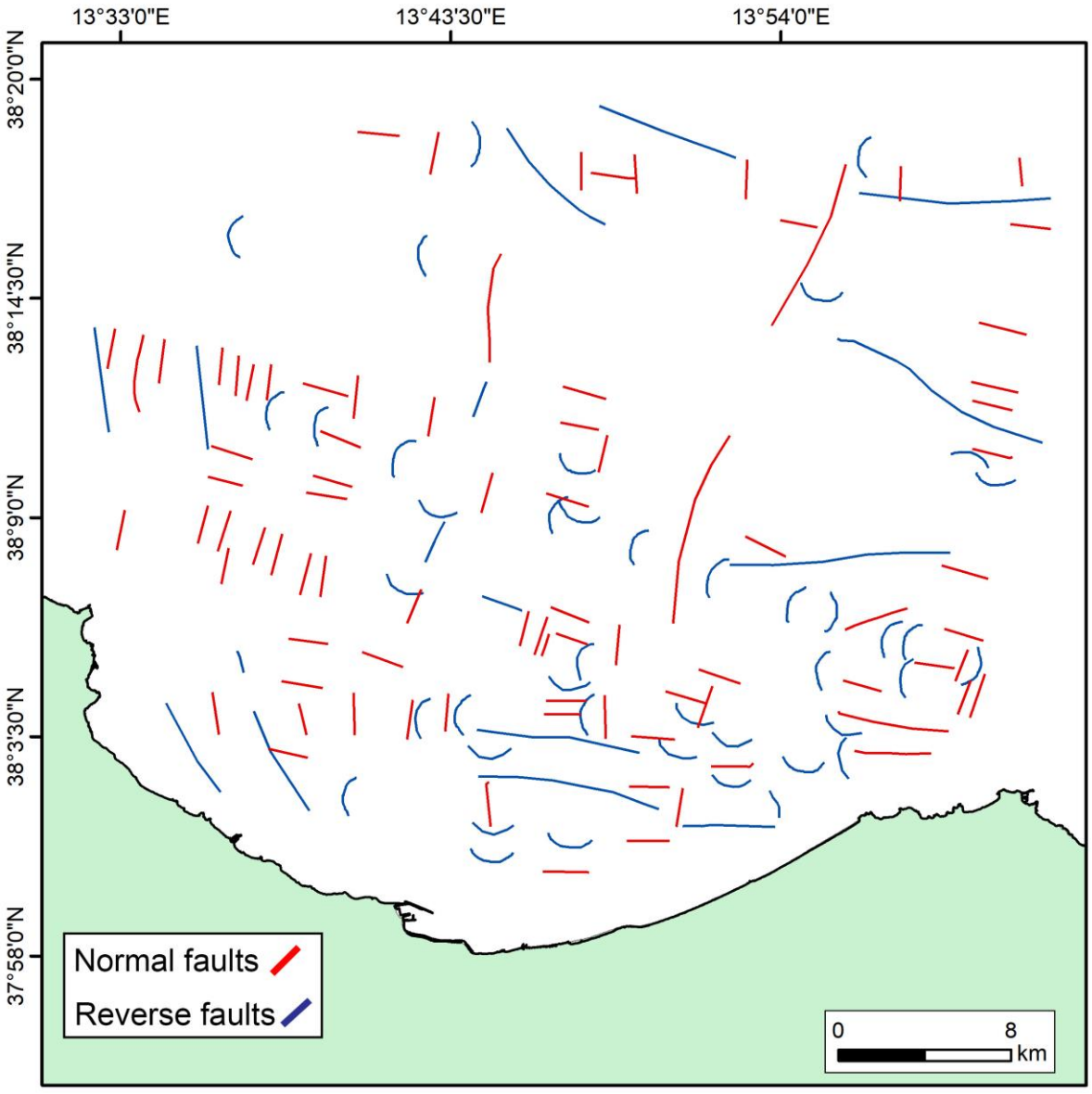

Fig. 11. Zizzo et al., 2019

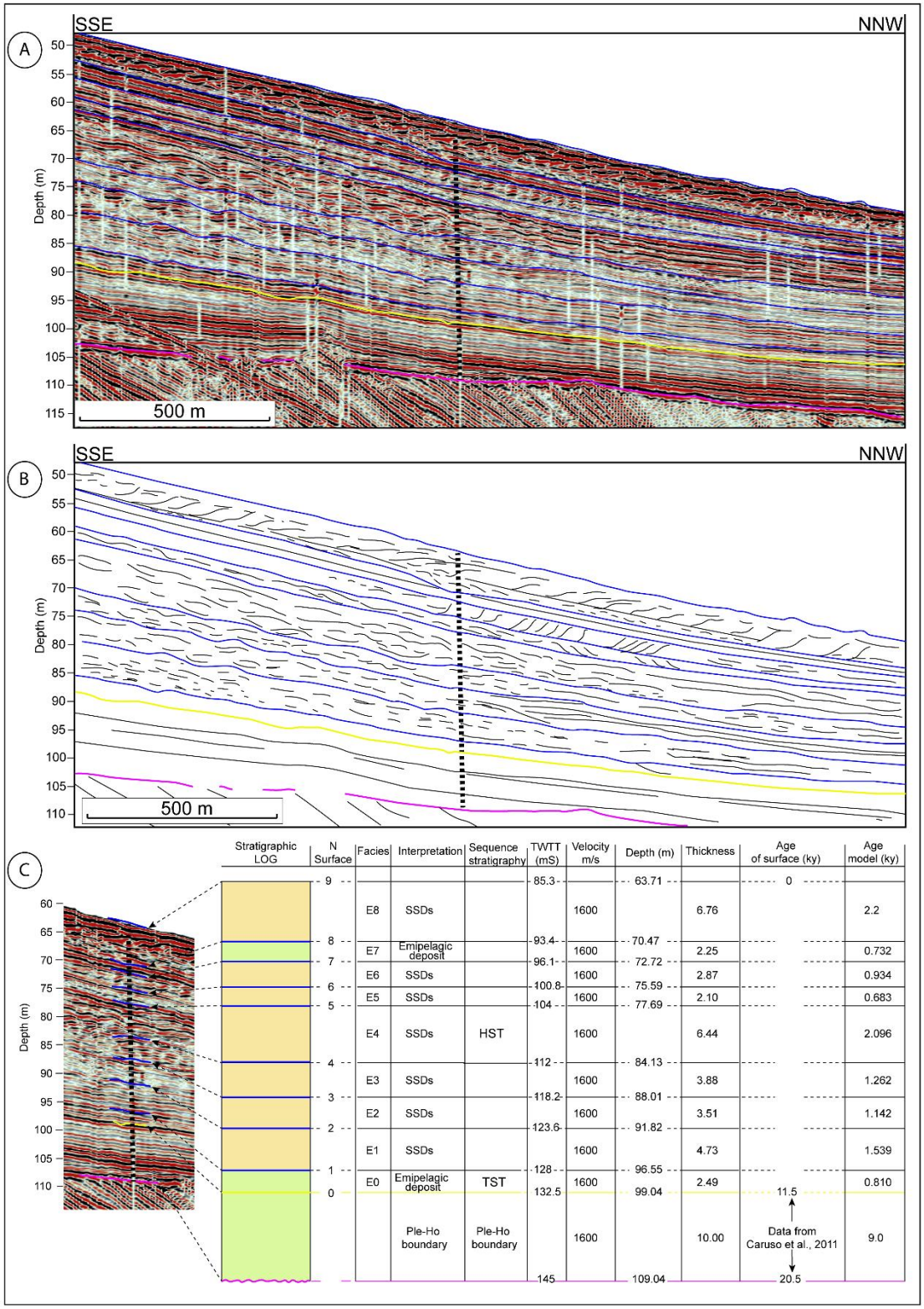

Fig. 12. Zizzo et al., 2019

ID	UTM 33N		GEOGRAPHIC	
	X	Y	LONGITUDE	LATITUDE
VC01	376851	4217703	13°35'43,7895" E	38°05'55,5001" N
VC01b	376851	4217703	13°35'43,7895" E	38°05'55,5001" N
VC02	376942	4217616	13°35'47,5787" E	38°05'52,7228" N
VC03	377033	4217528	13°35'51,3684" E	38°05'49,9130" N
VC04	377125	4217440	13°35'55,1991" E	38°05'47,1037" N
VC05	377260	4217355	13°36'00,7928" E	38°05'44,4127" N
VC06	377396	4217270	13°36'06,4274" E	38°05'41,7221" N
VC07	377531	4217184	13°36'12,0215" E	38°05'38,9985" N
VC07b	377531	4217184	13°36'12,0215" E	38°05'38,9985" N
VC08	377666	4217100	13°36'17,6142" E	38°05'36,3397" N
VC09	377781	4217003	13°36'22,3940" E	38°05'33,2493" N
VC10	377896	4216907	13°36'27,1730" E	38°05'30,1914" N
VC11	378010	4216810	13°36'31,9115" E	38°05'27,1005" N
VC12	378125	4216714	13°36'36,6903" E	38°05'24,0425" N
VC13	378241	4216666	13°36'41,4806" E	38°05'22,5418" N
VC14	378318	4216618	13°36'44,6702" E	38°05'21,0222" N
VC15	378395	4216570	13°36'47,8598" E	38°05'19,5026" N
VC16	378473	4216521	13°36'51,0910" E	38°05'17,9510" N

Table 1. Zizzo et al., 2019

Seismic Unit	Max Thickness (m)	Volume (m^3)	Interpretation
Sub-unit E8	14.4	40913	SSDS
Sub-unit E7	9.8	164550	Hemipelagic deposit
Sub-unit E6	7	388088	SSDS
Sub-unit E5	13.2	71733	SSDS
Sub-unit E4	9	25718	SSDS
Sub-unit E3	10.5	55238	SSDS
Sub-unit E2	9	10528	SSDS
Sub-unit E1	7.5	43876	SSDS

Table 2. Zizzo et al., 2019

CHAPTER 5

Potential Cyclic steps in a gully system of the Gulf of Palermo (Southern Tyrrhenian Sea)

NOTE This chapter is a scientific paper published in "Springer International Publishing Switzerland 2017 J.Guillén et al. (eds), Atlas of Bedorms in the Western Mediterranean". The authors are the followings: Claudio Lo Iacono, Mathieu Cartigny, Elisabetta Zizzo, Mauro Agate and Attilio Sulli. *DOI 10.1007/978-3-319-33940-5_36.*

Abstract
Multibeam bathymetric data revealed the occurrence of a train of bedforms along a gully system in the Gulf of Palermo, southern Tyrrhenian Sea. The observed gullies, located in the westernmost sector of the Gulf of Palermo, incise the outer shelf at a depth of 120 m and converge at the Zafferano Canyon, connecting to the Palermo Basin at a depth of 1300 m. Bedforms develop along these gullies and along the thalweg of the canyon, displaying an average wavelength of 200 m, with maximum values of 340 m. Their gully floor location combined with their wave length, upslope asymmetry and crescent shape point to a possible cyclic step origin of these bedforms. Preliminary numerical modelling suggests that, assuming that these bedforms were formed by cyclic steps in turbidity currents, these flows might have been few meters thick and have had velocities in the range of 0.2–1.5 m/s.

Keywords: Cyclic steps, Gullies, Submarine canyons, Turbidity currents, Gulf of Palermo, Tyrrhenian sea.

1. Introduction-Study Area

The submarine canyons of the Gulf of Palermo (northwestern Sicily, southern Tyrrhenian Sea) deeply carve the sedimentary sequence of the Palermo slope and basin system, most of them breaching the shelf margin, and extend to a depth of 1500 m, coinciding with the deepest area of the Palermo intraslope Basin (Lo Iacono et al. 2011, 2014). A train of bedforms occurs along a gully network in front of Cape Zafferano, in the easternmost sector of the gulf, where the continental shelf is no wider than 3 km (Fig. 1). The channel floor location of the bedforms, together with their wave length, crescent shape and upslope asymmetry, suggests that they might have developed as a result of a cyclic step process. In such a process, the downstream side of the bedform (the lee side of the bedform) is continuously eroded by a supercritical flow (Froude Number [Fr] > 1), while the flatter upstream side of the bedform is shaped by depositional subcritical flows (Fr < 1) (Parker 1996). This process leads to the formation of a series of asymmetrical upslope-migrating (often crescent-shaped) bedforms (Clarke et al. 2014). Similar bedforms have been observed in open slope environments (Migeon et al. 2000; Pratson et al. 2000; Hill et al. 2008; Urgeles et al. 2011) and more frequently along the thalweg of several submarine canyons and gullies (Fildani et al. 2006; Clark et al. 2014; Covault et al. 2014; Zhong et al. 2015) and could be interpreted as cyclic steps (Cartigny et al. 2011; Kostic 2011). Unfortunately, there are no available data to definitely confirm a cyclic step origin of the bedforms presented here, or even to proof their upslope migration over time.

These bedforms are interpreted here as cyclic steps purely on the basis of their geometry and location. We aim to present their morphologic interpretation and in second instance to roughly estimate the main characteristics of the flow potentially responsible for their formation, applying an hydraulic flow model.

2. Materials and methods

Swath-bathymetry multibeam (MB) data available for this study were acquired during two different oceanographic cruises in 2001 (CARG Project) and 2009 (MaGIC Project) (Chiocci and Ridente 2011). The MB system of the 2001 cruise was a Reson SeaBat 8111 generating 105 beams at a frequency of 100 kHz. The MB system of the 2009 cruise was a Reson SeaBat8160 generating 126 beams at a frequency of 50 kHz. The MB data were post-processed with the PDS-2000 system. Digital terrain models were produced with a footprint resolution of 20 m. For further details, see Lo Iacono et al. (2011, 2014). Global Mapper and Golden Software Surfer 9 were used to map the trains of bedforms and to calculate their main morphometric characteristics (Table 1). The bedform steepness has been defined as the step heights divided by the step lengths (h/L). The asymmetry index (AI) (Knaapen 2005) is defined as L2-L1/L, where L is the distance between two troughs, L1 is the distance between upslope trough and crest and L2 is the distance between the crest and the downslope trough. An AI > 0.02 indicates the presence of asymmetric bedforms. Negative AI values indicate a downslope asymmetry and positive AI values indicate an upslope asymmetry. The applied numerical model strongly simplifies the flows by averaging all flow parameters over the depth, by excluding any exchange of sediment in between the flow and the bed, and by limiting the downstream evolution of the flow to only include small variations as described in gradual varying flow theory. The numerical model uses an average grain size (medium sands) and the stoss and lee side slopes of observed bedforms as input data. The model runs several thousands of simulations for flows combining different discharges, Froude numbers and sediment concentrations. The synthetic bedform wavelengths and amplitudes predicted by these simulations are finally compared with the dimensions of the observed cyclic steps, and the most appropriate characteristics of their genetic flow are then fitted. More details on the model and its assumptions can be found in Cartigny et al. (2011).

3. Results-Discussion

The cyclic steps of the Gulf of Palermo were mapped in a depth range of 125–1050 m along a network of 9 gullies breaching the shelf-edge in front of Cape Zafferano, the eastern cape of the gulf (Figs1, 2). The gullies have an average width of 180 m and are up to 20 m deep. Some of the gullies display a smoothed and planed morphology of unclear origin within a depth range of 500–700 m (Fig 2). The mapped bedforms have a wavelength ranging from 110 to 340 m and an amplitude ranging from 0.8 to 5 m. Their steepness ranges from 0.007 to 0.01, this last value corresponding to the most morphologically pronounced bedforms, where steeper lee (downslope) and stoss (upslope) sides occur (Fig 3). These bedforms are also the most (upslope) asymmetric, with an AI of 0.27. The general slope gradient of the gullies along which the most asymmetric and steepest bedforms occur ranges from 7° to 10°.Based on the assumption that the bedforms developed as a result of a cyclic step process, rough estimations of the turbidity currents which generated the cyclic steps can be made using a simple numerical model for a given range of flow characteristics. The bedforms of Cape Zafferano

displaying a more pronounced morphology are here used as input for the model (Fig 3). The average characteristics for the selected bedforms (700–800 m water depth) are summarized in Table 1.

The model calculations indicate that the observed cyclic steps are likely generated by flows around 1 m thick, with average velocities of exceeding 1.0 m/s. The maximum velocities at the toe of the steep lee sides could reach values of ~1.5 m/s, whereas on the flatter stoss sides the flow reaches a maximum thickness exceeding 2 m combined with a minimum velocity of ~0.2 m/s (Fig 3). As the model makes several assumptions to simplify the flow dynamics, it is necessary to point out that these values are only very rough estimates, and are fully dependent on our cyclic step interpretation.

The occurrence of the studied bedforms along the Capo Zafferano Canyon and associated gullies likely suggests intense turbidity current or a variation in morphology and grain size along these incisions compared to the other canyons mapped in the Gulf of Palermo, where bedforms are apparently absent. This observation fits with previous considerations describing the easternmost canyons and gullies of each gulf along the northwestern Sicilian margin as the most intensely subject to downslope turbidity flows (Lo Iacono et al. 2014). The topography of the eastern Cape Zafferano and the corresponding decrease in the shelf width probably control the path of the along-shelf currents, which are diverted towards the canyon heads, promoting the creation of turbidity currents. Few insights are actually available about the age of the observed bedforms. The reduced steepness of most of the cyclic steps leads us to interpret these bedforms as no longer active and likely degraded in their height by sporadic diluted sedimentary flows and bioturbation processes.

4. Conclusions

Swath-bathymetry mapping along the Gulf of Palermo (southern Tyrrhenian) revealed the occurrence of trains of bedforms along a set of shelf incising gullies connected to the Zafferano Canyon. The observed bedforms are upslope asymmetric and display maximum lengths of 340 m.

Based on their location and geometry, these bedforms are here interpreted as formed by cyclic step processes in turbidity currents.

A preliminary and strongly simplified numerical reconstruction suggests that the flow controlling the development of such cyclic steps is a few meter thick (0.3–2.5 m) and might have reached peak velocities exceeding 1 m/s.

Acknowledgments

Data acquisition was made possible thanks to the Italian National Research Projects MaGIC (Marine Geological Hazard along the Italian Coast), funded by the Italian Civil Protection Department, and CARG (Geological Maps of Italy), funded by the ISPRA-Italian Geological Survey. Constructive reviews by two anonymous reviewers greatly improved the submitted version of the manuscript.

References

Cartigny, M. J., Postma, G., van den Berg, J. H., & Mastbergen, D. R. (2011). A comparative study of sediment waves and cyclic steps based on geometries, internal structures and numerical modeling. Marine Geology, 280(1), 40–56.Google Scholar

Chiocci F.L., Ridente D., (2011). Regional-scale seafloor mapping and geohazard assessment. The experience from the Italian project MaGIC (Marine Geohazards along the Italian Coasts). Mar. Geophys. Res. 32, 13–23.Google Scholar

Clarke, J. E. H., Vidiera Marques, C., Pratomo, D. (2014). Imaging active mass-wasting and sediment flows on a fjord delta, Squamish, British Columbia. In S. Krastel et al. (eds.), Submarine Mass Movements and Their Consequences, Advances in Natural and Technological Hazards Research 37, Springer.Google Scholar

Covault, J. A., Kostic, S., Paull, C. K., Ryan, H. F., & Fildani, A. (2014). Submarine channel initiation, filling and maintenance from sea-floor geomorphology and morphodynamic modelling of cyclic steps. Sedimentology, 61(4), 1031–1054.Google Scholar

Fildani, A., Normark, W. R., Kostic, S., & Parker, G. (2006). Channel formation by flow stripping: Large-scale scour features along the Monterey East Channel and their relation to sediment waves. Sedimentology, 53(6), 1265–1287.Google Scholar

Hill, P. R., Conway, K., Lintern, D. G., Meulé, S., Picard, K., & Barrie, J. V. (2008). Sedimentary processes and sediment dispersal in the southern Strait of Georgia, BC, Canada. Marine environmental research, 66, S39–S48.Google Scholar

Knaapen, M.A.F., (2005). Sandwave migration predictor based on shape information. J. Geophys. Res. 110, F04S11. doi: 10.1029/2004JF000195

Kostic, S. (2011). Modeling of submarine cyclic steps: Controls on their formation, migration, and architecture. Geosphere, 7(2), 294–304.Google Scholar

Lo Iacono C., Sulli A., Agate M., LoPresti V., Pepe F., Catalano R., (2011). Submarine canyon morphologies in the Gulf of Palermo (Southern Tyrrhenian Sea) and possible implications for geo-hazard. Marine Geophysical Researches 32, 127–138.Google Scholar

Lo Iacono C., Sulli A., Agate M., (2014). Submarine canyons of north-western Sicily (Southern Tyrrhenian Sea): Variability in morphology, sedimentary processes and evolution on a tectonically active margin. Deep-Sea Research II 104, 93–105.Google Scholar

Migeon S., Savoye B., Faugeres JC., (2000). Quaternary development of migrating sediment waves in the Var deep-sea fan: distribution, growth pattern, and implication for levee evolution. Sedimentary Geology 133, 265–293.Google Scholar

Parker, G. (1996). Some speculations on the relation between channel morphology and channel-scale flow structures. Coherent flow structures in open channels, 423.Google Scholar

Pratson L.F., Imran J., Parker G., Syvitski JPM., Hutton E., (2000). Debris flows versus turbidity currents: A modeling comparison of their dynamics and deposits. In: Bouma A.H. and Stone C.G. eds: Fine-Grained Turbidite Systems: American Association of Petroleum Geologists Memoir 72, SEPM (Society for Sedimentary Geology) Special Publication 68, 57–72.Google Scholar

Urgeles R., Cattaneo A., Puig P., Liquete C., De Mol B., Amblas D., Sultan N., Trincardi F., (2011). A review of undulated sediment features on Mediterranean prodeltas: distinguishing sediment transport structures from sediment deformation. Marine Geophysical Research 32, 1–1, 49–69.Google Scholar

Zhong, G., Cartigny, M.J.B., Kuang, Z., & Wang, L. (2015). Cyclic steps along the South Taiwan Shoal and West Penghu submarine canyons on the northeastern continental slope of the South China Sea. Geological Society of America Bulletin, B31003-1.

Figure captions

Fig 1 Bathymetric model of the study area. Cape Zafferano is the eastern cape of the Gulf of Palermo

Fig 2 Bathymetric model of the submarine gullies and of the Zafferano Canyon, where interpreted cyclic steps (CS) were mapped

Fig 3 3D bathymetric model of the most pronounced cyclic steps in the area, where numerical models were applied to reconstruct the intensity (U) and thickness (h) of the corresponding turbidity currents (section A–A′)

Table 1 Bedform characteristics of profile A–A′ in Fig 3.

Lo Iacono et al., 2017

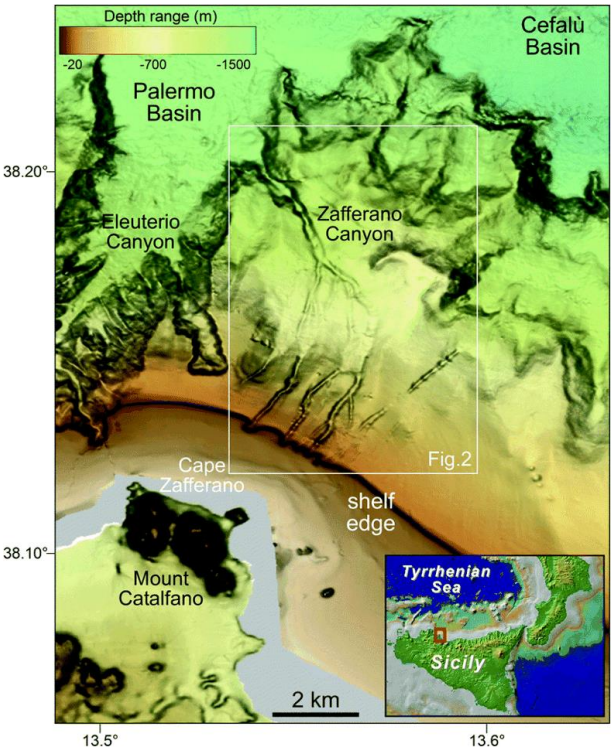

Fig 1. Lo Iacono et al., 2017

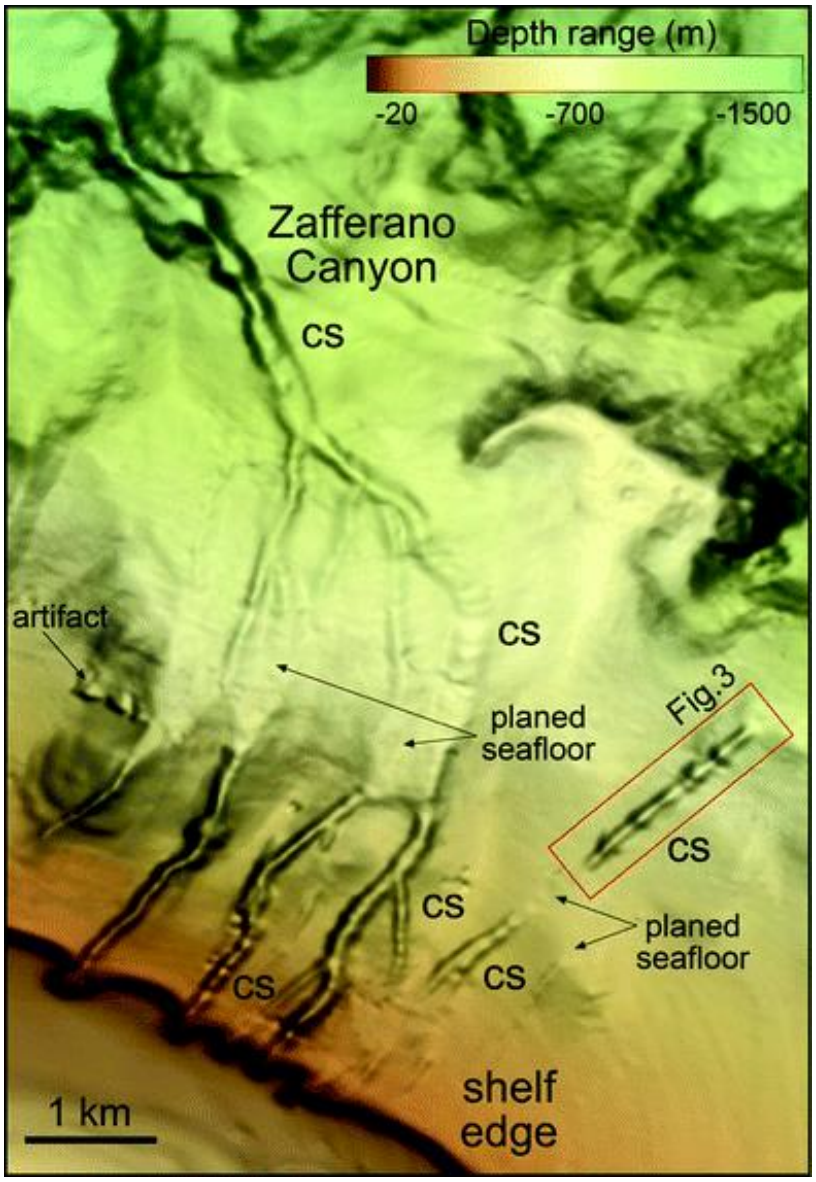

Fig 2. Lo Iacono et al., 2017

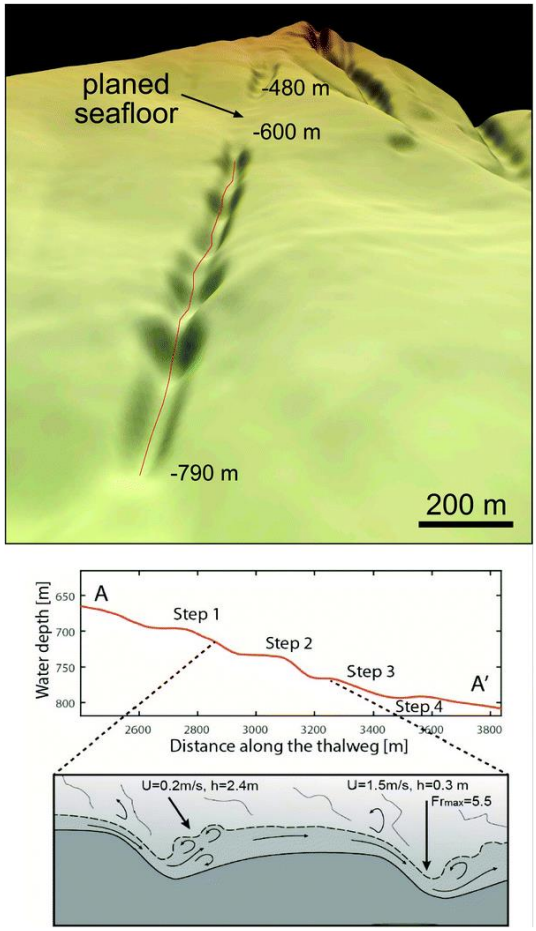

Fig 3. Lo Iacono et al., 2017

Table 1. Lo Iacono et al., 2017

Step #	Slope stoss side (m)	Slope lee side (–)	Length (m)	Amplitude (m)
Step 1	−0.008	0.164	224	5.8
Step 2	0.026	0.217	198	13.2
Step 3	0.003	0.110	249	3.1
Step 4	−0.038	0.063	286	5.0
Average	−0.004	0.138	239	6.8

CHAPTER 6

Seismotectonic map of the Northern Sicily Continental Margin (NSCM) and implications for Geohazard assessment

NOTE This chapter is a "working in progress" scientific paper in collaboration with: Attilio Sulli, Maurizio Gasparo Morticelli and Aaron Micallef.

1. Introduction and geological-geophysical setting

The Northern Sicily Continental Margin (NSCM) is a segment of the Appeninic-Tyrrhenian System whose upbuilding refers to both the post-collisional convergence between Africa and a very complex "European" crust (Bonardi et al., 2001) or AlKaPeKa (sensu Boullin, 1986) and the opening of the Tyrrhenian back-arc basin.

Seismo-stratigraphic and morpho-structural analysis of a large number of available (from ViDePi project) and unpublished (from Department of Earth and Marine Science of the University of Palermo) multichannel seismic reflection profiles acquired across the NSCM, together with new morphobathymetric data, allow us to produce a seismotectonic map, in order to obtain a useful tool for the assessment of the seismic hazard of the sea-land region.

The NSCM is suitable to test this approach because it is located in a transitional area between the Sicilian-Maghrebian chain to the south and the Tyrrhenian back-arc basin to the north. Along this transect the Moho depth ranges from about 10 km, in the Marsili bathyal plain, to about 40 km, towards the northern Sicily coast. The Bouguer anomalies change from 180 mGal in the Tyrrhenian region to negative anomalies in central Sicily (-100 mGal), while positive magnetic anomalies characterize the volcanic edifices, both submerged and buried. While, the heat flow shows very high values across the southern Tyrrhenian Sea (200 mW/m-2) that decrease (30-40 mW/m-2) towards the stable sector of the foreland area (Iblean plateau in SE Sicily).

2. Methodology

The seismotectonic map has been compiled from the overlapping of different geological layers that represent the main identified seafloor and sub-seafloor features (Fig. 1), such as geological map (Fig. 2), tectonic elements (normal and reverse faults), earthquakes, heat flow, gravimetric (Fig. 3) and magnetometric (Fig. 4) anomalies, Moho depth (Fig. 3), heat flow (Fig. 5), mass-wasting, fluid escape structures (e.g. pockmarks, mounds, gas flares, and gas chimneys), sedimentary successions (Fig. 1), ground acceleration and lateral/vertical motions (Fig. 6).

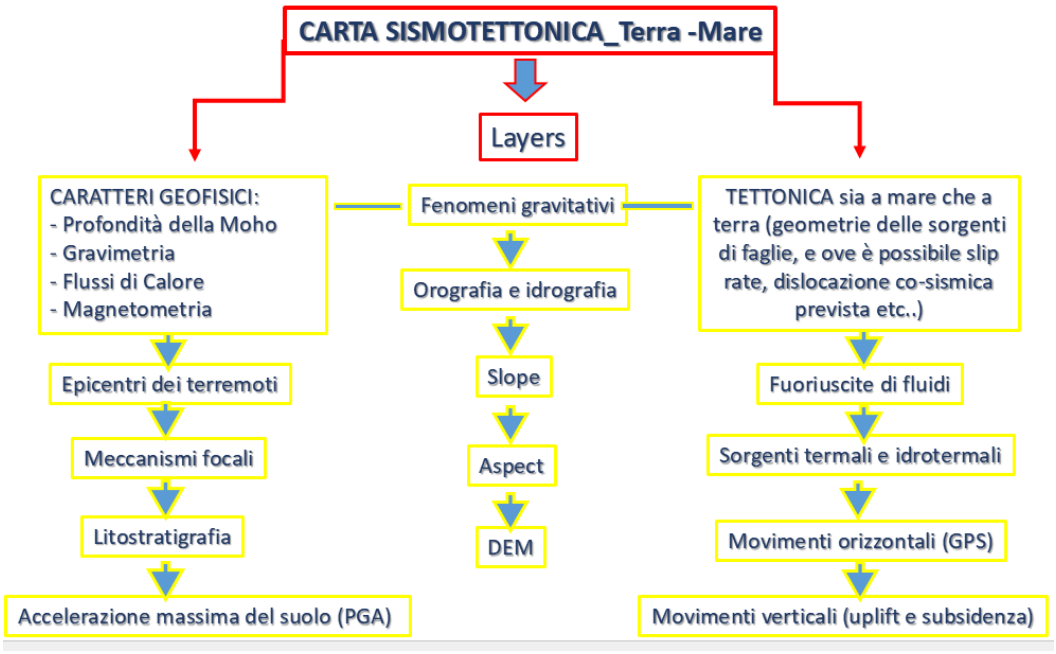

Fig. 1 Flow chart showing the different steps in the compilation of the seismotectonic map

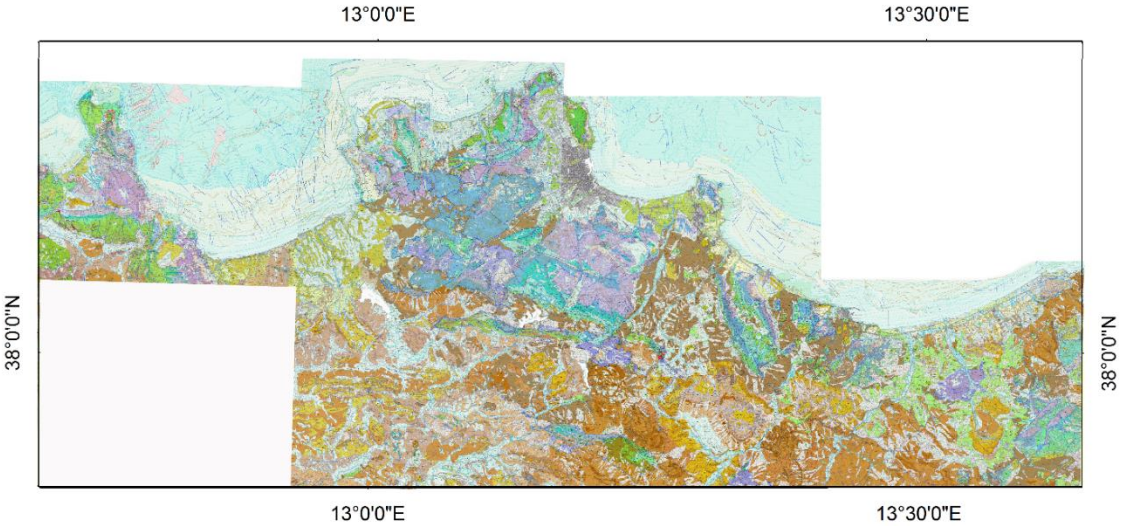

Fig. 2 Geological map of the study region

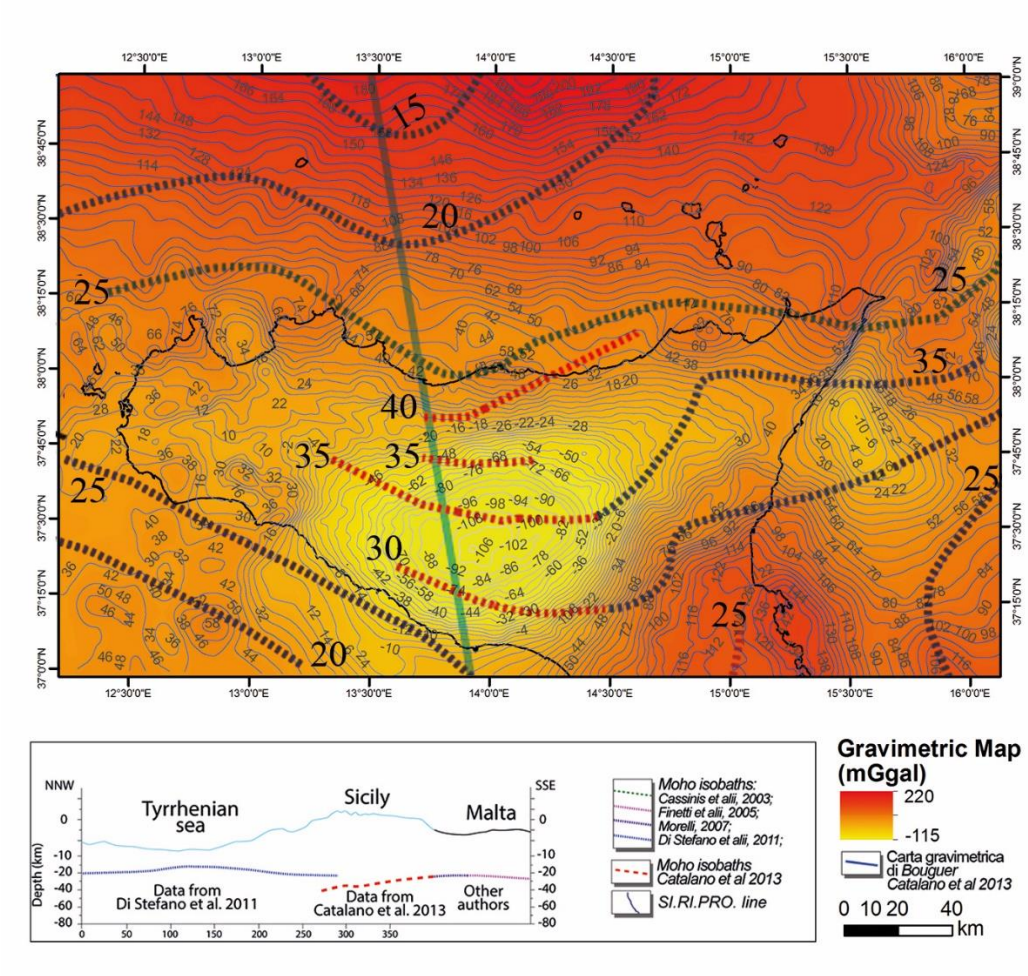

Fig. 3. Moho depth and gravimetric anomalies

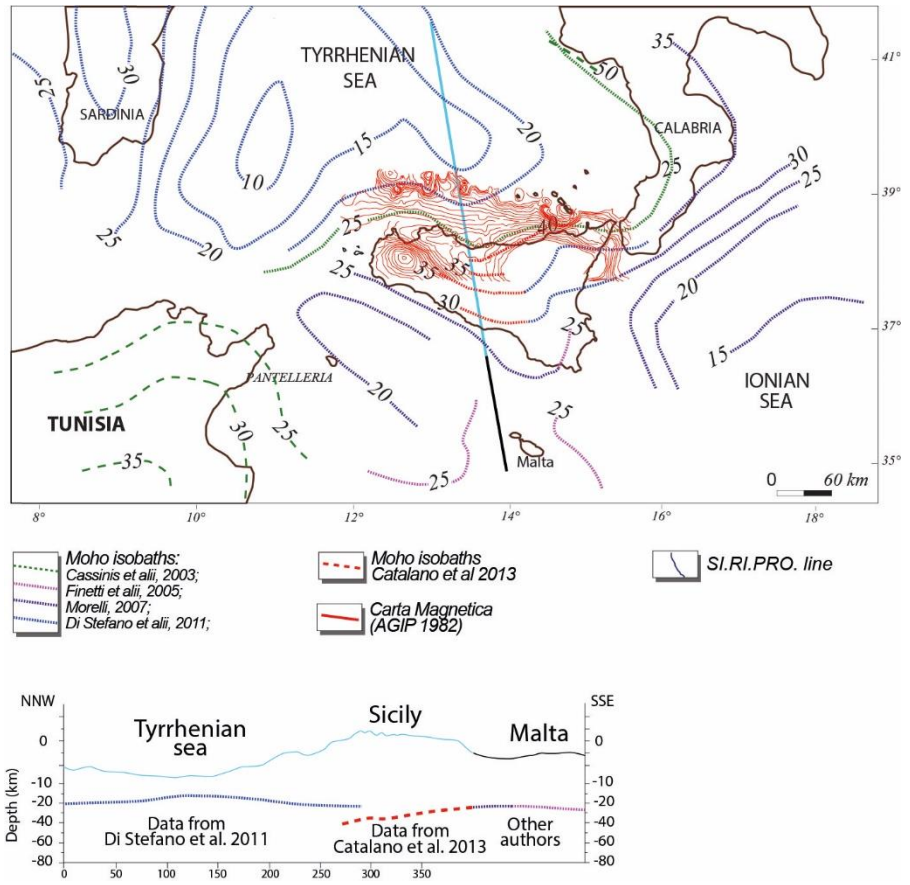

Fig. 4. Moho depth and magnetic anomalies

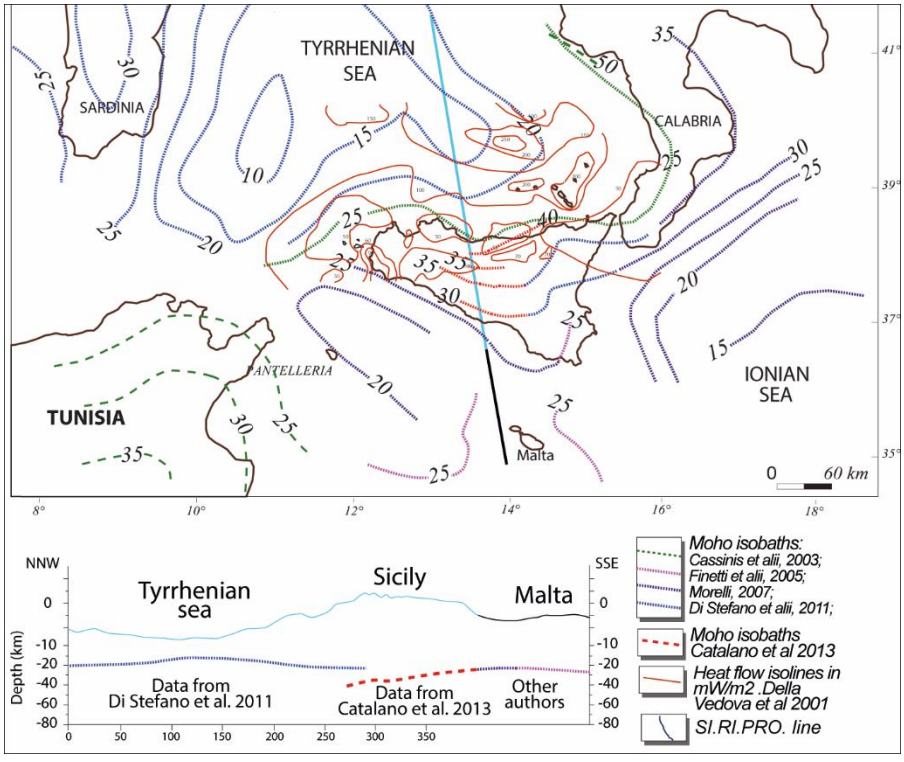

Fig. 5. Moho depth and heat flow

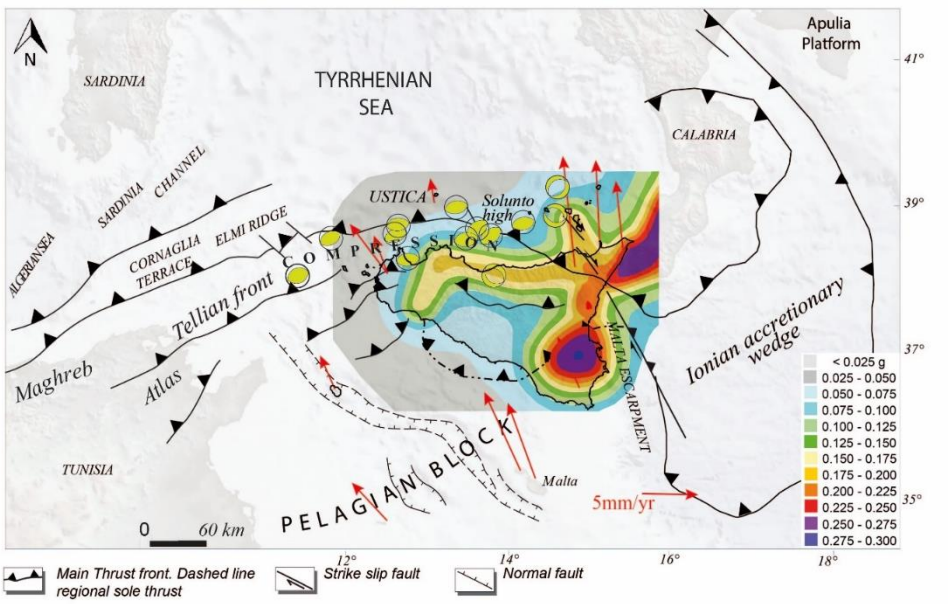

Fig. 6 Hazard map in terms of Peak Ground Acceleration, showing showing focal mechanisms, GPS values (data from D'Agostino and Selvaggi, 2004; Ferranti et al., 2006, Devoti et al., 2008, Serpelloni et al., 2007).

3. Recent and active tectonics and related processes

The eastern part of the Sicilian continental margin is characterised by a deeper seismicity related to the Ionian subduction, which is prevailingly linked both to extensional fault systems (Pollina, Messina strait) and to right-lateral NW-SE transcurrent systems (Vulcano-Lipari and Tindari-Giardini). While the western region shows shallow earthquakes (up to 25 km) of low to moderate magnitude (max Mw 5.9 on September 2002) occurring along an E-W trending belt and resulting from the brittle deformation of the Maghrebian chain. The focal mechanisms related to the main seismic shocks are in agreement with a dominant NW-SE compressive offset direction, with a right strike-slip component, and an antithetic NE-SW fault trend. Evidences of mass-wasting processes have been identified across the continental shelf and the continental slope and their spatial distribution, geometry, and seismic character suggest that the fluid seepage, oceanographic processes and the slope oversteepening could be important preconditioning factors, while the tectonic activity showing fault displacements during earthquakes is the main trigger. During the last 125 ky tectonic activity is evidenced by an uplift/subsidence patterns, decreasing from E to W. The continental regions are raised while offshore areas are subsiding, suggesting the occurrence of vertical differential movements. The GPS measurements document the active deformation with differential movements of individual blocks northward-directed, in agreement with the shallow seismicity, as well as with the convergence between Sicily and Sardinia, with values of about 2-6 mm/y.

4. The seismotectonic map of the Northern Sicily continental margin

This work produced the detailed seismotectonic map including both the terrestrial and marine areas (Fig. 7). We distinguished, at a regional scale, different shallow and deep seismogenetic volumes. Across the NSCM, we defined two main seismogenetic volumes that are produced by a NW-SE oriented compressional stress field defining an interplate shallow seismogenetic zone. Though these results are only preliminary, we provide a scientific product that can provide useful information in terms of seismic hazard in a complex region that includes both continental and marine sectors. Therefore, the identified geological features may be potentially geohazard elements for the neighbouring population and for the near goods, as well as submarine infrastructures (i.e. cables) and our seismotectonic map represent an important tool for monitoring the potentially seismogenic structures and assessing geohazards in marine and coastal environments.

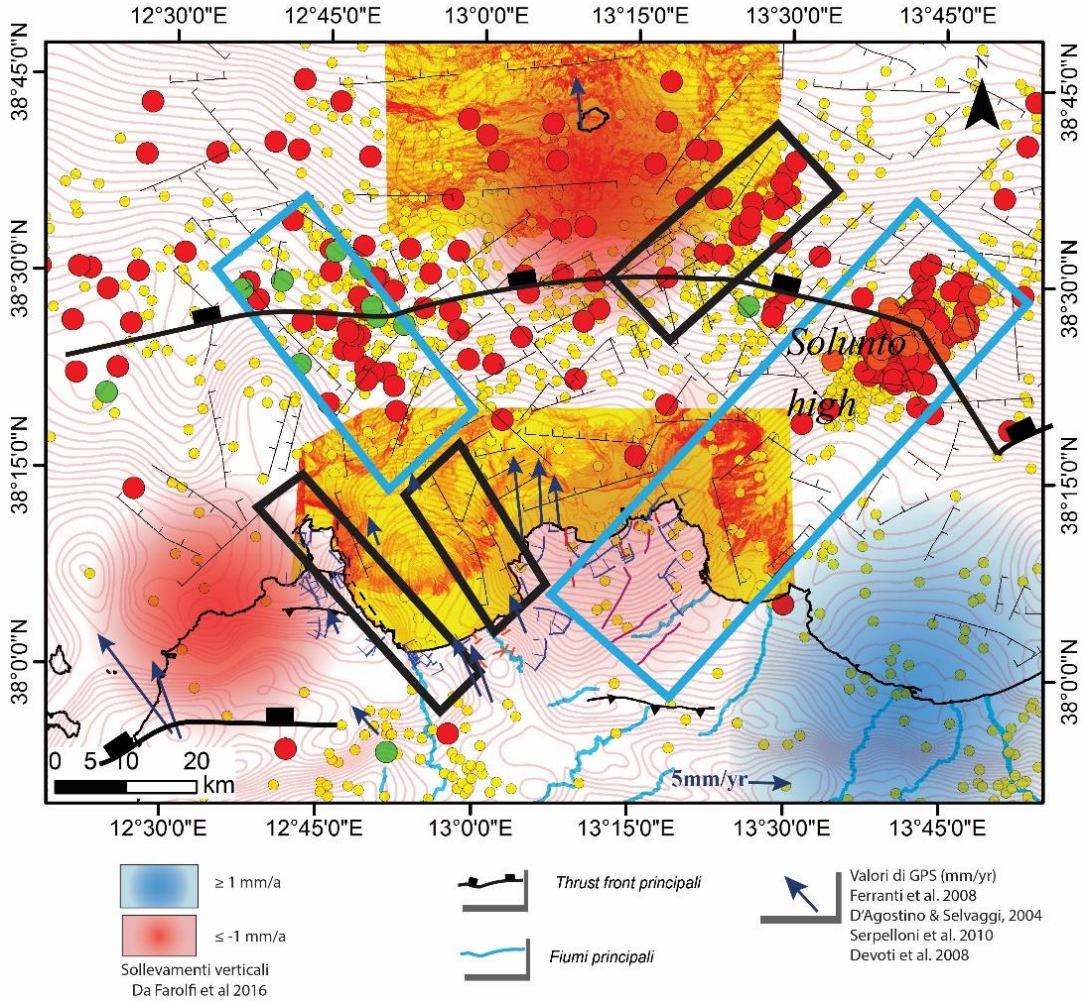

Fig. 7. Seismotectonic map of the NSCM. Blue boxes main seismogenetic volumes, including the 1998 and 2002 earthquakes. Black boxes: secondary zones, with strong seismicity and active tectonics.

References

AGIP s.p.a. 1994. Carta Aeromagnetica d'Italia Scala 1:1000000. Istituto Poligrafico e Zecca dello Stato. Servizio Geologico, Roma.

Bonardi, G., Cavazza, W., Perrone, V., & Rossi, S. (2001). Calabria-Peloritani terrane and northern Ionian Sea. In: G.B. Vai, & I.P. Martini (Eds.), *Anatomy of an Orogen: the Apennines and Adjacent Mediterranean Basins* (pp. 287-306). Springer, Dordrecht.

Boullin, J-P., Durand-Delga, M., & Olivier, P. (1986). Betic-Rifian and Tyrrhenian Arcs: distinctive features, genesis and development stages. In: WEZEL, F.C. (Ed.), *The Origin of Arcs*, (pp.281-304) Elsevier.

Cassinis, R., S. Scarascia, and A. Lozej (2003), The deep crustal structureof Italy and surrounding areas from seismic refraction data. A new synthesis, Boll. Soc. Geol. Ital.,122, 365–376.

Catalano, R., Valenti, V., Albanese, C., Accaino, F., Sulli, A., Tinivella, U., et al. (2013). Sicily's fold/thrust belt and slab rollback: The SI.RI.PRO. seismic crustal transect. Journal of the Geological Society, London, 170, 451-464.

D'Agostino, N., & Selvaggi, G. (2004). Crustal motion along the Eurasia-Nubia plate boundary in the Calabrian Arc and Sicily and active extension in the Messina Straits from GPS measurements. *Journal of Geophysical Research,* 109, B11402, doi:10.1029/2004JB002998.

Della Vedova B., Bellani S., Pellis G., Squarci P. (2001) Deep temperatures and surface heat flow distribution. In: Vai G.B., Martini I.P. (eds) Anatomy of an Orogen: the Apennines and Adjacent Mediterranean Basins. Springer, Dordrecht

Devoti, R., Riguzzi, F., Cuffaro, M., & Doglioni, C. (2008). New GPS constraints on the kinematics of the Apennines subduction. *Earth and Planetary Science Letters*, 273, 163–174.

Di Stefano, R., I. Bianchi, M. G. Ciaccio, G. Carrara, and E. Kissling (2011), Three-dimensional Moho topography in Italy: New constraints from receiver functions and controlled source seismology, Geochem. Geophys. Geosyst., 12, Q09006,doi:10.1029/2011GC003649.

Farolfi G., and Del Ventisette, C., (2016). Contemporary crustal velocity field in Alpine Mediterranean area of Italy from new geodetic data. In GPS Solut 20:715–722 Springer. DOI 10.1007/s10291-015-0481-1.

Ferranti, L., Antonioli, F., Mauz, B., Amorosi, A., Dai Pra, G., Mastronuzzi, G., et al., 2006. Markers of the last interglacial sea-level high stand along the coast of Italy: Tectonic implications. *Quaternary International* 145-146, 30-54, doi: 10.1016/j.quaint.2005.07.009.

Finetti, I.R., Lentini, F., Carbone, S., Del Ben, A., Di Stefano, A., Forlin, E., Guarnieri, P., Pipan, M. & Prizzon, A. (2005). – Geological out line of Sicily and litospheric tectono-

dynamics of its Tyrrenian margin from new CROP seismic data. In: I.R. Finetti, (Edr.), *CROP PROJECT: Deep seismic exploration of the Central Mediterranean and Central Italy*. – Atlas in Geosciences 1, Elsevier B.V., Amsterdam, 319-376.

Morelli C. (2007). Confirmations and apparent contradictions from the new geophysical deep constraints in the southern Apennines. Boll.Soc.Geol.It. (Ital.J.Geosci.), Spec. Issue No. 7 (2007), pp. 3-12.

Serpelloni, E., Vannucci, G., Pondrelli, S., Argnani, A., Casula, G., Anzidei, M., et al. (2007). Kinematics of the Western Africa–Eurasia plate boundary from focal mechanisms and GPS data. *Geophys. J. Int*., 169(3), 1180–1200. http://dx.doi.org/10.1111/j.1365-246X.2007.03367.x.

CHAPTER 7

Comparing methods for computation of run-up heights of landslide-generated tsunami in the Northern Sicily continental margin

NOTE This chapter is a scientific paper published in "*Geo-Marine Letters*" journal. The authors are the followings: Attilio Sulli, Elisabetta Zizzo & Ludovico Albano (2018). orcid.org/0000-0002-7705-3632.

Abstract

The North Sicily continental margin is a very active region located in the Central Mediterranean. Strong seismicity, active tectonics and volcanism, fluid escape, high sediment supply and widespread mass movements historically have exposed this region to marine geohazards, with a potential for tsunami generation. Morpho-bathymetric analysis revealed that one of the most common mechanisms associated with marine geo-hazards is due to submarine mass failure processes, genetically linked to the other processes active in this margin. With the aim to assess the risks associated to landslide-generated anomalous waves, we selected two sectors of this margin, Gulf of Palermo to the west and Patti offshore to the east. The working flow included analysis of the morpho-bathymetric data, morphometric characterization, calculation of parameters of landslide-generated waves, and computation of run-ups by using different algorithms. Assuming that each of the identified landslides could be a potential tsunamigenic source, we calculated the associated theoretical run-ups, referring to the main computation methodologies proposed in the scientific literature. In order to identify the methodology that better suits run-up values for landslide generated tsunami, we compared the known run-up values of actual, historical cases with those calculated through the different methodologies. The values obtained with the most suitable algorithm, both for theoretical and historical events, fit a curve that we used to formulate an empirical law describing the relationships between amplitude and depth, at the source point, and relative run-up. It can be used to calculate easily and promptly the run-up associated to a generic Landslide Generated Tsunami.

Keywords: tsunami, run-up, submarine landslide, geo-hazard, morpho-bathymetry, continental margin.

1. Introduction

Tsunamis are gravity-driven water waves, most of which generated by vertical displacement of the seabed that propagates through the water column to the surface. The resulting elevated surface wave collapses owing to gravity and then propagates outward from the source. Dispersion of the original wave generates a multiple wave train. Tsunamis are mainly (~80%) generated by earthquakes, but alternative mechanisms include subaerial and submarine landslides and volcanic collapse and eruption (Tappin 2017). Their main features are represented by both the long wave length (Charvet et al. 2013) and the height that can vary significantly from the open sea toward the coastal areas (Ezersky et al. 2013), giving the known destructive effect of tsunamis (e.g. the dramatic events in Indian Ocean 2004 and Japan 2011). Where the water depth gradually decreases, the wave slows dramatically, become compressed and grows steeper. Historically known events are referred to sensational episodes which registered significant values of run-up (Ru), accompanied by the highest risks with loss of life. So it is a commonplace that tsunamis are generated mostly by earthquakes, because of presence of seismic stations widespread on the ground that allows the phenomenon to be

easily attributed to a seismic event, and then focusing the study of the associated risks almost exclusively on seismic sources. In recent decades, morpho-bathymetric and high-resolution seismic surveys of extensive marine areas made it possible to investigate in detail the presence of large mass transport deposits, and other morphological features attributed to tectonics, volcanism and fluids seepage. As a consequence recent researches have been also addressed to tsunami sources other than earthquake, paying particular attention to landslides, which can generate large size tsunamis (Synolakis et al. 2002; Tinti et al. 2008; Liu et al. 2005; Glimsdal et al. 2013). Furthermore, medium-scale landslides are more hazardous as they occur at higher frequency (Casalbore et al. 2011). In order to produce an adequate assessment of the potential landslide-generated tsunami (LGT), there are several statistical, graphical, and analytical methods (Dao et al. 2013; Flouri et al. 2013). The latter are the most common methods for LGT assessment; they are founded generally on two characterizing parameters, length and amplitude of the wave near the point source, which can be determined with algorithms based on the morphometry of submarine landslides in the neighbor of the source area (McAdoo et al. 2004). The main parameter of tsunamis in the coastal area is the run-up, which is a measure of the maximum vertical raising of the wave, which is a function of both the height of the incident wave to the shore, and the morphology of the coastal sector where the water mass is impacting. Despite of some inaccuracies, these simulations can fruitfully be used for fast tsunami hazard assessments. For mapping coastal risk, a good estimate of the maximum height reached by the wave is essential because it is closely linked to the calculation of flooding. Overall, these data are used to define a buffer zone to protect the coastal infrastructure by tsunami events. Based on these assumptions, we analyzed the North Sicily continental margin (NSCM), because it is a tectonically active area with potential for tsunami generation, as in the cases of Messina (1908) (Aversa et al. 2014; Billi et al. 2010) and Stromboli (2002) (Chiocci et al. 2008; Tinti et al. 2005; Tinti et al. 2006). Morpho-bathymetric and seismic data, recently collected in the frame of MAGIC and CARG projects, revealed the occurrence of widespread submarine mass transport, genetically related to different processes affecting this margin (canyon, fluid seepage, volcanism, tectonics). In addition, the northern Sicily is characterized by coastal mountains and hills, which are part of the Sicily fold and thrust belt, which yields a great amount of sediments that contribute to the instability of the margin. We identified two different sectors of this margin, located in the western (Gulf of Palermo) and eastern (Patti offshore) coasts, chosen based on their morphological, stratigraphic and structural features, which could act as sources of tsunamis. Considering that most of models were proposed for open oceanic areas and they are rarely suited to semi-confined and narrow basins, the main aims of this paper are to assess the potential hazard associated to LGT in the NSCM, and to identify and verify a fast analytical methodology effective for a basin with the characteristics of the Mediterranean. We reached this purpose by comparing the results obtained with different methods of run-up computation applied to the potential Sicilian LGT with those related to actual events of LGT.

2. Geological setting

The NSCM extends in the southern Tyrrhenian Sea, from the north Sicily coastal belt to the Marsili bathyal plain (Fig 1). The margin is located in the transitional area between the Sicilian–Maghrebian chain to the south (Agate et al. 1993) and the Tyrrhenian back-arc basin to the north (Kastens et al. 1988). This region originated as a consequence of a complex interaction of compressional events, crustal thinning and strike-slip faulting (Pepe et al. 2005). Tectonic activity started in the Miocene with the thrusting of the Kabilian-Calabrian units followed by the deformation of the Sicilian–Maghrebian chain until the early Pliocene (Sulli 2000), while the opening of the Tyrrhenian Sea led to the subsidence of the margin since the Late Tortonian (Fabbri et al. 1981). E–W, NW–SE and NE–SW-trending both extensional and compressional faults with a local strike-slip component, exerted control on the morphology of the present day shelf and coastal areas during the Pleistocene. On the continental shelf, Pleistocene deposits are truncated by an erosional surface formed during the last glacio-eustatic oscillation. Prograding sedimentary wedges of coastal deposits, formed during the Last Glacial Maximum (LGM, about 20 ka), are present along the shelf margin (Caruso et al. 2011). In the Patti sector, the occurrence of fault segments and the alternation of rocks with different competence, namely the Hercynian metamorphic basement, its Meso-Cenozoic carbonate, Oligocene-Miocene terrigenous cover and Pleistocene deltaic sands and gravels (Carbone et al. 1998) produced a very uneven and steep submarine morphology. Due to active tectonics, sedimentation and sea-level fluctuations, both in the Gulf of Palermo (western NSCM) and the Patti offshore (eastern NSCM), swath-bathymetry shows a very active continental shelf-slope system, incised by several submarine canyons and related mass failure. The shaping of the canyons is due to both downslope evolution along tectonic lineaments, often in correspondence of the mouth of the torrential rivers, and concurrent up-slope retrogressive mass failures (Lo Iacono et al. 2011; Lo Iacono et al. 2014). The upper plate seismicity of the NSCM is defined by compressional focal mechanisms to the west and extensional to strike-slip mechanisms to the east. Shallow (<25 km) seismic events of low to moderate magnitude (max M 5.6 in September 2002) occur along an ENE–WSW trending belt, coinciding with the Kabilian-Calabrian thrust, coupled with a NW–SE compressive offset direction (Agate et al. 2000; Giunta et al. 2009). The main seismicity of the Patti area (max M 6.1 in 1978) is linked to right-lateral NNW-SSE transcurrent systems (Neri et al. 1996). High uplift rates during the last 125 ky were found along the eastern NSCM (0.8–1.63 mm/y), (Ferranti et al. 2010). The vertical rates show a decrease from E to W, and highlight coseismic activity between adjacent sectors, while comparison between onshore and offshore sectors suggests the activity of fault systems parallel to the coastline, causing differential vertical movements (subsidence vs. uplift) (Sulli et al. 2013). The western NSCM shows a present-day stability, except for local vertical movements in the Castellammare area, where uplift rates reach 0.1–0.2 mm/y (Mauz et al. 1997; Antonioli et al. 2006).

3. Materials and methods

To identify the landslides that could generate tsunamis in the NSCM, we used morpho-bathymetric data, acquired from 2001 to 2010 by the Marine GeoGroup of the University of Palermo, in the frame of CARG (national official geological cartography) and MAGIC (Marine Geohazards along the Italian Coasts) projects (oceanographic cruises DFP04, R/V Universitatis; EGUS2001, R/V Thetis; PUMA2009, R/V Universitatis; MACS2010, R/V Universitatis; Patti2003, R/V Thetis). In the EGUS2001 and Patti2003 cruises, a Reson SeaBat 8111 MultiBeam EchoSounder (MBES), generating 105 beams with a frequency of 100 KHz and operational range of 20-900 m bsl was used; in the cruises DFP04 and PUMA2009, a Reson SeaBat 8160 MBES, with a lower frequency (50 kHz), but able to investigate at higher depth (3000 m) was used. We post-processed the collected data with the software PDS2000, applying graphic removal of erroneous beams, noise filtering, processing of navigation data and correction for sound velocity. To obtain the Digital Terrain Model (DTM), we chose different footprint resolution depending on the depth, with a cell size of 10 m in the shelf and 20 m in the continental slope (mean resolution of 15 m). The workflow was developed through the following steps (Fig 2):

1) Analysis of the morpho-bathymetric data. The first step was to identify and to map a large amount of submarine landslides, potentially generating tsunamis, in the Gulf of Palermo and in the Patti offshore. Golden Software Surfer and Global Mapper were used to obtain 3D maps and bathymetric profiles DTM and to analyse the morpho-bathymetric features.

2) Morphometric characterization. We measured the main morphometric parameters useful to calculate the potential landslide-generated anomalous wave (Fig 3): length (*b*) and width (*w*) of landslide; its depth (*ds*) measured in the center point; slope angle at the source area (θ); thickness in the central point (*T*).

3) Calculation of parameters of the landslide-generated wave near the source point. Assuming each interpreted submarine landslide as tsunamigenic sources, we calculated the characterizing parameters of the landslide-generated wave near the source point, wave amplitude (*As*) [1], and length (*Ls*) [2] (Fig 3), by using McAdoo et al. (2004) equations.

$$[1]\ As = 0.224\,T\left(\frac{w}{w+Ls}\right)\left[\sin\theta^{1.29} - 0.746\sin\theta^{2.29} + 0.170\sin\theta^{3.29}\right]\left(\frac{b}{ds}\right)^{1.25}$$

$$[2]\ Ls = 3.8\left[\left(\frac{b\,ds}{\sin\theta}\right)^{0.5}\right]$$

Tsunami is characterized by large wave lengths, which remain basically unchanged, but the amplitude changes during propagation, in agreement with the principle of energy conservation, considering that the wave speed, which is function of water depth, decreases coastward due to the fast depth decrease. The wave speed near the coast (*c*) can be calculated using Zhao et al. (2010) equations [3].

$$[3]\ c = \sqrt{g\,(Ac + dc)}$$

where *dc* is the conventional interference depth of wave with sea bottom (10 m), *Ac* is the wave height near the coast, and *g* is the gravity acceleration. This parameter represents the shoaling process, that is

how the wave amplitude changes with the depth variation. To calculate *Ac* we used the Green law [4] that relates the wave amplitude at a generic point (*Ac*) to the amplitude at the source point (*As*).

$$[4]\ \ Ac = As\ \left(\frac{ds}{dc}\right)^{0.25}$$

4) Computation of run-ups with different algorithms. The run-up (*Ru*) is the main parameter that identifies the magnitude of a tsunami event. In order to estimate the tsunamigenic potential associated with submarine landslides we calculated the Ru of waves at the coast, through different algorithms (Synolakis 1987 [5]; Federici et al. 2006 [6]; Didenkulova et al. 2009 [7]; Zhao et al. 2010 [8]; Bryant 2014 [9]), obtained from simple empirical relationships, fluid dynamic laboratory simulations or numerical modelling (Fig 4), but we didn't consider dispersive wave models, not consistent with a rapid computation.

The equations proposed by Synolakis (1987), Zhao et al. (2010), and Bryant (2014), were formulated for events generated by earthquakes.

In order to simplify the computation, the equations refer to a theoretical coastal sector, where the height of the waves does not change with the morphology of the coast and during the propagation of the wave the energy does not decrease.

$$[5]\ \ Ru = dc\ 2.831\left(\sqrt{\cot\alpha}\right)\left(\frac{Ac}{dc}\right)^{5/4}$$

$$[6]\ Ru = Ac + \sqrt{\frac{c^2}{2g}\tan\alpha\left(Lc + \frac{Ac}{2\tan\alpha}\right)}$$

$$[7]\ Ru = 3.5\ Ac\sqrt{\frac{p}{Lc}}$$

$$[8]\ \ Ru = 3.043\ Ac\ \sqrt{c\sqrt{\frac{3Ac}{4\ dc^3}}\left(\frac{dc\cot\alpha}{\sqrt{g\ dc}}\right)}$$

$$[9]\ \ Ru = 2.83\ \sqrt{\cot\alpha}\ \ Ac^{5/4}$$

To apply these algorithms we had to get other parameters:

α- slope of the coastal strip (we assumed it equal to 1°);

p- Breaking point–coastline interval (considering a breaking point depth of 10 m and a constant slope of 1° it corresponds to a constant value of 588,23 m).

k – wave number (according to Zhao et al. 2010) [10]

$$[10]\ \ k = \sqrt{\frac{3Ac}{4\ dc^3}}$$

Lc – wave length near the coastal sector (according to Federici et al. 2006*)* [11]

$$[11]\ Lc = \frac{4\ q\ dc}{\sqrt{3\frac{Ac}{dc}}}$$

$Zmax$ - maximum raising reached by the water respect to the wave amplitude (according to Federici et al. 2006) [12]

$$[12]\ Zmax = \sqrt{\left(\frac{c^2}{2g}\right)\tan\alpha\left(Lc + \left(\frac{Ac}{2\tan\alpha}\right)\right)}$$

4.1) Computation of run-ups with different algorithms: run-ups of historical cases. The considered equations were applied to actual historical cases. We considered historical cases of LGT, extending worldwide because Mediterranean tsunamis are almost completely attributed to earthquakes.

We selected LGT with more detailed information, to apply the described equations and to compare computed theoretical results with real values, to identify the equation that provide more reliable results. Morphometric parameters were extrapolated from available data, or integrated with low resolution morpho-bathymetric data available on-line (http://www.gebco.net).

Following the selection of the best method to calculate the LGT run-ups, we put together actual LGT and potential Palermo Gulf and Patti offshore LGT, and drew the relative fitting curve to extrapolate a fast empiric equation that allows to calculate quickly run-ups.

4. Results

Throughout the study areas, we identified and parameterized, but not classified, 21 significant landslides, 18 in the Gulf of Palermo (Table 1) and 3 in the Patti offshore (Table 2) respectively, on the basis of bathymetric and morphological features, such as size, depth and distance from the coast.

4.1 The submarine mass failures in the NSCM. The Gulf of Palermo

The continental shelf in the Gulf of Palermo occupies an area of approximately 250 km^2 and is 8 km wide on average. The Gulf of Palermo shows a very active continental shelf-slope system, incised by several submarine canyons, which locally indent the shelf-edge, and flow into the Palermo intraslope basin, at a depth of around 1,300 m. Most of the mass failures of the area are related to canyon shaping processes and only few of them are not confined to the upper slope (Fig. 5). The continental shelf is characterized by mounds and pockmarks. The average height of the mounds is approximately 80 m and their maximum area is about 50000 m^2, while the average depth of pockmarks is about 20 m and the maximum area is 85000 m^2 (Fig 5). The canyons evolved through concurrent top-down turbiditic processes and bottom-up retrogressive mass failures, whose average length is about 5000 m, while the mean width is about 1000 m The main geological feature that controls the evolution of the canyons and induces sediment instability is the steep (1-10°) slope gradient. Faults and antiforms contributed to the regulation of mass failure processes, while the alignment of pockmarks and authigenic carbonates suggests a relationship between structural control, fluid escape processes and mass failures (Lo Iacono et al. 2011). The 18 main submarine landslides of the Palermo Gulf (Fig 5), observed along the upper slope, are presented from the east to the west in Table 1. The main mass failure is the well preserved

Priola landslide (PMO-10), affecting the uppermost slope, at a depth of 150 m. The scar (Fig 6), which is about 900 m wide and 100 m high, displays a semicircular shape and a failure plan flattening towards the detachment area, indicating a rotational component in a general translational mass movement. A detailed description of the morphometric characters of the landslides is presented in Table 1.

4.2 The submarine mass failures in the NSCM. The Patti offshore

In the Patti offshore, the shelf margin is strongly uneven and mainly located at a depth of 140-145 m (Fig 7). A dense network of canyons, gullies, channel-levee systems, structural steps and highs, submarine terraces and landslides, sedimentary creep features, show that the margin is very young and continuously reactivated by tectonic processes. The shaping of the canyons is due to both downslope evolution along tectonic lineaments, often in correspondence of the mouth of torrential rivers, and concurrent up-slope retrogressive mass failures. The landslides analyzed in the Patti offshore are presented in Table 2. The well-preserved Orlando landslide (PTT-01 in Table 2) is located in the upper slope, at a minimum depth of 153 m. The scar (Fig 8), which is about 586 m wide, has a detachment surface of 0.48 km^2 and a perimeter of 2.96 km, shows a semicircular shape and a plane flattening to the detachment zone, which indicates a rotational component in a translation mass movement. It is only 3.3 km far from the coast.

4.3 Landslides morphometry and run-up computation

With the aim to compute the expected run-up for theoretical LGT, we measured the morphometric parameters of each landslide (Table 3), considering them as potential source of anomalous waves. The morphometric analysis confirms that the Priola (PMO-10) landslide is the main feature in the Palermo Gulf, while the Orlando (PTT-01) landslide is the most prominent feature in the Patti offshore. The *As* and *Ls* values were calculated to model the hypothetical wave generated near the source point from the identified submarine landslides, by using the McAdoo et al. (2004) equations, and obtained the related wave lengths and amplitudes (Table 4). Starting from these values, we calculated the basic parameters to compute the expected run-ups for each landslide (Table 5). In Table 5 we can notice that the slope was considered as a constant values (1.0°) to simplify the model, while the major wave amplitude near the coast is 1,04 m (PMO-10), the minor values is 0,04 m (PMO-15); the major wave length near the coast is relative to PMO-15, the minor values is for PMO-10.

Subsequently, we computed the values of run-ups referred to the interpreted submarine landslides (Table 6). By applying the different equations, the run-up values change strongly for the analyzed landslides. In particular, from the comparison of the different methods used in both sectors (Gulf of Palermo and Patti offshore), characterized by different geological and morphological characteristics, the higher values are those obtained with the Bryant (2014) method (PMO-10 and PTT-O1 for Palermo and Patti respectively), while the lower values are those calculated with Didenkulova et al. (2009). From our results it is also evident that there are not valuable differences among the run-up

values obtained with the methods proposed by Zhao et al. (2010) and Synolakis (1987), even if the Federici et al. (2006) method provide more mean values and minor differences among the obtained values (Table 6).

5. Discussion

In general, the results show that most of the submarine landslides are confined on canyon walls. As a consequence they could propagate without significant loss of energy, representing therefore a significant hazard and a possible threat of tsunamis along the coast. Moreover they could be,element of potential risk also for underwater installations or cables. But the comparison among swift methods used to assess run-ups relative to both landslide- and earthquake-generated tsunamis showed that the obtained theoretical values are very different among them. In order to identify the best method to obtain the most realistic value of LGT run-ups, we tested all the algorithms with historical events, in order to verify the values obtained with different equations with actual values.

To do this, we selected historical events of LGT where we found thorough data sufficient to get the parameters that we have to enter into the equations. In particular we analysed four cases of LGT:

- *Mona Passage* (between Hispaniola and Puerto Rico), occurred on October 11, 1918 (López-Venegas et al. 2008)
- *Valdez* (Alaska), where on March 27, 1964, a strong earthquake triggered a large submarine landslide that generated a tsunami, with run-ups of 6 m (Parson et al., 2014; Nicolsky et al. 2010);
- *Nice* (France), occurred on October 16, 1979 (Labbé et al. 2012);
- *Papua* (New Guinea) occurred on July 17, 1998 (Tappin et al. 2008; Heinrich et al. 2000);

For these events we calculated the morphometric parameters that are reported in Table 7.

Subsequently we calculated the parameters relative to the height and length of the anomalous wave near the source point (Table 8) and near the coast (Table 9). Based on these parameters we computed with the different algorithms the theoretical values of run-up (Table 10) and compared the results with the actual values. The comparison showed that with the methods proposed by Zhao et al. (2010), Synolakis (1987) and Bryant (2014), for events generated by earthquakes, as well as those coming from the Didenkulova et al. (2009) algorithm, we obtained theoretical values diverging very much from the actual values of run-ups. Differently, the method proposed by Federici et al. (2006) return theoretical values comparable with the actual run-ups.

The results coming from the algorithm of Federici et al. (2006) returned theoretical values very similar to the real run-ups for all the considered events, and further the expected values are always higher than the measured ones. This is a very important aspect because it represents a precautionary element for the assessment of the geological hazard of LGT. For this reason, we took into account the values returned by this algorithm to draw a graph in order to relate the expected run-up values (relative to

both the NSCM and actual LGT events), according to Federici et al. (2006), to the wave amplitude near the source point (Fig 9). Analysing the resulting graph, it is clear that the distribution is ordered according to a curve where the highest values of run-ups are in direct proportionality, as expected, with the wave amplitude. Nevertheless, a small section of the curve shows an opposite trend: for very low wave amplitude (<0.4 m) values, an increase in run-up values is observed whit decreasing amplitudes. It means that for amplitudes less than 0.4 m the major contribution to the run-up derives from the raising (Z_{max}), while for higher values the greater contribution is given by the value of the amplitude.

Based on the drawn curve we deduced an empirical equation [13] linking the wave amplitude to the expected run-ups and fitting the plotted values:

$$[13]\ Ru = \frac{3As^2 + 5As + 0.075}{As}$$

This equation has been applied both to the hypothetical LGT events in the NSCM studied areas and to the historical actual events. The results (Table 11), compared to the run-up values of the actual events are surprisingly more fitting than those obtained from Federici et al. (2006), even if the differences are minimal. In this way, we propose an empirical method of tsunami computation that, notwithstanding the lack of theoretical backing, allows obtaining very promptly run-up values of LGT, which can be used in rapid assessment or to draw flooding maps in large regions.

6. Conclusions

Analysing the morpho-bathymetry data of the northern Sicily continental margin, a tectonically active sector of the central Mediterranean characterized by widespread instability, several submarine landslides were identified. Assuming that each of them could be a potential tsunamigenic source, we calculated the associated theoretical run-ups, referring to the main computation methodologies proposed in the scientific literature. In order to identify the methodology that better suits LGT values, we compared the known run-up values of actual cases with those calculated through the different methodologies. Once verified that the Federici et al. (2006) method better approximates the values of actual LGT events, we formulated an empirical law that allows calculating promptly the run-up associated to a generic LGT having as starting data the amplitude of the wave near the source point.

Acknowledgements: Funding for research was provided by CARG, MAGIC Projects (CONISMA/URL Palermo) and MIUR/University of Palermo (PJ_AUTF_008539) (resp. A. Sulli).

References

Agate M, Beranzoli L, Braun T, Catalano R, Favali P, Frugoni F, Pepe F, Smriglio G, Sulli A (2000) The 1998 offshore NW Sicily earthquakes in the tectonic framework of the southern border of the Tyrrhenian Sea. Mem Soc Geol It. 55: 103–114

Agate M, Catalano R, Infuso S, Lucido M, Mirabile L, Sulli A (1993) Structural evolution of the Northern Sicily continental margin during the Plio-Pleistocene. In: Max, M.D., Colantoni, P. (Eds.), Geological Development of the Sicilian–Tunisian Platform. UNESCO Report In Marine Science 58: 25–30

Antonioli F, Kershaw S, Renda P, Rust D, Belluomini G, Cerasoli M, Radtke U, Silenzi S (2006) Elevation of the last interglacial highstand in Sicily (Italy): A benchmark of coastal tectonics. Quaternary International 145-146: 3–18

Aversa M, Bussoletti G, Fea M, Torre R (2014) I maremoti nell'area dello Stretto di Messina - The seaquakes in the Messina Strait area. Mem. Descr. Carta Geol. d'It. XCVI: 87-128

Bigi G, Bonardini G, Catalano R, Cosentino D, Lentini F, Parotto M, Sartori R, Scandone P, Turco E (1992) Structural Model of Italy, 1:500.000. Consiglio Nazionale delle Ricerche, Rome.

Billi A, Minelli L, Orecchio B, Presti D (2010) Constraints to the Cause of Three Historical Tsunamis (1908, 1783, and 1693) in the Messina Straits Region, Sicily, Southern Italy. Seismological Research Letters 81, 6: 907-915 doi: 10.1785/gssrl.81.6.907

Bryant E A (2014) Tsunami, The Underrated Hazard. Springer International Publishing Switzerland. doi:10.1007/978-3-319-06133-7_2, 222 P

Carbone S, Lentini F, Vinci G (1998) Carta geologica del settore occidentale dei Monti Peloritani (Sicilia nord-orientale). S.EL.CA., Firenze

Caruso A, Cosentino C, Pierre C, Sulli A (2011) Sea-level changes during the last 41,000 years in the outer shelf of the southern Tyrrhenian Sea: Evidence from benthic foraminifera and seismostratigraphic analysis. Quaternary International 232: 122-131 doi:10.1016/j.quaint.2010.07.034

Casalbore D, Romagnoli C, Bosman A, Chiocci F L (2011) Potential tsunamigenic landslides at Stromboli Volcano (Italy): Insight from marine DEM analysis. Geomorphology 126,42–50. doi:10.1016/j.geomorph.2010.10.026

Charvet I, Eames I, Rossetto T (2013) New tsunami runup relationships based on long wave experiments. Ocean Modelling 69: 79–9

Chiocci F L, Romagnoli C, Bosman A (2008) Morphologic resilience and depositional processes due to the rapid evolution of the submerged Sciara del Fuoco (Stromboli Island) after the December 2002 submarine slide and tsunami. Geomorphology 100: 356–365. doi:10.1016/j.geomorph.2008.01.008

Dao M.H, Xu H, Chan E S, Tkalich P (2013) Modelling of tsunami-like wave run-up, breaking and impact on a vertical wall by SPH method. Natural Hazards and Earth System Sciences, 13: 3457–3467. doi:10.5194/nhess-13-3457-2013

Didenkulova I I, Pelinovsky E N, Soomere T (2009) Runup Characteristics of Symmetrical Solitary Tsunami Waves of ‘‘Unknown’’ Shapes. Pure and Applied Geophysics. 165: 2249–2264.doi:10.1007/s00024-008-0425-6

Ezersky A, Tiguercha D, Pelinovsky E (2013) Resonance phenomena at the long wave run-up on the coast. Natural Hazards and Earth System Sciences, 13: 2745–2752. doi:10.5194/nhess-13-2745-2013

Fabbri A, Gallignani P, Zitellini N (1981) Geological evolution of the peri-Tyrrhenian sedimentary basins. Tecnoprint, Bologna: 101–126

Federici B, Bacino F, Cosso T, Poggi P, Rebaudengo Landò L, Sguerso D (2006) Analisi del rischio tsunami applicata ad un tratto della costa Ligure. Geomatics Workbooks, 6: 1-19

Ferranti L, Antonioli F, Anzidei M, Monaco C, Stocchi P (2010) The timescale and spatial extent of vertical tectonic motions in Italy: insights from relative sealevel changes studies. Journal of the Virtual Explorer, Electronic Edition. ISSN:1441-8142 ISSN: 1441-8142, 36, paper 23

Flouri E T, Kalligeris N, Alexandrakis G, Kampanis N A, Synolakis C E (2013) Application of a finite difference computational model to the simulation of earthquake generated tsunamis. Applied Numerical Mathematics 67: 111–125. doi:10.1016/j.apnum.2011.06.003

Gasparo Morticelli M, Valenti V, Catalano R, Sulli A, Agate M, Avellone G, Albanese C, Basilone L, Gugliotta C (2015) Deep controls on foreland basin system evolution along the Sicilian fold and thrust belt. Bulletin de la Societé géologique de France, Special Pubbl. 186: 273–290.

Giunta G, Luzio D, Agosta F, Calò M, Di Trapani F, Giorgianni A, Oliveri E, Orioli S, Perniciaro M, Vitale M, Chiodi M, Adelfio G (2009) An integrated approach to investigate the seismotectonics of northern Sicily and southern Tyrrhenian. Tectonophysics 476: 13–21. doi:10.1016/j.tecto.2008.09.031

Glimsdal S, Pedersen G K, Harbitz C B, Løvholt F (2013) Dispersion of tsunamis: does it really matter? Natural Hazards and Earth System Sciences, 13: 1507–1526. doi:10.5194/nhess-13-1507-2013

Heinrich P, Piatanesi A, Okal E, Hèbert H (2000) Near-field modeling of the july 17, 1998 tsunami in Papua New Guinea. Geophysical research letters, 27, 19: 3037-3040

Kastens K, Mascle J, Auroux C, Bonatti E, Broglia C, Channell J, Curzi P, Emeis K C, Glacon G, Asegawa S, Hieke W, Mascle G, McCoy F, McKenzie J, Mendelson J, Muller C,

Rèhault J P, Robertson A, Sartori R, Sprovieri R, Tori M (1988) ODP Leg 107 in the Tyrrhenian Sea: insights into passive margin and back-arc basin evolution. Geol. Soc. Am. Bull., 100: 1140–1156

Labbé M, Donnadieu C, Daubord C, Hébert H (2012) Refined numerical modeling of the 1979 tsunami in Nice (French Riviera): Comparison with coastal data. Journal of Geophysical Research, 117, F01008. 17 doi:10.1029/2011JF001964

Liu P-F, Wu T-R, Raichlen F, Synolakis C E, Borrero J C (2005) Runup and rundown generated by three-dimensional sliding masses. J. Fluid Mech. 536: 107-144

Lo Iacono C, Sulli A, Agate M (2014) Submarine canyons of north-western Sicily (Southern Tyrrhenian Sea): Variability in morphology, sedimentary processes and evolution on a tectonically active margin. Deep-Sea Research Part II: Topical Studies in Oceanography, 104: 93-105

Lo Iacono C, Sulli A, Agate M, Lo Presti V, Pepe F, Catalano R (2011) Submarine canyon morphologies in the Gulf of Palermo (Southern Tyrrhenian Sea) and possible implications for geo-hazard. Marine Geophysical Research, 32, 1: 127-138. doi:10.1007/s11001-011-9118-0

López-Venegas A M, ten Brink U S, Geist E L (2008) Submarine landslide as the source for the October 11, 1918 Mona Passage tsunami: Observations and modeling. Marine Geology 254: 35–46. doi:10.1016/j.margeo.2008.05.001

Mauz B, Buccheri G, Zöller L, Greco A (1997) Middle to upper Pleistocene morphostructural evolution of the NW-coast of Sicily: Thermoluminescence dating and palaeontological-stratigraphical evaluations of littoral deposits. Palaeogeography, Palaeoclimatology, Palaeoecology, 128: 269–285

McAdoo B G & Watts P (2004) Tsunami hazard from submarine landslides on the Oregon continental slope. Marine Geology. 203: 235-245. doi:10.1016/S0025-3227(03)00307-4

Neri G, Caccamo D, Cocina O, Montalto A. (1996) Geodynamic implications of recent earthquake data in the Southern Tyrrhenian Sea. Tectonophysics.258: 233-249

Nicolsky D J, Suleimani E N, Hansen R A (2010) Numerical modeling of the 1964 Alaska tsunami in western Passage Canal and Whittier, Alaska. Natural Hazards and Earth System Sciences, 10: 2489–2505. doi:10.5194/nhess-10-2489-2010

Parsons T, Geist E L, Ryan H F, Lee H J, Haeussler P J, Lynett P, Hart P E, Sliter R, Roland E (2014) Source and progression of a submarine landslide and tsunami: The 1964 Great Alaska earthquake at Valdez. Journal of Geophysical Research: Solid Earth, 119: 8502–8516. doi:10.1002/2014JB011514.

Pepe F, Sulli A, Bertotti G, Catalano R (2005) Structural highs formation and their relationship to sedimentary basins in the north Sicily continental margin (southern Tyrrhenian Sea): Implication for the Drepano Thrust Front. Tectonophysics 409: 1–18

Sulli A (2000) Structural framework and crustal characteristics of the Sardinia Channel Alpine transect in the central Mediterranean. Tectonophysics 324: 321–336

Sulli A, Lo Presti V, Gasparo Morticelli M, Antonioli F (2013) Vertical movements in NE Sicily and its offshore: Outcome of tectonic uplift during the last 125 ky. Quaternary International, 288: 168-182. doi:10.1016/j.quaint.2012.01.021

Synolakis C E (1987) The runup of solitary waves. J. Fluid Mech. 185: 523-545

Synolakis C E, Bardet J-P, Borrero J C, Davies H L, Okal E A, Silver E A, Sweet S, Tappin D R (2002) The slump origin of the 1998 Papua New Guinea Tsunami. Mathematical, Physical and Engineering Sciences, 458: 763-789

Tappin D R (2017) The Generation of Tsunamis. Encyclopedia of Maritime and Offshore Engineering. PP1–10

Tappin D R, Watts P, Grilli S T (2008) The Papua New Guinea tsunami of 17 July 1998: anatomy of a catastrophic event. Natural Hazards and Earth System Sciences, 8: 243–266

Tinti S, Manucci A, Pagnoni G, Armigliato A, Zaniboni F (2005) The 30 December 2002 landslide-induced tsunamis in Stromboli: sequence of the events reconstructed from the eyewitness accounts. Natural Hazards and Earth System Sciences, Copernicus publications on behalf of the European Geosciences Union, 5 (6): 763-775

Tinti S, Maramai A, Armigliato A, Graziani L, Manucci A, Pagnoni G, Zaniboni F (2006) Observations of physical effects from tsunamis of December 30, 2002 at Stromboli volcano, southern Italy. Bull Volcanol, 68: 450–461. doi:10.1007/s00445-005-0021-x

Tinti S, Zaniboni F, Pagnoni G, Manucci A (2008) Stromboli Island (Italy): Scenarios of Tsunamis Generated. Pure and Applied Geophysics. 165: 2143–2167.doi:10.1007/s00024-008-0420-y

Trincardi F & Zitellini N (1987) The Rifting of the Tyrrhenian Basin. Geo-Marine Letters 7: 1-6

Wezel F C, Savelli D, Bellagamba M, Tramontana M, Bartole R (1981) Plio-Quaternary depositional style of sedimentary basins along insular Tyrrhenian margin. In: F.C. Wezel (ed), Sedimentary Basins of Mediterranean Margins. C.N.R. Italian Project of Oceanography, Tecnoprint Bologna pp 239-269

Zhao X L, Wang B, Liu H (2010) Propagation and runup of tsunami waves with Boussinesq model. Proceedings of the 32nd International Conference on Coastal Engineering, Shanghai, 1-14.

Figure captions

Fig 1 Structural map of the NSCM with the main tectonic features (data from Bigi et al. 1992; Sulli 2000). In the bottom left corner the regional setting of the central Mediterranean (from Gasparo Morticelli et al. 2015).

Fig 2 The workflow used in this analysis.

Fig 3 Morphometric characterization of the landslide and related landslide generated wave (for symbols see the text).

Fig 4 Schematic models of run-up computation proposed by different authors: a) Zhao et al. (2010), b) Federici et al. (2006), c) Synolakis (1987), d) Bryant (2014), Didenkulova et al. (2009). See text for explanation of abbreviations.

Fig 5 Morpho-bathymetric model of the Gulf of Palermo and localization of the 18 mapped landslides. A detail of the Priola landslide (PMO-10) is shown in the top right. Canyons, gullies and pockmarks lie in the continental slope as well as the related pockmark-scars and landslides.

Fig 6 Line drawing from the DTM (above) and longitudinal profile (below) of the Priola landslide (PMO-10)

Fig 7 Morpho-bathymetric model of the Patti offshore and localization of the 3 mapped landslides. A detail of the Orlando landslide (PTT-01) is shown in the inset.

Fig 8 Line drawing of the 3-D model (above) and longitudinal profile (below) of the Orlando landslide (PTT-01).

Fig 9 Relationship between the wave amplitude near the source point and computed run-ups of NSCM (blue dots) and actual (red dots) LGT. The occurrence of a critical amplitude value is outlined at 0.4 m. The R^2 is higher than 0.7, pointing out a good fitting between values and curve.

Table

Table 1 Main morphometric features of the landslides in the Gulf of Palermo.

Table 2 Main morphometric features of the landslides in the Patti offshore.

Table 3 Morphometric parameters calculated for submarine mass failures in the NSCM.

Table 4 Wave length and amplitudes values at the source point.

Table 5 Basic parameters useful for the calculation of the run-up. The calculations were carried out considering a theoretical coastal sector characterized by a slope of 1° (average value of inner continental shelf) and by a depth of interference with the seafloor of 10 m.

Table 6 Computed run-ups, obtained by using 5 methods proposed by different Authors.

Table 7 Morphometric parameters of the submarine mass failures responsible for historical events.

Table 8 Wave parameters near the source point for historical events.

Table 9 Wave parameters near the coast for historical events. We considered a theoretical slope of 1° in the coastal sector.

Table 10 Theoretical values of run-ups for historical events obtained with the different methodologies. The last column shows their actual run-ups values.

Table 11 Spread (Δ) between the results obtained with the empirical equation compared to those obtained from Federici et al. (2006), both in relation to the values of actual LGT.

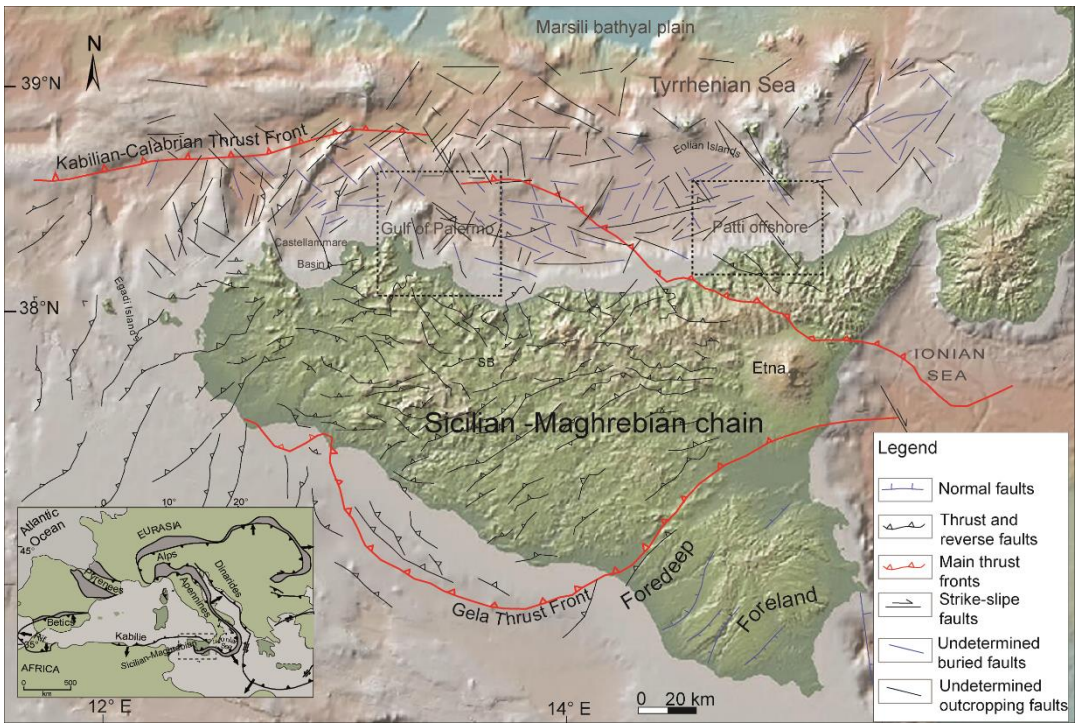

Fig 1 Sulli et al.,2018

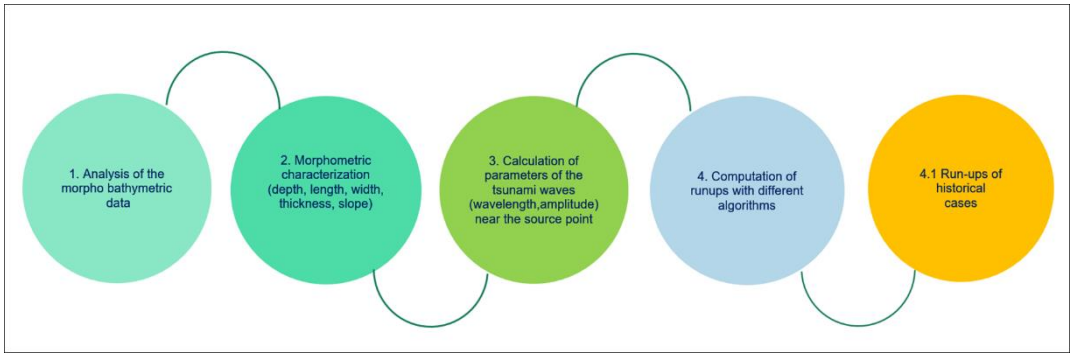

Fig 2 Sulli et al.,2018

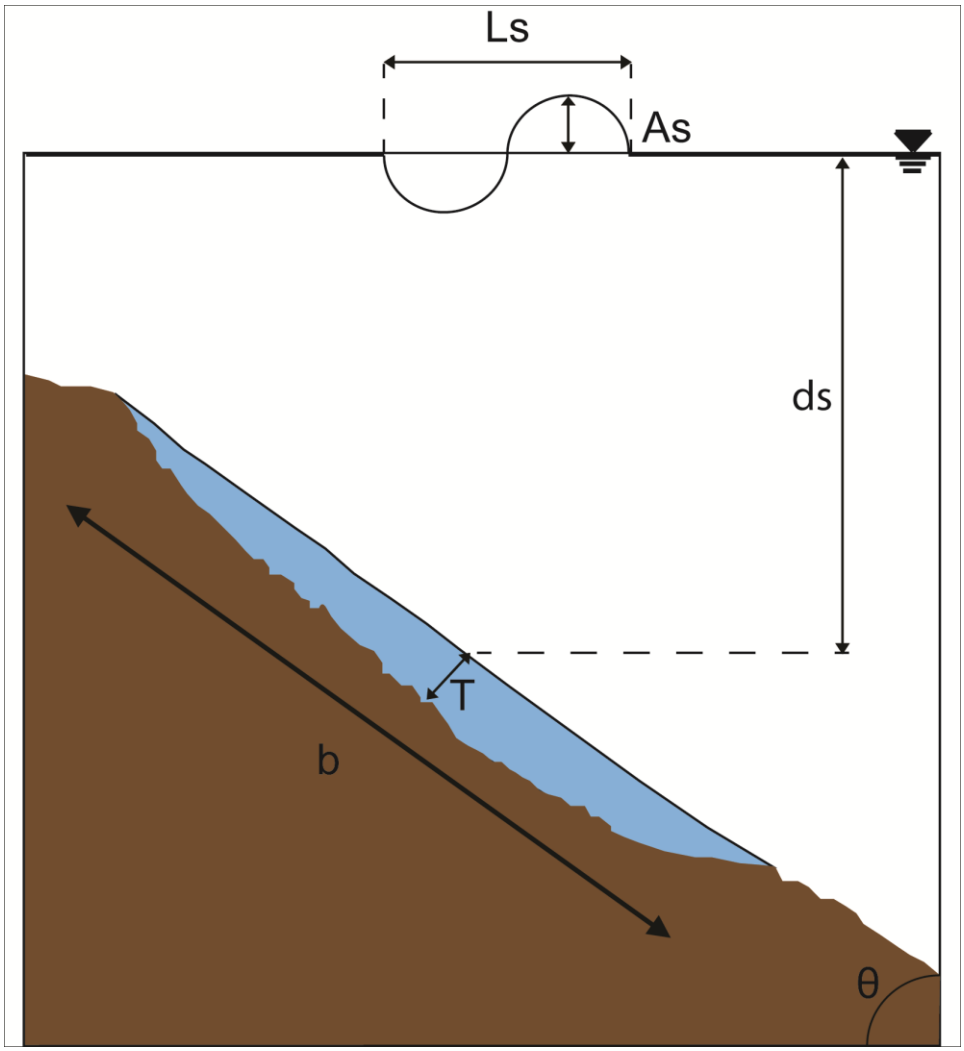

Fig 3 Sulli et al.,2018

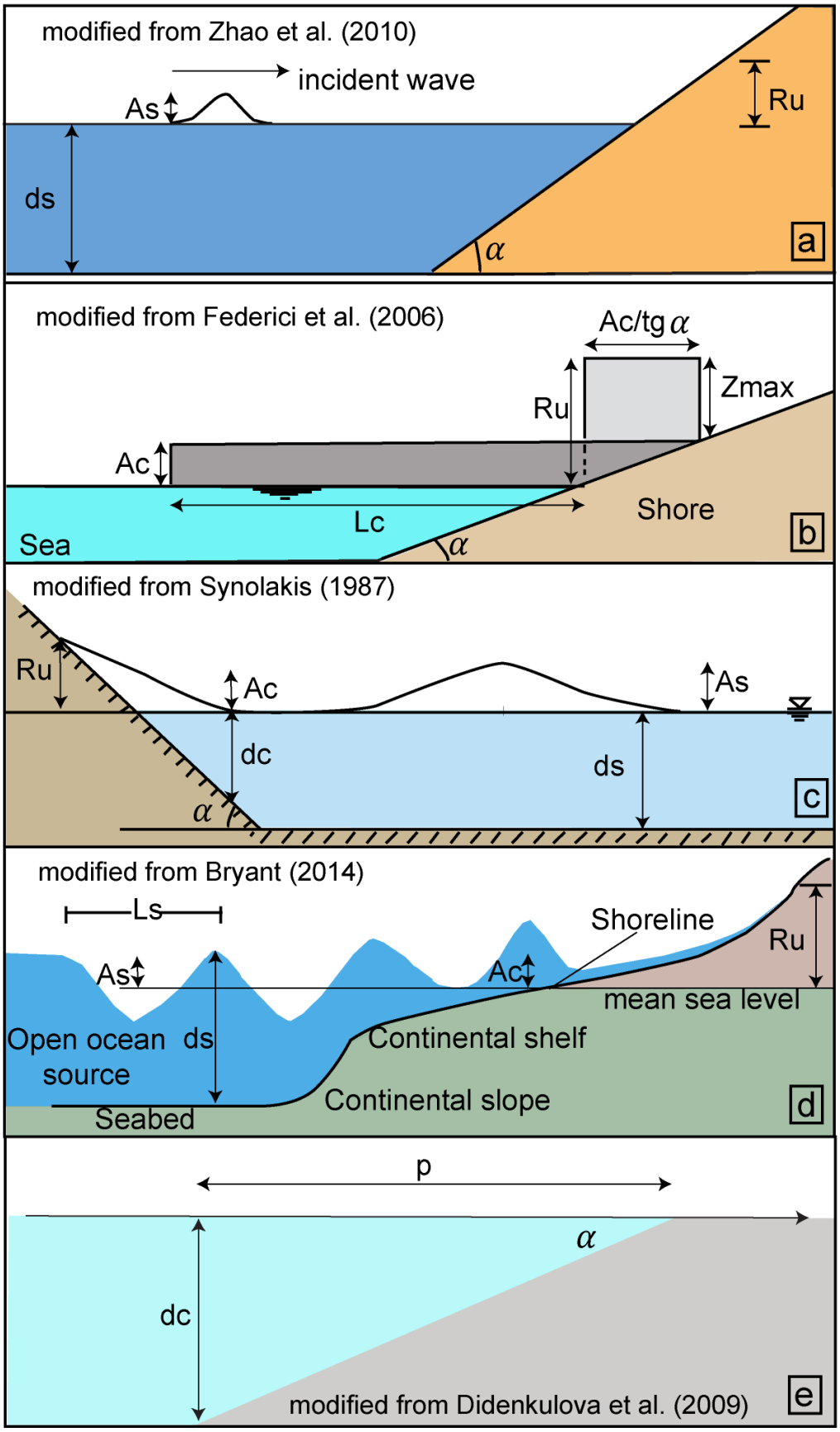

Fig 4 Sulli et al.,2018

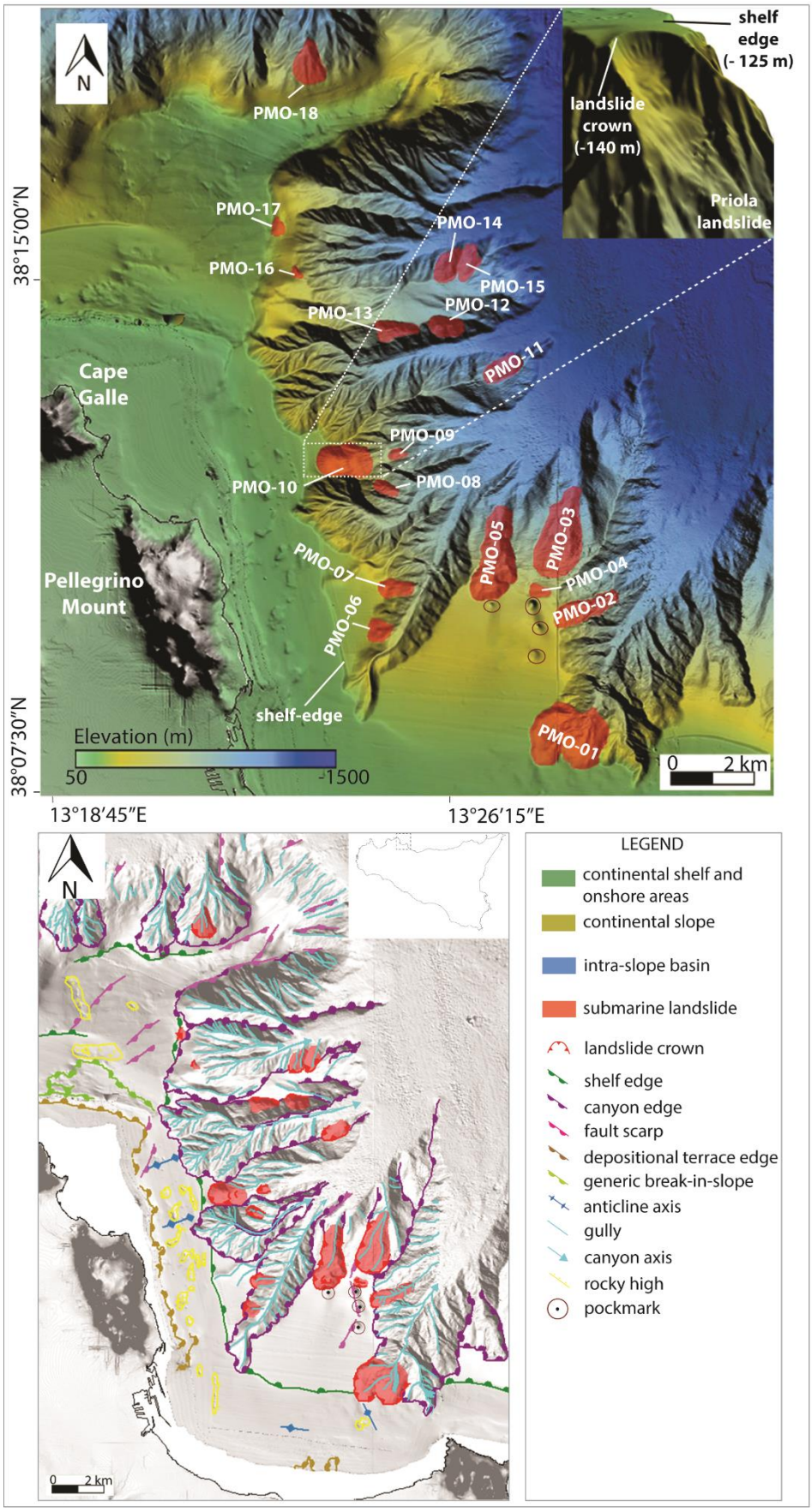

Fig 5 Sulli et al.,2018

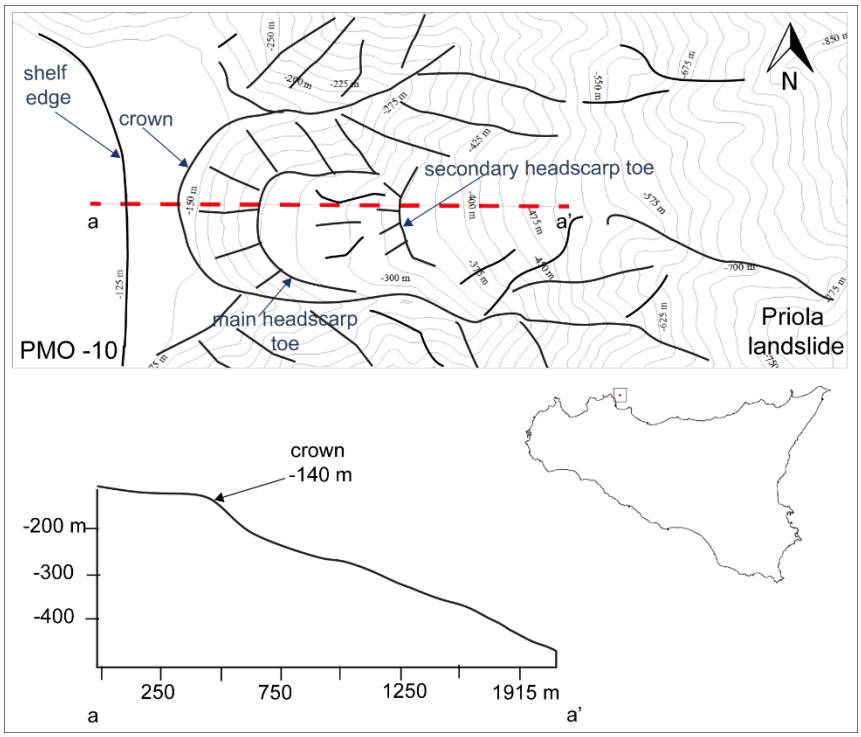

Fig 6 Sulli et al.,2018

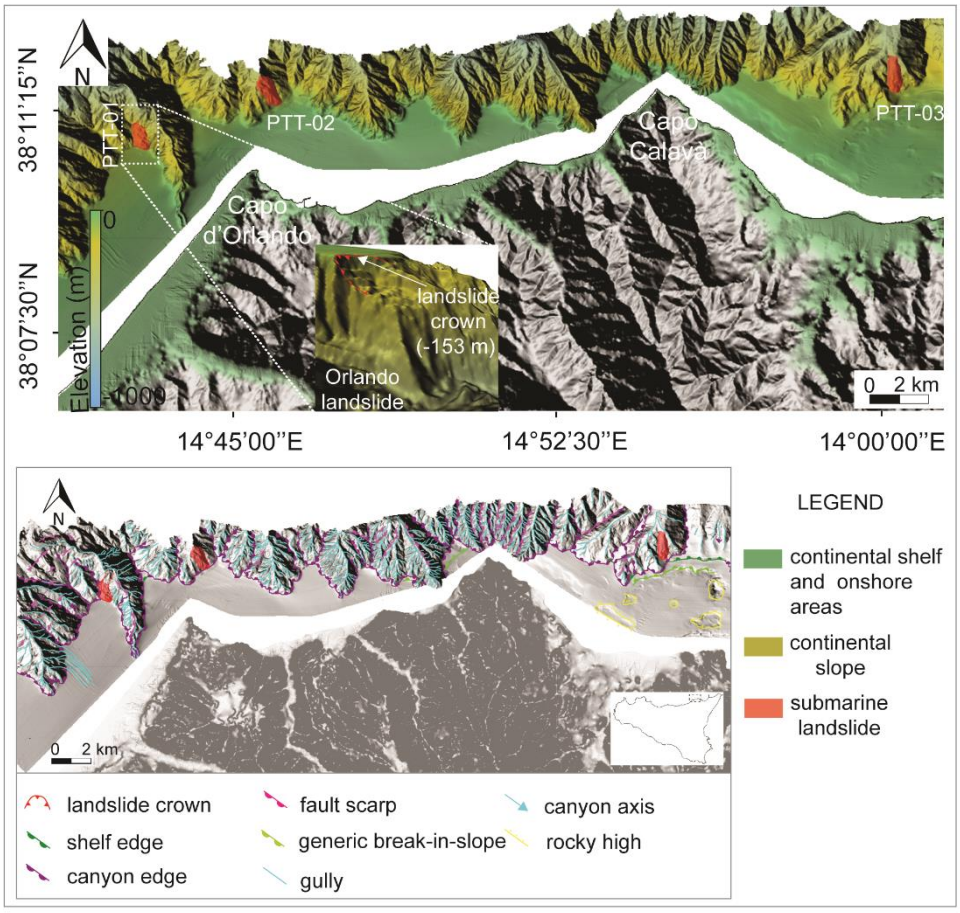

Fig 7 Sulli et al.,2018

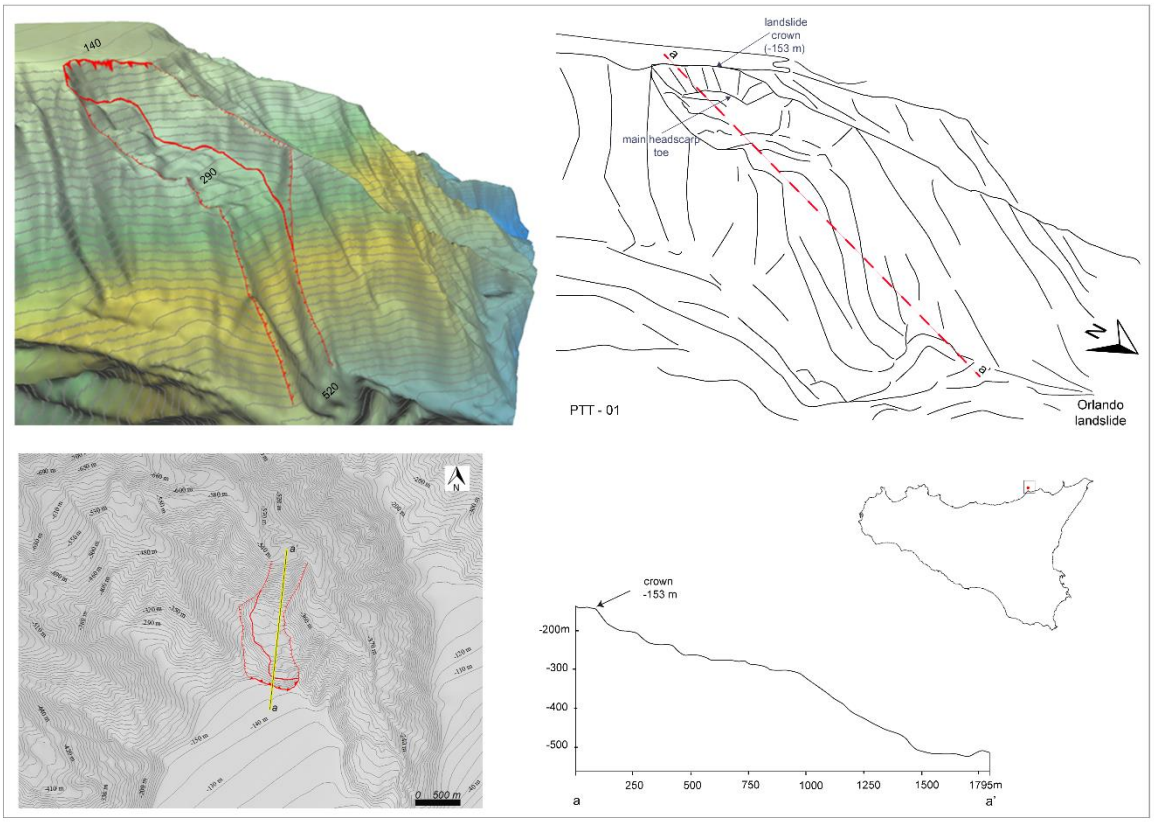

Fig 8 Sulli et al.,2018

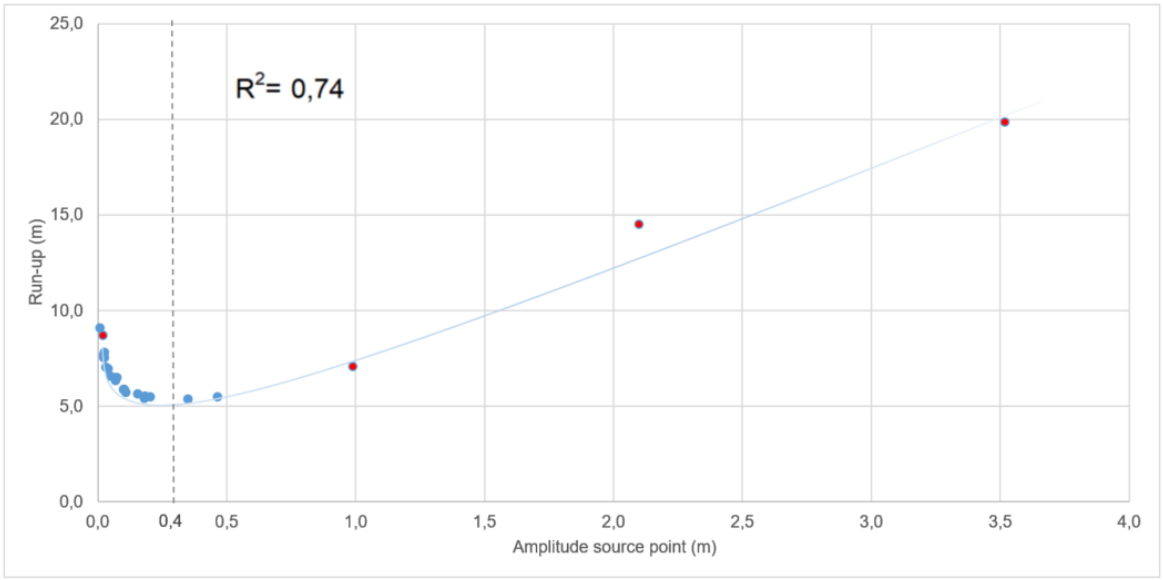

Fig 9 Sulli et al.,2018

Table 1

LGT	*Detachment Surface*	*Perimeter*	*Distance from coast*	*Crown Depth*	*Coordinates*	
	(km^2)	(km)	(m)	(m)	latitude	longitude
PMO-01	3.04	7.91	2.5	118.0	38°08'28.06"N	13°28'31.08"E
PMO-02	0.96	4.53	6.4	331.0	38°10'18.36"N	13°28'45.00"E
PMO-03	2.36	6.48	7.3	540.0	38°11'04.35"N	13°28'19.71"E
PMO-04	0.18	1.68	7.05	415.0	38°10'34.17"N	13°27'56.55"E
PMO-05	2.22	6.81	6.5	383.0	38°10'47.98"N	13°27'03.27"E
PMO-06	0.36	2.27	3.4	187.0	38°09'55.10"N	13°24'58.97"E
PMO-07	0.41	2.61	4.0	228.0	38°10'31.21"N	13°25'17.65"E
PMO-08	0.22	1.89	44.6	440.0	38°12'01.50"N	13°25'03.80"E
PMO-09	0.13	1.40	15.4	570.0	38°12'31.50"N	13°25'12.89"E
PMO-10	1.22	4.26	3.5	140.0	38°12'22.97"N	13°24'10.33"E
PMO-11	0.59	3.03	8.8	975.0	38°13'52.43"N	13°27'09.10"E
PMO-12	0.49	2.77	8.2	825.0	38°14'26.59"N	13°26'05.60"E
PMO-13	0.50	3.19	7.1	675.0	38°14'22.45"N	13°25'11.57"E
PMO-14	0.53	2.80	9.3	900.0	38°15'18.46"N	13°26'01.24"E
PMO-15	0.46	2.83	9.7	995.0	38°15'25.75"N	13°26'35.72"E
PMO-16	0.08	1.11	6.9	305.0	38°15'12.85"N	13°23'18.98"E
PMO-17	0.15	1.55	6.9	135.0	38°15'49.48"N	13°22'52.91"E
PMO-18	0.79	3.47	10.5	420.0	38°18'14.50"N	13°23'26.52"E

Table 2

LGT	*Detachment Surface*	*Perimeter*	*Distance from coast*	*Crown Depth*	*Coordinates*	
	(km^2)	(km)	(m)	(m)	latitude	longitude
PTT-01	0.48	2.96	3.3	153.0	38°10'38.82"N	14°42'07.42"E
PTT-02	0.59	3.37	2.4	128.0	38°11'31.84"N	15°00'50.32"E
PTT-03	0.59	3.24	4.5	191.0	38°11'16.86"N	14°45'31.06"E

Table 3

LGT	Length **b** (m)	Depth **ds** (m)	Slope **θ** (°)	Thickness **T** (m)	Width **w** (m)
PMO-01	1055.0	250.0	12.0	6.0	1250.0
PMO-02	800.0	500.0	18.0	10.0	750.0
PMO-03	1600.0	700.0	16.0	10.0	1000.0
PMO-04	600.0	450.0	15.0	15.0	700.0
PMO-05	1200.0	490.0	13.0	11.0	770.0
PMO-06	450.0	270.0	16.0	6.0	550.0
PMO-07	900.0	400.0	15.0	7.0	580.0
PMO-08	800.0	550.0	16.0	10.0	400.0
PMO-09	550.0	650.0	16.5	13.0	350.0
PMO-10	900.0	250.0	13.0	20.0	800.0
PMO-11	900.0	1000.0	15.0	10.0	1000.0
PMO-12	600.0	950.0	15.0	10.0	850.0
PMO-13	678.6	749.6	14.5	13.2	894.0
PMO-14	772.3	1000.0	18.0	10.0	593.0
PMO-15	500.0	1000.0	15.0	9.0	550.0
PMO-16	367.0	355.1	18.5	8.0	226.0
PMO-17	368.0	176.3	13.5	5.5	490.0
PMO-18	1300.0	667.3	18.9	15.1	933.0
PTT- 01	950.0	150.0	12.0	9.0	586.0
PTT- 02	1300.0	250.0	16.0	7.0	460.0
PTT- 03	1380.0	260.0	15.5	6.0	480.0

Table 4

LGT	Wave length **Ls** (m)	Wave amplitude **As** (m)
PMO-01	4358.81	0.20
PMO-02	4403.01	0.10
PMO-03	7801.01	0.11
PMO-04	3952.71	0.10
PMO-05	6256.85	0.10
PMO-06	2569.39	0.07
PMO-07	4564.19	0.07
PMO-08	4889.54	0.04
PMO-09	4341.88	0.03
PMO-10	3870.42	0.47
PMO-11	7216.62	0.03
PMO-12	5743.15	0.02
PMO-13	5516.11	0.05
PMO-14	6118.05	0.02
PMO-15	5378.95	0.01
PMO-16	2480.17	0.03
PMO-17	2040.18	0.08
PMO-18	6333.24	0.18
PTT- 01	3203.90	0.35
PTT- 02	4202.27	0.19
PTT- 03	4484.23	0.16

Table 5

LGT	Slope **α** (°)	Wave amplitude **Ac** (m)	Wave length **Lc** (m)	Speed **c** (m/s)	Depth **dc** (m)
PMO-01	1.0	0.5	261.4	10.1	10.0
PMO-02	1.0	0.3	339.8	10.0	10.0
PMO-03	1.0	0.3	313.3	10.1	10.0
PMO-04	1.0	0.3	340.4	10.0	10.0
PMO-05	1.0	0.3	340.3	10.0	10.0
PMO-06	1.0	0.2	445.6	10.0	10.0
PMO-07	1.0	0.2	421.2	10.0	10.0
PMO-08	1.0	0.1	525.0	10.0	10.0
PMO-09	1.0	0.1	627.0	9.9	10.0
PMO-10	1.0	1.0	172.6	10.4	10.0
PMO-11	1.0	0.1	536.3	10.0	10.0
PMO-12	1.0	0.1	654.3	9.9	10.0
PMO-13	1.0	0.1	458.6	10.0	10.0
PMO-14	1.0	0.1	630.4	9.9	10.0
PMO-15	1.0	0.0	934.9	9.9	10.0
PMO-16	1.0	0.1	678.4	9.9	10.0
PMO-17	1.0	0.2	445.4	10.0	10.0
PMO-18	1.0	0.5	245.0	10.2	10.0
PTT- 01	1.0	0.7	211.9	10.2	10.0
PTT- 02	1.0	0.4	273.5	10.1	10.0
PTT- 03	1.0	0.4	298.0	10.1	10.0

Table 6

LGT	**Ru** Synolakis 1987 (m)	**Ru** Federici et al. 2006 (m)	**Ru** Didenkulova et al. 2009 (m)	**Ru** Zhao et al. 2010 (m)	**Ru** Bryant 2014 (m)
PMO-01	4.51	5.46	2.39	4.56	14.46
PMO-02	2.34	5.85	1.24	2.36	11.12
PMO-03	2.86	5.70	1.52	2.89	12.06
PMO-04	2.33	5.85	1.24	2.34	11.10
PMO-05	2.33	5.85	1.24	2.35	11.10
PMO-06	1.19	6.47	0.63	1.19	8.48
PMO-07	1.37	6.33	0.73	1.37	8.97
PMO-08	0.79	6.94	0.42	0.79	7.20
PMO-09	0.51	7.52	0.27	0.51	6.03
PMO-10	12.72	5.46	6.75	13.04	21.90
PMO-11	0.75	7.01	0.40	0.75	7.05
PMO-12	0.45	7.67	0.24	0.46	5.78
PMO-13	1.11	6.55	0.59	1.11	8.24
PMO-14	0.50	7.54	0.26	0.50	5.99
PMO-15	0.19	9.09	0.10	0.19	4.04
PMO-16	0.42	7.80	0.22	0.42	5.57
PMO-17	1.19	6.47	0.63	1.19	8.49
PMO-18	5.30	5.40	2.81	5.36	15.42
PTT- 01	7.61	5.34	4.04	7.74	17.83
PTT- 02	4.03	5.51	2.14	4.07	13.82
PTT- 03	3.25	5.63	1.72	3.28	12.68

Table 7

LGT Cases history	*Length* ***b*** *(m)*	*Depth* ***ds*** *(m)*	*Slope* ***θ*** *(°)*	*Thickness* ***T*** *(m)*	*Width* ***w*** *(m)*
MONA PASSAGE (1918)	8500.0	1900.0	9.0	100.0	8500.0
VALDEZ (1964)	450.0	150.0	2.0	10.0	1300.0
NICE (1979)	4000.0	450.0	6.0	25.0	4800.0
PAPUA (1998)	4000.0	1100.0	5.0	600.0	4100.0

Table 8

LGT Cases history	*Wave length* ***Ls*** *(m)*	*Wave amplitude* ***As*** *(m)*
MONA PASSAGE (1918)	39321.6	2.1
VALDEZ (1964)	5382.1	0.0
NICE (1979)	16059.4	1.0
PAPUA (1998)	27497.3	3.5

Table 9

LGT Cases history	*Slope* ***α*** *(°)*	*Wave length* ***Lc*** *(m)*	*Wave amplitude* ***Ac*** *(m)*
MONA PASSAGE (1918)	1.0	63.2	7.8
VALDEZ (1964)	1.0	845.5	0.0
NICE (1979)	1.0	110.0	2.6
PAPUA (1998)	1.0	52.2	11.4

Table 10

LGT Cases history	Theoretical values					actual values
	Ru *Synolakis 1987* *(m)*	***Ru*** *Federici et al. 2006* *(m)*	***Ru*** *Didenkulova et al. 2009* *(m)*	***Ru*** *Zhaoet al. 2010* *(m)*	***Ru*** *Bryant 2014* *(m)*	***Ru*** *(m)*
MONA PASSAGE (1918)	156.98	14.47	14.47	181.37	59.83	3.50
VALDEZ (1964)	0.24	8.66	8.66	0.24	4.47	6.00
NICE (1979)	39.21	7.06	7.06	41.53	34.35	12.50
PAPUA (1998)	252.55	19.82	19.82	305.57	72.37	6.00

Table 11

LGT	***Ru*** *Federici et al. 2006* *(m)*	***Ru*** *our equation* *(m)*	***Δ*** *Ru Federici et al. 2006 – Ru our equation* *(m)*
PMO-01	5.46	5.98	-0.52
PMO-02	5.85	6.04	-0.19
PMO-03	5.70	6.01	-0.31
PMO-04	5.85	6.03	-0.18
PMO-05	5.85	6.04	-0.19
PMO-06	6.47	6.30	0.18
PMO-07	6.33	6.28	0.04
PMO-08	6.94	6.93	0.01
PMO-09	7.52	7.77	-0.26
PMO-10	5.46	6.56	-1.10
PMO-11	7.01	7.30	-0.29
PMO-12	7.67	8.29	-0.62
PMO-13	6.55	6.64	-0.09
PMO-14	7.54	8.10	-0.57
PMO-15	9.09	11.70	-2.61
PMO-16	7.80	7.79	0.01
PMO-17	6.47	6.21	0.26
PMO-18	5.40	5.96	-0.56
PTT- 01	5.34	6.27	-0.93
PTT- 02	5.51	5.96	-0.45
PTT- 03	5.63	5.95	-0.32
MONA PASSAGE (1918)	14.47	11.34	3.13
VALDEZ (1964)	8.66	8.46	0.20
NICE (1979)	7.06	8.05	-0.99
PAPUA (1998)	19.82	15.59	4.23

LGT	***Ru*** actual values *(m)*	***Ru*** *our equation* *(m)*	***Δ*** *Ru* actual values *– Ru our equation* *(m)*
MONA PASSAGE (1918)	6.00	11.34	-5.34
VALDEZ (1964)	6.00	8.46	-2.46
NICE (1979)	3.50	8.05	-4.55
PAPUA (1998)	12.50	15.59	-3.09

Conclusions

Putting together the results obtained in the different topics addressed during the research work, based on the acquisition, processing and analysi of marine geological and geophysical data, we provided new insights into the sedimentary, tectonic and geodynamic processes of the NSCM, as well as the assessment of related coastal and marine geo-hazards.

We used seismostratigraphic tools to identify a complex multilayer composed of:

1) Kabylian-Calabrian crystalline rocks, including their Tertiary cover;

2) Sicilian-Maghrebian carbonate successions, including their Tertiary cover;

3) Messinian layers;

4) Plio-Quaternary sequences including gravitational instability deposits, buried or emerging mounds, and fluid escapes features. The uppermost portions were attributed to the Late Quaternary depositional sequence composed of Falling Stage, Lowstand, Transgressive, and Highstand Systems Tracts. They were correlated with the sea level change curve (Silenzi 2004) and tentatively dated as deposited during different intervals of the Late Pleistocene-Holocene. Their characteristic geometry, stratal pattern and mutual relationships were useful to create a reference to date geomorphic, depositional, and tectonic processes.We analysed also several core samples to define the sedimentological characters of these deposits. The Plio-Quaternary deposits have variations in thickness and tectonic style, recording the effects of the tectono-stratigraphic events.

On the whole the tectonic edifice is composed mostly of Meso-Cenozoic carbonate units, arranged as a pile of tectonic units with apparent vergence towards ESE, involved, since the upper Pliocene, in the extensional and/or transtensional tectonics. The main events, recognized also in the outcropping sectors, are the following: i) compressional deformation involving the Meso-Cenozoic carbonates up to the Messinian layer, producing folds and reverse faults with NNE-SSW direction and vergence towards ESE; ii) extensional (to transtensional) deformation that involve the post-Messinian deposits represented by W-dipping listrical growth normal faults with large displacements. These structures generated a system of structural high and depressions; iii) NNW-SSE to ENE-WSW trending faults involving more recent deposits (mainly up to middle Pleistocene) rarely displacing the seabed. Minor N-S and E-W trending faults show also a strike-slip component. These faults are responsible for the current configuration of the shelf-slope system and they have their surface morphological expression in the crowns of the retrogressive landslides and in the development of bypass zones (canyons, channels, rills). The tectonic processes are still very active, as evidenced by the strong seismicity of the submerged sector, which was recently revealed by the earthquakes of 1998 and 2002, whose epicenters are located in areas respectively southwest and east of Ustica.

One of the main novelty of this research is represented by widespread south-dipping, north-verging thrusts in the internal sectors of the Sicilian FTB (northern coastal belt and south-western Tyrrhenian sea). Some of them seem to be responsible of the main submerged structural high geometry (e.g. the Solunto high) controlling the morphostructural evolution of the NSCM. In some cases, they appear

very recent and involve the more recent Quaternary deposits, affecting also the sub-bottom sequences. In the NW sector of the study area (Sardinia channel) the seismic profiles shows that north-verging thrusts involve also the deepest part of the tectonic edifice. These structures, correlated with seismicity and GPS measurements, are likely indicative of an important change in the distribution and orientation of deformation in agreement with the continuous convergence of African and European plates, and representative of a late collision phase in the mountain building of northern Sicily, following the ongoing collision of the African promontory with oceanic sectors. The GPS values document the active deformation with differential movements of individual blocks northward-directed, in agreement with the shallow seismicity, as well as the convergence between Sicily and Sardinia, with values of about 2-6 mm/y.

In the Ustica offshore we studied the products of the morphostructural processes affecting a volcanic complex occurring along the Africa-Europe plate margin. Morpho-bathymetric and sub-seafloor information lead to individuate different sectors with peculiar morphological and structural features. The northern sector is characterized by the occurrence of several volcanic centres with different morphologic characters, such as height, diameter and volume. The larger volcanic structures and the alignment of small volcanic edifice can be attributed to magmatic upwelling associated to faulting, producing a genetic link between tectonics and volcanism. The location of the recent volcanic activity suggest a shift of the deep source northward and/or a movement of the Ustica crustal block southward, in agreement with the present convergence between Africa and Eurasia plates. The south-western sector is characterized by fault escarpments and ridges, such as the large N-S ridge and overall the 8 km-long, ENE-WSW trending Arso structure, as well as minor, synthetic faults in the same area. The south-eastern sector is characterized by a narrow continental shelf, widely affected by erosional processes, and very steep continental slope. The eastern sector is dominated by channelized features, as linear furrows, incisions and erosional channels, which develop along the steep and irregular slope down to a depth of 1500 m.

To provide a chronostratigraphic characterization of the active tectonics along the NSCM we studied the relationships between the uppermost Pleistocene-Holocene sedimentary sequence and the faults systems. In the southern margin of the Termini Basin we detected both extensional/transtensional and hinterland verging reverse faults affecting the oldest reflecting horizons belonging to the LQDS. The large scale study of the morphological features of the study area brought to the individuation of different types of elements: pockmarks and mounds, landslides, fault escarpment, canyons and channels. Some of them were considered as induced by seismic events, particularly the several landslides recognized both in the continental shelf and slope. Correlating them to the systems tracts and unconformities of the LQDS, as interpreted following the sequence stratigraphy model, and using the chronology coming from vibracores collected in this region, we tentatively dated the occurrence of landslides and calculated the recurrence time of earthquakes that triggered them, considering the age-model based on a constant sedimentation rate during the Holocene. This is an important outcome that

can be used to assess the frequency of seismic events in this region. In detail we found almost seven seismic-induced landslides occurring in the last 11.5 ky, with a recurrence time between 680 and 2200 years.

The detailed study of the morpho-bathymetry highlighted sedimentary processes active in different sectors of the margin. In the Capo Zafferano offshore we mapped trains of bedforms in a depth range of 125-1050 m along a network of 9 gullies breaching the shelf-edge. The mapped bedforms were interpreted as cyclic steps, generated by turbidity currents, with wavelength from 110 to 340 m and amplitude from 0.8 to 5m. The model calculations indicate that the observed cyclic steps are likely generated by flows around 1 m thick, with average velocities of exceeding 1.0 m/s. The occurrence of the bedforms along the Capo Zafferano Canyon and associated gullies likely suggests intense turbidity current, even if these structures anre degraded by sporadic diluted sedimentary flows and bioturbation processes.

In order to assess the parameters of anomalous waves and tsunami run-ups we studied two very active segments of the margin, the Gulf of Palermo and Patti offshore. We identified several submarine landslides mainly confined on canyon walls. Consequently, if they generate anomalous waves they could propagate without significant loss of energy, representing therefore a significant hazard and a threat of tsunamis along the coast. We parameterized 21 significant landslides, 18 in the Gulf of Palermo and 3 in the Patti offshore respectively, based on bathymetric and morphological features, such as size, depth, and distance from the coast. The measurement of the morphometric parameters of each landslide confirms that they can be considered as a potential source of waves of the tsunami. Assuming that all the landslides could be potential tsunamigenic sources, we calculated the associated theoretical run-ups, comparing approximation methods proposed in the literature. Subsequently, we selected historical events of landslide-generated tsunamis (LGT) and calculated their morphometric parameters. Through the calculation of the parameters relative to the height and length of the tsunami wave near the source point and near the coast, we computed with different equations the theoretical values of run-up and compared the results with the actual values. The highest values of run-ups are in direct proportionality with the wave amplitude, although a small section of the curve shows for very low wave amplitude values (< 0.4 m) an increase in run-ups with decreasing amplitudes. Finally, we formulated an empirical law that allows calculating promptly the run-up associated with a generic LGT having as starting data the amplitude of the wave near the source point.

As final outcome of the PhD research, collecting and overlapping all the interpreted data, we defined two seismogenetic volumes in the study area, produced by a NW-SE oriented compressional stress field, defining an interplate shallow seismogenetic zone linked to the convergence of Africa-Europe. For this purpose we produced a georeferenced map that is composed of overlapping layers representing features, as lithostratigraphy, tectonic elements, seismicity, heat flow, gravimetry, magnetometry, Moho depth, horizontal and vertical movement rates, landslides, fluid escape. It is a basic tool to highlight their mutual relationships and active structures. The seismogenic source, which

extends in an east-west direction from the Sardinia Channel to the Aeolian Islands, about 50 km off the northern Sicilian coast, is a compressional belt that accommodates most of the Africa-Europe convergence (5-8 mm/y). The compressional stress field is consistent with the motion vectors of the plates derived from the GPS data. These compressional deformations, mainly ENE-WSW oriented, are also accompanied by extensional faults (normally oriented NNW-SSE) and strike-slip, both right-lateral (NW-SE) and left-lateral (NE-SW), in agreement with an Andersonian model of deformation. This source could coincide with the north-vergent reverse faults and thrusts, both onland and in the submerged areas. This outcome could have important implication for the assessment of seismic risk in the Central-Western Mediterranean and for the understanding of active structures in marine areas that could be responsible for marine geological hazard.